# *IRAS* Galaxies Behind The Milky Way

by

Frank de Ruyter

A thesis

submitted for the degree of Master of Science

of

The Australian National University.

16 December 1997

Mount Stromlo and Siding Spring Observatories

Institute of Advanced Studies

The Australian National University

Canberra

*To Mum and Dad*

# Disclaimer

I hereby declare that the work in this thesis is that of the candidate alone, except for the following figures and tables in Chapter one:

- Figures 1.1, 1.2 and 1.3 have been copied from Yamada *et al.* (1993*a*)
- Table 1.2 has been copied from Yamada *et al.* (1993*a*).

I have also been able to use unpublished redshift data from Dr N. Visvanathan and Dr Yamada (in Chapter 3).

Everything else, including the clustering program whose output is presented in chapter six, is the work of the candidate.

Signed: _____

Frank de Ruyter

**Errata**

1. Line 8 on page 29 contains the number "754". It should read "745".
2. Lines 21 and 23 of page 42 should read "z = 0.022", not "z=0.22".
3. Line 14 of page 66 has the statement "$25^o < \mathbf{b} < -25^o$".
   Of course, this should read "$-25^o < \mathbf{b} < 25^o$".
4. The second sentence in the footnote on page 72 was inadvertently not deleted during recent editing.

# Acknowledgements

Thanks are due to my supervisor Dr Natarajan Visvanathan for suggesting the original thesis topic, and for his enthusiasm and guidance throughout this work. I am extremely grateful for his patience at my constant forays to his office early in the piece for help with *IRAF* problems and for the introduction he gave me to observing with the 2.3-metre telescope at Siding Springs. Thanks also to Matthew Colless for helpful comments regarding the clarity of some sections of this work.

Thanks are also collectively due to Dr N. Visvanathan, Dr T. Yamada and Dr K. Fisher for having given me access to unpublished redshift data.

Lastly, nothing would have been possible without the benefit of an ANU post-graduate scholarship, so I am indebted to the Australian National University for making this available to me.

**A word or two from the author...**

Take a look at the text which starts off the Bible:

*"In the beginning God created the heavens and the earth." (Genesis1:1)*

In Hebrew, the sentence looks like this:

בְּרֵאשִׁית בָּרָא אֱלֹהִים אֵת הַשָּׁמַיִם וְאֵת הָאָרֶץ׃

That's seven Hebrew words with a total gematria of nine hundred and ninety-nine. "Gematria", by the way, is a nice little toy for the mystics among us. It is the principle by which each Hebrew letter has a number value, and so, by adding letter values, each word and sentence takes a value too. The mystics take secret meanings out of these number tallies: they see "coded" meanings in the numbers.

For a mystic there is a lot going on in Genesis 1:1. It is a good start to get a sentence with seven words, as "7" is the number of "divine authorship". That speaks for itself in this context. And if you've ever studied gematria (or dabbled, as I have) then you'll soon find out about the number "9" - it's the number which means "to bring to completion". What's pretty cool about Genesis 1:1 is that you get a triple "9" - i.e. "999". I think that means "complete completeness". A completely complete statement cannot really have anything added to it to make a fuller statement. It's like the Big Guy saying to us "Any questions?"

And I guess that brings me to this thesis. Like anyone who would go to the trouble of doing all this work, I suppose I do it because the subject drives me. If you're astronomically inclined, you'll know what I mean. And I think that I am also basically religious - and driven by a desire to know about divine matters.

From the stance of scientific enquiry I think - like a lot of astronomers, professional or otherwise - that motivation comes because I have so many questions and feel that there is a better than fair chance that I can have most of them answered. And when I started to put

together this thesis I felt as if I was playing a part in providing some of the answers. Possibly this thesis will answer some questions for you - who knows. Or maybe it will never be read again.

In a nutshell, my view is that at the end of the day we've got to admit that the world, along with its intellectual property, all belong to God. Well, if you believe in God that is. If you do, then you'll see that really it's just part of His "copyright" on the place. And its not just the world, either. If you go along with Job, God "can bind the chains of the Pleiades, (and) loosen the cords of Orion" (Job 38:31). That's pretty impressive. Okay, so maybe Job is a poetic book, and maybe someone like Solomon actually wrote it. But we still receive it as "inspired" text. And I have a feeling it really is.

God poses another question of Job: "Who has put wisdom in the inward parts; or who has given understanding to the mind?". Its supposed to be a closed question, and we get the point. We're just observers, and it is God who gave us the eyes to see. That's good - it suggests that God is quite happy for us to see a lot. As God has never forbidden mankind to make enquiry, I think we can assume that it is okay to ask questions - in fact, it is probably required. And there doesn't seem to be any restriction on the size of the question!

None of us were there when everything started - that is true. But at least, for the astronomer, theres a bit of a "time-delay" on the information we're working with. We've still got a bit of a chance of figuring out some of those things that happened way back when ... (well, as far back as a telescope will take us). And I think that that's what makes it fun, whatever angle you might come at it from.

Well - that's my spiel. I've just put it in to remind myself in years to come that science isn't everything. Whatever your own slant on things might be - even if radically in disagreement of or unable to identify with my ramblings above - I hope that the thesis will hold something of interest for you.

# Abstract

The results of a systematic search for $IRAS$ galaxies at Galactic latitudes $|\mathbf{b}| < 15^{\circ}$, and Galactic longitudes $210^{\circ} < |\mathbf{l}| < 360^{\circ}$, are presented in this thesis. The $IRAS$ flux-limited ($f_{60} > 0.6\,Jy$) galaxy sample has been chosen for our sample. From 966 $IRAS$ sources identified as being galaxies by Yamada *et al.* (1993*a*) from Schmidt plate searches, the spectra of 176 have been newly observed and reduced, and redshifts recovered for 136 of these.

This brings the total number of available redshifts for $IRAS$ galaxies at $|\mathbf{b}| < 15^{\circ}$ up to 745. The sample of redshift-identified $IRAS$ galaxies is estimated to be $\sim 55\%$ complete at southern latitudes and $\sim 70\%$ complete in the northern, after comparison with the Rowan-Robinson *et al.* (1991) all-sky 60-micron $IRAS$ galaxy survey. In several areas $IRAS$-galaxy number densities show real over- and under-densities.

Redshift data were input to a clustering program, which was able to identify several new groups and clusters of galaxies behind the Milky Way. The results of this analysis appear in Chapter 6.

Large scale structures seen in the ESO catalogue, and in the CfA survey for optical galaxies outside the "zone of avoidance", appear to continue across the Milky Way in three places in the $IRAS$ map of the sky, which extends to much lower Galactic latitudes. The approximate longitudes at which these structures cross the Galactic equator are $\mathbf{l} = 240^{\circ}$ (and therefore in the constellation of Puppis), $\mathbf{l} = 280^{\circ}$ (in the constellation of Vela) and $\mathbf{l} = 330^{\circ}$ (in the Centaurus/Lupus region). The latter structure, crossing in Centaurus, appears to extend over more than $90^{\circ}$ in latitude, at a mean redshift of $\sim 3700\,km\,s^{-1}$. The long dimension of this structure therefore exceeds $80\,h^{-1}\,Mpc$ in size. The structure crossing in Vela, by comparison, has a longest dimension of $\sim 45\,h^{-1}\,Mpc$.

The number density of $IRAS$ galaxies for which $f_{60} > 0.6\,Jy$ (for a galaxy sample restricted to $cz \leq 6500\,km\,s^{-1}$) found at $|\mathbf{b}| > 4^{\circ}$, between $\mathbf{l} = 210^{\circ}$ and $\mathbf{l} = 360^{\circ}$, is close to 0.21 $IRAS$

galaxies per square degree - three times larger than the 0.07 $IRAS$ galaxies per square degree found for galaxies with $f_{60} > 1.936\,Jy$ in a search at all longitudes by Strauss *et al.* (1992*a*). In the optically thinnest parts of the Milky Way the number density equals about 0.30 galaxies per square degree, beginning to approach the all-sky average number density of 0.42 $IRAS$ galaxies per square degree, determined by Rowan-Robinson *et al.* (1991) from a one-in-six sample of $IRAS$ galaxies at higher latitudes, with lower average foreground extinctions.

Galactic extinction *has* affected the optical galaxy counts, and therefore the observed distribution of optically confirmed $IRAS$ galaxies. Nevertheless, the present analysis suggests strongly that large-scale structures *do* cross behind the Milky Way, and that a series of under- and over-dense regions at redshifts below $50\,h^{-1}\,Mpc$ in the background population of galaxies have been correctly identified. A series of $log\,N$ versus $log\,f_{60}$ plots, presented in Chapter 5, indicate that the 60-micron sample is, however, highly complete, and indicate that source confusion may have been an important factor in producing lower galaxy detection rates behind the Milky Way at $|\mathbf{b}| < 4^{\circ}$ than elsewhere.

# Contents


**1 Introduction** 1

1.1 Motivation for the Survey . . . . . 1

1.2 Selection Criteria . . . . . 2

1.2.1 Identifying Galaxies on the Schmidt Plates . . . . . 9

1.3 Selection Effects . . . . . 12

**2 Extinction Analysis** 15

2.1 Effects of Extinction ($A_V$) on the Identified Sample . . . . . 15

2.1.1 Converting $A_V$ to $A_I$ . . . . . 17

2.2 Summary of Extinction Effects . . . . . 25

**3 Measuring Redshifts** 27

3.1 Acquisition of Spectra . . . . . 27

3.2 Tabulation of Data . . . . . 29

**4 Sample Completeness** 31

**5 Distribution of the IRAS Galaxies** 37

5.1 Distribution of *IRAS* Galaxies on the Sky and in Redshift Space . . . . . 37

5.2 Evidence for Density Fluctuations: The $LogN$ versus $Log\ f_{60}$ plot . . . . . 44

5.3 A Universal Luminosity Function for *IRAS* Galaxies? . . . . . 47

**6 Clustering Program** 53

6.1 Setting Program Parameters . . . . . 53

6.1.1 Distance to, and Size of, the Virgo Cluster . . . . . 53
6.1.2 Running the Program . . . . . 55
6.2 Groups and Clusters of *IRAS* Galaxies: Program Results . . . . . 66
6.2.1 Identifying Groups and Clusters . . . . . 66
6.3 Comparison to the CfA Survey Data . . . . . 71
6.4 Superclusters in Vela and Centaurus? . . . . . 74
6.5 The "Great Wall" at Southern Latitudes? . . . . . 84

**7 Conclusions** **87**
7.1 Summary of Results . . . . . 87

**8 References** **93**

**9 Appendices** **99**
9.1 Previously Identified Groups and Clusters of Galaxies within $cz < 6500\,km\,s^{-1}$. 100
9.2 New Seyfert-like Galaxies in the Sample. . . . . 103
9.3 Galaxy Data for *IRAS* Galaxies between l = 210° and l = 360° behind the Milky Way. . . . . 104

# List of Figures


1.1 The CIAs (CGMW-*IRAS* Associations) of Saito *et al.*, 1990, 1991. . . . . 5

1.2 Yamada's criteria for identifying *IRAS* sources as stars, applied to the 307 CIAs. 8

1.3 Yamada's criteria for classifying *IRAS* sources as *HII* regions, Galactic cirrus or PMS stars, applied to the 307 CIAs. . . . . 9

2.1 Situation of bins between $\mathbf{l} = 235^{\circ}$ and $\mathbf{l} = 360^{\circ}$ near the Galactic equator. . . 21

5.1 *IRAS* galaxies in the $(\mathbf{l}, \mathbf{b})$ plane: all redshifts. . . . . 38

5.2 *IRAS* galaxies at $cz < 6500\, km\, s^{-1}$ in the $(\mathbf{l}, \mathbf{b})$ plane. . . . . 38

5.3 Locations of *IRAS* galaxies in the longitude-redshift plane. . . . . 39

5.4 Locations of *IRAS* galaxies in the latitude-redshift plane. . . . . 39

5.5 Pie-chart ($\mathbf{b}$ suppressed) showing location of all *IRAS* galaxies with redshifts. 40

5.6 Variation of total galaxy counts with redshift. . . . . 41

5.7 Comparison of redshift distributions as they appear in the one-in-six survey of Rowan-Robinson *et al.* (1990) and in the current survey. . . . . 43

5.8 *Log N* versus *log* $f_{60}$ for 925 *IRAS* galaxies situated at $0^{\circ} < |\mathbf{b}| < 15^{\circ}$. . . . . 45

5.9 *Log N* versus *log* $f_{60}$ for 835 *IRAS* galaxies situated at $4^{\circ} < |\mathbf{b}| < 15^{\circ}$. . . . . 48

5.10 *Log N* versus *log* $f_{60}$ for 90 *IRAS* galaxies situated at $|\mathbf{b}| < 4^{\circ}$. . . . . 49

5.11 Regression "best fit" to the *log N* versus *log* $f_{60}$ relation, for galaxies situated at $0^{\circ} < |\mathbf{b}| < 15^{\circ}$. . . . . 50

5.12 Regression "best fit" to the *log N* versus *log* $f_{60}$ relation, for galaxies situated at $4^{\circ} < |\mathbf{b}| < 15^{\circ}$. . . . . 51

6.1 Clustering of *IRAS* galaxies for $cz < 6500\, km\, s^{-1}$. . . . . 61

6.2 Clustering of $IRAS$ galaxies in 750 $km\,s^{-1}$ slices in redshift space, out to $cz <$ 6500 $km\,s^{-1}$. Note that the slices overlap by 250 $km\,s^{-1}$ with each neighbouring slice. . . . . 62

6.3 Combination of CfA and $IRAS$ survey data. . . . . 77

6.4 Distribution in the (**l**, **b**) plane of groups and clusters associated with the supercluster-like structure crossing the Galactic equator near **l** = 240°. . . . . 78

6.5 Distribution in redshift-space (**l** coordinate suppressed) of groups and clusters associated with the supercluster-like structure crossing the Galactic equator near **l** = 240°. . . . . 78

6.6 Distribution in redshift-space (**b** coordinate suppressed) of groups and clusters associated with the supercluster-like structure crossing the Galactic equator near **l** = 240°. . . . . 79

6.7 Distribution in the (**l**, **b**) plane of groups and clusters associated with the supercluster-like structure crossing the Galactic equator near **l** = 280°. . . . . 80

6.8 Distribution in redshift-space (**l** coordinate suppressed) of groups and clusters associated with the supercluster-like structure crossing the Galactic equator near **l** = 280°. . . . . 80

6.9 Distribution in redshift-space (**b** coordinate suppressed) of groups and clusters associated with the supercluster-like structure crossing the Galactic equator near **l** = 280°. . . . . 81

6.10 Distribution in the (**l**, **b**) plane of groups and clusters associated with the supercluster-like structure crossing the Galactic equator near **l** = 320°. . . . . 82

6.11 Distribution in redshift-space (**l** coordinate suppressed) of groups and clusters associated with the supercluster-like structure crossing the Galactic equator near **l** = 320°. . . . . 82

6.12 Distribution in redshift-space (**b** coordinate suppressed) of groups and clusters associated with the supercluster-like structure crossing the Galactic equator near **l** = 320°. . . . . 83

9.1 Locations of the Seyfert and "multiple"-source galaxies in the distribution of *IRAS* galaxies behind the Milky Way. . . . . 103

# List of Tables


1.1 Yamada's 1993*a* infra-red flux-density and colour criteria. . . . . 6

1.2 *IRAS* point sources found in various surveys at $|\mathbf{b}| < 12^{\circ}$ until 1992. . . . . 7

2.1 Conversion between Feitzinger & Stuwe opacity classes and magnitudes of extinction at $V$. . . . . 17

2.2 Variation of Absorption with Wavelength (normalized to $A_V = 1.0$). . . . . 18

2.3 Mean $I$-band extinctions (magnitudes) in adjacent $(\mathbf{b} \times \mathbf{l}) = (3^{\circ} \times 5^{\circ})$ & $(4^{\circ} \times 5^{\circ})$ regions in the Milky Way. . . . . 20

2.4 Mean $I$-band extinctions (magnitudes) in $(\mathbf{b} \times \mathbf{l}) = (11^{\circ} \times 5^{\circ})$ strips in the Milky Way. . . . . 22

2.5 Mean $I$-band extinctions in $(3^{\circ} \times 75^{\circ})$ and $(4^{\circ} \times 75^{\circ})$ strips for $|\mathbf{b}| < 15^{\circ}$. . . . 23

2.6 Mean $I$-band extinctions & total galaxy counts for $(3^{\circ} \times 150^{\circ})$ and $(4^{\circ} \times 150^{\circ})$ strips in Table 2.5. . . . . 24

4.1 Galaxy number densities (optically identified *IRAS* galaxies per square degree) & estimated sample completenesses in $(\mathbf{b} \times \mathbf{l}) = (3^{\circ} \times 75^{\circ})$ and $(4^{\circ} \times 75^{\circ})$ constant-latitude strips in the Milky Way, restricted to $4^{\circ} < |\mathbf{b}| < 15^{\circ}$. . . . 34

4.2 *IRAS* galaxy number densities & estimated sample completenesses in all-longitude (i.e. $360^{\circ} > \mathbf{l} > 210^{\circ}$) constant-latitude strips in the Milky Way, for $4^{\circ} < |\mathbf{b}| < 15^{\circ}$. . . . . 35

6.1 Results of the Clustering Analysis - Table 1 . . . . . 59

6.2 Results of the Clustering Analysis - Table 2 . . . . . 60

6.3 Old and New Groups in the Milky Way. . . . . 70

9.1 Centaurus Clusters near the Milky Way, for $cz \leq 6500\,km/s$ - Table 1. . . . . 100
9.2 Previously Identified Groups and Clusters at $|\mathbf{b}| < 25°$ - Table 2. . . . . 101
9.3 Previously Identified Groups and Clusters at $|\mathbf{b}| < 25°$ - Table 3. . . . . 102

# Chapter 1

# Introduction

## 1.1 Motivation for the Survey

The distribution of $IRAS$[1] galaxies in the Local Universe has, in the last few years, been quite well mapped in both northern and southern latitudes of the Milky Way (e.g. Rowan-Robinson *et al.*, 1991; Strauss *et al.*, 1992*a*; Fisher *et al.*, 1995). The $IRAS$ survey is a complete all-sky[2] mid/far-infra-red survey, obtained entirely on one instrumental system. It is generally unaffected by the atmospheric extinction and absorption which affect ground-based infra-red and optical surveys.

Observations to date suggest that the bright galaxy number densities remain enhanced above average values as surveys approach ever more closely to the Galactic equator in such regions as the Hydra-Centaurus-Pavo-Indus supercluster (commonly referred to as the "Great Attractor") and the Perseus-Pisces supercluster (see e.g. Strauss *et al.*, 1992*a*), suggesting that these structures may actually continue right across the heavily obscured part of the Milky Way. There is also the possibility that other as-yet-undiscovered over-densities could exist near the Galactic equator. Filamentary and sheetlike structures are documented on both sides

[1]The Infra-red Astronomical Satellite was developed and operated by the U.S. National Aeronautics and Space Administration (N.A.S.A.), the Netherlands Agency for Aerospace Programs (N.I.V.R.) and the U.K. Science and Engineering Research Council (S.E.R.C.). This satellite simultaneously produced a scan of the sky in four wave-bands: $12\mu m$, $25\mu m$, $60\mu m$ and $100\mu m$.

[2]Excluding just 4% of the sky.

of the Milky Way (Strauss *et al.*, 1992*b*), so it is obviously desirable to trace these structures down to the lowest possible Galactic latitudes. The possible existence of coherent large-scale structures which completely cross the Milky Way is discussed in Yamada *et al.* (1993*a*).

The galaxy distribution at Galactic latitudes $|\mathbf{b}| < 15°$, comprising effectively 25% of the sky, has not been properly mapped before[3]. Mapping of this region will not only amplify knowledge of how large scale structures continue to propagate behind the Milky Way, but will also provide more data which will help to calculate the net gravity vector which induces the peculiar motion of the Local Group (e.g. Lynden-Bell *et al.*, 1989; Rowan-Robinson *et al.*, 1990).

## 1.2 Selection Criteria

Galaxies account for $\sim$ 10% of the 240 000-odd *IRAS Point Source Catalog* (IPSC, 1988) sources. Most of these galaxies are spirals, detected because of far-infra-red radiation from their plentiful dust lanes. It is difficult to identify the galaxies among the multitude of other Galactic infra-red sources. Most Milky Way *IRAS* sources are not background galaxies. In fact the majority are either supergiant stars, planetary or reflection nebulae, warm isolated dust clouds, Galactic "cirrus" or *HII* regions (IPSC, 1988).

A number of researchers (see Table 1.2) have until now applied a variety of flux and colour criteria to the sources listed in the *IRAS* catalogue in an attempt to obtain a maximal selection of galaxy candidates from among the many infra-red sources. Once applied, these criteria generate a list of *IRAS* "candidate" galaxies, after which it still remains to verify the given candidate lists by checking whether probable sources appear to correspond with anything which resembles a galaxy on an optical or near-infra-red photographic plate.

Once galaxies have been identified as such from Schmidt plates, or else from the results of earlier galaxy surveys, the next step is to obtain optical spectra, so that redshifts - and therefore distances - can also be ascertained for each of the *IRAS* galaxies.

---

[3]Throughout this report, the notation $(\mathbf{l}, \mathbf{b})$ is used to denote $(l^{II}, b^{II})$.

Several surveys of galaxies behind the Milky Way have already been performed. Investigations of Schmidt plates by Kraan-Korteweg (1989) and Saito *et al.* (1990, 1991) have filled in galaxy counts for various longitudinal sections of the sky behind the Milky Way. Specifically, Kraan-Korteweg searched at $|\mathbf{b}| \lesssim 15^{\circ}$ in the range $\mathbf{l} = 270^{\circ}$ to $295^{\circ}$, visually identifying $\sim 200$ objects as galaxies down to 0.2 arcminutes in diameter on the U.K. Schmidt $IIIa-J$ ($J$-plate) Atlas plates. Saito *et al.* (1990) performed a similar visual search at $|\mathbf{b}| \lesssim 12^{\circ}$ in the range $\mathbf{l} = 205^{\circ}$ to $250^{\circ}$, using the U.K. Schmidt Atlases compiled by Hartley & Dawe (1981), identifying $\sim 7000$ objects down to 0.1 arcminutes in diameter as galaxies or galaxy-like, the results being listed also Saito (1991).

Overlapping with these surveys, Strauss *et al.* (1990, 1992*a*, 1992*b*) and Fisher *et al.*, (1995)[4] variously produced a selection of $60\mu m$ *IRAS* galaxy candidates from the I.P.S.C. with $f_{60}$ fluxes greater than $1.936\,Jy$ and $1.2\,Jy$, respectively, taken over the whole sky. Both surveys were reasonably complete for $|\mathbf{b}| > 15^{\circ}$, but that of Strauss *et al.* (1992*b*) was much less complete than Fisher's at lower latitudes.

The *IRAS* galaxies discovered in the present survey were originally selected as candidates after applying criteria defined and applied by Yamada *et al.*(1993*a*), as outlined below. Redshifts for many of the galaxies found by Yamada were obtained by Visvanathan in three observing runs in 1993 at Siding Springs Observatory using the double-beam spectrograph (DBS) on the 2.3-metre telescope. The author also assisted in the acquisition of data for this program in an observing run in 1993.

Yamada *et al.* (1993*a*) developed their flux-based selection criteria after first creating a list of all *IRAS* point sources behind the Milky Way directly associated with optical galaxies in the CGMW (*Catalog of Galaxies Behind the Milky Way* - Saito, 1991). The list so compiled contained 307 "CIAs"[5]. One hundred and ninety of these galaxies also had $f_{60} > 0.6\,Jy$, which matched the completeness limit achieved by the *IRAS* survey at $60\mu m$ at much higher Galactic

[4] References in this thesis, with one exception, extend only to 1995, as the main analysis was completed in that year.

[5] "CIAs" is shorthand for CGMW-*IRAS* Associations; Saito *et al.*, 1990, 1991: these CIAs are plotted in Figure 1.1.

latitudes (*IRAS Explanatory Supplement, 1988* (ES))[6]. Half of these 190 CIAs furthermore had confirmed redshifts and were already definitely identified as galaxies (Takata, 1992; Yamada & Saito, 1993). The selection criteria then defined and applied by Yamada *et al.* (1993*a*) were able to pick up 173 of the 190 ($f_{60} > 0.6\,Jy$) *IRAS* galaxies in their CIA list, and so appear to be $\sim 91\%$ efficient in finding *IRAS* galaxies with $f_{60} > 0.6\,Jy$ in the CGMW region. The same criteria were also found to recover 95% of the catalogued *IRAS* galaxies outside the Milky Way region (cf. Takata, 1992). Therefore, although optical verification becomes increasingly difficult from photographic plates because of high optical extinctions near the Galactic equator, it is nevertheless anticipated that Yamada's criteria will "blindly" detect up to 90% of all detectable galaxies in the extended region dealt with in this survey, if one uses *IR* plates and extends the survey to smaller galaxy diameters.

In fact, comparative Schmidt Atlas studies by Saito *et al.* (1990, 1991) and Yamada & Saito (1993) lead them to claim that the CIAs comprise nearly a complete set of *IRAS* galaxies for $f_{60} > 0.6\,Jy$ within $120h^{-1}\,Mpc$ in the CGMW region[7], although some of the faintest galaxies, because extinction has caused their diameters on Schmidt Atlas plates to be reduced, have probably been lost from the sample for $|\mathbf{b}| \lesssim 5^{o}$. It is also possible that some distant but luminous ($L_{fIR} \gtrsim 10^{10}\,L_{\odot}$) galaxies, which are both fainter and a little bluer, have also been missed in the CGMW for $|\mathbf{b}| < 5^{o}$, and this seems to be supported by the fact that the average $60\mu m$ flux and the $log(f_{100}/f_{60})$ colour of the CIAs (with $\Theta_{\mathrm{I}} < 0.3$ arcminutes[8] and $f_{60} > 0.6\,Jy$) are $1.15\,Jy$ and 0.27 for $|\mathbf{b}| > 5^{o}$ but are $1.38\,Jy$ and 0.53 for $|\mathbf{b}| < 5^{o}$ !

To exclude stars, Yamada includes the requirement that $f_{60}^{2} > f_{12}f_{25}$ (following Strauss *et al.* (1990) in this regard - see Figure 1.2). To eliminate both Galactic cirrus and young stellar objects emitting at and longward of $100\mu m$, and warm *HII* regions emitting at and shortward of $60\mu m$, a limitation that $0.8 < f_{100}/f_{60} < 5.0$ has also been imposed (see Figure 1.3). Each

---

[6]The criteria of Rowan-Robinson *et al.* (1991) were as efficient as those of Yamada *et al.* but were not published at the time Yamada *et al.* began their search.

[7]Where $h = H_{o}/(100\,km\,s^{-1}\,Mpc^{-1})$.

[8]$\Theta_{\mathrm{I}}$ = apparent diameter on the Schmidt *I*-plates.

Figure 1.1: The CIAs (CGMW-*IRAS* Associations) of Saito *et al.*, 1990, 1991. These are *IRAS* point sources behind the Milky Way, directly associated with the optical galaxies in the *Catalog of Galaxies behind the Milky Way* of Saito, 1990. Key: open circles = galaxies with $f_{60} > 0.6\,Jy$ (190 galaxies); closed circles = galaxies with $f_{60} < 0.6\,Jy$ (117 galaxies). The criteria in Table 1.1 select 173 of the galaxies with $f_{60} > 0.6\,Jy$.

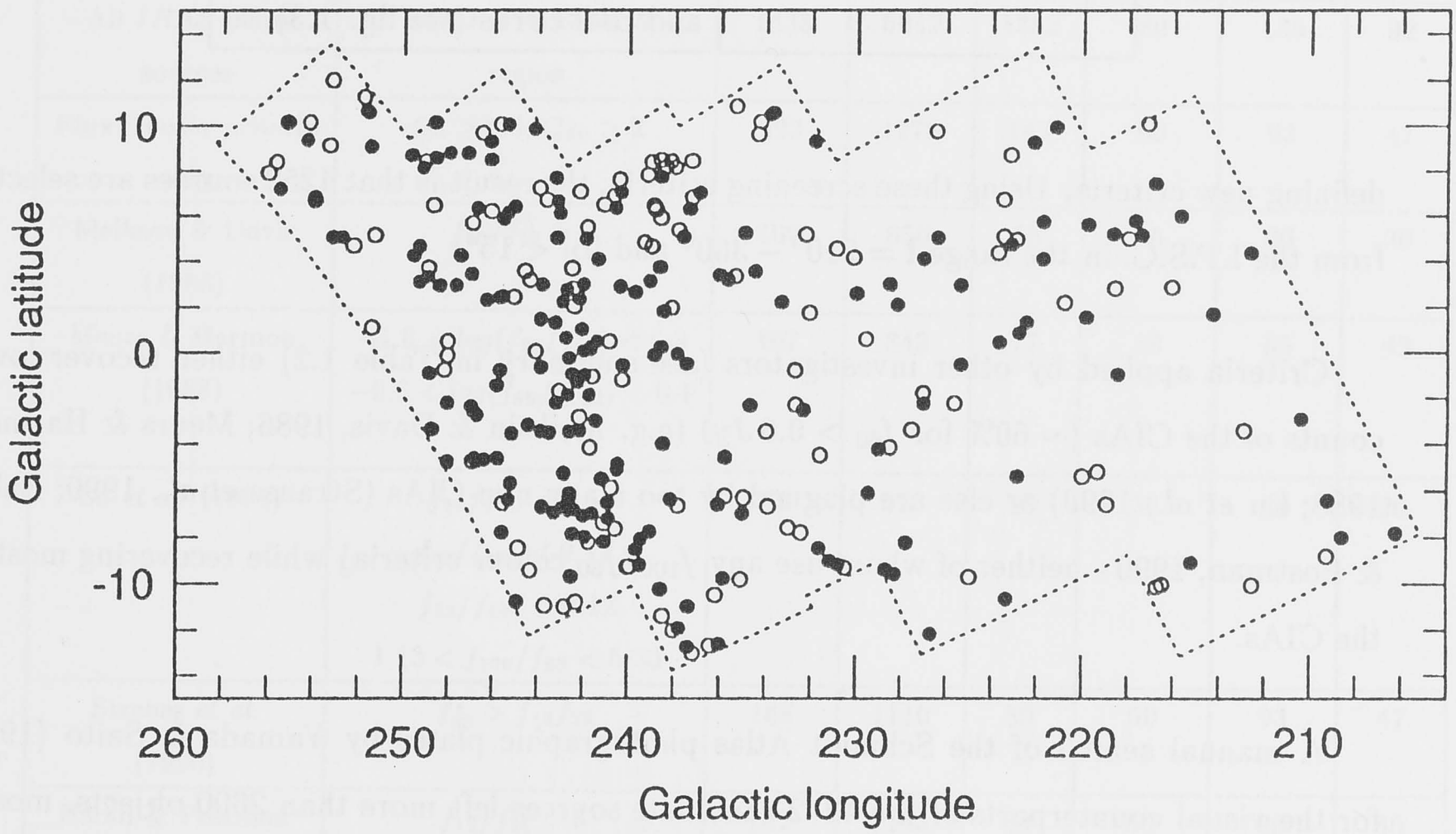


$60\mu m$ source needs also to have been detected at least twice ($Q_{60} \geq 2$) by the satellite to confirm the flux measurement. As measured earlier, these four criteria on their own already select $\sim$ 90% of the CIAs with $f_{60} > 0.6\,Jy$, as well as 95% of catalogued *IRAS* galaxies outside the Milky Way region (Takata, 1992). The other $\sim$ 10% are mainly included among the brightest objects at $f_{100}$.

Although these criteria also pick up twice as many non-CIA sources[9] as CIA sources between $5° < |\mathbf{b}| \lesssim 12°$, and six times as many for $|\mathbf{b}| < 5°$, this is not so many as to warrant

[9]It is observed that in all four bands the non-galaxy sources have significantly higher flux densities than the galaxies.

Table 1.1: Yamada's 1993*a* infra-red flux-density and colour criteria.

| Criterion | Meaning of Criterion |
|---|---|
| (i) $Q_{60} \geq 2$ | Quality of $60\mu m$ flux density |
| (ii) $f_{60} > 0.6\,Jy$ | Range of $60\mu m$ flux density |
| (iii) $f_{60}^2 > f_{12} f_{25}$ | Exclusion of stars (see fig. 1.2) |
| (iv) $0.8 < f_{100}/f_{60} < 5.0$ | Exclusion of hot $HII$ regions and cool cirrus (see fig. 1.3) |

defining new criteria. Using these screening criteria, the result is that 4252 sources are selected from the I.P.S.C. in the range $\mathbf{l} = 210° - 360°$ and $|\mathbf{b}| < 15°$.

Criteria applied by other investigators (see summary in Table 1.2) either recover lower counts of the CIAs ($\sim 60\%$ for $f_{60} > 0.6\,Jy$) (e.g. Meiksin & Davis, 1986; Meurs & Harmon, 1988; Lu *et al.*, 1990) or else are plagued by too many non-CIAs (Strauss *et al.*, 1990; Babul & Postman, 1990 - neither of whom use any $f_{100}/f_{60}$ colour criteria) while recovering most of the CIAs.

A manual search of the Schmidt Atlas photographic plates by Yamada & Saito (1993) for the visual counterparts of the 4252 candidate sources left more than 2600 objects, mostly within 3° of the Galactic equator, unidentified. Many of these could still be galaxies. Of those positively identified *IRAS* sources, 966 were found to be galaxies. The remainder of the candidate sources were matched with objects within the Milky Way. Of the 966 identified galaxies, 423 were already catalogued in the *Catalog of Galaxies and Quasars in the IRAS Survey*, but most of the 543 remaining candidates were newly identified as galaxies in their search.

In the survey of Strauss *et al.* (1990), ADDSCAN corrections were applied to all fluxes to compensate for suspected systematic underestimation of fluxes due to aperture effects. However, Yamada *et al.* (1993*a*) estimate, from data presented in Strauss *et al.* (1990), that the ratio of ADDSCANed to catalogued $60\mu m$ flux-densities is less than 1.5 for nearly all

Table 1.2: *IRAS* point sources found in various surveys at $|\mathbf{b}| < 12^{\circ}$ until 1992.
Superscripts: (1) Numbers of *IRAS* Point Sources (including *CIA*s [*CGMW/IRAS* associations]) recovered by each criterion in each zone (2) Numbers of recovered *CIA*s.

| Authors | Criteria | $IPS^1$ | | | $CIAs^2$ | | |
|---|---|---|---|---|---|---|---|
| | | $\mathbf{b} < -5$ | $\|\mathbf{b}\| < 5$ | $\mathbf{b} > 5$ | $\mathbf{b} < -5$ | $\|\mathbf{b}\| < 5$ | $\mathbf{b} > 5$ |
| All *IRAS* point sources | All *IPS* in CGMW region | 1838 | 5042 | 1352 | 80 | 135 | 92 |
| Flux density criteria only | $f_{60} \geq 0.6$; $Q_{60} \geq 2$ | 223 | 1278 | 143 | 50 | 93 | 47 |
| Meiksen & Davis (1986) | $f_{60}/f_{12} > 3$ | 109 | 850 | 55 | 36 | 66 | 30 |
| Meurs & Harmon (1988) | $-1.0 < log(f_{25}/f_{60}) < 0.2$ $-0.6 < log(f_{60}/f_{100}) < 0.1$ | 107 | 343 | 77 | 38 | 65 | 42 |
| Lu *et al.* (1990) | $f_{25}/f_{60} < 0.5$, $f_{12}/f_{100} < 0.12$, $f_{12}/f_{100} < 0.12$ $1.13 < f_{100}/f_{60} < 5.30$ | 87 | 523 | 28 | 36 | 60 | 20 |
| Strauss *et al.* (1990) | $f_{60}^2 > f_{12}f_{25}$ | 168 | 1110 | 89 | 50 | 93 | 47 |
| Babul & Postman (1990) | $f_{12}/f_{25} > 3$ $f_{60}/f_{25} > 2$ | 162 | 1143 | 84 | 50 | 90 | 46 |
| Rowan-Robinson *et al.* (1991) | $log(f_{60}/f_{25}) > -0.3$, $log(f_{60}/f_{100}) < 0.6$ $log(f_{60}/f_{100}) < 0.6$ (and $log(f_{60}/f_{12}) > 0$, $log(f_{100}/f_{25}) > -0.3$ $log(f_{25}/f_{12}) < 1.0$ if detections occur at at $12\mu m$ and $25\mu m$) | 122 | 467 | 85 | 46 | 75 | 46 |
| Yamada *et al.* (1993*a*) | see Table 1.1 | 131 | 593 | 82 | 47 | 80 | 46 |

Figure 1.2: Yamada's criteria for identifying *IRAS* sources as stars, applied to the 307 CIAs. Exclusion of stars is by criterion (iii) in Table 1.1. Objects to the right of the dashed line fulfill the criterion that $f_{60}^2 > f_{12} f_{25}$, and are therefore unlikely to be stars. It is noticeable that objects to the left of the line (which accounts for $\sim 5\%$ of the CIAs) all have low flux levels.

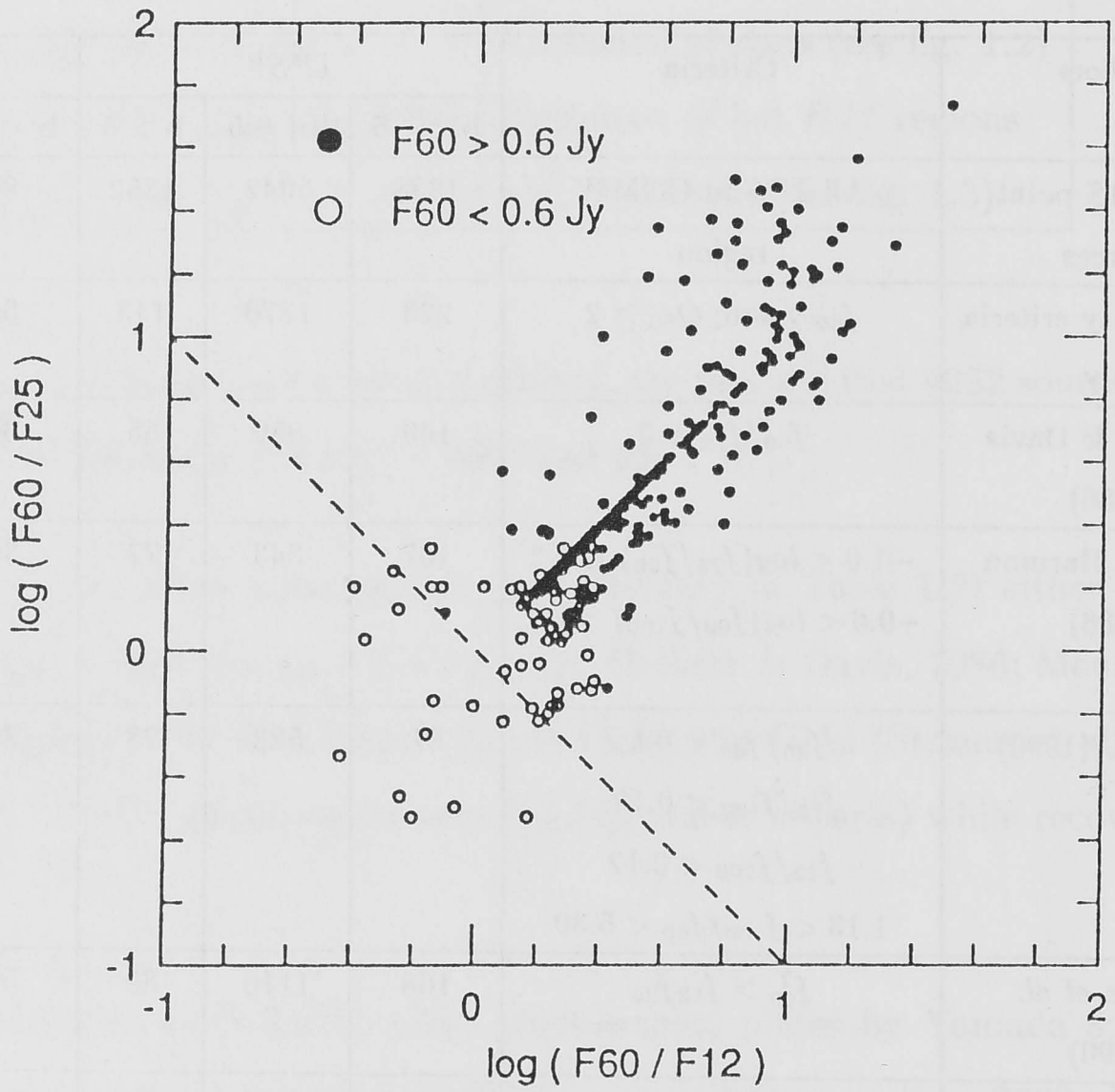


of the 66 sources with $f_{60} > 1.936\,Jy$ found at $|\mathbf{b}| < 5^{\circ}$. Strauss *et al.* (1990) also estimated that the uncertainties in $f_{60}$ and $f_{100}$ fluxes due to detector hysteresis (i.e. heightened detector response shortly after the *IRAS* detectors have passed over a bright object) would have altered fluxes by less than 2%. Consequently, Yamada *et al.* (1993*a*) did not feel it generally necessary to correct for either of these effects in the data used for the present survey and analysis[10].

[10] Fisher *et al.*, (1992), also tested for the need to make colour corrections to P.S.C. fluxes. The reason for this is that the "flux densities" calculated in the P.S.C. come with the assumption that the spectral energy distribution, $f_\nu$, is proportional to $\nu^{-1}$ - i.e.

$$F = f_\nu^{\mathrm{PSC}}(\nu_0) \int (\nu_0/\nu)\, R_\nu \, d\nu,$$

where $\nu_0$ is the frequency at the bandpass centre and $R_\nu$ is the responsivity of the detector. They found that generally only negligible colour corrections would be needed, if at all. Those few galaxies listed with ADDSCANed fluxes in this report's Appendix 9.3 are those for which *both* Strauss *et al.* (1990) and Fisher

Figure 1.3: Yamada's criteria for classifying $IRAS$ sources as $HII$ regions, Galactic cirrus or PMS stars, applied to the 307 CIAs.

Exclusion of hot $HII$ regions, exclusion of cool patches of Galactic cirrus, and exclusion of YSOs is by criterion (iv) in Table 1.1 from the sample of CIAs. $HII$ regions should lie below the lower dashed line at $f_{100}/f_{60} = 0.8$, while cirrus and Y.S.O.s should lie above the upper dashed line at $f_{100}/f_{60} = 5.0$.

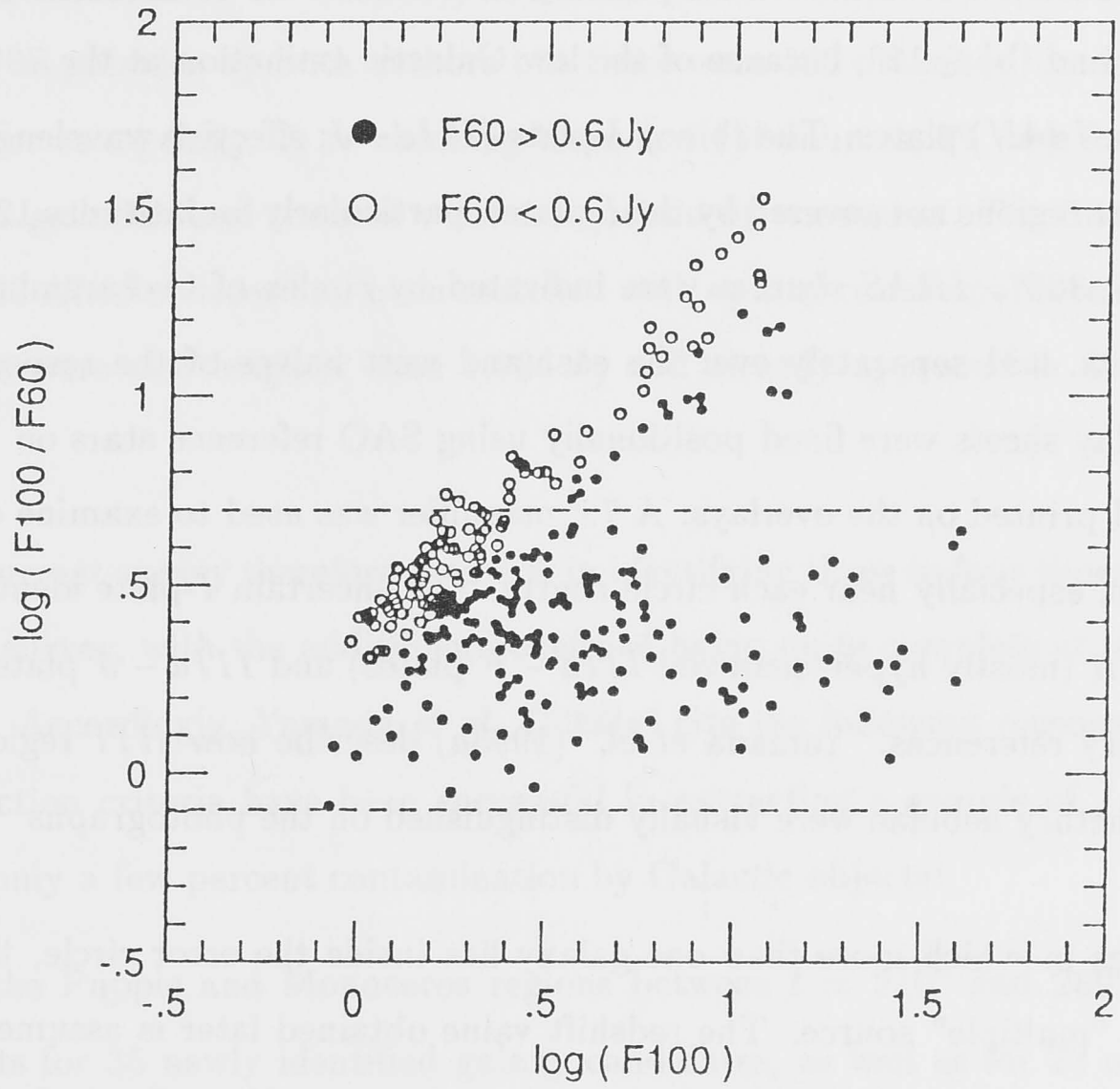


### 1.2.1 Identifying Galaxies on the Schmidt Plates

The physical process of seeking to identify galaxies from amongst the possible optical counterparts to the 4252 $IRAS$ candidate sources on the U.K. Schmidt ($I$-band and $IIIa-J$) plates is a tedious one. $IRAS$ has a $1\sigma$ pointing accuracy of fifteen arcseconds in the cross-scan direction (ES). Yamada's group (1993$a$) sought to positively match $IRAS$ sources to galaxies by searching for galaxy-like objects on the Schmidt Atlas plates using magnifying glasses and a finding circle as large as two arcminutes around the stated $IRAS$ point source positions.

---

*et al.* (1992) have continued with ADDSCANed fluxes, and have been indicated as such by the appendix "A" after the $f_{60}$ fluxes.

Because Galactic extinction diminishes both the brightness, size[11] and density of objects in Schmidt exposures, it follows that any identified sample must necessarily constitute a lower-limit[12] to the already flux-limited ($f_{60} > 0.6\,Jy$) sample of $IRAS$ galaxies behind the Milky Way.

The red $I$-plate Schmidt Atlas was the primary reference for the fields included in the region $210^{\circ} \lesssim \mathrm{l} \lesssim 360^{\circ}$ and $|\mathbf{b}| \lesssim 12^{\circ}$, because of the low Galactic extinction at the $790\,nm$ effective wavelength of the $I$ $(4N)$ plates. The (blue) $J$-plate ($IIIa-J$; effective wavelength $\sim 470\,nm$) Atlas was used for regions not covered by the $I$-plates, particularly for latitudes $12^{\circ} \lesssim |\mathbf{b}| < 15^{\circ}$ from $230^{\circ} \lesssim \mathrm{l} \lesssim 360^{\circ}$. $IRAS$ sources were indicated by circles of two arcminute radius on overlapping sheets, laid separately over the east and west halves of the respective Schmidt Atlas. The overlay sheets were fixed positionally using SAO reference stars on both Schmidt Atlas plates, and printed on the overlays. A 7× magnifier was used to examine each circle for extended objects, especially near each circle centre. For uncertain $I$-plate identifications, the U.K. Schmidt $SR$ (mostly hypersensitized $IIIa-F$ plates) and $IIIa-J$ plate Atlases were used as secondary references. Yamada *et al.* (1993*a*) describe how $HII$ regions, reflection nebulae and planetary nebulae were visually distinguished on the photographs[13].

In those cases in which more than one galaxy lies inside the error circle, the source has been listed as a "multiple" source. The redshift value obtained later is assumed to apply to the object with the strongest emission. In a great many cases, Yamada *et al.* (1993*a*) found

---

[11] Fisher *et al.* (1995), in describing their $1.2\,Jy$ survey, mention the problem that very nucleated galaxies, such as starburst galaxies, would be difficult to distinguish optically from stars on photographic plates, even at moderate extinction levels.

[12] For cluttered sources the mediocre resolution of the $IRAS$ satellite also leads to a loss of completeness in the sample contained in the I.P.S.C. (see ES $VIII-D$). At $12\mu m$ the sample with $f_{12} > 1\,Jy$ is estimated to be only 63% complete. However, most galaxies are brightest at $60\mu m$ or $100\mu m$, where the completeness is luckily much higher.

[13] In short, Galactic $HII$ regions are usually associated with dark nebulae, and compact $HII$ regions are always seen brighter on the $SR$-plates than on the $I$-plates. Reflection nebulae are always associated with stars. Planetary nebulae are observed less commonly than other infra-red objects, and both reflection and planetary nebulae appear more distinctly on $J$-plates than on $I$-plates. Various catalogues listing such objects were also used to make the identifications - cf. description in Saito *et al.*, 1990.

nothing but an optically "empty field" but, in general, these occur in the vicinity of molecular clouds in $HII$ maps. The assumption is made that in *most* such cases these dust clouds in our Galaxy are hiding faint objects.

The object matching was, to preserve objectivity, performed independently by two of the authors in Yamada *et al.* (1993*a*), and their results combined. Nine hundred sources were identified as galaxies by both authors but there were 100 other sources identified by only one or the other as a galaxy. In re-checking these last 100 sources, 29 were found to be catalogued already as galaxies, and the rest were categorised by consensus. The final result was that 966 of the 4252 *IRAS* sources had been matched with optical counterparts resembling galaxies. Of these, 273 were also brighter than $1.936\,Jy$ and already appeared in Strauss *et al*'s (1992*a*) sample.

The current survey therefore succeeds in identifying three to four times as many galaxies as Strauss's survey, with the additional benefit of being quite complete at latitudes greater than $|\mathbf{b}| = 4^{\circ}$. Accordingly, Yamada *et al.* (1993*a*) cite the following reasons for their belief that their selection criteria have been successful in extracting a sample of $IRAS$ galaxies which contains only a few percent contamination by Galactic objects:

- In the Puppis and Monoceros regions between $\mathrm{l} = 210^{\circ}$ and $260^{\circ}$ they obtained redshifts for 35 newly identified galaxy candidates, as well as for 23 objects catalogued in CGQ$IRAS$[14] without redshifts (Takata, 1992; Yamada & Saito, 1993; Yamada *et al.*, 1993*b*) and find that only one of the 58 objects is possibly a Galactic object.
- The newly identified galaxy candidates are distributed in a manner similar to the objects catalogued in CGQ$IRAS$, both as functions of Galactic latitude and longitude (see Figure 5, Yamada *et al.*, 1993*a*). (If the newly identified sample were heavily contaminated by Galactic objects then one would not expect those sources to be distributed in the same way as galaxies.) Furthermore, the number of the newly identified objects *decreases* with Galactic latitude closer to the Galactic plane against the *increasing* density of Galactic $IRAS$ sources (see Figure 4, Yamada *et al.*, 1993*a*.)

[14]CGQ$IRAS$ = Catalog of Galaxies and Quasars in the $IRAS$ Survey (Lonsdale *et al.*, 1989)

- Strauss *et al.* (1992*a*, *b*) had previously investigated the distribution of *IRAS* galaxies with $f_{60} > 1.936\,Jy$ down to $|\mathbf{b}| = 5°$. Out of 206 sources in Yamada's sample with $f_{60} > 1.936\,Jy$ at $|\mathbf{b}| > 5°$, 190 (92%) were also found catalogued by Strauss *et al.* (1992*b*) with redshifts. Twelve of the remaining sixteen sources were listed as Galactic sources (seven as cirrus, three as stars, one as a reflection nebula and one as an *HII* region) from their appearance in the Schmidt Survey Atlas but the other four sources were missed. Even if half of the sixteen sources are Galactic objects, these account for less than a few percent of the $1.936\,Jy$ sample.

As mentioned, the vast majority of *IRAS* sources ($\sim$ 2600 of the initial 4252 candidates) tagged as "possible" galaxies were without visible counterparts in the optical photographic plates. This does not indicate that they are not galaxies - only that they are too faint on the photographic plates to be seen so as to be identified. The possibility of their later identification as galaxies, and later inclusion, means there is still some potential for an alteration of the present apparent distribution of *IRAS* galaxies on the sky.

Of the 966 optically identified galaxies, only those 745 with currently measured redshifts can be shown in redshift plots in this report, so it follows that perhaps as few as 55%[15] of all the *IRAS* galaxies that may actually exist in the survey region are represented here.

## 1.3 Selection Effects

Essentially, *IRAS* fluxes measure infra-red emission from dust lanes embedded in the arms of bright warm spiral and irregular galaxies, and so the sample is biased for galaxies of this type. Elliptical galaxies, and even quiescent spirals, will therefore be highly undersampled. These omitted galaxies may additionally account for something on the order of a third to a

[15]The number density of *IRAS* galaxies in the zone of avoidance would not be expected to deviate too radically from the all-sky average, by which reasoning no more than half of these 2600 sources should also turn out to be galaxies. But, since most of these 2600 sources lie at latitudes below 5°, where the density of Galactic objects is also expected to rise steeply, probably significantly *more* than half of the unidentified sources are likely to be Galactic objects. If, conservatively, 15% of these 2600 unidentified sources are galaxies, then the total galaxy count would be around 1360, and a plot of those 745 galaxies with measured redshifts would then represent $\sim$ 55% of the total number of "dusty" galaxies actually present.

half of the galaxies actually present behind the Milky Way. For those galaxies whose emissions make them candidates for detection, the two dominating selection effects which then apply are, firstly, sample incompleteness stemming from the range of intrinsic galaxy brightnesses in the sample[16] and, secondly, the variable extinction associated with different lines of sight through the Galactic disk, limiting optical identifications and acquisitions of redshifts.

The intrinsic brightness effect is concerned with the fact that with increasing distance fainter galaxies (whether optically or in the infra-red) must be increasingly undersampled with respect to brighter galaxies in the sample. Superimposed onto this effect, when making optical identifications, is the role played by dust in absorbing optical and near-infra-red light in its passage through the dark molecular clouds distributed along the Galactic plane. Optically faint galaxies are again lost from the identifiable sample more quickly than optically bright galaxies, as line-of-sight extinctions increase. This latter condition is the chief source of sample incompleteness (as far as a sample in redshift-space goes) for the current survey.

Another important selection effect is source confusion. In some cases this means that a galaxy lies directly behind a foreground object (that is, is separated from it by an angular distance smaller than the resolution of the *IRAS* camera - this is a more critical problem as one nears the Galactic equator, where the source density is higher; hence the region $|\mathbf{b}| < 4^{\circ}$ is avoided in the analysis that follows) but in the main it pertains to those galaxies which are listed as multiple sources. Of the 745 galaxies presented with redshifts, 150 of these are listed as multiple sources. While some of these are chance alignments of galaxies along a line of sight, most multiple sources tend to be physically associated. There are also four definite and ten possible Seyfert galaxies discovered in the sample, which are possibly in the class of merging or post-merger galaxies[17].

---

[16] For those spirals optically identified in photographic plates there is also a bias toward selection of the *largest* galaxies.

[17] A brief examination indicates that nearly all of the definite and possible Seyferts, and the majority of the multiple sources, fall in regions where galaxies are already most densely concentrated. If counted as double or triple counts, these would only contribute to any observed density enhancements.

Since only those *IRAS* galaxies identified optically in the Schmidt *I* and *J* plates have been targeted for the redshift survey, any sample bias introduced through selection effects at optical wavelengths will be reflected in the resulting distribution of *IRAS* galaxies. In outlining the dominant selection effects it is therefore apparent that the possibility exists that any galaxy distribution observed in the (**l**, **b**) plane from this survey, as depicted in Figures 5.1 and 5.2, could be partly an artifact of the variable Galactic extinction near the Galactic plane.

# Chapter 2

# Extinction Analysis

## 2.1 Effects of Extinction ($A_V$) on the Identified Sample

Galactic extinction rises with decreasing Galactic latitude according to $csc|\mathbf{b}|$. It also increases rapidly within 10° in longitude (for $|\mathbf{b}| < 5°$) of the centre of the Galaxy. Yamada *et al.* (1993*a*) report from their catalogue that for $350° < \mathbf{l} < 360°$ the sample seems to be highly incomplete, and so they omit data from this region in their analysis. Additionally, Galactic extinction is quite patchy at scales of about one square degree along much of the length of the Galactic equator, most noticeably so for $0° < \mathbf{l} < 60°$ and $320° < \mathbf{l} < 360°$ (Feitzinger & Stuwe, 1984). The average extinction is, however, less variable on a coarser scale and reasonably representative average Galactic extinctions can therefore be calculated for regions[1] of 10-20 square degrees.

The "average" reddening in each region is estimated approximately from opacity maps of the Milky Way published by Feitzinger & Stuwe (1984, 1986*c*). In their later paper a set of ten maps, based on the dark cloud catalogues of Lynds (1962) and Feitzinger & Stuwe (1984, 1986*a*), are presented. The southern sky survey of Feitzinger & Stuwe (1984) was actually planned and executed to match the Lynds catalogue (which covers the whole sky at $\delta > -33°$) as closely as possible in the region of overlap. An account of their methodology appears in Feitzinger & Stuwe (1986*b*). In following Lynds, these authors describe the extinction in any

[1] We will call them "areal bins".

given region in terms of "opacity class". The classes range from zero to six, with six denoting the highest opacity, and thus maximum extinction.

Feitzinger & Stuwe (1986*c*) have published three maps to cover the region $-40° < \mathbf{b} < 40°$ for $0° < \mathbf{l} < 360°$ - one map shows all opacity class 1 & 3 objects, another all the class 2 objects, and the third shows all class 4, 5 & 6 sources. In their earlier paper (Feitzinger & Stuwe, 1984), they presented a single map which showed all six classes superposed, in a presentation which emulated the actual appearance of the Milky Way. Unfortunately this earlier map covered only $0° < \mathbf{l} < 15°$ and $235° < \mathbf{l} < 360°$, so it has been necessary to combine this with the later maps to obtain a full record of the Galactic extinctions for the region spanning $\mathbf{l} = 210°$ to $\mathbf{l} = 360°$. A copy of this map[2] is included below for reference.

These opacity classes were then calibrated by Feitzinger & Stuwe (1986*b*) against actual visual extinctions ($A_V$) . Their method involved using empirical absorption data obtained for dark clouds by Neckel & Klare (1980) to set up a correlation between $V$-band absorptions and their own opacity classes. The linear-regression best-fit relationship derived by them is:

$$A_V = 0.724\,(\mathbf{OC}) + 0.5\ \textit{magnitudes}$$

where **OC** stands for the opacity class. The scatter about this best-fit relation is 0.6 magnitudes. Simply described, $\mathbf{OC} = 0$ defines a region in which the mean absorption in the $V$ band is 0.5 magnitudes, while $\mathbf{OC} = 6$ defines $\sim 4.8$ magnitudes of extinction. The conversions are calculated exactly in Table 2.1 below.

The smallest scale at which individual opacity classes are indicated on these maps is 0.01 square degrees. For present purposes, it proves to be sufficiently accurate, and repeatable to better than 5% accuracy, simply to judge by eye the fractional occupation of each areal bin by the respective opacity classes. For each areal bin, an area-weighted "mean" opacity class was determined, and the equivalent mean $A_V$ for each bin derived from this. The smallest regions averaged over in this manner are 15 square degrees ($3° \times 5°$) in size; the largest individual areas

[2]The region $210° < \mathbf{l} < 235°$ is only found represented in individual opacity classes, so, to save space, has not been included here. The binning is, however, similar.

Table 2.1: Conversion between Feitzinger & Stuwe opacity classes and magnitudes of extinction at $V$.

| OC | $A_V$ (mag.) |
|---|---|
| 0 | 0.500 |
| 1 | 1.224 |
| 2 | 1.948 |
| 3 | 2.672 |
| 4 | 3.396 |
| 5 | 4.120 |
| 6 | 4.844 |

(those containing few or no molecular clouds, so that a larger region can safely be averaged over) are as large as 55 square degrees ($11^\circ \times 5^\circ$).

The survey region ($210^\circ < \mathbf{l} < 360^\circ$, $|\mathbf{b}| < 15^\circ$) has been cut up in two different ways - first by taking cuts at regular steps in longitude and binning across the latitudes (excluding data for $|\mathbf{b}| < 4^\circ$, $245^\circ < \mathbf{l} < 360^\circ$) and secondly by taking cuts at regular steps in latitude and binning across the longitudes (excluding data for $|\mathbf{b}| < 4^\circ$ at all longitudes).

### 2.1.1 Converting $A_V$ to $A_I$

The mean weighted extinctions at the $I$ band are graphically tabulated in Table 2.3. The conversion from $V$ band extinctions to $I$ band extinctions was made under the assumption that extinction varies inversely with wavelength through the visible part of the spectrum, which is evident from the data presented in Table 2.2, below, taken from Allen (1973; page 264).

The effective wavelength of the photographic $4N$ ($I$)-plates is 790 $nm$ (Hartley & Dawe, 1981), whereas the Feitzinger & Stuwe opacity classes are given for extinctions at an effective

Table 2.2: Variation of Absorption with Wavelength (normalized to $A_V = 1.0$).

| Band | $1/\lambda$ | $\lambda$ | $A_\lambda/A_V$ |
|---|---|---|---|
| | $\mu^{-1}$ | $\mu$ | |
| | 0.5 | 2.00 | 0.11 |
| | 1.0 | 1.00 | 0.38 |
| $I$ | 1.11 | 0.90 | 0.46 |
| | 1.5 | 0.67 | 0.74 |
| $V$ | 1.81 | 0.553 | 1.00 |
| | 2.0 | 0.50 | 1.13 |
| $B$ | 2.28 | 0.44 | 1.32 |
| | 2.5 | 0.40 | 1.45 |
| $U$ | 2.74 | 0.365 | 1.58 |
| | 3.0 | 0.333 | 1.69 |
| | 5.0 | 0.200 | 2.8 |
| | 10.0 | 0.100 | 4.2 |

wavelength[3] of 553 $nm$. Normalized extinctions at the $I$ band need to be interpolated from the data in Table 2.2, while those at the $V$-band can be read directly from the table. Interpolation yields a normalized value for $A_{790nm}$ of 0.631 magnitudes of extinction per magnitude of extinction at $V$. For $A_{470nm}$ (the absorption associated with images on the IIIa-J plate: effective wavelength 470 $nm$) a normalized value of 1.225 magnitudes of extinction per magnitude of extinction at $V$. Every value of $A_V$ calculated from the Feitzinger & Stuwe maps is therefore multiplied by 0.631 to bring it to the equivalent amount of extinction at $\lambda_{\rm I} = 790\,nm$, or by 1.225 to give the equivalent extinction at $\lambda_{\rm J} = 470\,nm$, with an error expected to be less than 10%. The average $I$-band extinctions for the areal bins into which the survey region has been split are represented in Tables 2.3, 2.4, 2.5 and 2.6, below. $A_B$ is calculated as 1.32 magnitudes per magnitude of extinction at $V$.

[3]The 790 $nm$ effective wavelength is the convolution of filter transmission, the transmission of the Earth's atmosphere, the transmission of the telescope optics and the colour sensitivity of the emulsion for a solar-type source. The sensitivity of the photographic plates may vary by a few percent from plate to plate.

Table 2.3: Mean $I$-band extinctions (magnitudes) in adjacent $(\mathbf{b} \times \mathbf{l}) = (3^\circ \times 5^\circ)$ & $(4^\circ \times 5^\circ)$ regions in the Milky Way.
Northern latitudes are at the right.

| l\b | $-15^\circ - -12^\circ$ | $-12^\circ - -8^\circ$ | $-8^\circ - -4^\circ$ | $4^\circ - 8^\circ$ | $8^\circ - 12^\circ$ | $12^\circ - 15^\circ$ |
|---|---|---|---|---|---|---|
| 357.5 | 0.316 | 0.333 | 0.440 | 0.658 | 0.412 | 0.611 |
| 352.5 | 0.316 | 0.316 | 0.462 | 0.397 | 0.316 | 0.326 |
| 347.5 | 0.316 | 0.415 | 0.419 | 0.549 | 0.316 | 0.379 |
| 342.5 | 0.316 | 0.316 | 0.470 | 0.923 | 0.838 | 0.316 |
| 337.5 | 0.316 | 0.316 | 0.349 | 1.295 | 0.867 | 0.421 |
| 332.5 | 0.316 | 0.316 | 0.343 | 0.840 | 0.426 | 0.316 |
| 327.5 | 0.316 | 0.316 | 0.323 | 0.423 | 0.316 | 0.316 |
| 322.5 | 0.316 | 0.316 | 0.404 | 0.368 | 0.328 | 0.316 |
| 317.5 | 0.333 | 0.316 | 0.584 | 0.491 | 0.316 | 0.316 |
| 312.5 | 0.324 | 0.329 | 0.459 | 0.473 | 0.316 | 0.316 |
| 307.5 | 0.316 | 0.380 | 0.446 | 0.558 | 0.316 | 0.316 |
| 302.5 | 0.655 | 0.552 | 0.456 | 0.361 | 0.407 | 0.316 |
| 297.5 | 0.604 | 0.379 | 0.513 | 0.378 | 0.316 | 0.316 |
| 292.5 | 0.316 | 0.322 | 0.436 | 0.278 | 0.324 | 0.316 |
| 287.5 | 0.316 | 0.334 | 0.461 | 0.457 | 0.336 | 0.316 |
| 282.5 | 0.316 | 0.316 | 0.316 | 0.361 | 0.367 | 0.316 |
| 277.5 | 0.316 | 0.316 | 0.385 | 0.444 | 0.327 | 0.316 |
| 272.5 | 0.345 | 0.527 | 0.530 | 0.466 | 0.316 | 0.316 |
| 267.5 | 0.434 | 0.624 | 0.898 | 0.605 | 0.316 | 0.316 |
| 262.5 | 0.362 | 0.316 | 0.600 | 0.324 | 0.316 | 0.316 |
| 257.5 | 0.422 | 0.430 | 0.403 | 0.316 | 0.340 | 0.316 |
| 252.5 | 0.316 | 0.416 | 0.550 | 0.316 | 0.316 | 0.316 |
| 247.5 | 0.316 | 0.316 | 0.570 | 0.316 | 0.316 | 0.316 |
| 242.5 | 0.316 | 0.316 | 0.324 | 0.316 | 0.316 | 0.316 |
| 237.5 | 0.316 | 0.316 | 0.504 | 0.316 | 0.316 | 0.316 |
| 232.5 | 0.316 | 0.316 | 0.316 | 0.316 | 0.316 | 0.316 |
| 227.5 | 0.316 | 0.316 | 0.316 | 0.316 | 0.316 | 0.316 |
| 222.5 | 0.316 | 0.316 | 0.316 | 0.316 | 0.316 | 0.316 |
| 217.5 | 0.316 | 0.318 | 0.316 | 0.316 | 0.316 | 0.316 |
| 212.5 | 0.326 | 0.317 | 0.316 | 0.316 | 0.316 | 0.316 |

Figure 2.1: Situation of bins between $l = 235°$ and $l = 360°$ near the Galactic equator.

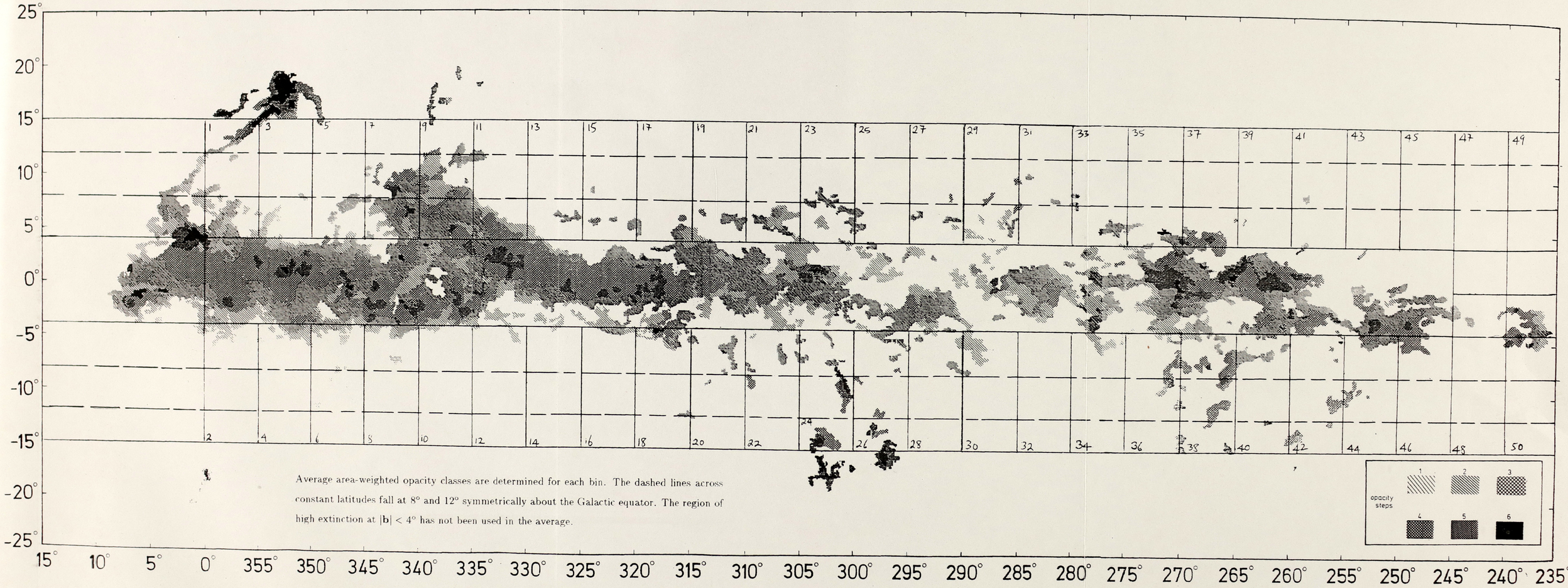


Average area-weighted opacity classes are determined for each bin. The dashed lines across constant latitudes fall at 8° and 12° symmetrically about the Galactic equator. The region of high extinction at $|b| < 4°$ has not been used in the average.

The distribution of dark clouds
(area > 0.01 sqdeg) in galactic coordinates.

Table 2.4: Mean $I$-band extinctions (magnitudes) in $(\mathbf{b} \times \mathbf{l}) = (11^\circ \times 5^\circ)$ strips in the Milky Way.
Bins in Table 2.3 have been combined along lines of constant longitude.

| l | $-4^\circ > \mathrm{b} > -15^\circ$ | $4^\circ < \mathrm{b} < 15^\circ$ | Mean for $4^\circ < \lvert\mathrm{b}\rvert < 15^\circ$ | Galaxies at $4^\circ < \lvert\mathrm{b}\rvert < 15^\circ$ |
|---|---|---|---|---|
| 357.5 | 0.356 | 0.571 | 0.465 | 6 |
| 352.5 | 0.366 | 0.347 | 0.358 | 3 |
| 347.5 | 0.372 | 0.684 | 0.529 | 8 |
| 342.5 | 0.375 | 0.765 | 0.569 | 4 |
| 337.5 | 0.327 | 1.019 | 0.674 | 10 |
| 332.5 | 0.328 | 0.614 | 0.472 | 20 |
| 327.5 | 0.318 | 0.354 | 0.337 | 27 |
| 322.5 | 0.348 | 0.329 | 0.339 | 21 |
| 317.5 | 0.443 | 0.379 | 0.411 | 17 |
| 312.5 | 0.381 | 0.373 | 0.378 | 33 |
| 307.5 | 0.399 | 0.404 | 0.400 | 16 |
| 302.5 | 0.599 | 0.393 | 0.495 | 9 |
| 297.5 | 0.492 | 0.339 | 0.416 | 8 |
| 292.5 | 0.365 | 0.358 | 0.364 | 24 |
| 287.5 | 0.368 | 0.379 | 0.374 | 22 |
| 282.5 | 0.316 | 0.348 | 0.333 | 40 |
| 277.5 | 0.388 | 0.378 | 0.383 | 32 |
| 272.5 | 0.479 | 0.368 | 0.424 | 23 |
| 267.5 | 0.661 | 0.424 | 0.543 | 5 |
| 262.5 | 0.434 | 0.322 | 0.379 | 11 |
| 257.5 | 0.435 | 0.324 | 0.380 | 6 |
| 252.5 | 0.441 | 0.316 | 0.379 | 9 |
| 247.5 | 0.407 | 0.316 | 0.362 | 17 |
| 242.5 | 0.332 | 0.332 | 0.332 | 24 |
| 237.5 | 0.413 | 0.413 | 0.413 | 18 |
| 232.5 | 0.316 | 0.316 | 0.316 | 6 |
| 227.5 | 0.316 | 0.316 | 0.316 | 4 |
| 222.5 | 0.320 | 0.316 | 0.317 | 4 |
| 217.5 | 0.316 | 0.316 | 0.316 | 4 |
| 212.5 | 0.318 | 0.316 | 0.317 | 2 |
| | | | Mean=0.424 | Mean=14.43 |
| | | | $\sigma = 0.091$ | $\sigma = 10.30$ |

Table 2.5: Mean $I$-band extinctions in $(3^\circ \times 75^\circ)$ and $(4^\circ \times 75^\circ)$ strips for $|\mathbf{b}| < 15^\circ$. (Galaxy numbers at $cz < 6500\, km\, s^{-1}$ are also indicated.)

| **b/l** | $360^\circ > \mathbf{l} > 285^\circ$ | $285^\circ > \mathbf{l} > 210^\circ$ |
|---|---|---|
| $12^\circ - 15^\circ$ | Strip 1 : $0.347 \pm 0.080$ : 53 Gal. | Strip 7 : $0.316 \pm 0.000$ : 39 Gal. |
| $8^\circ - 12^\circ$ | Strip 2 : $0.410 \pm 0.184$ : 49 Gal. | Strip 8 : $0.322 \pm 0.014$ : 48 Gal. |
| $4^\circ - 8^\circ$ | Strip 3 : $0.564 \pm 0.270$ : 27 Gal. | Strip 9 : $0.358 \pm 0.083$ : 33 Gal. |
| $-4^\circ - -8^\circ$ | Strip 4 : $0.437 \pm 0.065$ : 25 Gal. | Strip 10 : $0.444 \pm 0.166$ : 30 Gal. |
| $-8^\circ - -12^\circ$ | Strip 5 : $0.348 \pm 0.064$ : 38 Gal. | Strip 11 : $0.365 \pm 0.095$ : 31 Gal. |
| $-12^\circ - -15^\circ$ | Strip 6 : $0.359 \pm 0.110$ : 34 Gal. | Strip 12 : $0.336 \pm 0.039$ : 25 Gal. |

Table 2.6: Mean $I$-band extinctions & total galaxy counts for $(3^\circ \times 150^\circ)$ and $(4^\circ \times 150^\circ)$ strips in Table 2.5.

| **b** | Mean Extinction at $I$ (mags.) | Strips Combined | Total Galaxies |
|---|---|---|---|
| $12^\circ - 15^\circ$ | 0.331 | 1 & 7 | 92 |
| $8^\circ - 12^\circ$ | 0.366 | 2 & 8 | 97 |
| $4^\circ - 8^\circ$ | 0.461 | 3 & 9 | 60 |
| $-4^\circ - -8^\circ$ | 0.441 | 4 & 10 | 55 |
| $-8^\circ - -12^\circ$ | 0.358 | 5 & 11 | 69 |
| $-12^\circ - -15^\circ$ | 0.348 | 6 & 12 | 59 |
| | Mean Overall Extinction ($A_I$) is $0.383 \pm 0.070$ $(1\,\sigma)$ or $0.383 \pm 18.4\%$ | | Mean Number of Galaxies per Combined Strips is $432/6 = 72.0 \pm 18.1$ $(1\,\sigma)$ or $72.0 \pm 25.1\%$ |

## 2.2 Summary of Extinction Effects

The smallest *IRAS* galaxy number density for $15^{o} > |\mathbf{b}| > 5^{o}$, in the $f_{60} > 0.6\,Jy$ sample, is less than half of the all-sky average. To account for this singly in terms of variations in *HI* column densities[4], the necessary increase in the column density in these least populated regions must be greater by at least $4 \times 10^{21}\,cm^{-2}$ than for adjacent regions (see analysis of Saito *et al.*, 1990, 1991; Yamada & Saito, 1993). However, Bloemen (1983) did not find evidence for this kind of variation in column densities.

More importantly, if molecular clouds are indeed the main cause for low galaxy counts in certain regions, then one would expect to find low galaxy counts in association with a prevalence of objects normally associated with molecular clouds in the same areas. This is *not* observed anywhere, however, so the evidence indicates that diminished counts are most likely to be intrinsic to the galaxy distributions.

Nevertheless, it can be verified from plots of mean extinction ($A_I$) versus galaxy counts in areal bins that a *weak* correlation seems evident in regions where average extinctions are lower than 0.4 magnitudes. That is, the numbers of optically identified galaxies are, *in general*, enhanced in the bins where lowest extinction appears (or, to put it conversely, are generally diminished in all bins with extinctions greater than 0.4 magnitudes). This correlation is not universally seen, however, as several regions show *both* extinction and counts as simultaneously high or low.

The overall impression from these plots (not included here) is that while galactic extinction *does* affect the *number* of galaxies identified in many of the bins so as to reduce the counts, the overall galaxy *distribution* is, at best, only mildly modified by galactic extinction.

---

[4]Dust and *HI* gas tend to be found together inside molecular clouds, and the dust column density within molecular clouds can be linked broadly to that of the *HI* gas, although the gas-to-dust ratio in the Galaxy can be quite variable at smaller scales (cf. Burstein & Heiles, 1982). The size of the areal bins allows small-scale discrepancies in the gas-to-dust ratio to be evened out. The link between dust and *HI* gas column densities was also the original basis for converting *HI* column densities into effective opacities (and, hence, for designating opacity classes).

# Chapter 3

# Measuring Redshifts

## 3.1 Acquisition of Spectra

Spectra were obtained by Visvanathan & Yamada for 176 of Yamada's 966 galaxies, using the double beam spectrograph (DBS) on the 2.3-metre telescope at Siding Springs Observatory, during three runs in 1993. These were reduced by the author.

For the run of 17 February a 300 line/mm diffraction grating was used, covering a spectral region from $\sim 6400 - 7400\mathring{A}$. For the observing runs of 19-22 April and 26-29 May a 600 line/mm grating was used, covering a spectral region from $\sim 6400 - 6900\mathring{A}$. Only red spectra were used in the analysis. The DBS arrangement simultaneously acquires blue and red spectra using a CCD detector. The dispersion direction is perpendicular to the long slit aperture. For present purposes, only the section containing the $H_\alpha/[NII]$ triplet redshifted from 6563, 6716 and $6731\mathring{A}$ and the $[SII]$ doublet redshifted from 6548 and $6583\mathring{A}$ was reduced. For the best spectra, heliocentric redshifts could be determined to a precision of $\sim 20 - 40\, km\, s^{-1}$.

Astronomical seeing ranged between one and two arcseconds on all nights and a two-arcsecond slit was consistently used, oriented along the long axis of the object, whenever this could be discerned. Typical exposure times were 200-500 seconds, but some faint sources were exposed for 1000 seconds. Reference arcs, and flat fields and dark fields in both filters, were all acquired at the beginning and end of each night.

All spectra were referenced against both Cu-Ar and Ne arc spectra. These in turn were calibrated using the *IRAF* routines **ident**, **reident**, **fitcoords** and **transform**, all being **longslit** routines found inside the **twodspec** package. The residuals in the eleven arc-reference calibrations were at worst about $0.05\mathring{A}$. The estimated mechanical and thermal spectrograph stability of 0.5 pixels over a night represents a redshift uncertainty of $\sim 20\,km\,s^{-1}$ for the 600 line/mm grating arrangement or $\sim 35\,km\,s^{-1}$ for 300 line/mm.

Once the calibration was completed, reduction of the 176 spectra commenced, again using routines from the **longslit** package. The spectra were cut (using **imcopy**), transformed (using **transform**), background-subtracted (**background**) and combined into single-row spectra (using **scombine**).

The final spectra were analyzed for redshifts using the **rv** package. Within this package the **fxcor** routine searched for cross-correlations between a 5-line (the $H_\alpha/[NII]$ triplet and the $[SII]$ doublet) template and the spectral emission lines, and returned a radial velocity measurement. Cross-correlation peaks were not always sharp and so the error in that procedure returned an uncertainty of $10-30\,km\,s^{-1}$, occasionally exceeding $50\,km\,s^{-1}$ for under-exposed spectra. From a total of 176 spectra, definite redshifts were extracted for 136 (77%), while 40 spectra were under-exposed.

The adopted spectral cut restricted redshifts to a range of $16500\,km\,s^{-1}$ ($z = 0.055$) if using all five template lines or, if using only the $H_\alpha(\lambda 6562.82\mathring{A})/[NII](\lambda\lambda 6548, 6583\mathring{A})$ triplet, to a range of $\sim 22000\,km\,s^{-1}$ ($z \approx 0.07$). Redshifts were calculated using the formulae $z = (\lambda - \lambda_o)/\lambda_o$ and $v = cz$. Measured redshifts were reduced to the heliocentric system by the standard reduction of the Earth's motion. No correction has, however, been applied to account for the motion of the Sun relative to the centroid of the Local Group.

## 3.2 Tabulation of Data

Appendix 9.3 includes Yamada's 966 identified *IRAS* galaxies within the boundaries defined by $\mathrm{l} = 210° - 360°$ and $|\mathrm{b}| < 15°$. These were originally listed in Yamada *et al.* (1993*b*) and in the current work 136 new redshifts have been obtained. Several supplementary redshifts have also been derived from various sources, including Fisher *et al.*, (1995)and Will Saunders (May and November, 1993: private communication), and some updates by Yamada. In cases where several authors have provided redshifts for a source for which no redshift was obtained at Siding Springs, an average of those values has been adopted. Redshifts are presented for 754 of Yamada's 966 galaxies[1]. The list in Appendix 9.3 contains 103 galaxies besides those of Yamada, obtained from various catalogues and other recent work[2]. The redshift acquisition rate from all researchers working on Yamada's data is currently $\sim 78\%$. The success rate for the data obtained at Siding Springs Observatory is coincidentally also $\sim 77\%$.

The table in Appendix 9.3 is laid out as follows: column 1 lists the *IRAS* Point Source Catalogue names of each of the galaxies, columns 2 and 3 list the Galactic longitudes and latitudes corresponding to the stated *IRAS* positions, columns 4 and 5 give the *IRAS* Point Source Catalogue 60- and 100-micron flux densities, column 6 confirms source identity, column 7 gives the morphological type (e.g. S = spiral, E = elliptical) of identified galaxies, column 8 states whether sources are multiple (P=pair), columns 9 and 10 list respectively the estimated B-plate major diameters (in mm) and $B$ magnitudes of the galaxies and column 11 lists estimated extinction in magnitudes at the $B$ band. Columns 12 - 14 provide the redshifts, their uncertainties, and their sources. An asterisk in column 14 indicates a redshift that was obtained from a private version (Huchra, 1993) of the redshift catalogue ("zcat") without carrying over the original reference from that source. Finally, columns 15 - 17 contain cross-identifications, where they exist, of the listed galaxies. The first two galaxies listed in the table, falling just outside the $\mathrm{l} > 210°$ survey limit, have not been included in any of the analysis or discussion.

---

[1]Note that the 150 multiple sources go as single listings, with the listed redshifts being those of the brightest galaxy in each case.

[2]This excludes data collected by Visvanathan and others since the analysis stage of this thesis.

# Chapter 4

# Sample Completeness

It is difficult to provide a confident estimate of the completeness of the sample of *IRAS* galaxies behind the Milky Way, especially without reference to an existing standard. No such standard exists for galaxies situated in the zone of avoidance, but it should not be unreasonable to assume that galaxy number densities behind the Milky Way should emulate, or may even slightly exceed[1], those measured at Galactic latitudes higher than $|\mathbf{b}| = 15^{\circ}$.

To compare galaxy number densities at low latitudes (for galaxies discovered after applying Yamada's criteria) with the all-sky *IRAS* galaxy number density determined by Rowan-Robinson *et al.* (1991), using their criteria[2] for sources contained at absolute latitudes higher than 5°, it will be assumed that the density of galaxies behind the Milky Way should be similar to the Rowan-Robinson all-sky average measured substantially at higher latitudes. Completeness in this survey is therefore stated in comparison with the estimate of completeness in that survey.

---

[1] Given that the deviation of the infall of the Local Group (LG) of galaxies from a direct motion towards the centre of the Virgo cluster has led to the suggestion that a concentration of galaxies may exist at low latitudes in the direction of the "Great Attractor", at something above the all-sky average.

[2] Their study uses data for 31% of the sky at $|\mathrm{b}| < 5^{\circ}$ and 82% of the sky overall. It excludes about 3% of the sky which did not achieve two hours of confirmed *IRAS* coverage, as well as areas labelled as having high source-density in any of the four bands. Their one-in-six sample is considered to be 99% complete for *IRAS* galaxies having $f_{60} > 0.6\,Jy$, out to a cosmological redshift distance of $\sim 5000\,km\,s^{-1}$.

Since extinction increases according to a cosec($|\mathbf{b}|$) law as one approaches the Galactic equator perpendicularly, along a line of constant longitude, it is obviously more sensible to estimate the sample completeness within strips of constant Galactic latitude (where levels of Galactic extinction should remain approximately constant). The survey region has accordingly been divided into three strips, with counts taken in the areas demarcated by latitudes $15^{\circ} > \mathbf{b} > 4^{\circ}$, $4^{\circ} > \mathbf{b} > -4^{\circ}$ and $-4^{\circ} > \mathbf{b} > -15^{\circ}$. The areal coverage represented by these three strips is 1650 $sq.^{\circ}$, 1200 $sq.^{\circ}$ and 1650 $sq.^{\circ}$, respectively.

The *IRAS* galaxy number densities per square degree in these strips are found to be $487/1650 = 0.30$ galaxies per square degree, $107/1200 = 0.09$ galaxies per square degree and $372/1650 = 0.23$ galaxies per square degree respectively, resulting in completenesses of 70.3%, 21.4% and 53.7% in the respective regions[3], with an overall average density of 0.21 galaxies per square degree over all Milky Way latitudes, with no redshift ceiling imposed. The low figure for $4^{\circ} > \mathbf{b} > -4^{\circ}$ derives from low numbers of definite candidates and depleted counts in the source-confused regions adjacent to the Galactic equator. Omitting the $4^{\circ} > \mathbf{b} > -4^{\circ}$ region returns an average density of $\sim 0.27$ galaxies per square degree, which is about 63% of the Rowan-Robinson *et al.* (1991) all-sky $f_{60} > 0.6\,Jy$ *IRAS* average galaxy density of 0.42.

In the zone $\mathbf{l} = 230^{\circ} - 260^{\circ}$, where *CO* observations by May *et al.* (1988) indicate far lower obscuration by molecular clouds, the average number density of galaxies is found to be only 0.29 per square degree, which again approaches $\sim 70\%$ of the Rowan-Robinson *et al.* (1991) average number density for the whole sky. Of course, this 30° section may straddle a void, in which case the comparison would not be very useful.

When Yamada *et al.* (1993*a*) obtained their average completeness levels relative to Rowan-Robinson *et al.* (1991) they did so after having excluded the regions $210^{\circ} < \mathbf{l} < 230^{\circ}$ (for

[3] Accounting for a total of 966 *IRAS* galaxy candidates. These completeness estimates also count those *IRAS* sources for which redshifts have not yet been successfully obtained, judging these to be galaxies from the colour and flux selection criteria, other galaxy catalogues and Schmidt plate searches. The 966 *IRAS* galaxies identified by Yamada *et al.* are supplemented in the data table by a further 101 optically identified galaxies listed with redshifts, mainly obtained from Huchra (1993). A few other previously uncatalogued galaxies with redshifts have also been obtained from private sources.

lack of any U.K. Schmidt Atlas plates for $\mathbf{b} \geq 12^{\circ}$ in this region) and $350^{\circ} - 360^{\circ}$ (because of the extreme incompleteness predicted near the Galactic Centre in this longitude range) from their calculations. If these same exclusions are adopted here, the average number densities obtained for optical identifications for the zones used by Yamada *et al.* (1993*a*) - namely, $5^{\circ} < \mathbf{b} < 15^{\circ}$, $-5^{\circ} < \mathbf{b} < 5^{\circ}$ and $-15^{\circ} < \mathbf{b} < -5^{\circ}$ (for $350^{\circ} > \mathbf{l} > 230^{\circ}$) - are 0.36, 0.10 and 0.25 *IRAS* galaxies per square degree, respectively. Comparison with the 0.42 *IRAS* galaxies per square degree of Rowan-Robinson *et al.* (1991) then returns nominal *optical detection* rates of 86%, 23% and 60% in these 10°-wide strips. The fact that the rate is consistently higher for northern latitudes stems from the higher average *HI* column densities at the southern latitudes ($-15^{\circ} < \mathbf{b} < -5^{\circ}$) compared to counterpart northern regions. This is evidently due to a warp in the *HI* disc towards negative latitudes in the southern outer Galaxy (Burton & te Lintel Hekkert, 1986).

The average overall completeness, therefore, taken as a measure of the optically detected galaxies at $15^{\circ} > |\mathbf{b}| > 4^{\circ}$ and compared to *IRAS* galaxies identified as galaxies by Rowan-Robinson *et al.* (1990) at $|\mathbf{b}| > 5^{\circ}$, appears to be $\sim 70\%$. If Yamada's selection criteria are efficient, one should expect to approach the Rowan-Robinson *et al.* (1991) all-sky average number densities in galaxy counts, as dust obscuration should not significantly affect $f_{60}$ detections. However, one might not expect the same completeness if comparing *optically* identified galaxies within the Milky Way to those counted outside $|\mathbf{b}| \geq 10^{\circ}$.

Despite the low detection rate of *IRAS* galaxies in the current search, the *IRAS* galaxy densities exceed the all-sky average of Rowan-Robinson *et al.* (1991) in three longitude regions in both hemispheres; number density peaks occur in narrow regions near $\mathbf{l} = 245^{\circ}, 280^{\circ}$ and $310^{\circ}$ for $5^{\circ} < \mathbf{b} < 15^{\circ}$, and near $\mathbf{l} = 240^{\circ}, 280^{\circ}$ and $330^{\circ}$ for $-15^{\circ} < \mathbf{b} < -5^{\circ}$, indicating the possible presence of three long structures which cross the Milky Way at an angle. These regions of enhanced density, with widths of order 10°, appear to be located as the extensions of three[4] filamentary structures in the ESO galaxy distribution (ESO Catalogue, 1982) around the Milky Way region (see Figures 1 and 4 of Yamada *et al.*, 1993*a*).

---

[4] Or, indeed, *six* such structures, according to the recent claims of Takata *et al.*, 1996.

Table 4.1: Galaxy number densities (optically identified *IRAS* galaxies per square degree) & estimated sample completenesses in $(\mathbf{b} \times \mathbf{l}) = (3^\circ \times 75^\circ)$ and $(4^\circ \times 75^\circ)$ constant-latitude strips in the Milky Way, restricted to $4^\circ < |\mathbf{b}| < 15^\circ$.

The table includes only galaxies with known redshifts but without an upper-limit on redshift. There are 42 galaxies in the excluded zone. Completeness is estimated with respect to the Rowan-Robinson *et al.* (1991) all-sky number density of 0.42 galaxies per square degree.

| b | $360^\circ > \mathbf{l} > 285^\circ$ | $285^\circ > \mathbf{l} > 210^\circ$ |
|---|---|---|
| $12^\circ - 15^\circ$ | 53 Galaxies: 0.231: 56.1% | 77 Galaxies: 0.342: 81.5% |
| $8^\circ - 12^\circ$ | 77 Galaxies: 0.257: 61.1% | 86 Galaxies: 0.287: 68.3% |
| $4^\circ - 8^\circ$ | 50 Galaxies: 0.167: 39.7% | 40 Galaxies: 0.133: 31.7% |
| $-4^\circ - -8^\circ$ | 47 Galaxies: 0.157: 37.3% | 39 Galaxies: 0.130: 31.0% |
| $-8^\circ - -12^\circ$ | 64 Galaxies: 0.213: 50.8% | 67 Galaxies: 0.223: 53.1% |
| $-12^\circ - -15^\circ$ | 51 Galaxies: 0.227: 54.0% | 52 Galaxies: 0.231: 55.0% |

Whether the densities presented here ($|\mathbf{b}| > 4^\circ$) or in Yamada *et al.* (1993*a*) ($|\mathbf{b}| > 5^\circ$), (the number densities of optically identified galaxies can, even in areas obscured by Galactic dust, still exceed the Rowan-Robinson *et al.* (1991) all-sky average,) produce some initial confidence that the over-dense regions observed are real or not, one could say certainly that the background galaxy distribution is far from uniform. Since over-densities are typically no more than $\sim 25\%$ above mean densities, and this is emulated in the current sample, there is a further basis for confidence that the "candidates" contained in this sample constitute in the order of 90% of all actual *IRAS* galaxies. It also follows that, for latitudes $|\mathbf{b}| > 4^\circ$, and out to a redshift distance of $cz \approx 6500\, km\, s^{-1}$, the optical identification must have been successful for between 60% and 85% of these. The loss of completeness seen in the redshift-identified galaxies could be mainly due to the scattering and absorbing effects of Galactic gas and dust, rather than to the selection criteria.

Table 4.2: *IRAS* galaxy number densities & estimated sample completenesses in all-longitude (i.e. $360° > \mathrm{l} > 210°$) constant-latitude strips in the Milky Way, for $4° < |\mathrm{b}| < 15°$.

| b | Number of galaxies: Density: Completeness |
|---|---|
| $12° - 15°$ | 130 : 0.289 : 68.8% |
| $8° - 12°$ | 163 : 0.272 : 64.7% |
| $4° - 8°$ | 90 : 0.150 : 35.7% |
| $-4° - -8°$ | 86 : 0.143 : 34.1% |
| $-8° - -12°$ | 131 : 0.218 : 52.0% |
| $-12° - -15°$ | 103 : 0.229 : 54.5% |

As the *IRAS* sample evidently contains quite a high completeness for *IRAS* galaxies, it follows that the structures traced in the (l, b)-plane by the *IRAS* population (with or without available redshifts) should be quite indicative of the real projected structures which propagate behind the Milky Way.

# Chapter 5

# Distribution of the IRAS Galaxies

## 5.1 Distribution of *IRAS* Galaxies on the Sky and in Redshift Space

The distribution of 745 *IRAS* galaxies for which redshifts are available are plotted in Figures 5.1 and 5.2, the latter plot truncating the data to $cz < 6500\,km\,s^{-1}$. These plots merely give the projection on the sky of the *IRAS* sample. Figures 5.3 and 5.4 plot the locations of *IRAS* galaxies in the longitude-redshift and latitude-redshift planes, respectively.

A pie chart of the distribution follows in Figure 5.5. This is a polar plot with galactic latitudes suppressed. It shows how the *IRAS* galaxies are distributed in redshift space and longitudinally across the sky. This plot has the added utility of serving as an approximate means of identifying the completeness limit of the sample. To assist with this latter question, Figure 5.6 has also been plotted. Figure 5.6 shows that there seems to be a general underdensity centred at $cz \sim 4000\,km\,s^{-1}$. The pie chart and figure also combine to suggest that sample completeness has diminished by $\sim 7000\,km\,s^{-1}$, with this incompleteness possibly setting in as early as $\sim 6500\,km\,s^{-1}$.

Figure 5.1: *IRAS* galaxies in the (l, b) plane: all redshifts.

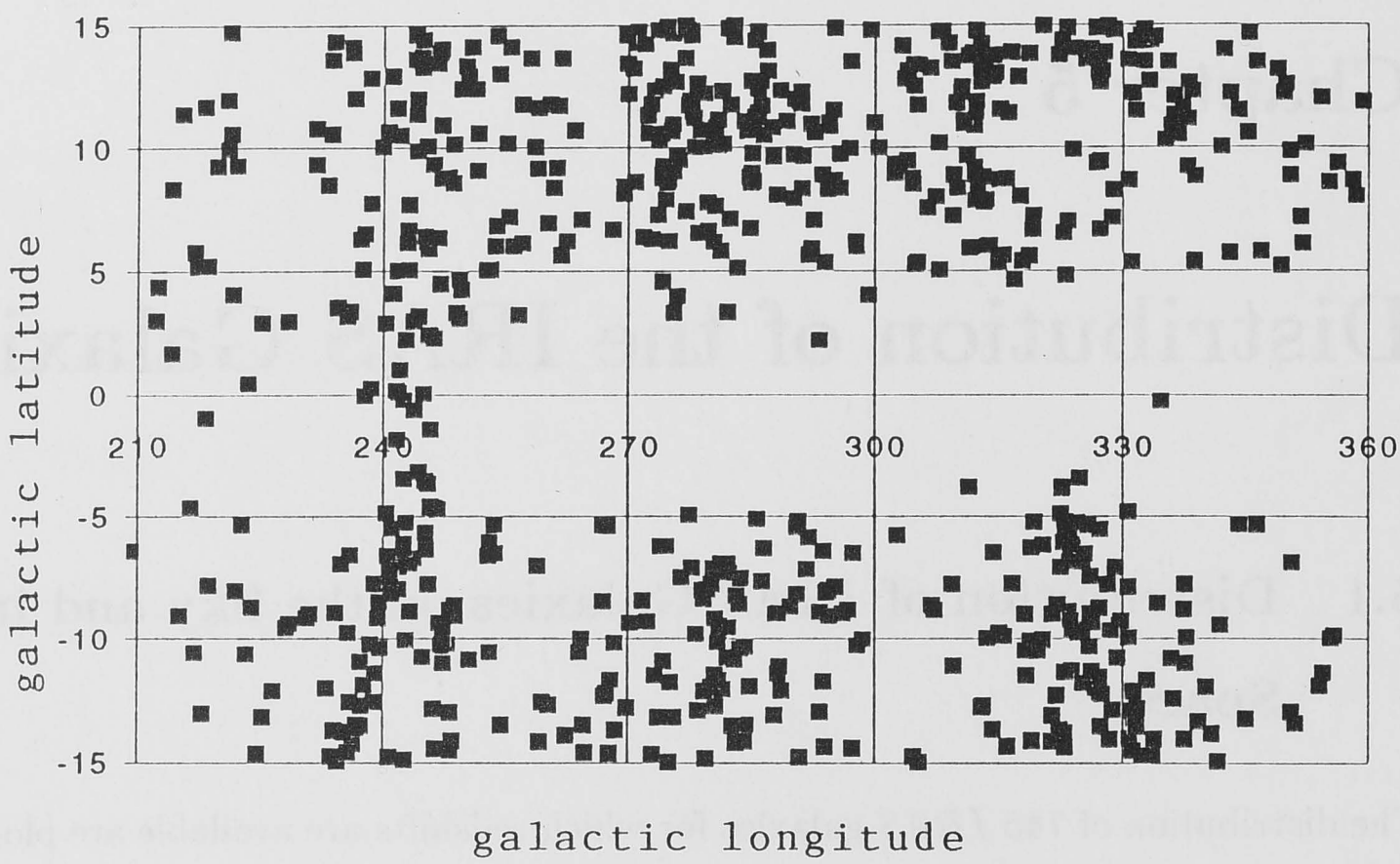


Figure 5.2: *IRAS* galaxies at $cz < 6500\,km\,s^{-1}$ in the (l, b) plane.

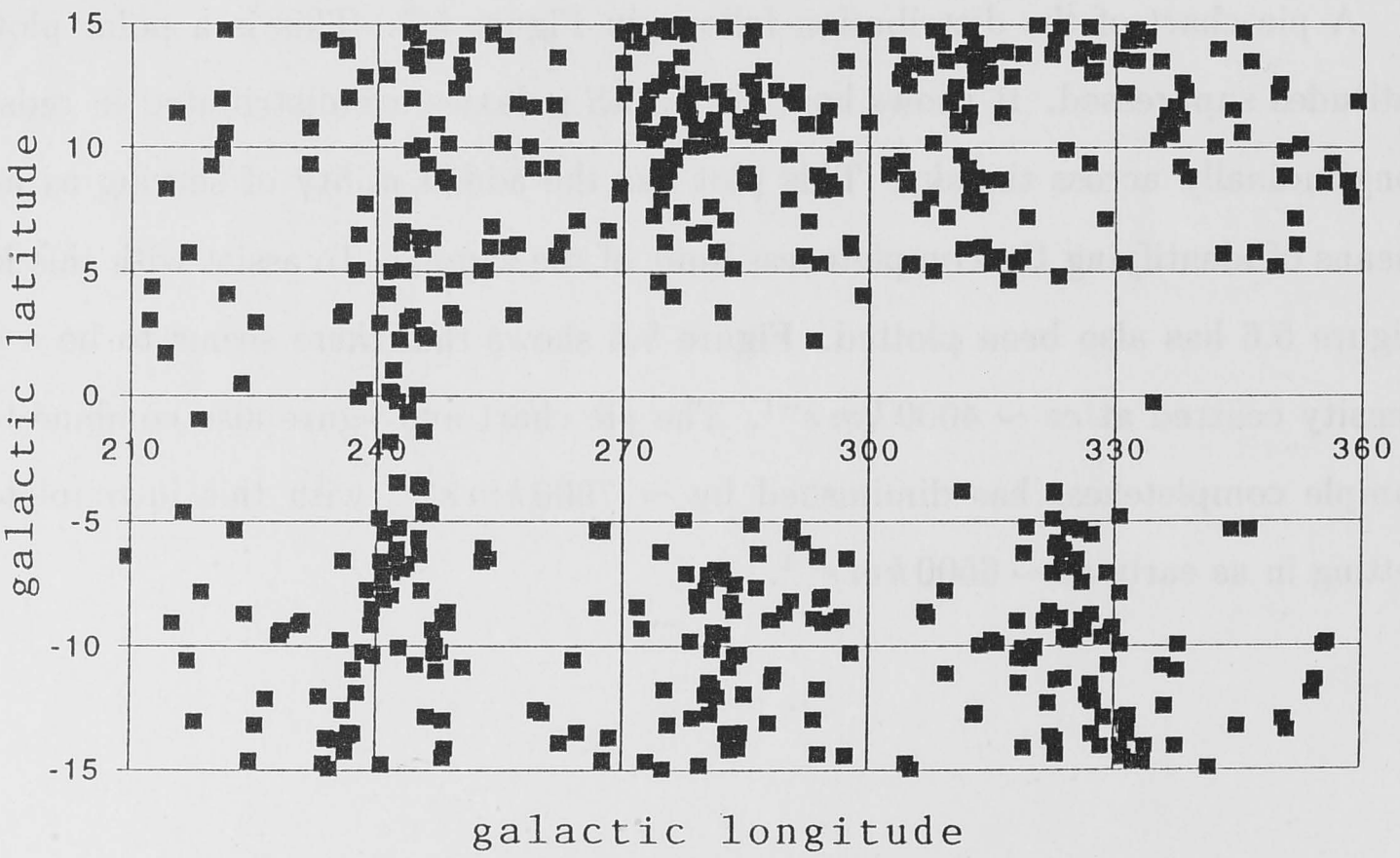

Figure 5.3: Locations of *IRAS* galaxies in the longitude-redshift plane.

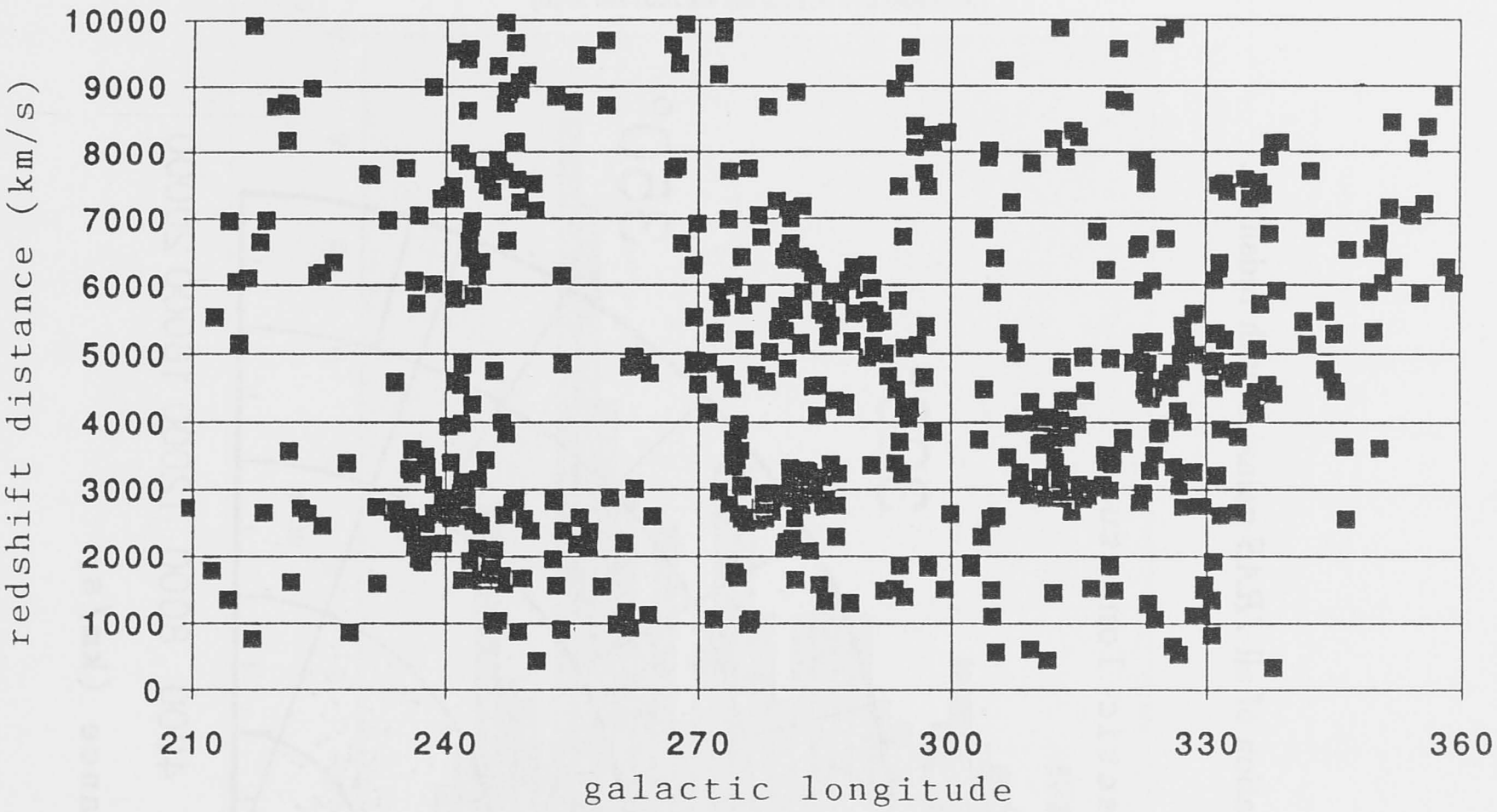


Figure 5.4: Locations of *IRAS* galaxies in the latitude-redshift plane.

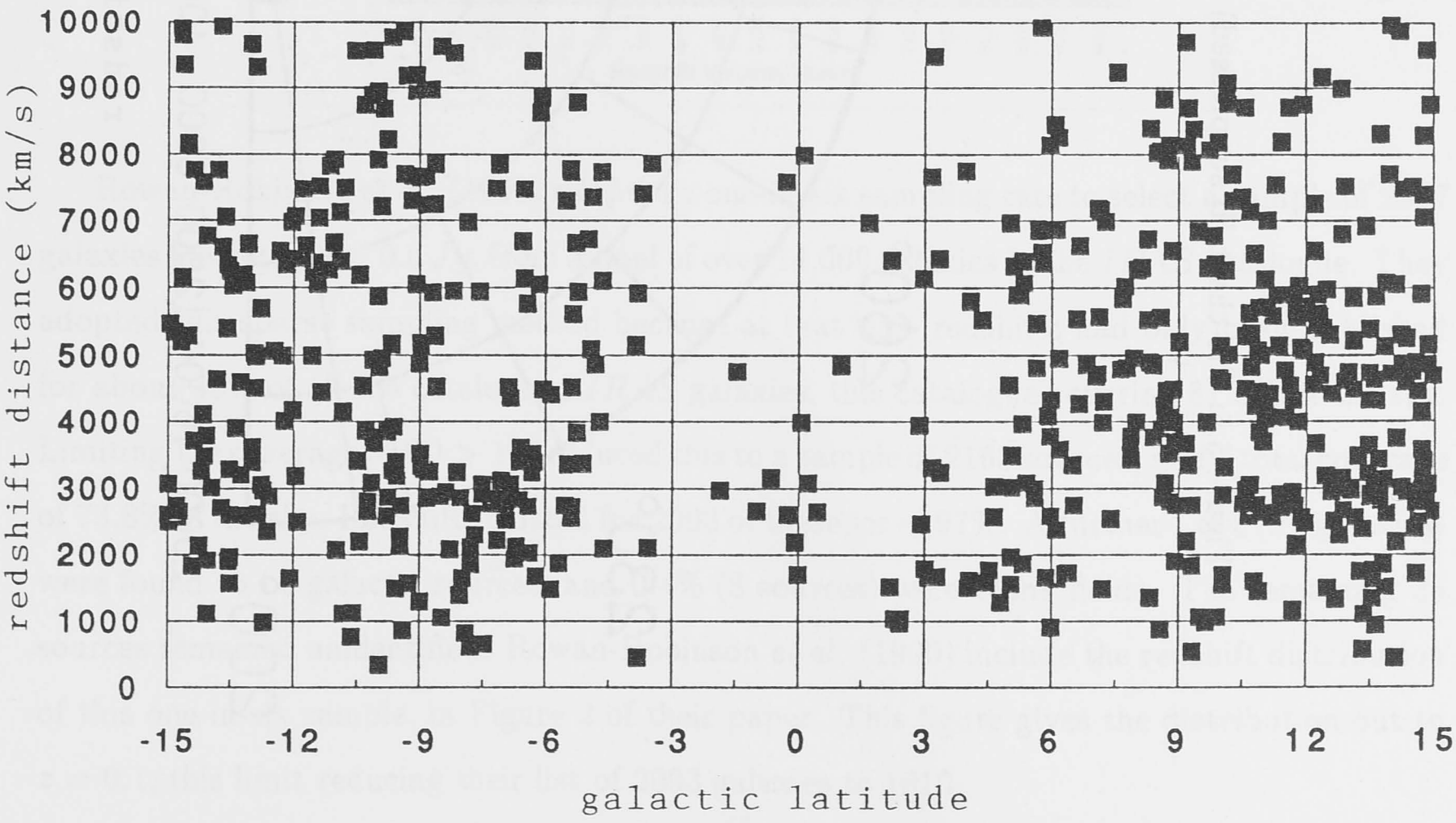

Figure 5.5: Pie-chart (**b** suppressed) showing location of all $IRAS$ galaxies with redshifts.

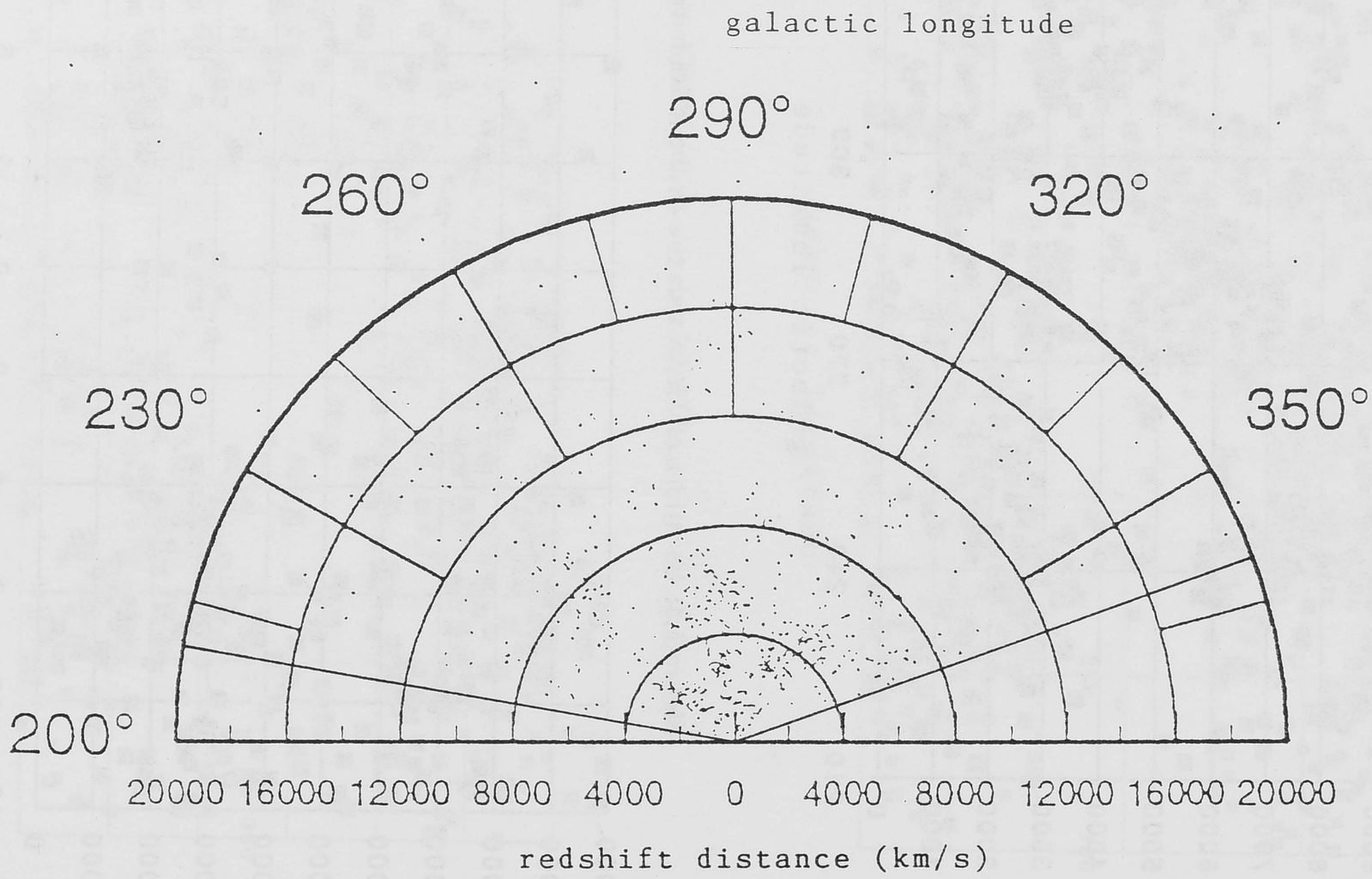

Figure 5.6: Variation of total galaxy counts with redshift.

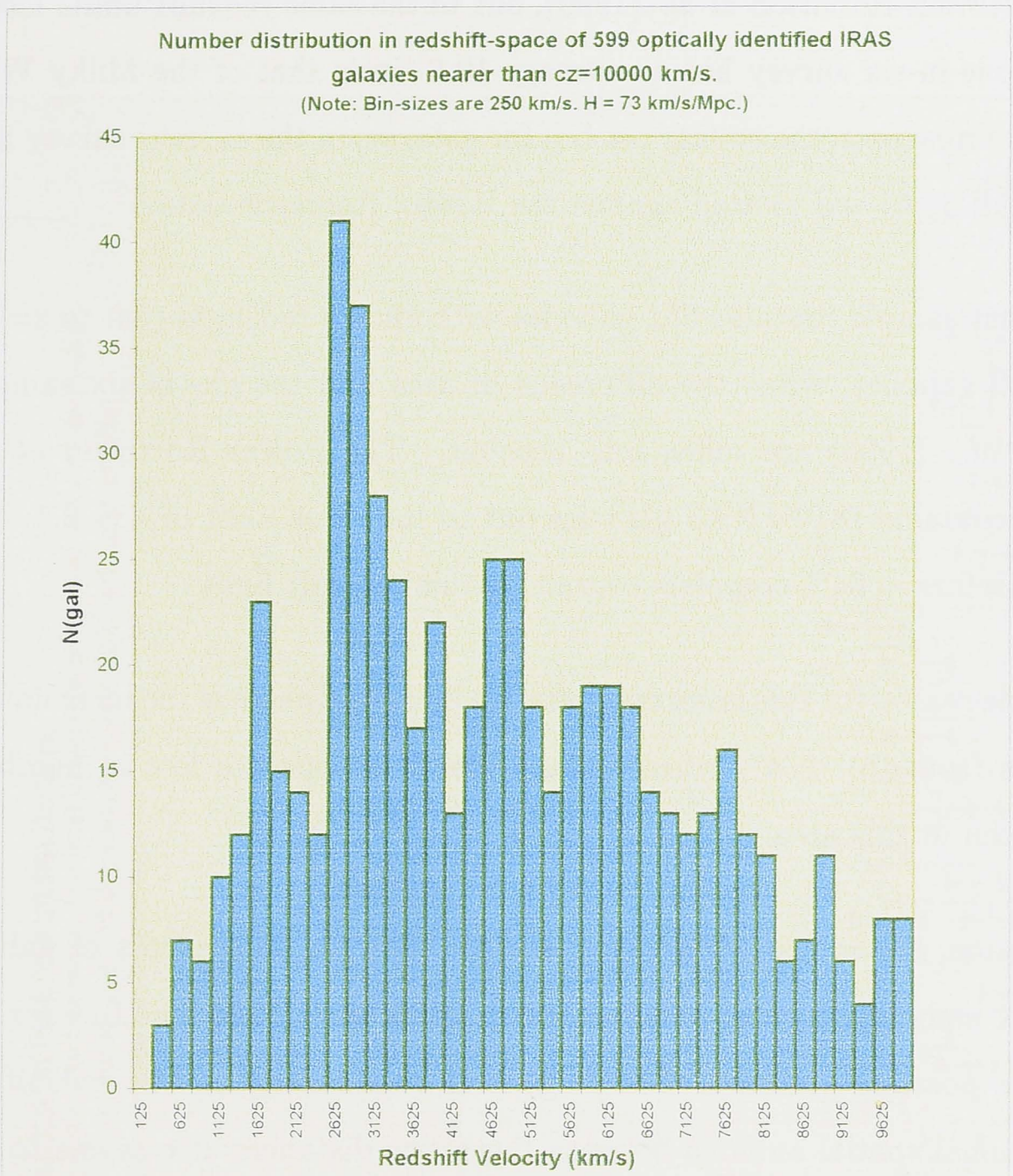


Rowan-Robinson *et al.* (1990) adopted a one-in-six sampling rate to select a sample of 2387 galaxies having $f_{60} > 0.6\,Jy$, from a pool of over 14,000 galaxies in the $IRAS$ catalogue. They adopted this sparse sampling method because at that time redshifts had only been published for about 30% of all the catalogued $IRAS$ galaxies, this catalogue covering 81.8% of the sky. Limiting the coverage to $|\mathrm{b}| > 10^{\circ}$ reduced this to a sample of 2163 sources, and a total coverage of 73.8% of the sky. Redshifts existed for 2093 of these, or $\sim 97\%$. A further 1.2% (27 galaxies) were found to be galactic sources, and 0.4% (8 sources) were blank fields. The remaining 35 sources remained unidentified. Rowan-Robinson *et al.* (1990) include the redshift distribution of this one-in-six sample, in Figure 2 of their paper. This figure gives the distribution out to $z = 0.1$, this limit reducing their list of 2093 galaxies to 1810.

Figure 5.7, on the next page, compares the redshift distribution seen in the current sample with that of Rowan-Robinson *et al.* (1990), out to the same redshift limit. Covering 73.8% of the sky, the one-in-six survey has a coverage 10.6 times that of the Milky Way sample. For purposes of comparison, the counts per bin for galaxies in the current survey have been scaled by 1.77 (i.e. 10.6 / 6) and plotted against the Rowan-Robinson data.

The current sample contains 651 galaxies with known redshifts (out to z=0.1), or a scaled count of 1152 galaxies, when the difference in area and the one-in-six sampling of Rowan-Robinson *et al.* (1990) are taken into account. The Rowan-Robinson *et al.* sample, by comparison, contains 1810 *IRAS* galaxies out to the same limit of $z = 0.1$. The Milky Way sample is therefore $\sim$ 64% complete overall, to this redshift limit.

A probable reason for this large comparative incompleteness is the inclusion into our survey of the counts from $|\mathbf{b}| < 4^{o}$, where galaxy identifications are low in number due to large extinctions seen in this area.

All the same, the scaled Milky Way sample shows a 50% excess of galaxies relative to the one-in-six sample between z=0.008 (cz = 2400 km/s) and z=0.014 (cz = 4200 km/s), indicating the possible presence of some general over-density at this redshift distance. The three-dimensional spatial annulus between these two distances also seems to be overdense in Figure 1.5. Immediately beyond this distance, between z=0.016 and z=0.020, the galaxy counts fall rapidly until they are relatively fewer than the 1-in-6 counts.

The current distribution, to a large extent, emulates that of Rowan-Robinson in its overall shape, out to the nominal completeness limit of z=0.22 ($cz \sim 6500\, km\, s^{-1}$), although counts in the current survey stand at between 50% and 90% of those in Rowan-Robinson *et al.*, 1990.

Perusal of Figure 5.7 shows clearly that at all redshifts greater than z=0.22 the Milky Way sample seldom has more than 50% of the completeness of the Rowan-Robinson *et al.* sample.

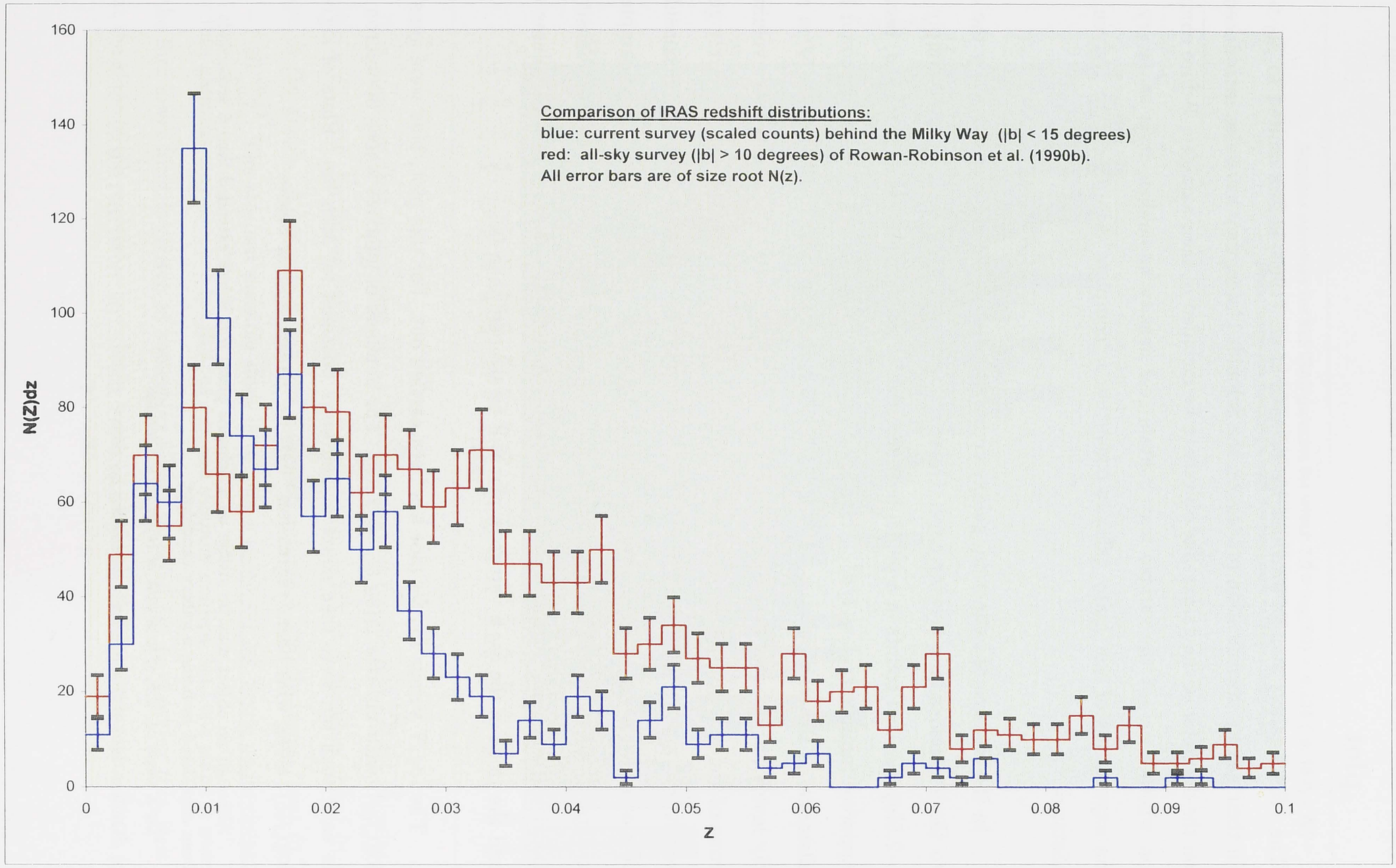


Figure 5.7: Comparison of redshift distributions as they appear in the one-in-six survey of Rowan-Robinson *et al.* (1990) and in the current survey.

## 5.2 Evidence for Density Fluctuations: The $LogN$ versus $Log\, f_{60}$ plot

The $IRAS$-galaxy sample provided by Yamada *et al.* (1993) is flux-limited to $f_{60} > 0.6\, Jy$. In their galaxy identification process on the Schmidt plates, they have also introduced a limit on the diameter of the galaxy-like objects to be included in their sample[1]. Before commenting on whether or not the sample may contain real density anomalies, it is necessary to have an expectation of how many galaxies constitute a "complete" sample out to a given redshift distance.

In the absence of extinction, galaxy counting rates ($n$) should be affected by the distance to those galaxies in a viewing cone. Galaxy magnitudes could be calculated simply as $m = -2.5 log\, L_{60}$, and counts in a pencil beam should fall predictably with distance, $d$, because the apparent luminosity $L \propto 1/d^2$. The average apparent magnitudes of galaxies should fall with distance, as the relation $m = -2.5 log\, L_{60}$ implies that $m \propto -2.5 log(d^{-2})$: that is, $m \propto 5 log d$. By inversion, this last expression implies that $d$ varies as $10^{m/5}$. However, the volume of the cone of vision naturally increases as $d^3$, so that $n \propto d^3$, and it is therefore a purely geometric result that $n \propto 10^{3m/5}$, or $log\, n \propto 0.6m$, after combining this with the previous consideration. A plot of $log\, n$ versus $m$ should therefore yield a slope of 0.6 for a complete sample[2] and a generally homogeneous background distribution of galaxies. With a real over-density in the Local Universe, one would expect that $n$ would increase at a faster rate with volume than $d^3$, and the slope of the $log\, n$ versus $m$ plot will be steeper[3] than 0.6.

The $log\, N$ versus $log\, f_{60}$ plot has been carried out. For this plot, bins were generated in $\log(f_{60})$, with bin-size $\Delta log\, f_{60} = 0.025$. The numbers of galaxies whose 60-micron flux fell in each such bin were then counted, and $\log N$ obtained for each bin. Plots of $\log N$ versus $\log(f_{60})$, along with linear regression "best fit" slopes, appear below.

---

[1] Although an object may be visible on a Schmidt plate, if it is less extended than 6 arcseconds it has not been considered as being a galaxy candidate.

[2] Or a slope of -1.5, if in a plot of $log\, n$ versus $log\, f_{60}$.

[3] Or less than -1.5 in the $log\, n$ versus $log\, f_{60}$ plot.

Figure 5.8: $Log\,N$ versus $log\,f_{60}$ for 925 $IRAS$ galaxies situated at $0° < |\mathrm{b}| < 15°$.

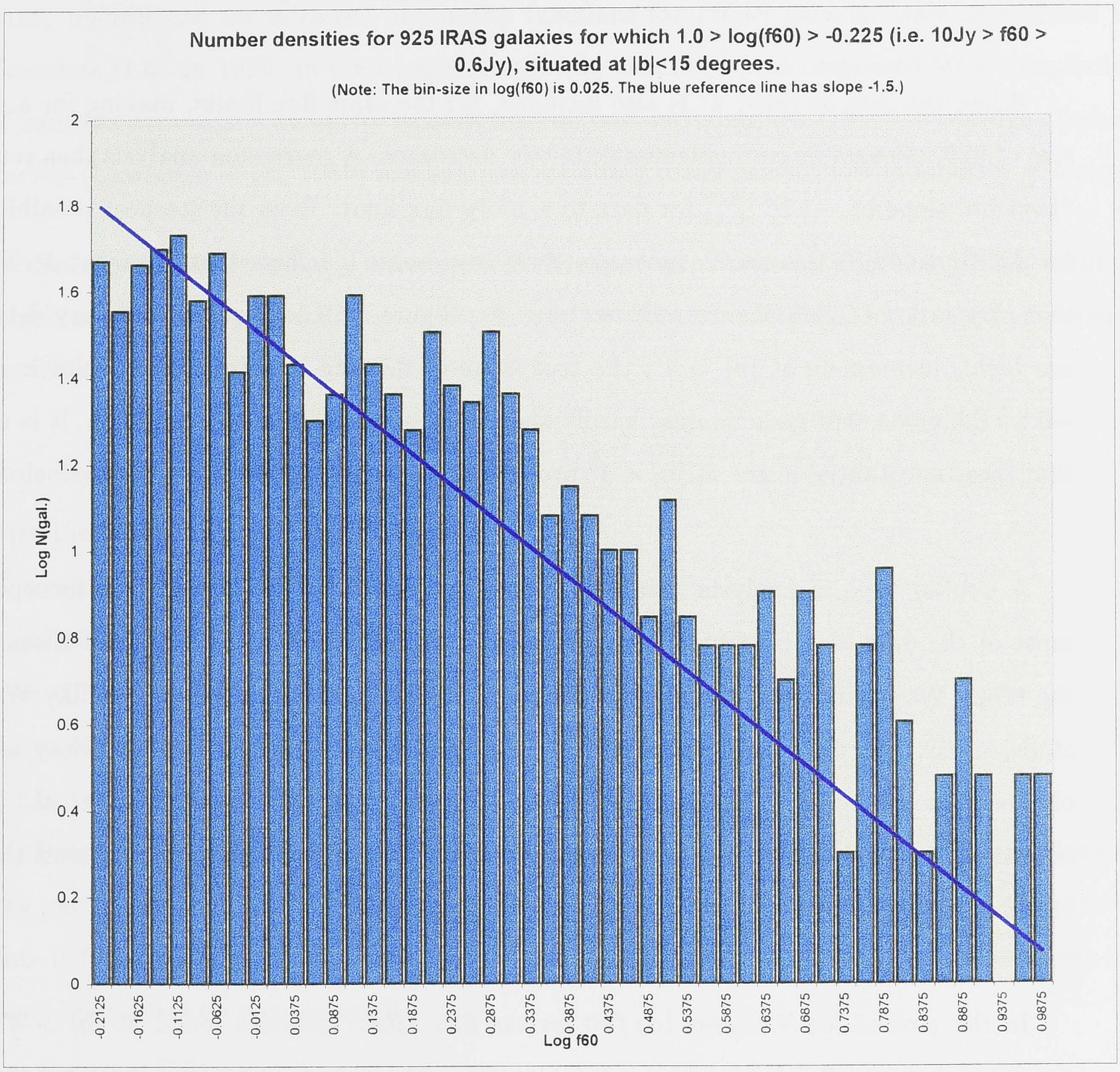


It is apparent that in the plot of $log\,N$ versus $log\,f60$ for the 835 $IRAS$ galaxies found at $|\mathrm{b}| > 4°$, with $f_{60}$ fluxes between $0.6\,Jy$ and $10\,Jy$, $-1.5$ is a possible visual fit to the slope of the graph. A regression analysis, however, returns a slightly lower "best fit" slope of $-1.20\,^{+0.27}_{-0.13}$. The steepest possible slope is therefore about $-1.33$. Some under-detection of low flux galaxies may account for this, as one can visually confirm that the slope is steepened if the flux lower limit is chosen at something higher than $0.6\,Jy$. In checking this, it is found that the slope of the regression line climbs to $\sim -1.45$ if only those galaxies with fluxes greater

than $1\,Jy$ are taken. This seems to support the view, then, that the $f_{60}$ sample at $|\mathbf{b}| > 4^{\circ}$ *is* highly complete, but mainly for those galaxies with $f_{60} > 1.0\,Jy$.

When the data at $|\mathbf{b}| < 4^{\circ}$ is also included, for the same flux limits, making for a sample size of 925, the sample completeness definitely decreases. A regression analysis then returns a "best fit" slope of $-1.16\,^{+0.29}_{-0.14}$ for data to a $10\,Jy$ flux limit. Even the steepest possible value for the slope admits that source incompleteness is present. It follows that this must derive from that population of galaxies situated at $|\mathbf{b}| < 4^{\circ}$. Figure 5.10 confirms that galaxy detections are *highly* incomplete at $|\mathbf{b}| < 4^{\circ}$; the true slope of this $log\,N$ versus $log\,f_{60}$ plot is around $-0.6$. So, given that galactic dust hardly absorbs or scatters infra-red radiation, it is evident that these substantial losses at $|\mathbf{b}| < 4^{\circ}$ are mainly to be attributed to source confusion.

A similar type of analysis[4], since published by Takata *et al.* (1996), and incorporating most of the data also presented here (but also including a few other longitude slices across the Milky Way), finds that the number densities of $IRAS$ galaxies behind the Milky Way (i.e. at $|\mathbf{b}| < 15^{\circ}$), in the range $0.5\,Jy < f_{60} < 10\,Jy$, fall very much in the same way as those observed at $|\mathbf{b}| > 15^{\circ}$ in the data of the QMW catalog of Rowan-Robinson *et al.* (1991), indicating no substantial difference in the completeness of the Takata survey and the high estimated completeness of the Rowan-Robinson survey.

In the plot of $log\,N$ versus $log\,f60$ for the 835 $IRAS$ galaxies found at $|\mathbf{b}| > 4^{\circ}$, with $f_{60}$ fluxes between $0.6\,Jy$ and $10\,Jy$, the regression fit slope of $-1.20\,^{+0.27}_{-0.13}$ indicates that $n$ in the local universe increases on average as $d^{2.4}$. There is no evidence of a *general* large scale overdensity of galaxies behind the Milky Way, based on this result. Both the number densities and the way in which the numbers of $IRAS$ galaxies increase with redshift are similar both behind and outside the Milky Way. Any over-densities or voids must therefore have smaller scales.

---

[4] In fact, a plot of $log\,N_{\rm gal}$ *per steradian* versus $f_{60}$.

## 5.3 A Universal Luminosity Function for *IRAS* Galaxies?

Sixty micron and far infra-red luminosity functions for *IRAS* galaxies were determined by Saunders *et al.* in 1990. In their paper, luminosity functions were compared for a compilation of samples with highly complete redshift information, including the QMC-Cambridge-Durham survey (Lawrence *et al.*, 1989) and samples including many nearby, low-luminosity galaxies.

Saunders *et al.* eventually opted for a STY (Sandage, Tammann & Yahil (1979)) solution which behaves as a power law for $L << L_*$ *and* as a Gaussian in $log\, L$ for $L >> L_*$, choosing as "best" solution:

$$\phi(L) = C(L/L_*)^{1-\alpha}\, exp[-1/2\sigma^2\, log_{10}^2(1 + L/L_*)],$$

with the four parameters having values:

$C = (2.6 \pm 0.8) \times 10^{-2}\, h^3\, Mpc^{-3}$

$\alpha = 1.09 \pm 0.120$

$\sigma = 0.724 \pm 0.031$

$L_* = 10^{(8.47 \pm 0.23)}\, h^{-2}\, L_\odot$.

Despite this, their survey is still based upon an incomplete sample, so no serious meaning can yet be attached to the above result. The luminosity function generated from the present data is found to be consistent with the solution of Saunders *et al.* (1990), but suffers from the same limitations on completeness.

Figure 5.9: $Log\,N$ versus $log\,f_{60}$ for 835 $IRAS$ galaxies situated at $4^{o} < |\mathrm{b}| < 15^{o}$.

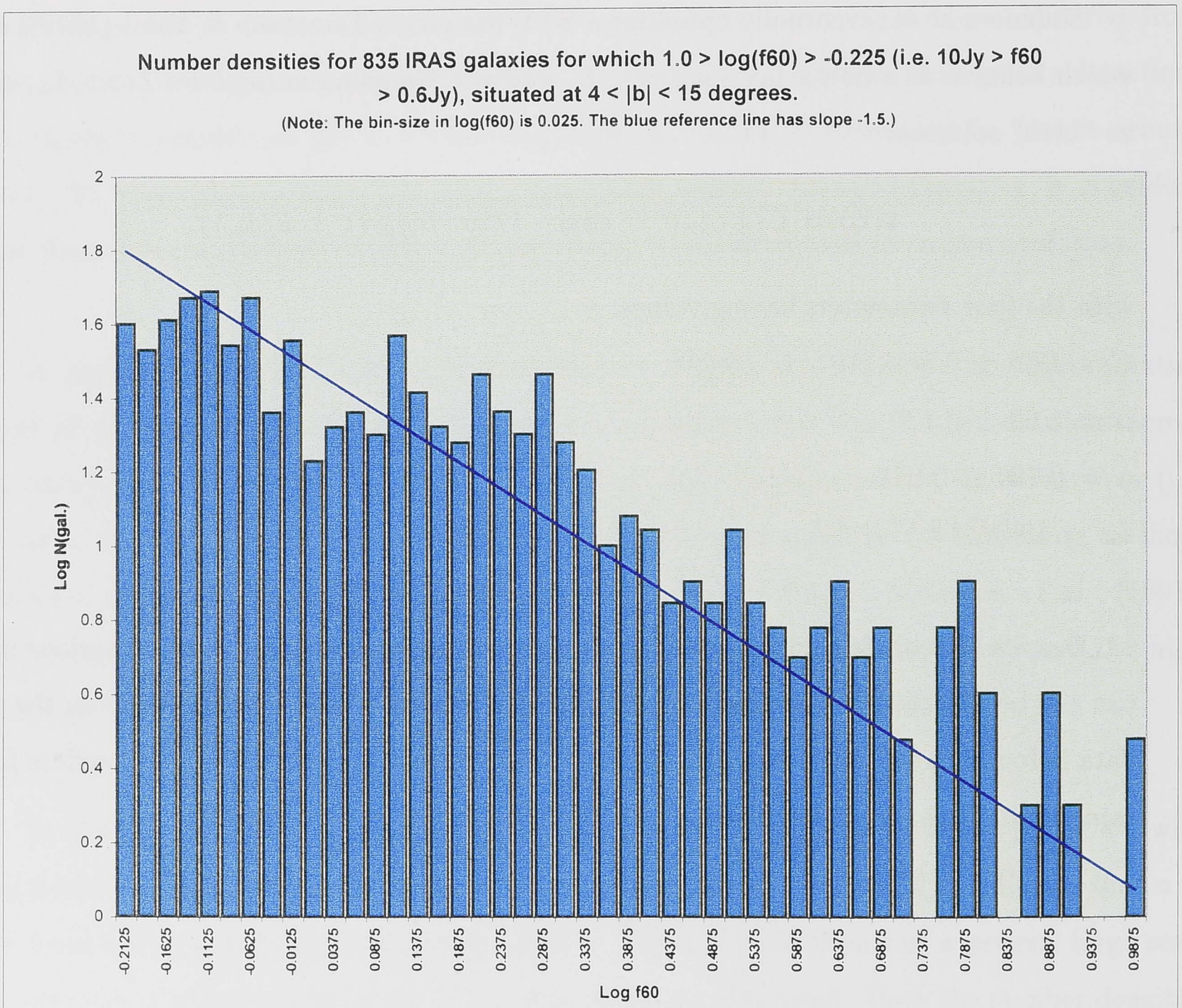

Figure 5.10: *Log N* versus *log* $f_{60}$ for 90 *IRAS* galaxies situated at $|\mathbf{b}| < 4°$.

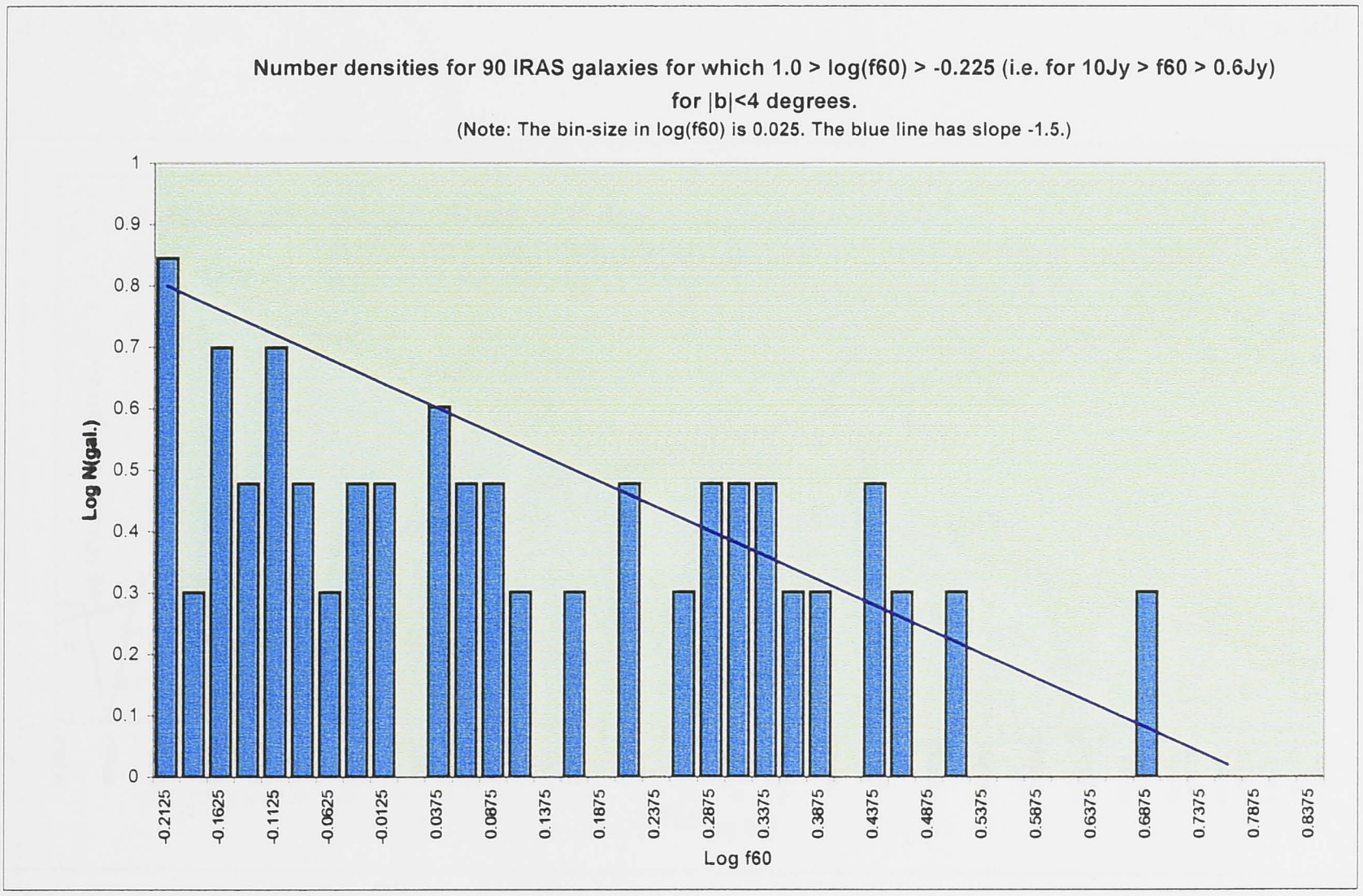

Figure 5.11: Regression "best fit" to the $log\, N$ versus $log\, f_{60}$ relation, for galaxies situated at $0° < |\mathbf{b}| < 15°$.

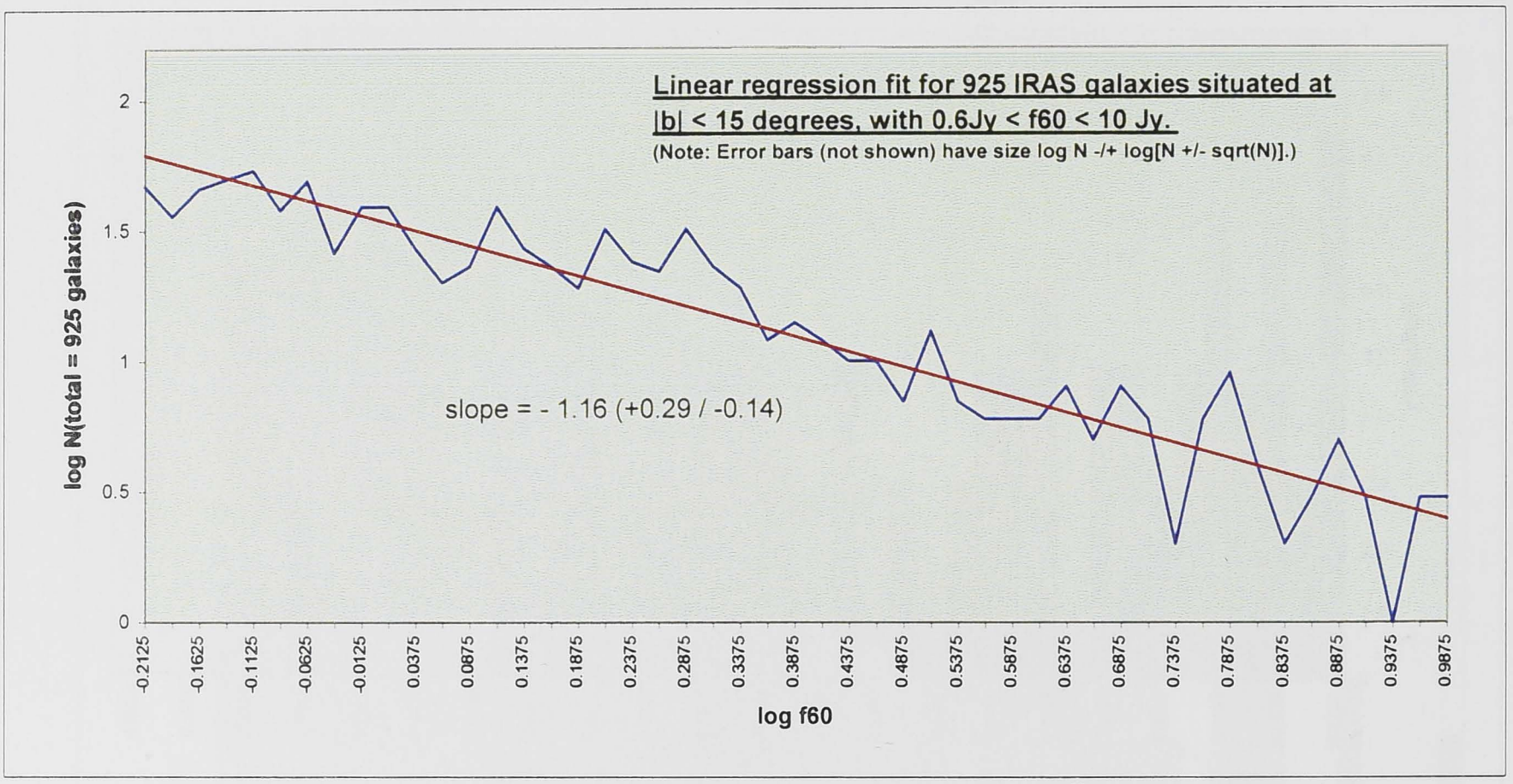

Figure 5.12: Regression "best fit" to the $log\ N$ versus $log\ f_{60}$ relation, for galaxies situated at $4° < |b| < 15°$.

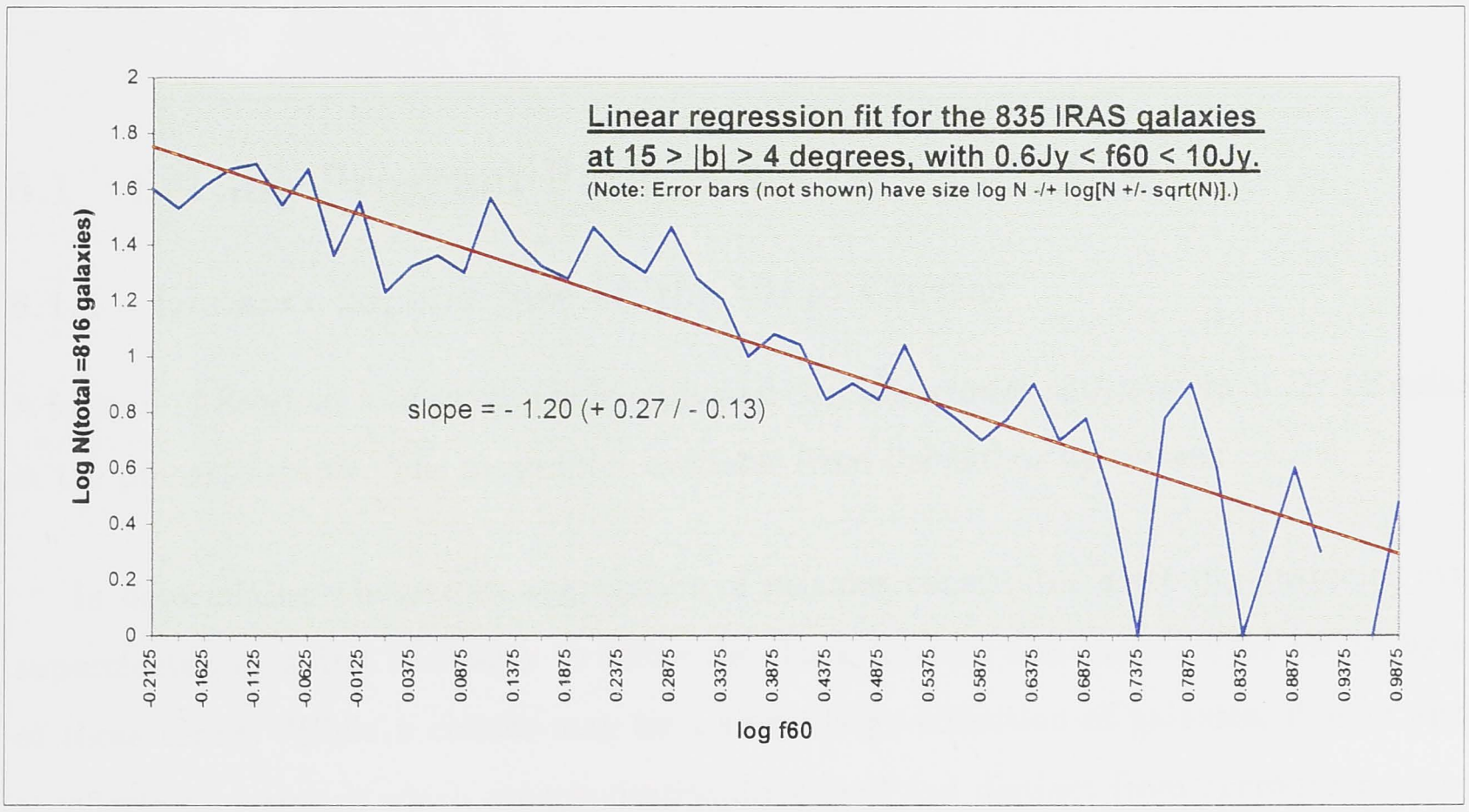

# Chapter 6

# Clustering Program

## 6.1 Setting Program Parameters

### 6.1.1 Distance to, and Size of, the Virgo Cluster

A fortran 77 program was written to identify and describe groups and clusters of $IRAS$ galaxies in the present sample. The program is available from the author by request.

In determining whether an aggregation of galaxies constitutes a group, cluster or even a supercluster, it is first necessary to define the characteristics and spatial sizes meant by each of these terms. While a cluster may be a single large collection of galaxies, it may also be a collection of groups which are gravitationally bound and distinct from surrounding groups. Groups are of order $0.25 - 1.0\,Mpc$ in diameter whereas clusters span around $2 - 5\,Mpc$. Clusters are typically separated from one another by distances in the order of $10 - 30\,Mpc$. Superclusters are much larger structures - often longer than 100 Mpc, and at least $15 - 20\,Mpc$ across. These are usually arranged in the form of walls, or sheets, of clusters, groups and individual field galaxies.

A working size scale is provided by comparing the dimensions of identified concentrations of galaxies with those of the Virgo cluster. The Virgo cluster is suitably nearby ($\sim 17\,Mpc$) and is rich in both spiral and elliptical galaxies, which has historically enabled a number of different distance tests to be applied.

There has been some discrepancy in the inferred distance to (and, thus, in the inferred size of) the Virgo cluster, with quoted distances which range from 15 to 24 Mpc (cf. Jacoby *et al.*, 1992 and Sandage & Tammann, 1993).

A recent study (see Freedman *et al.*, 1994) using the Hubble Space Telescope data has not completely clarified the distance issue, but it has at least established the distance to a probable Virgo cluster member with a greater accuracy than before. In the Hubble study, high-quality light curves were obtained for classical Cepheids with periods of 20-65 days in the member galaxy M100. Application of the Period-Luminosity law for classical Cepheids enabled a distance accurate to within 10% to be established for this galaxy. The brightness of M100 Cepheids was then compared with the brightness of similar LMC Cepheids, to obtain a ratio of distances (M100/LMC) from the brightness ratios. The only uncertainty that would be expected to exist in the distance to M100 would therefore be a combination of the uncertainties in the distance to the LMC and reddening corrections. Errors introduced through zero-point shifts in the Period-Luminosity relation, because of different average metallicities in M100, the LMC and the Galaxy, are not important when compared to these dominating uncertainties. Freedman *et al.* give the distance to the cluster as $17.1 \pm 1.8\, Mpc$[1].

The real difficulty with the Hubble result is the issue of whether the distance to M100 is truly representative of the distance to the Virgo cluster as a whole. This uncertainty drives the overall uncertainty in the distance to the Virgo cluster up to a conservative 20%.

Given that the Virgo cluster spans $\approx 12^{\circ}$ on the sky, the true linear extent of the cluster is $3.59 \pm 0.38\, Mpc$, using the Freedman *et al.* distance. As a guide in what follows, any object that would be larger than $9^{\circ}$ on the sky at the distance of the Virgo cluster will be called a "cluster". Anything from a binary galaxy system up to a collection of galaxies extending over $6^{\circ}$ will be described as a "group", and from $6^{\circ} - 9^{\circ}$ as a "large group". Finally, large-scale associations of galaxies projected over $> 90^{\circ}$ on the sky at $17\, Mpc$ are likely to be superclusters.

---

[1] Incidentally, if the recession velocity preferred by Huchra (1988) (adjusted for the infall of the Local Group) of $1404 \pm 80\, km\, s^{-1}$ is adopted with the Freedman *et al.* (1994) distance, a resultant value of $H_{\circ} = 1404 \pm 80/17.1 \pm 1.8 = 82 \pm 17\, km\, s^{-1}\, Mpc^{-1}$ is obtained for the Hubble constant.

### 6.1.2 Running the Program

The program relies on a number of input parameters, including the adopted value of the Hubble constant (in km/s/Mpc) and the radii of the finding spheres which determine whether or not galaxies are associated into groups or clusters, or groups into clusters, or clusters and groups into superclusters. The problem of how to accommodate large velocity dispersions, the major obstacle in the identification of small groups, will be described.

Another important set of initial values are those which will decide whether the latest collection of galaxies is a pair, a group, a large group, a filament or a cluster. (There are also some intermediate cases such as "probable cluster", "filamentary large group", etc.)

The next most important parameter is probably that which estimates the aspect ratios of collections of galaxies. Once the aspect ratio exceeds a certain value, the object could become defined as a filament, or as a filamentary large group or cluster. The aspect ratio is simply the major axis length of an associated collection of galaxies, divided by the minor axis length.

The velocity dispersion ($\sigma_v$) for $IRAS$ galaxies is expected to be of order $70 - 150\,km\,s^{-1}$ in a large group, and may be as much as $500\,km\,s^{-1}$ in a large cluster like the Coma cluster. Rood & Dickel (1978) and Tully (1987) find that typical line-of-sight velocity dispersions for small groups in the optical CfA survey are $\leq 200\,km\,s^{-1}$. Surveys to smaller depths (i.e. which incorporate only brighter galaxies), such as the $IRAS$ survey, have lower apparent velocity dispersions, and this is why, in the present survey, dispersions higher than $\sim 130\,km\,s^{-1}$ should seldom be encountered.

In the program used here, the finding circle was simply enlarged to allow for the possibility of broad velocity dispersions, but it is acknowledged that this is far from an elegant solution. A weakness in this approach is the risk that large velocity differences are too readily taken as representing large differences in distance. That is, a program like this does not always account well for galaxies which may be quite close to each other in space but which seem far apart because of the large radial velocity differences between them, this difference actually arising mainly from high peculiar velocities. The opposite effect - that galaxies which appear, on the

basis of radial velocities, to be closely associated are actually distant from each other - is also possible, for the same reasons.

An excessively large search circle, though, opens up the more problematic possibility of an erroneous association of unrelated galaxies into common groups. While properly accommodating velocity dispersions would involve a more statistically-oriented programming approach than adopted here, a simple enlargement of the finding circle size is nearly as effective for present purposes because of the relatively sparse nature of the *IRAS* sample.

The data set, cut to $cz \leq 6500\, km\, s^{-1}$, was input to the program, and all groups, clusters and other associations identified. Because of variable extinction, identifications based upon galaxy count criteria have the potential of being inconsistent. If the associated extinction at the position of a group or cluster centre is more than $2\,\sigma$ above the mean overall extinction for the sample the chance is high that the program will misclassify the object in the direction of a smaller object, since the level of incompleteness will have increased steeply.

The approach of letting the program read in a table of extinctions, and then adjusting the numbers of galaxies in each group or cluster to some presumably "corrected" number, has been avoided: one cannot presume to know anything about galaxies that have never been seen - no previous survey is available to indicate what the number densities behind the Milky Way should be! The criteria as applied then, pertain to a sample treated as if it were uniformly shrouded at the mean extinction level of the whole survey region.

Since the sample was, moreover, selected using optical identification of galaxies on Schmidt plates, incompleteness is necessarily much higher for galaxies at higher redshifts. Since the stronger criterion in the program for classifying associations is their spatial extent (rather than total numbers of associated galaxies), the program has some robustness against depleted numbers. All the same, classification into groups, large groups and clusters becomes increasingly subject to error with increasing redshift. All groupings with an average redshift greater than $6350\, km\, s^{-1}$ may also be incomplete, since the $\sigma_v$ implies that a redshift of $6700\, km\, s^{-1}$ may nevertheless indicate a galaxy which is nearer than the nominated sample limit of $6500\, km\, s^{-1}$.

Because the output file is quite large, the output of the program has been summarized in Tables 6.1 and 6.2, which follow below. These tables share the same format, in which columns 1 and 2 give the galactic $l^{II}$ and $b^{II}$ coordinates, columns 3 and 4 the mean redshift and estimated velocity dispersion for each identified grouping, column 5 the apparent diameter in megaparsecs of each grouping, based on the galaxy positions in that grouping, and column 6 the apparent sizes of the groupings if placed at a distance of $17\,Mpc$, given the mean redshift distances in each case and a Hubble constant of $73\,km\,s^{-1}\,Mpc^{-1}$. This figure in column 6 is only calculated for groupings which contain more than two galaxies, for reasons discussed in Section 6.2. The number of galaxies found in each grouping is recorded in column 7, along with the galaxy types - the key appearing at the head of the table. The final column describes the nature of grouping in each case, with the key also appearing in the table header.

The program was run with the Hubble constant set to $73\,km\,s^{-1}\,Mpc^{-1}$ and[2] the finding circles set to $1.75\,Mpc$ (to find associated galaxies), $3.54\,Mpc$ (to find groups associated at the small scale into clusters) and $14\,Mpc$ (to find groups and clusters that might be associated at the large-scale in superclusters). The output of the program is quite sensitive to the exact values adopted for the three finding circles - most critically to the smallest finding circle - and to the value chosen for the Hubble constant.

The value of $1.75\,Mpc$, adopted for the program variable "circle", is approximately half the diameter of the Virgo cluster (estimated in the preceding discussion to be $\sim 3.5\,Mpc$). The assumption is made that the Virgo cluster, which is close to the Local Group, is of typical cluster size. Adopting the radius of a cluster as a finding length should certainly be generous enough to find any galaxies in the cluster without including only loosely associated field galaxies. The problem with picking up field galaxies at the edge of too large a finding sphere is that each of these then becomes the centre of a new search, and a large number of "stray" galaxies may become included into the list of cluster members.

[2] A value favoured by Visvanathan (1990). At this stage the newest value for the Hubble constant, described in a previous footnote, has not been adopted, pending further verification of the distance to M100, and of its definite membership of the Virgo cluster.

The value of 3.54 $Mpc$, adopted for the program variable "secondcircle", is merely the nominally defined "maximum cluster size", divided by the square root of two. Clusters have been treated as entities that may range in diameter from between two and five megaparsecs. A collection of galaxies with a radius of, say, 1.75 $Mpc$ is still a large group, rather than a cluster. A collection of galaxies more extensive than 5 $Mpc$ is larger than a cluster and may be some collection of clusters and groups on a larger scale. The factor of 1.414 means that effectively half of the maximum area subtended by a maximal size cluster is searched for groups that may together constitute a cluster, so there is the quality of a geometrical mean size to this second finding circle.

Again, to set the sphere too large is to erroneously infer the association of groups (already shown to be isolated from one another to some degree by the action of the first search, and the first finding circle), some of which might be separated from each other at well above the diameter of a cluster. This should be avoided, if possible, especially as it is the role of the third finding circle to pick out the more extended structural associations.

The value of 14 $Mpc$, adopted for the program variable "thirdcircle", was chosen because this is approximately the radius of the local Virgo supercluster, divided by the square root of two, so defined for reasons similar to those just cited above in reference to "secondcircle". The Local Group is situated about 17 $Mpc$ from the centre of the Virgo cluster. It lies near the outer reaches of the supercluster, which has the Virgo cluster at its centre.

It is better to use the program than one's own perusal of the ($\mathbf{l}$ $vs$ $\mathbf{b}$), ($\mathbf{b}$ $vs$ $cz$) and ($\mathbf{l}$ $vs$ $cz$) diagrams to find galaxy associations. The $\mathbf{l}$, $\mathbf{b}$, and $cz$ axes in diagrams like Figures 5.1, 5.3 & 5.4 are usually not on the same scale, making three-dimensional structures hard to visualize, and also because any more than a few hundred galaxies cause the above diagrams to become very congested, making visual analysis both tedious and increasingly subject to error.

The associations of $IRAS$ galaxies identified by the clustering program are illustrated more clearly in the following set of diagrams, which show how the groupings are distributed with redshift.

Table 6.1: Results of the Clustering Analysis - Table 1

Key to *IRAS* galaxy associations (ID): g = group, lg = large group, cp = close pair, pcl = probable cluster, cl = cluster. Key to Types: S = spiral, S? = probable spiral, E = elliptical, E? = probable elliptical, U = unknown.

| Centre of Grouping | | $cz$ | $\sigma_v$ | Grp Dia. | Size at | No. of | Types | ID |
|---|---|---|---|---|---|---|---|---|
| l | b | (km/s) | (km/s) | ($Mpc$) | 17 $Mpc$ (°) | Galaxies | | |
| 233.9 | -14.2 | 2686 | 26 | 0.9 | | 2 | 2S | g |
| 235.8 | 3.3 | 3273 | 38 | 0.9 | | 2 | 2S | g |
| 236.3 | 14.0 | 6055 | 13 | 0.5 | | 2 | 2U | g |
| 237.1 | -13.5 | 1923 | 29 | 0.7 | | 2 | 2S | g |
| 238.8 | -9.0 | 2631 | 25 | 1.7 | | 2 | 2S | g |
| 240.0 | -2.0 | 2195 | 11 grps & | clusters: | | | s/cluster? | |
| 242.2 | -6.9 | 3093 | 31 | 0.8 | | 2 | 1S 1U | g |
| 244.8 | -5.9 | 1992 | 23 | 4.4 | 9.2 | 7 | 5S 1E 1U | pcl |
| 245.8 | 2.4 | 1003 | 19 | 1.0 | 4.2 | 3 | 3S | g |
| 245.9 | 8.4 | 1672 | 12 | 5.3 | 13.3 | 12 | 12S | cl |
| 248.1 | -9.5 | 2821 | 26 | 1.2 | | 2 | 2S | g |
| 251.1 | 7.3 | 882 | 22 | 1.3 | | 2 | 1S 1E | g |
| 256.3 | 12.9 | 2166 | 18 | 1.5 | | 2 | 1S 1U | g |
| 269.4 | 8.4 | 4865 | 27 | 0.6 | | 2 | 1S 1S? | g |
| 274.3 | 8.6 | 3435 | 57 | 2.5 | 3.0 | 3 | 3S | g |
| 274.8 | 8.6 | 3921 | 58 | 1.3 | | 2 | 2S | g |
| 275.2 | -11.8 | 6413 | 2 | 0.06 | | 2 | 1S 1U | cp |
| 276.1 | 9.6 | 1009 | 50 | 1.1 | | 2 | 2S | g |
| 276.9 | 12.4 | 2620 | 14 | 4.2 | 6.7 | 8 | 8S | pcl |
| 277.7 | 14.7 | 2762 | 6 | 0.2 | | 2 | 2S | cp |
| 278.4 | 11.4 | 2920 | 17 | 2.3 | 3.3 | 3 | 2S 1U | lg |
| 278.7 | -7.8 | 2885 | 27 | 1.9 | 2.7 | 3 | 2S 1S? | g |
| 280.4 | -11.7 | 6396 | 35 | 1.3 | | 2 | 2S | g |
| 280.0 | 1.0 | 2625 | 14 grps & | clusters: | | | s/cluster? | |
| 281.3 | -8.2 | 2163 | 35 | 3.3 | 6.3 | 4 | 4S | lg |
| 281.5 | -9.8 | 3136 | 61 | 1.7 | | 2 | 1S 1E? | g |
| 282.2 | -7.1 | 2822 | 52 | 2.6 | 3.8 | 3 | 2S 1U | g |
| 282.9 | -12.8 | 1598 | 51 | 1.7 | | 2 | 2S | g |
| 282.9 | -13.9 | 3271 | 14 | 0.7 | | 2 | 2S | g |

Table 6.2: Results of the Clustering Analysis - Table 2

Key to ID: as for Table 6.1.

| Centre of Grouping | | $cz$ | $\sigma_v$ | Grp Dia. | Size at | No. of | Types | ID |
|---|---|---|---|---|---|---|---|---|
| l | b | (km/s) | (km/s) | ($Mpc$) | 17 $Mpc$ (°) | Galaxies | | |
| 285.0 | 10.9 | 5606 | 25 | 1.5 | | 2 | 2S | g |
| 285.4 | 9.5 | 2779 | 23 | 2.5 | 3.8 | 5 | 5S | lg |
| 290.1 | -8.4 | 5935 | 9 | 1.3 | | 2 | 2S | g |
| 290.7 | 11.9 | 5594 | 36 | 1.3 | | 2 | 2S | g |
| 290.8 | 11.9 | 5091 | 26 | 0.6 | | 2 | 2S | g |
| 293.2 | -7.0 | 1426 | 54 | 1.6 | | 2 | 2S | g |
| 302.4 | 9.1 | 1852 | 43 | 1.0 | | 2 | 1S? 1U | g |
| 305.0 | -14.9 | 2582 | 20 | 0.6 | | 2 | 2S | g |
| 310.5 | 11.6 | 3675 | 17 | 1.2 | | 2 | 2S | g |
| 311.2 | 10.2 | 4014 | 13 | 4.5 | 4.7 | 6 | 4S 2U | pcl |
| 311.7 | 13.4 | 3027 | 10 | 6.1 | 8.4 | 13 | 10S 1E 2U | cl |
| 312.7 | 7.9 | 3731 | 23 | 3.9 | 4.4 | 5 | 2S 3U | lg |
| 313.0 | -12.8 | 3006 | 54 | 1.2 | | 2 | 2S | g |
| 317.8 | 5.2 | 3026 | 29 | 1.7 | 2.3 | 3 | 2S 1U | g |
| 320.3 | -10.1 | 3714 | 57 | 1.3 | | 2 | 2S | g |
| 322.6 | -4.4 | 5122 | 36 | 1.5 | | 2 | 2S | g |
| 323.2 | -6.3 | 4407 | 40 | 2.1 | 2.0 | 3 | 1S 2U | g |
| 323.0 | -1.0 | 3716 | 21 groups & | clusters: | | | s/clust? | |
| 324.6 | -9.7 | 3874 | 48 | 1.1 | | 2 | 2S | g |
| 326.3 | 13.5 | 4693 | 35 | 2.6 | 2.3 | 3 | 1S 1S? 1U | g |
| 327.3 | -9.1 | 3279 | 27 | 2.4 | 3.1 | 3 | 2S 1S? | g |
| 327.6 | 13.5 | 5174 | 55 | 1.6 | | 2 | 2S | g |
| 327.8 | -12.2 | 4983 | 5 | 2.8 | 2.3 | 3 | 2S 1U | g |
| 328.7 | -7.4 | 2740 | 4 | 3.0 | 4.6 | 3 | 2S 1U | g |
| 329.0 | -12.4 | 1103 | 5 | 0.9 | | 2 | 1S 1U | g |
| 329.8 | -9.4 | 1521 | 48 | 1.1 | | 2 | 2S | g |
| 331.7 | -13.5 | 6282 | 51 | 1.2 | | 2 | 2S | g |
| 331.8 | -14.6 | 5239 | 48 | 1.7 | | 2 | 1S 1U | g |
| 333.3 | 14.1 | 4705 | 34 | 2.2 | 2.0 | 3 | 1S 2U | g |
| 338.0 | 11.9 | 4413 | 0.5 | 1.5 | | 2 | 1s 1U | g |

Figure 6.1: Clustering of $IRAS$ galaxies for $cz < 6500\,km\,s^{-1}$.

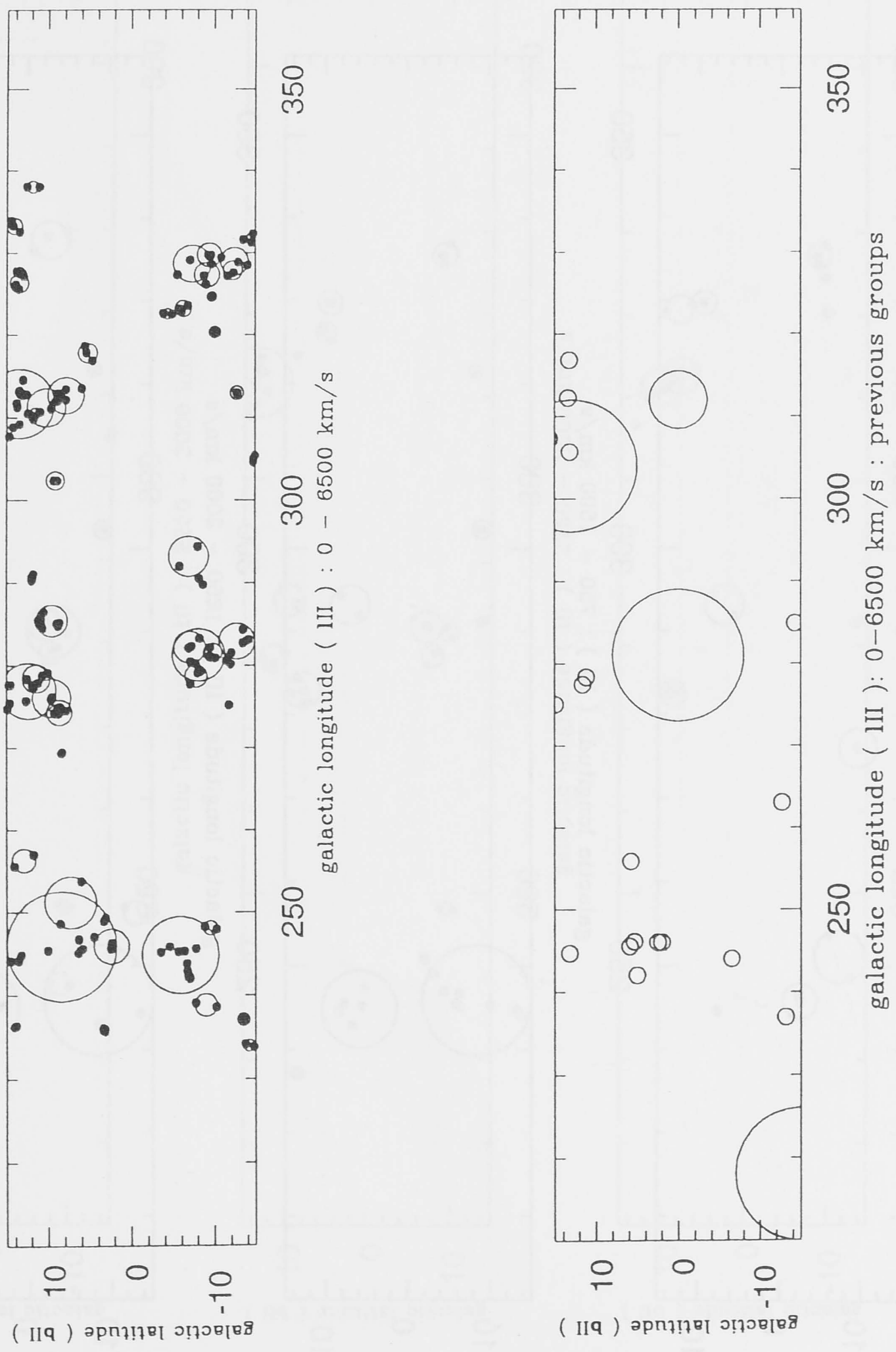

Figure 6.2: Clustering of $IRAS$ galaxies in $750\,km\,s^{-1}$ slices in redshift space, out to $cz < 6500\,km\,s^{-1}$. Note that the slices overlap by $250\,km\,s^{-1}$ with each neighbouring slice.

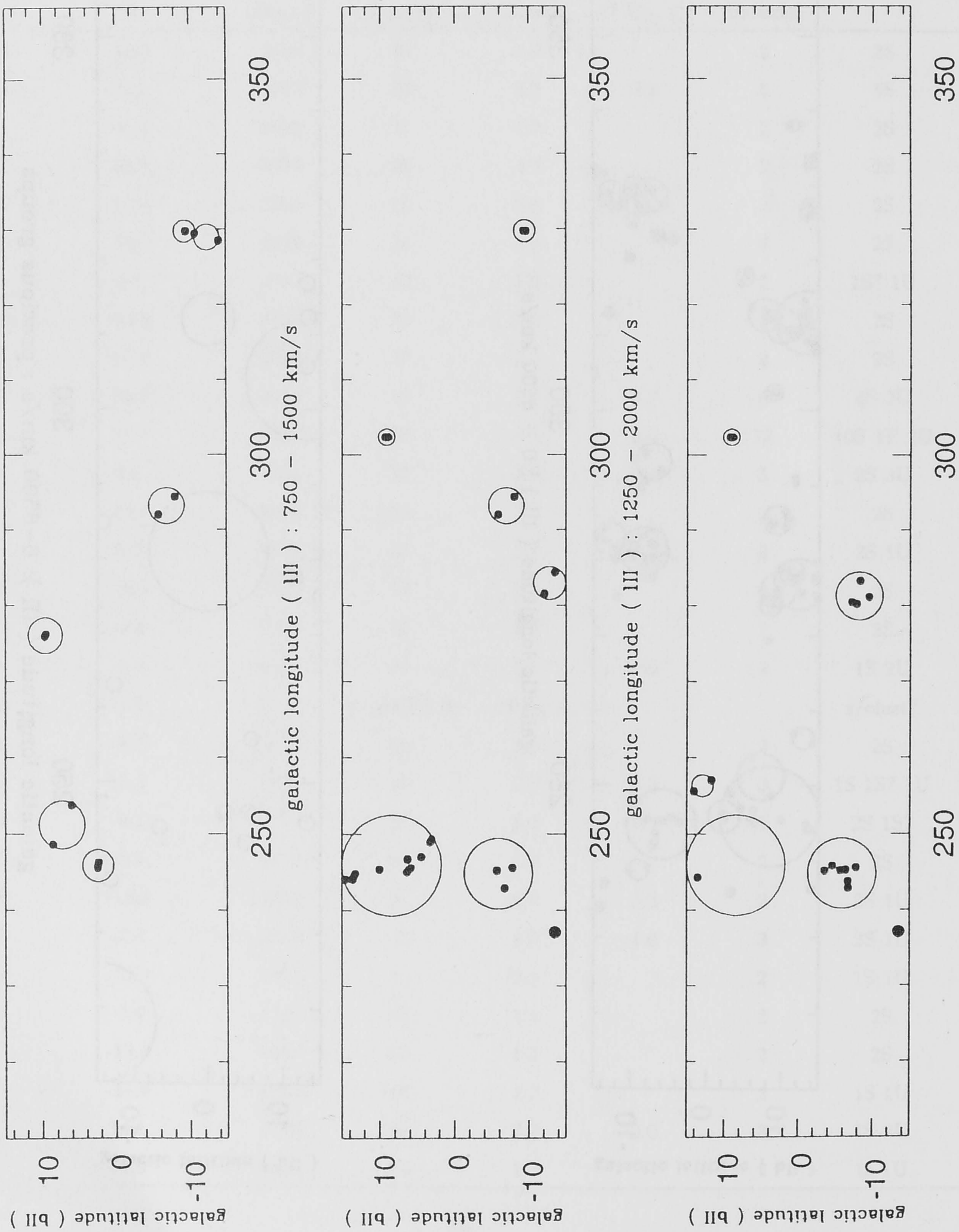

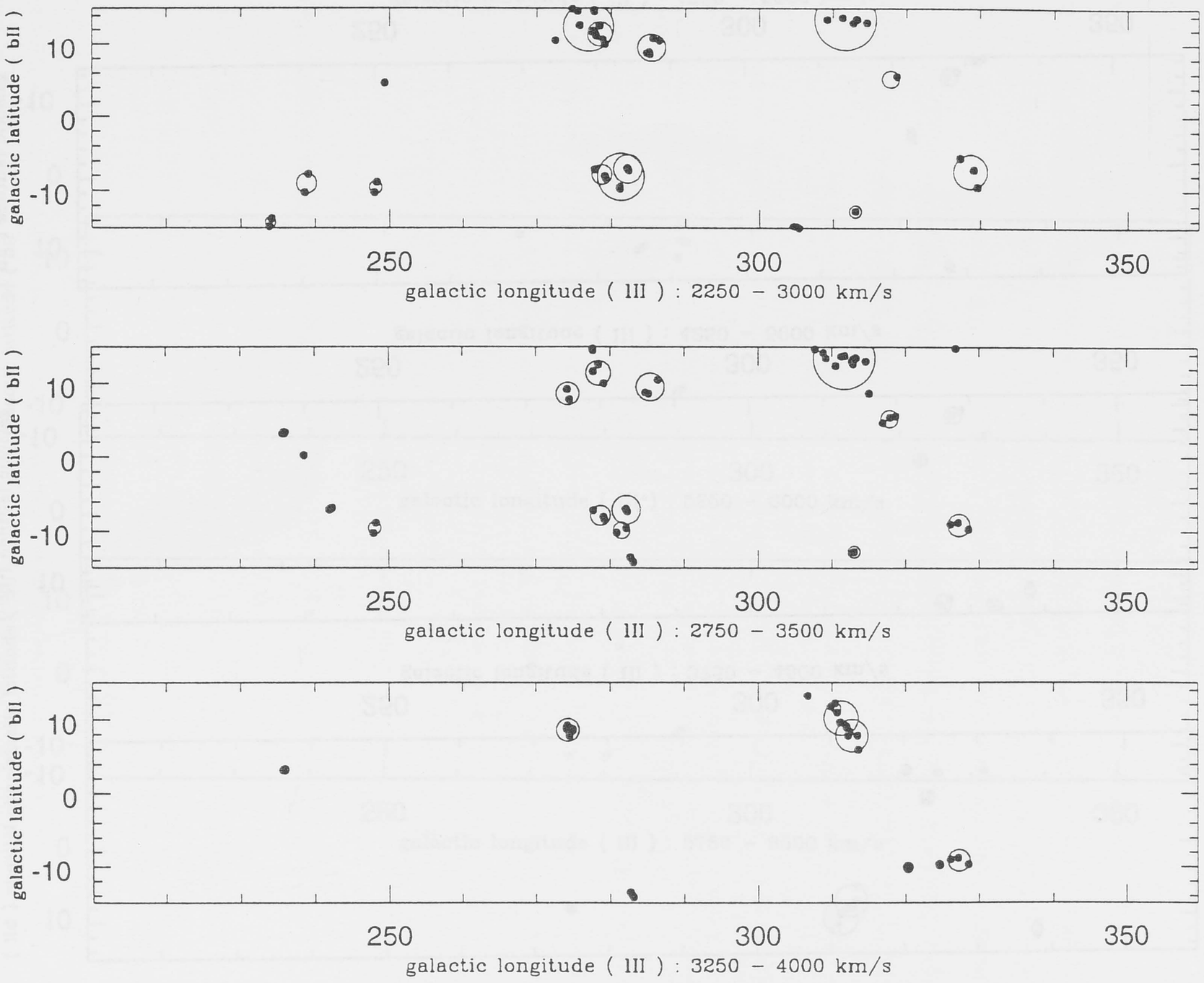
galactic latitude ( bII )
10
0
-10
250
300
350
galactic longitude ( lII ) : 2250 – 3000 km/s
galactic latitude ( bII )
10
0
-10
250
300
350
galactic longitude ( lII ) : 2750 – 3500 km/s
galactic latitude ( bII )
10
0
-10
250
300
350
galactic longitude ( lII ) : 3250 – 4000 km/s

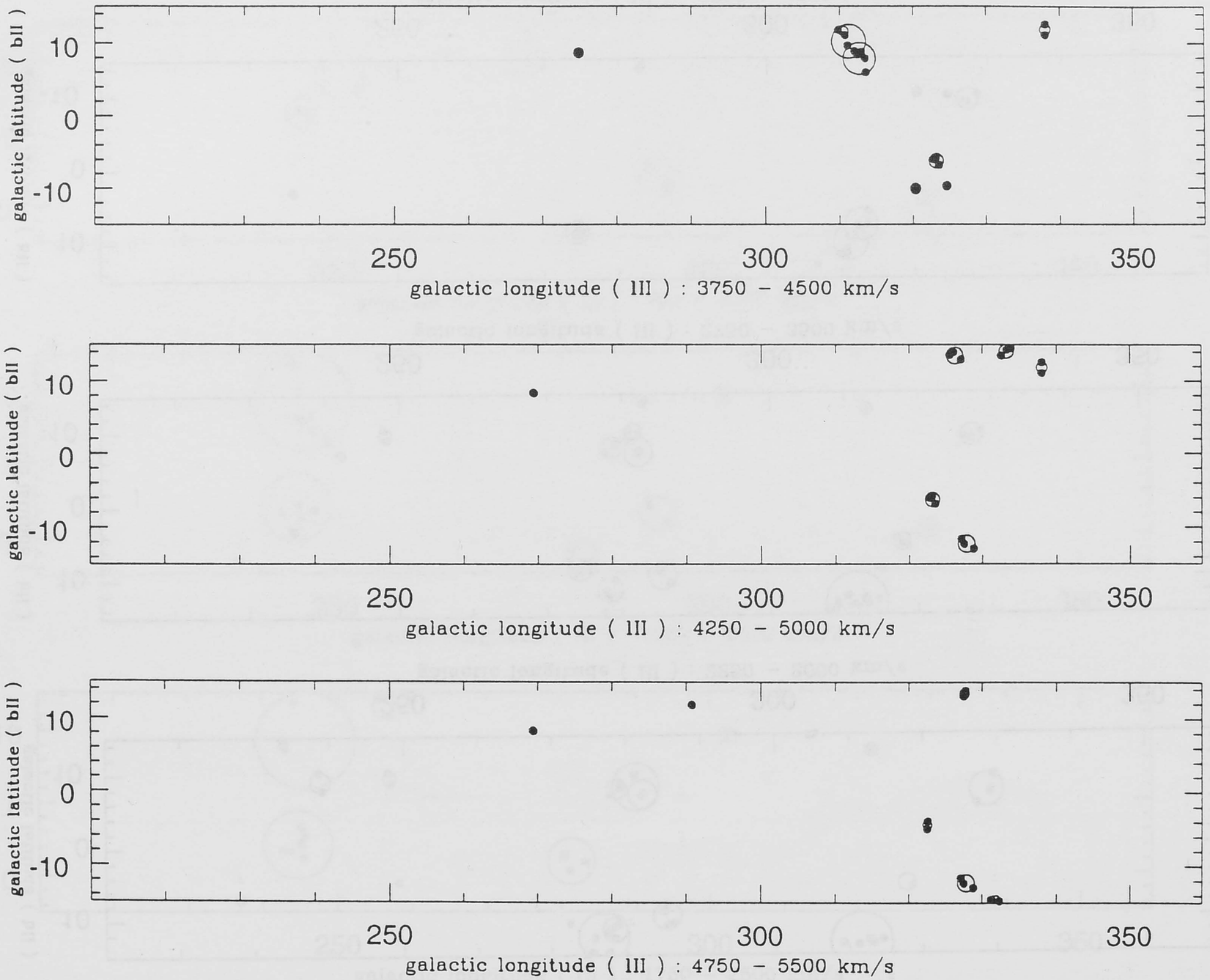
galactic latitude ( bII )
10
0
-10
250
300
350
galactic longitude ( lII ) : 3750 – 4500 km/s
galactic latitude ( bII )
10
0
-10
250
300
350
galactic longitude ( lII ) : 4250 – 5000 km/s
galactic latitude ( bII )
10
0
-10
250
300
350
galactic longitude ( lII ) : 4750 – 5500 km/s

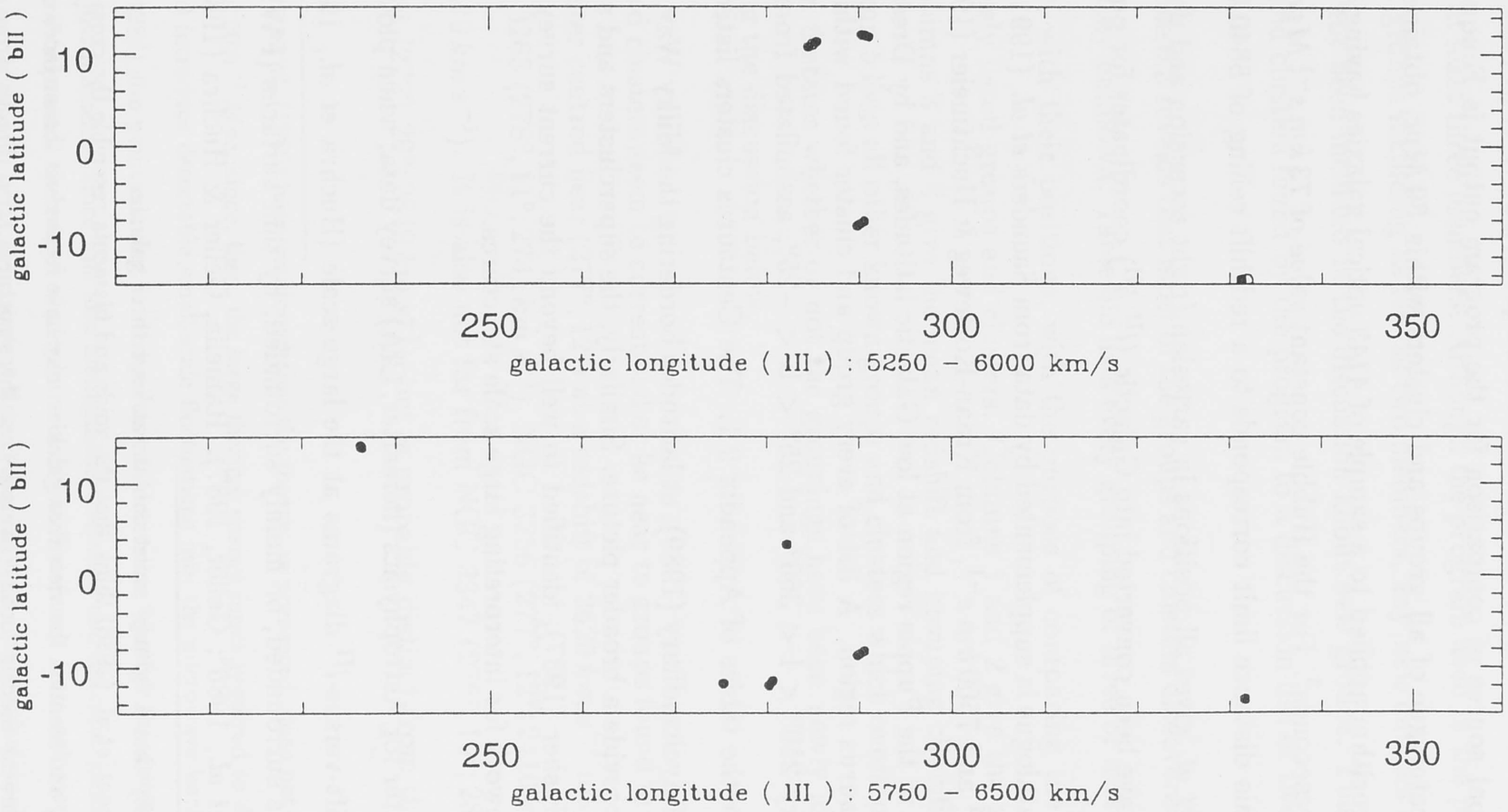
galactic latitude ( bII )
10
0
-10
250
300
350
galactic longitude ( lII ) : 5250 – 6000 km/s
galactic latitude ( bII )
10
0
-10
250
300
350
galactic longitude ( lII ) : 5750 – 6500 km/s

## 6.2 Groups and Clusters of *IRAS* Galaxies: Program Results

### 6.2.1 Identifying Groups and Clusters

The principal source of comparison for the program output is Fouque *et al.* (1992). They present a catalogue of all groups and clusters within $80\,Mpc$, obtained by means of a heirarchical algorithm applied to a sample of 4143 optical galaxies having diameters ($D_{25}$) larger than 100 arcseconds[3]. For the Hubble constant value of $73\,km\,s^{-1}\,Mpc^{-1}$ used in the fortran program, this distance limit corresponds to a redshift ceiling of $5840\,km\,s^{-1}$. The catalogue of Fouque *et al.* gives all positions in cartesian (right ascension and declination) coordinates, and these have been converted into Galactic $(l^{\rm II}, b^{\rm II})$ coordinates for purposes of comparison.

Their catalogue is supplemented by data from Saunders *et al.* (1991) for redshifts between $5500\,km\,s^{-1}$ and $7500\,km\,s^{-1}$, from Kraan-Korteweg & Huchtmeier (1992), to the same limit, for galaxies in the Puppis region at low Galactic latitudes, and by Dressler (1991) for clusters in the Centaurus region. A list of every group and cluster found within $7500\,km\,s^{-1}$, within the boundary $210^{\rm o} < {\rm l} < 360^{\rm o}$ and $25^{\rm o} < {\rm b} < -25^{\rm o}$, assimilated from the sources above, is presented in the tables of Appendix 9.1. The Centaurus clusters listed by Scaramella *et al.* (1989) and Raychaudhury (1989), at latitudes bordering the Milky Way, have been included in this list to provide a broader picture. Similarly, the superclusters and supercluster complexes of Tully & Fisher (1987), identified to well beyond the current survey limits, provide a still larger framework for interpreting large scale structures.

The Center for Astrophysics (hereafter, CfA) survey data, when plotted in redshift-versus-$b^{\rm II}$ or redshift-versus-$l^{\rm II}$ diagrams at the large scale (Huchra *et al.*, 1983), characteristically display voids surrounded, or mainly surrounded, by thin surfaces (FWHM $\approx 500\,km\,s^{-1}$; de Lapparent *et al.*, 1986[4]; Geller, 1987). Ramella, Geller & Huchra (1989) state that as many

[3]They specify that a "group" must contain at least three galaxies.

[4]De Lapparent *et al.* (1986) think that the voids and filaments resemble the cross-sectional view of bubble-like structures, and mention the view that galaxies may have formed on the surfaces of expanding shock waves. While most current models ideally assume that the structures form directly from gravity acting on matter perturbations, the sharpness of the transition from high-density regions to voids in the CfA survey suggested to Ostriker & Cowie (1981) that hydrodynamic processes might be important in the formation of galaxies.

as one third of small (3-4 member) groups are spurious, and that they are just an accident of the geometry of large-scale structure in which the surfaces are so thin, and the velocity dispersions[5] of groups so high, that individual galaxies from different groups can appear to be closer to each other than to their own group centres. This is a strong motivation for requiring a "group" to contain at least three members. Although the program used in the present analysis was allowed to find groups including as few as two members, any *new* entities containing just two members have not been included in the discussion about new groups. This reduces a list of fifty-six groups and clusters found by the program to a discussion list of twenty-seven.

A perusal of Table 6.3 reveals that most of the groups and clusters discovered in the current survey were previously unknown. Table 6.3 lists every grouping of three or more galaxies from Tables 6.1 and 6.2, with their positions, with the purpose of comparing the locations with those of all previously listed groups and clusters. Columns 1 and 2 give the galactic $l^{II}$ and $b^{II}$ coordinates, columns 3 and 4 give the mean redshift and grouping classification for each grouping, and column 5 lists all other known groups and clusters which overlap with the listed groupings. Column 6 states whether or not the groupings have been newly identified in this survey, summarising the discussion below.

Some groups and clusters seem to correspond or lie near to groups found in earlier surveys. For example, a cluster centred near $(277°, 12°)$ at a redshift of $2620\,km\,s^{-1}$ may correspond to all or any of NGC 3263 $(278°, 11°; 2741\,km\,s^{-1})$, NGC 3256 $(277°, 12°; 2410\,km\,s^{-1})$ or NGC 3250 $(275°, 15°; 2570\,km\,s^{-1})$. It is also not far from NGC 3347 $(276°, 19°; 2805\,km\,s^{-1})$ and the Antlia cluster at $(272°, 20°; 2849\,km\,s^{-1})$, but is probably distinct from these.

---

However, de Lapparent *et al.* (1986) have cautioned that the theory, as presented, does not appear to account for bubbles as large as $20\,h^{-1}\,Mpc$, since, then, the large thermal energy input required to drive the expansion of such bubbles should introduce detectable small-scale fluctuations into the microwave background spectrum. De Lapparent *et al.* (1986) also point out that it is important to determine whether these structures are actually portions of shells, or just filaments, since this also distinguishes between two different generic geometries.

[5]These "dispersions" represent the range of peculiar velocities that result from galaxies moving in gravitationally bound systems, or from large-scale coherent flows (that may also be gravitationally driven). Hence, maps in redshift space must be distortions of maps in three-dimensional space.

A cluster found at $(312°, 13°; 3027\,km\,s^{-1})$ forms a new neighbour to the group NGC 5090 $(308°, 19°; 3309\,km\,s^{-1})$, and probably includes the group NGC 5064 $(307°, 16°; 2809\,km\,s^{-1})$ in its membership. A cluster at $(246°, 8°; 1672\,km\,s^{-1})$ seems to lie neatly tucked alongside the massive group described by Kraan-Korteweg & Huchtmeier (1992) at $(246°, 6°; 1450\,km\,s^{-1})$ (which they interpret as forming part of a "wall" that crosses the Galactic Plane vertically at that longitude, and which may be the same as the group NGC 2559 $(246°, 5°; 1456\,km\,s^{-1})$. This cluster and the nearby group(s) are probably distinct, unless a very large cluster exists.

A probable cluster, centred near $(311°, 10°; 4014\,km\,s^{-1})$, has its nearest counterpart in NGC 5333, a group identified at $(312°, 13°; 2749\,km\,s^{-1})$. The two objects are probably distinct, considering the difference in their mean redshifts, indicating that a new cluster has been found. Another cluster, at $(245°, -6°; 1992\,km\,s^{-1})$, matches no previous cluster, and is also newly discovered. A large group with coordinates $(313°, 8°; 3731\,km\,s^{-1})$ also appears to have been discovered for the first time, the nearest group in the region , IC 4296, only as near as $(313°, 28°; 3622\,km\,s^{-1})$.

Among the many smaller groups, those situated near to previously identified neighbours are a group of two at $(237°, -14°; 1923\,km\,s^{-1})$ (near NGC 2280 at $(237°, -13°; 1732\,km\,s^{-1})$), a group of three at $(278°, 11°; 2920\,km\,s^{-1})$ (near NGC 3256 at $(277°, 12°; 2410\,km\,s^{-1})$), a group of two at $(283°, -13°; 1598\,km\,s^{-1})$ (near NGC 2836 at $(285°, -14°; 1357\,km\,s^{-1})$), a group of two at $(239°, -9°; 2631\,km\,s^{-1})$ (near NGC 2280 at $(237°, -13°; 1732\,km\,s^{-1})$), a group of two at $(234°, -14°; 2686\,km\,s^{-1})$ (near NGC 2207 at $(229°, -17°; 2559\,km\,s^{-1})$), and a group of two at $(278°, 15°; 2762\,km\,s^{-1})$, not far from Centaurus 27 (Raychaudhury, 1989) at $(275°, 15°, 2725\,km\,s^{-1})$ and near NGC 3347 at $(276°, 19°; 2805\,km\,s^{-1})$, NGC 3250 at $(275°, 15°; 2570\,km\,s^{-1})$, NGC 3263 at $(278°, 11°; 2741\,km\,s^{-1})$ and perhaps NGC 3256 at $(277°, 12°; 2410\,km\,s^{-1})$.

Other groups of two or three, to which more distant previous groups may (but probably do not) correspond, include a group of two at $(256°, 13°; 2166\,km\,s^{-1})$ (NGC 2663 is situated at $(256°, 6°; 1918\,km\,s^{-1})$), a group of two at $(302°, 9°; 1852\,km\,s^{-1})$ (NGC 4976 is at $(306°, 13°; 1261\,km\,s^{-1})$), a group of two at $(281°, -8°; 2163\,km\,s^{-1})$ (near NGC 2836 at

$(285°, -14°; 1357\,km\,s^{-1})$), a group of three at $(246°, 5°; 1003\,km\,s^{-1})$ (surrounded by NGC 2559 at $(246°, 5°; 1456\,km\,s^{-1})$ and two groups discovered by Kraan-Korteweg & Huchtmeier (1992) at $(246°, 3°; 750\,km\,s^{-1})$ and $(246°, 6°; 1450\,km\,s^{-1})$, respectively (the latter of which appears to correspond with NGC 2559)).

Finally, groups of three or more, not associated with previously identified groups or clusters, include the following: a group of five at $(285°, 9°; 2779\,km\,s^{-1})$, and ten groups of three at $(329°, -7°; 2740\,km\,s^{-1})$, $(327°, -9°; 3279\,km\,s^{-1})$, $(274°, 9°; 3435\,km\,s^{-1})$, $(282°, -7°; 2822\,km\,s^{-1})$, $(279°, -8°; 2885\,km\,s^{-1})$, $(323°, -6°; 4407\,km\,s^{-1})$, $(326°, 14°; 4693\,km\,s^{-1})$, $(333°, 14°; 4705\,km\,s^{-1})$, $(328°, -12°; 4983\,km\,s^{-1})$ and $(318°, 5°; 3026\,km\,s^{-1})$, respectively. Although even groups of three could be spurious, most or all of them are probably real, and newly discovered, in this survey. The results of this comparison are summarised in Table 6.3.

Scaramella *et al.* (1989), in an optical survey, found two substantial concentrations of galaxies near the Great Attractor, at $v \sim 3300\,km\,s^{-1}$ and at $v \sim 4500\,km\,s^{-1}$. Each of these concentrations can be resolved into two clusters[6], centred around each of these redshifts. Well beyond the present *IRAS* survey limit, they find a very rich concentration of galaxy clusters (at least twenty-four clusters, between 9900 & $20000\,km\,s^{-1}$, with the main complex of ten clusters (the "Shapley Concentration") centred at around $14,600\,km\,s^{-1}$), which may be influential in affecting Local Group velocities[7]. The centre of mass of all of these clusters lies about 10° away from the Faber & Burstein position of the Great Attractor. The ten Shapley clusters also lie within 10° of Shapley 8 (A3558) at $(\mathbf{l}, \mathbf{b}) = (312°, 31°)$. The four clusters that lie within $5000\,km\,s^{-1}$ appear in Appendix 9.1.

---

[6] Although Burstein *et al.* (1990) suggest that these two concentrations at $3300\,km\,s^{-1}$ and $4500\,km\,s^{-1}$ may be connected, given the attendant velocity dispersions. They also note that these clusters have a net peculiar motion of $\sim 750\,km\,s^{-1}$, consistent with the overall Great Attractor flow, making it unlikely that these clusters are themselves the gravitational source of the global infall.

[7] Although Rowan-Robinson *et al.* (1990) estimate that these contribute no more than 10% to the motion of the Local Group. Neither can these concentrations, by themselves, be the Great Attractor (see Burstein *et al.*, 1990), since the peculiar velocities of galaxy clusters in Centaurus fall to zero near $4500\,km\,s^{-1}$. If the concentration of clusters near $14000\,km\,s^{-1}$ were the Great Attractor, there would be a continuing rise in velocities out to the Shapley clusters.

Table 6.3: Old and New Groups in the Milky Way.

Note: Only groups with more than two members and centred within $cz \leq 6250\,km\,s^{-1}$ are included.

| Centre of Grouping | | $cz$ | Object | Similar | Newly |
|---|---|---|---|---|---|
| l | b | (km/s) | Description | Groups | Identified? |
| 277 | 12 | 2620 | cluster | NGC 3263; NGC3256; NGC 3250 near NGC 3347 and Antlia cluster | No |
| 312 | 13 | 3027 | cluster | includes NGC 5064; near NGC 5090 | Yes |
| 246 | 8 | 1672 | cluster | near KKH1 and NGC 2559 | Yes |
| 311 | 10 | 4014 | prob. cluster | near NGC 5333 | Yes |
| 245 | -6 | 1992 | cluster | none | Yes |
| 313 | 8 | 3731 | large group | near IC 4296 | Yes |
| 237 | -14 | 1923 | group | NGC 2280 | No |
| 278 | 11 | 2920 | group | NGC 3256 | No |
| 283 | -13 | 1598 | group | NGC 2836 | No |
| 239 | -9 | 2631 | group | near NGC 2280 | Yes |
| 234 | -14 | 2686 | group | NGC 2207 | No |
| 278 | 15 | 2762 | large group? | with NGC 3347; NGC 3250; NGC 3263 near NGC 3256 | No |
| 256 | 13 | 2166 | group | near NGC 2663 | Yes |
| 302 | 9 | 1852 | group | near NGC 4976 | Yes |
| 281 | -8 | 2163 | group | near NGC 2836 | Yes |
| 246 | 5 | 1003 | group | near NGC 2559=KKH3? and NGC KKH2 | Yes |
| 285 | 9 | 2779 | large group | none | Yes |
| 329 | -7 | 2740 | group | none | Yes |
| 327 | -9 | 3279 | group | none | Yes |
| 274 | 9 | 3435 | group | none | Yes |
| 282 | -7 | 2822 | group | none | Yes |
| 279 | -8 | 2885 | group | none | Yes |
| 323 | -6 | 4407 | group | none | Yes |
| 326 | 14 | 4693 | group | none | Yes |
| 333 | 14 | 4705 | group | none | Yes |
| 328 | -12 | 4983 | group | none | Yes |
| 318 | 5 | 3026 | group | none | Yes |

## 6.3 Comparison to the CfA Survey Data

Apart from the clustering program, there are two other approaches that can be adopted in testing whether the galaxies in the present sample are truly clustered. The first, a mainly theoretical approach, would be to carry out a $log\, n\ vs\ m$ approach for the narrow cone on the sky in the direction of an alleged cluster. Low numbers of galaxies however prevent this from being a useful approach for small regions of the sky. The $log\, n\ vs\ m$ carried out in Chapter 4 could only give an idea of whether a *general* over-density exists in the survey region, as it considered data for the whole survey region at once.

The second alternatve approach involves setting the distributions which seem to appear in the present data set against those arising from a galaxy survey carried on outside the zone of avoidance. First of all, the external data will not be affected to the same degree at optical wavelengths by extinction, or by the variability of extinction which occurs at low Galactic latitudes. No dark molecular clouds are found at $|\mathbf{b}| > 30°$ (Feitzinger & Stuwe, 1984).

Regions outside the zone of avoidance have been mapped in both optical and $IRAS$ surveys, and while the optical surveys are rather more complete, the same general clustering features have been seen in both types of survey. The clustering features seen outside the zone of avoidance are therefore regarded as being real, and as providing a reliable template to fit around the present survey plots. If over-dense regions in the external sample are observed to join smoothly with similar structures in the Milky Way sample, and if the voids are likewise continuous with the sparse regions in the current sample, one could be reasonably confident, at least to a first approximation, that any apparent concentrations would be real. Conversely, if structures are shown to be discontinuous at the boundary of the two samples, it will force the conclusion that incompleteness must have been unacceptably high, and that the filaments and voids which are described as passing behind the Milky Way are quite probably not real.

The data set chosen for this comparison is that of the second CfA survey. The objective of the CfA survey was to map the general galaxy distribution on the sky outside the Milky Way. This survey was an optical ground-based survey, which mapped the sky to a depth of

$cz \leq 15000\,km\,s^{-1}$, in bands of constant declination at all right ascensions. The survey is most complete at northern declinations, owing to most of the observing having taken place in the northern hemisphere. The second phase of the CfA survey extended observations further to the south, generating sufficient data for the present *IRAS* sample to be bracketed by the CfA data for $15° < |\mathbf{b}| < 25°$, between $210° < \mathbf{l} < 360°$.

To elicit fairer comparison, only the CfA data for $cz \leq 6500\,km\,s^{-1}$ has been retained. Because the CfA data is incomplete at $15° \geq |\mathbf{b}| \geq 10°$, and extremely so at $|\mathbf{b}| < 10°$, all data for $|\mathbf{b}| < 15°$ has also been left from the sample. Instead, the CfA survey for $15° < |\mathbf{b}| < 25°$ has been combined with the *IRAS* galaxy data from the present survey for $|\mathbf{b}| < 15°$, and a plot of the combined data appears below[8] as Figure 6.3.

The CfA survey data is, due to the much lower extinctions at the latitudes for which the data is retained, much more complete than the supplementary *IRAS* data, given that the completeness of the *IRAS* sample relies on the optical identification of galaxies on Schmidt plates in the highly obscured Milky Way, and also because of the difference in the observing wavelengths of the two surveys.

The large-scale features in the CfA survey are quite evident, even though information about the distribution of galaxies in redshift space is suppressed in the plot. Diagonal features approach the Milky Way ($|\mathbf{b}| < 15°$) from both hemispheres, although the different $\mathbf{l}$ and $\mathbf{b}$ scales in the plot make the large-scale features look narrower than they actually are on the sky. The continuation of these structures would cross the Galactic equator near the latitudes $\mathbf{l} = 240°$, $\mathbf{l} = 278°$ and $\mathbf{l} = 318°$, crossing the zone of avoidance at slightly different angles in each case.

The clustering program suggests, on the basis of a $14\,Mpc$ radius finding circle, that three large-scale associations may exist near $(\mathbf{l}, \mathbf{b}) = (240°, -2°)$, $(\mathbf{l}, \mathbf{b}) = (280°, 1°)$ and $(\mathbf{l}, \mathbf{b}) = (323°, -1°)$, at mean redshifts of $2195\,km\,s^{-1}$, $2625\,km\,s^{-1}$ and $3716\,km\,s^{-1}$, respectively.

[8] A similar plot, setting the CfA optical data against the current optically identified *IRAS* sample, but with Seyfert galaxies identified, is given in Appendix 9.2. Lines are drawn across both plots at $\mathbf{b} = 15°$ and $\mathbf{b} = -15°$ to make it clearer where the two data sets meet.

The extent of the first such structure, which is an association of eleven groups and clusters, is something like 50 $Mpc$, although the filament is not distinct along its whole length north of latitude 15°. The extent of the second large-scale structure, which is an association of fourteen groups and clusters, is approximately 60 $Mpc$, and that of the third, which involves twenty-one groups and clusters, about 54 $Mpc$. Additionally there are three other regions of smaller extent, one centred near $(\mathbf{l}, \mathbf{b}) = (331°, 13°)$, at a redshift of 4650 $km\,s^{-1}$ (four groupings), another near $(\mathbf{l}, \mathbf{b}) = (287°, 12°)$, at a redshift of $\sim$ 5300 $km\,s^{-1}$ (three groupings), and the third near $(\mathbf{l}, \mathbf{b}) = (278°, -12°)$, near 6400 $km\,s^{-1}$ (two groups). This is approximately in agreement with what might have been expected from the CfA survey data, without the new $IRAS$ data, and encourages the belief that the apparent density fluctuations in the $IRAS$ sample are indeed intrinsic to the sample.

Between $\mathbf{l} = 210°$ and $\mathbf{l} = 240°$, the $IRAS$ sample is quite sparse. This would seem to be significant, because the extinction for the same region is the *lowest* for the whole Milky Way. The CfA survey also finds an under-density at these longitudes, which extends to $\mathbf{b} \sim 30°$ in the north, and to $\mathbf{b} \sim 25°$ in the south. It is likely that a large void occupies this whole domain and that a "wall", defining the edge of this void, is that structure which propagates across the Milky Way near $\mathbf{l} = 240°$, and which includes the large groups or clusters in the Puppis region.

The two low-density regions which cross between $\mathbf{l} = 250° - 270°$ and $\mathbf{l} = 285° - 305°$ have number densities which are only a little lower than the $IRAS$ survey average, and they are not as under-dense as the peripheral longitudes. Consequently, they are probably not so under-dense as to be true voids.

Extensions do seem to be in evidence at the three places in the three originally predicted areas of the Milky Way, and the broadest but most diffuse of these is the Puppis filament near $\mathbf{l} = 240°$. The Vela filament passes through the Hydra cluster, at $(\mathbf{l}, \mathbf{b}) = (270°, 26°)$. The over-density seen down to $\mathbf{b} = 5°$ in both hemispheres, near $\mathbf{l} = 320°$, is the most crisply defined, probably because the extension of this feature in the plot of the CfA sample is so strongly emphasized in both hemispheres. The over-density is also emphasized because so many $IRAS$ galaxies are detected there at low Galactic latitudes, despite the $(1\,\sigma)$ above-average extinctions

at those longitudes.

There is, therefore, every confidence, based on the extended features in the optically-based CfA survey for $|\mathbf{b}| > 15^{\circ}$, that the three main regions of over-density which seem to appear in the *IRAS* survey do, indeed, represent the true location of over-densities of galaxies behind the Milky Way, and the voids likewise. Figures 6.4 - 6.12 plot out the three extended features as viewed in the $(\mathbf{l}, \mathbf{b})$ plane, and in the $cz$ versus $\mathbf{b}$ and $cz$ versus $\mathbf{l}$ planes.

## 6.4 Superclusters in Vela and Centaurus?

The clustering program has also reported the possibility of at least two superclusters which run through, or into, the region obscured by the Milky Way. The first, centred near $(\mathbf{l}, \mathbf{b}) = (280^{\circ}, 1^{\circ})$, and crossing the Galactic equator at an angle (parallel to a line of constant longitude) of $\sim 27^{\circ}$, lies mainly in the constellation of Vela. It has a mean redshift of $2625\, km\, s^{-1}$. The fourteen associated groups and clusters form a structure which stretches across $\sim 20\, Mpc$ within the limits of the Milky Way. This elongated structure extends initially from a group near $cz = 1009\, km\, s^{-1}$, then through a set of clusters and large groups scattered in both hemispheres between redshifts of $2163\, km\, s^{-1}$ and $2920\, km\, s^{-1}$, and accompanied by ten groups distributed between $\mathbf{l} = 272^{\circ}$ & $295^{\circ}$ and $\mathbf{b} = -14^{\circ}$ and $12^{\circ}$, and finally to a group found at $cz = 3921\, km\, s^{-1}$, which marks its other extremity.

The structure is about $(2929/73 = \sim 40)\, Mpc$ deep, $\sim 18^{\circ}$ wide (at $2625\, km\, s^{-1}$, this is about $11\, Mpc$), and stretches some $31^{\circ}$ ($20\, Mpc$) obliquely across Galactic latitudes. Outside the zone of avoidance, the Vela filament flows through the Hydra cluster, seen in the CfA plot near $(270^{\circ}, 27^{\circ})$. There seems to be no distinct southern latitude continuation of the structure below $\sim -20^{\circ}$. The northern extension into the CfA data region accounts for perhaps another $25\, Mpc$, making the filament $\sim 45\, Mpc$ long, in total.

The second possible supercluster is centred near $(323^{\circ}, -1^{\circ})$, in the direction of the constellation Centaurus, and has a central redshift of $3716\, km\, s^{-1}$. It incorporates twenty-one

groups and clusters, distributed between $1103\,km\,s^{-1}$ & $5239\,km\,s^{-1}$, spread along $\sim 35°$ ($\sim 31\,Mpc$) of sky behind the Milky Way, with clusters and large groups centred at 3027, 3731 and $4014\,km\,s^{-1}$, respectively, surrounded by eighteen groups. The large group near $3731\,km\,s^{-1}$ marks out the approximate centre of this association, as it passes behind the Milky Way. The structure is quite narrow - about 8° in width ($\sim 7\,Mpc$) - but quite extended into redshift space, spanning a range of $4136\,km\,s^{-1}$ ($\sim 56\,Mpc$). This gives it the appearance of a sheet, or "wall", of galaxies.

The Centaurus supercluster crosses the Milky Way at an angle of $\sim 41°$, and, in the CfA data, continues to greater southern and northern latitudes, until finally spreading across $> 90°$ on the sky, extending in the north in the general direction of the Great Attractor, the centre of which Faber & Burstein (1988) give as $(309°, 18°)$.

The CfA survey data certainly seems to contain a galaxy over-density near these coordinates: the concentration of clusters near $(303°, 21°)$, which combine to produce probably the most pronounced feature of the CfA plot, appears to fall within the broad domain of the Great Attractor ("GA"). Indeed, the mean redshift of the supercluster ($3731\,km\,s^{-1}$) falls towards the centre of the redshift domain ($2000 - 6000\,km\,s^{-1}$) of the GA. The Centaurus concentrations, near $4300\,km\,s^{-1}$, are at the same redshifts as a group and probable cluster in the present survey, found at lower latitudes, reinforcing the picture of a continuity of the northern Centaurus system of clusters and groups across the Milky Way, and of their inclusion into a supercluster structure which passes behind the Milky Way near $l = 320°$, and which lies adjacent to the region described as the Great Attractor.

The Centaurus sheet is also more flattened than the structure which crosses in Vela. The concentrations which lie adjacent to the Centaurus supercluster, at slightly higher average Galactic longitudes, are probably a series of clusters which are falling into the Centaurus supercluster because of the large over-density in the Centaurus region. They are not really distant enough from the Centaurus clusters to be described as a separate association.

At the distance of the Virgo cluster, these two large structures would both subtend angles

well in excess of 90° on the sky. By the definitions presented at the beginning of this chapter, the two structures are both at the scale of superclusters.

The Vela supercluster is flanked by something of a void between $\mathbf{l} = 250° - 275°$ for $-15° < \mathbf{b} < 5°$, and comes close to being attached to the Puppis filament near $\mathbf{b} = 25°$. Bridges seem to exist (see CfA data) near $\mathbf{b} = 25°$ and $\mathbf{b} = 32°$ (and possibly near $\mathbf{b} = 10°$), spanning $\mathbf{l} = 245° - 290°$, $260° - 295°$ and $270° - 290°$, respectively, and these possibly link the Puppis filament, near $\mathbf{l} = 245°$, to the Vela and Centaurus superclusters, in a rung-like manner.

Figure 6.3: Combination of CfA and *IRAS* survey data.

The CfA survey data has been cut to $cz \leq 6500\, km\, s^{-1}$ for $|\mathbf{b}| > 15^{o}$ and has been supplemented by *IRAS* data to the same redshift limit.

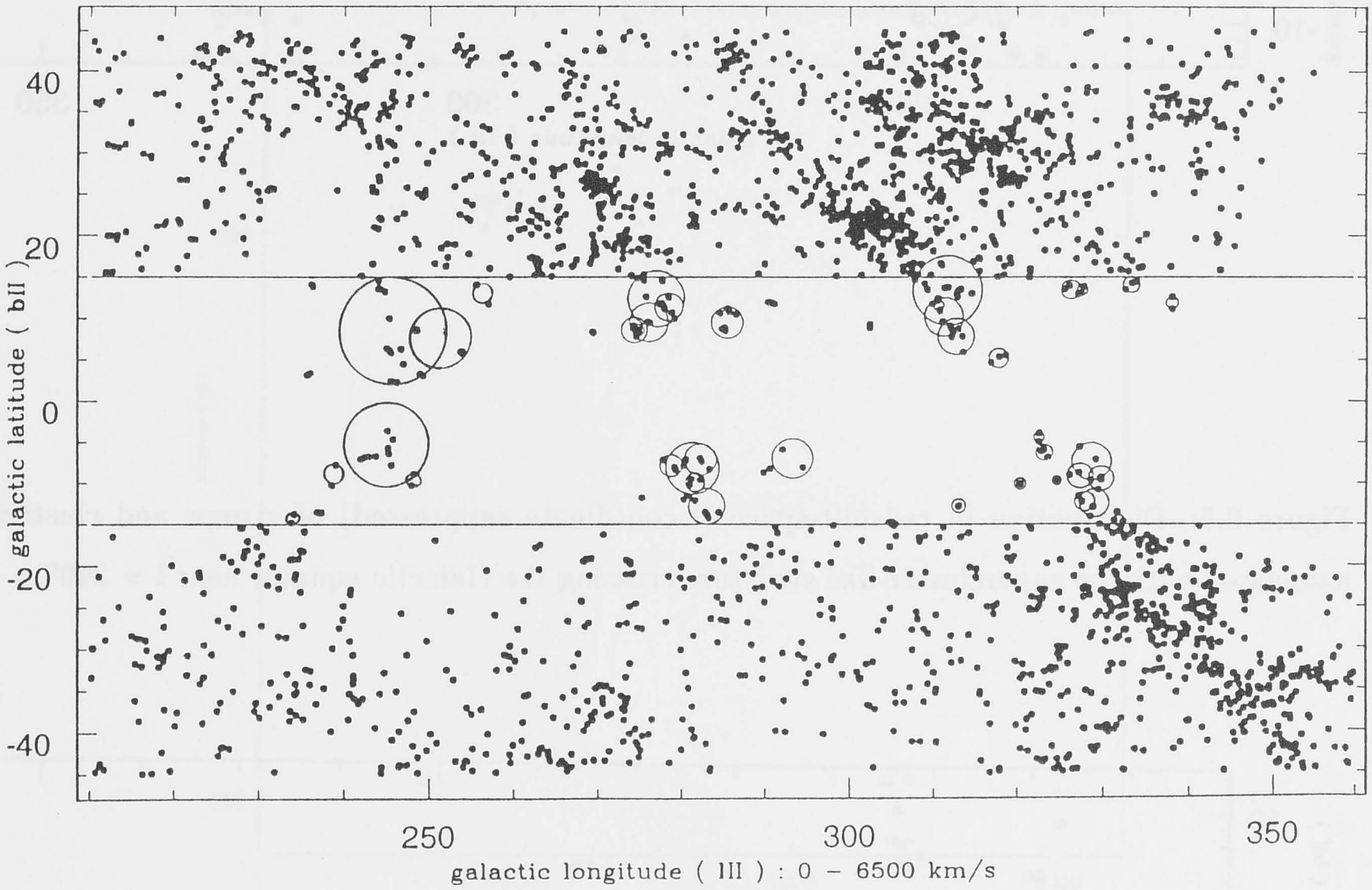

Figure 6.4: Distribution in the $(\mathbf{l}, \mathbf{b})$ plane of groups and clusters associated with the supercluster-like structure crossing the Galactic equator near $\mathbf{l} = 240°$.

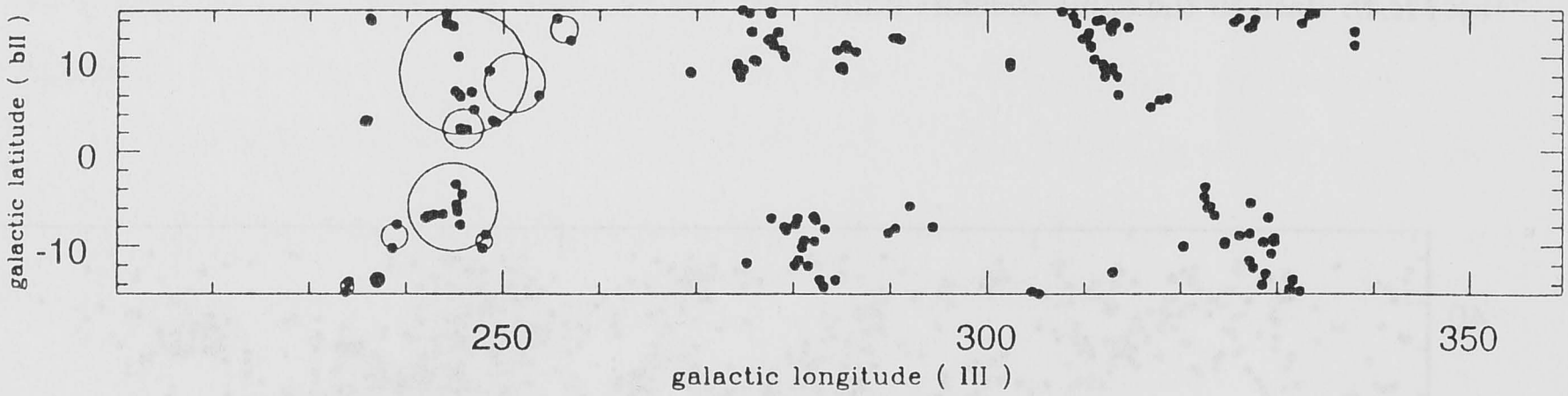


Figure 6.5: Distribution in redshift-space (**l** coordinate suppressed) of groups and clusters associated with the supercluster-like structure crossing the Galactic equator near $\mathbf{l} = 240°$.

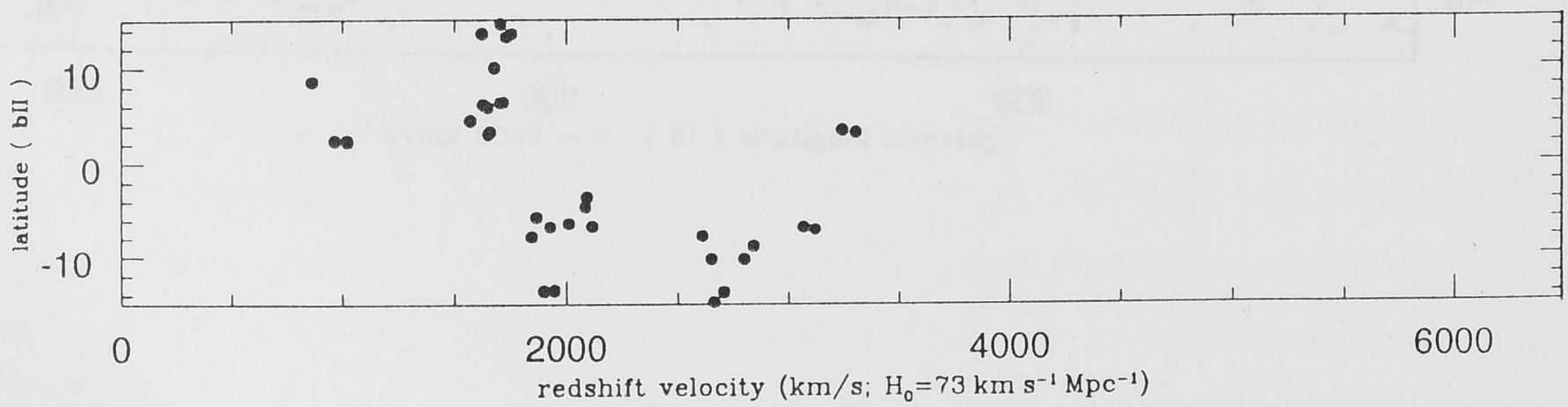

Figure 6.6: Distribution in redshift-space (**b** coordinate suppressed) of groups and clusters associated with the supercluster-like structure crossing the Galactic equator near $l = 240°$.

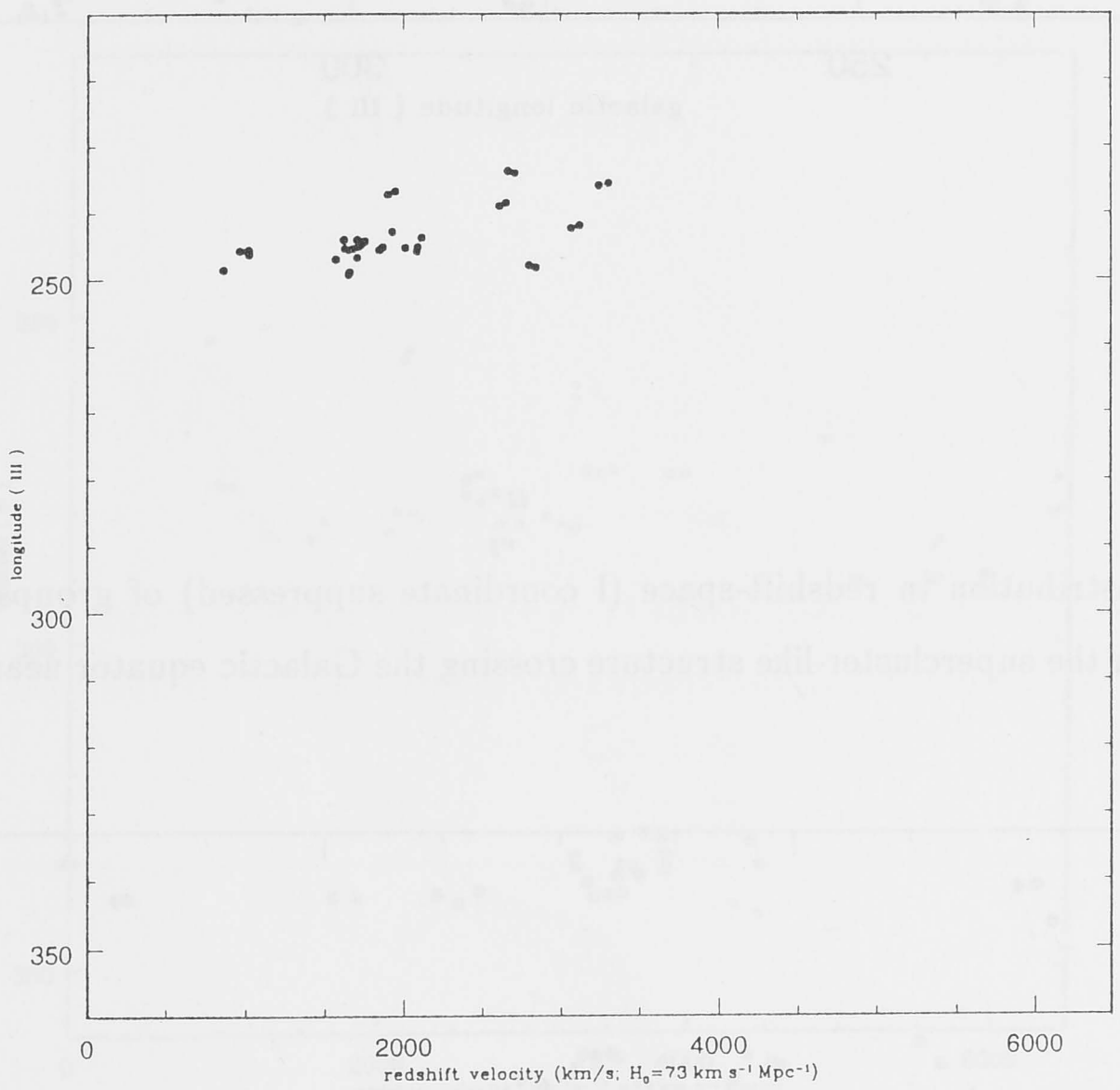

Figure 6.7: Distribution in the $(\mathbf{l}, \mathbf{b})$ plane of groups and clusters associated with the supercluster-like structure crossing the Galactic equator near $\mathrm{l} = 280^{\mathrm{o}}$.

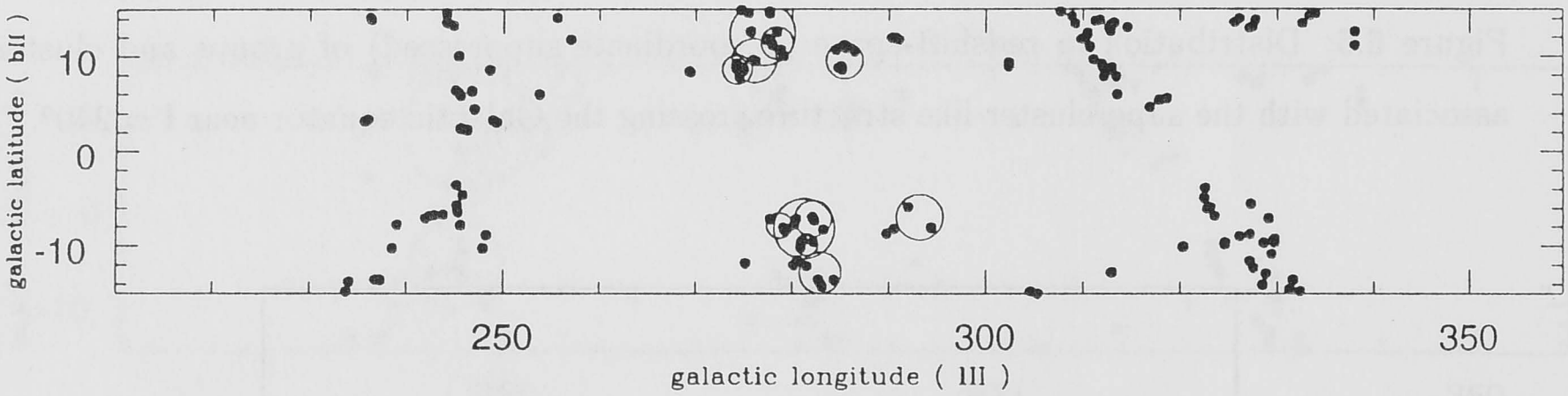


Figure 6.8: Distribution in redshift-space (l coordinate suppressed) of groups and clusters associated with the supercluster-like structure crossing the Galactic equator near $\mathrm{l} = 280^{\mathrm{o}}$.

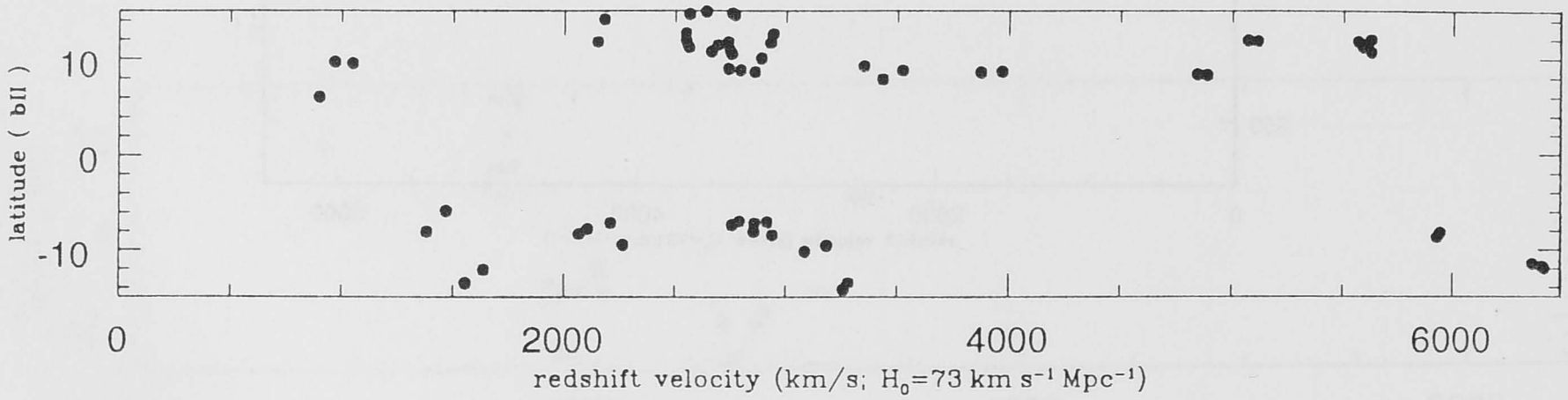

Figure 6.9: Distribution in redshift-space (**b** coordinate suppressed) of groups and clusters associated with the supercluster-like structure crossing the Galactic equator near $\mathbf{l} = 280°$.

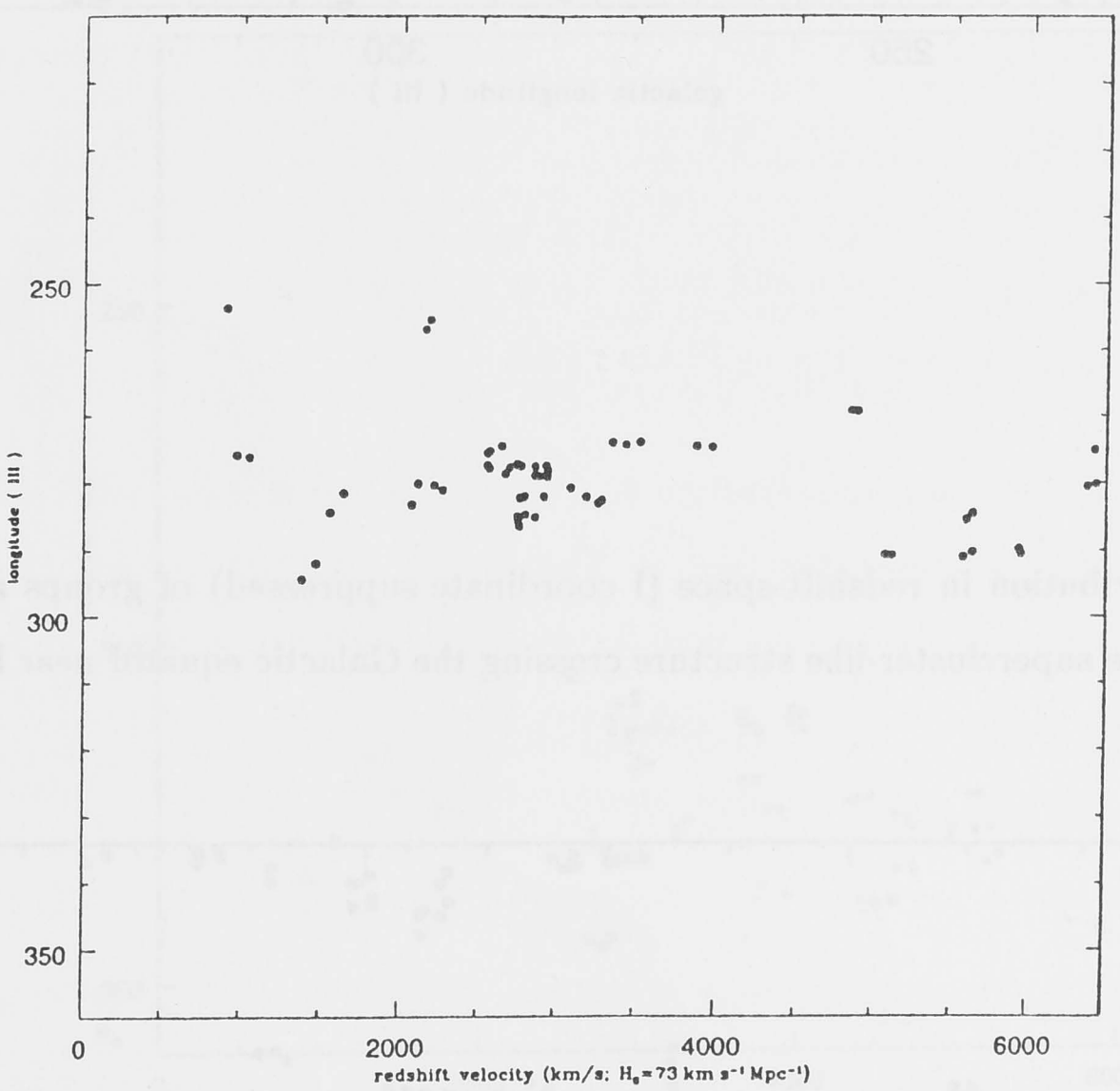

Figure 6.10: Distribution in the $(\mathbf{l}, \mathbf{b})$ plane of groups and clusters associated with the supercluster-like structure crossing the Galactic equator near $\mathbf{l} = 320°$.

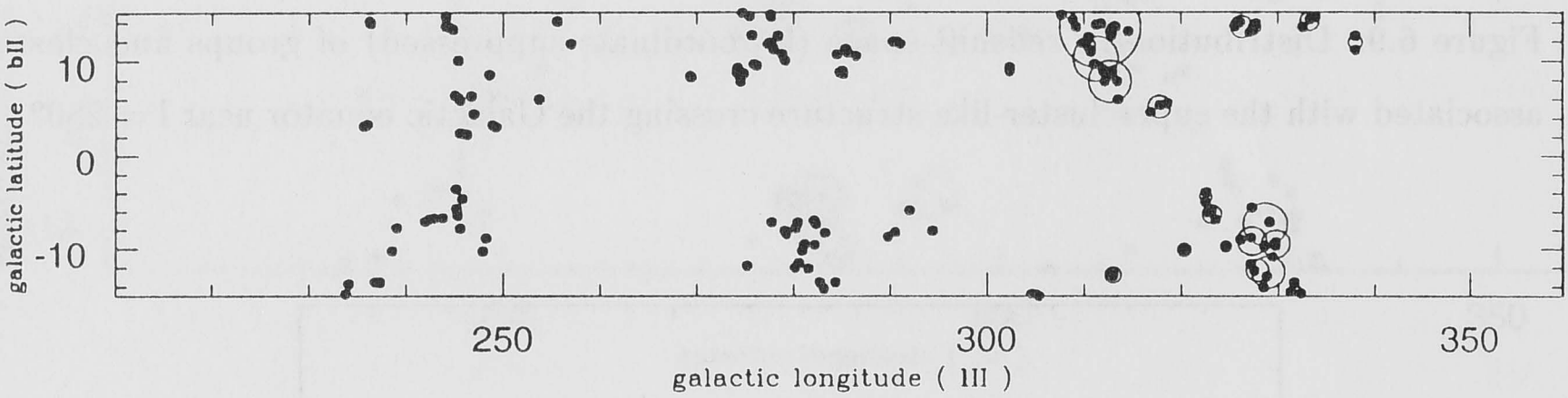


Figure 6.11: Distribution in redshift-space (**l** coordinate suppressed) of groups and clusters associated with the supercluster-like structure crossing the Galactic equator near $\mathbf{l} = 320°$.

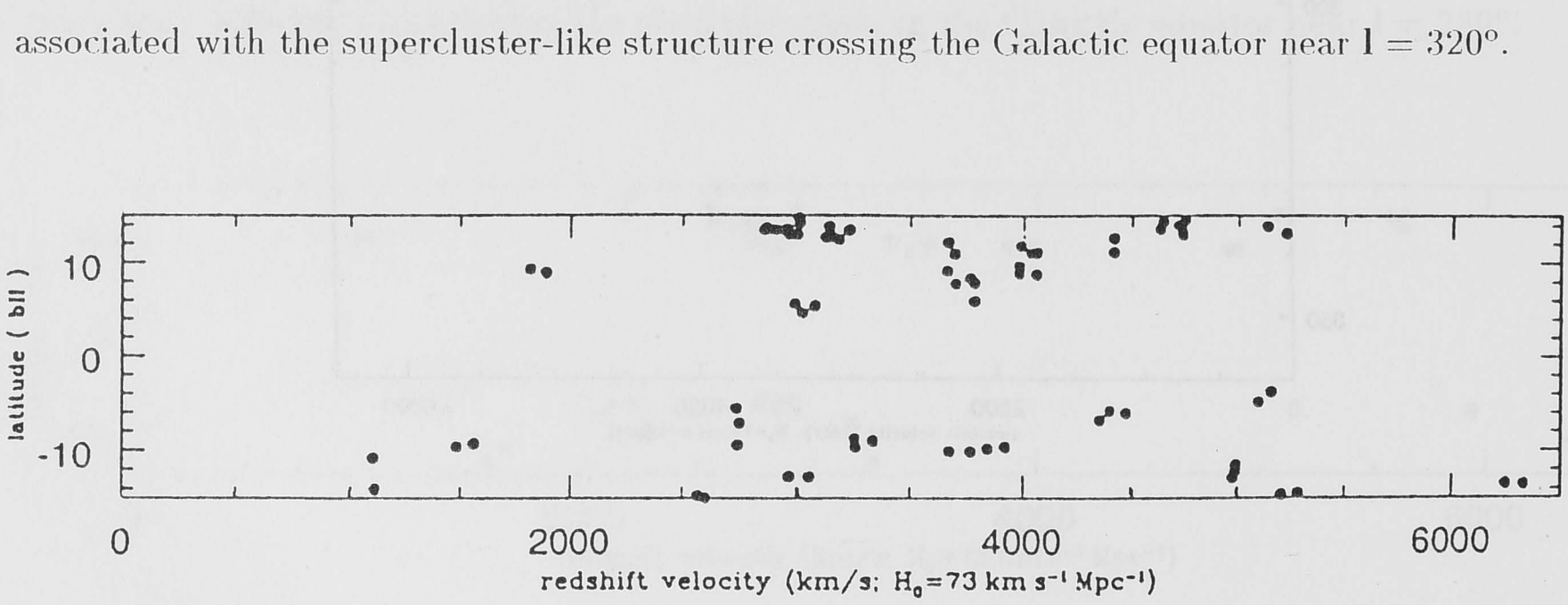

Figure 6.12: Distribution in redshift-space (**b** coordinate suppressed) of groups and clusters associated with the supercluster-like structure crossing the Galactic equator near $l = 320°$.

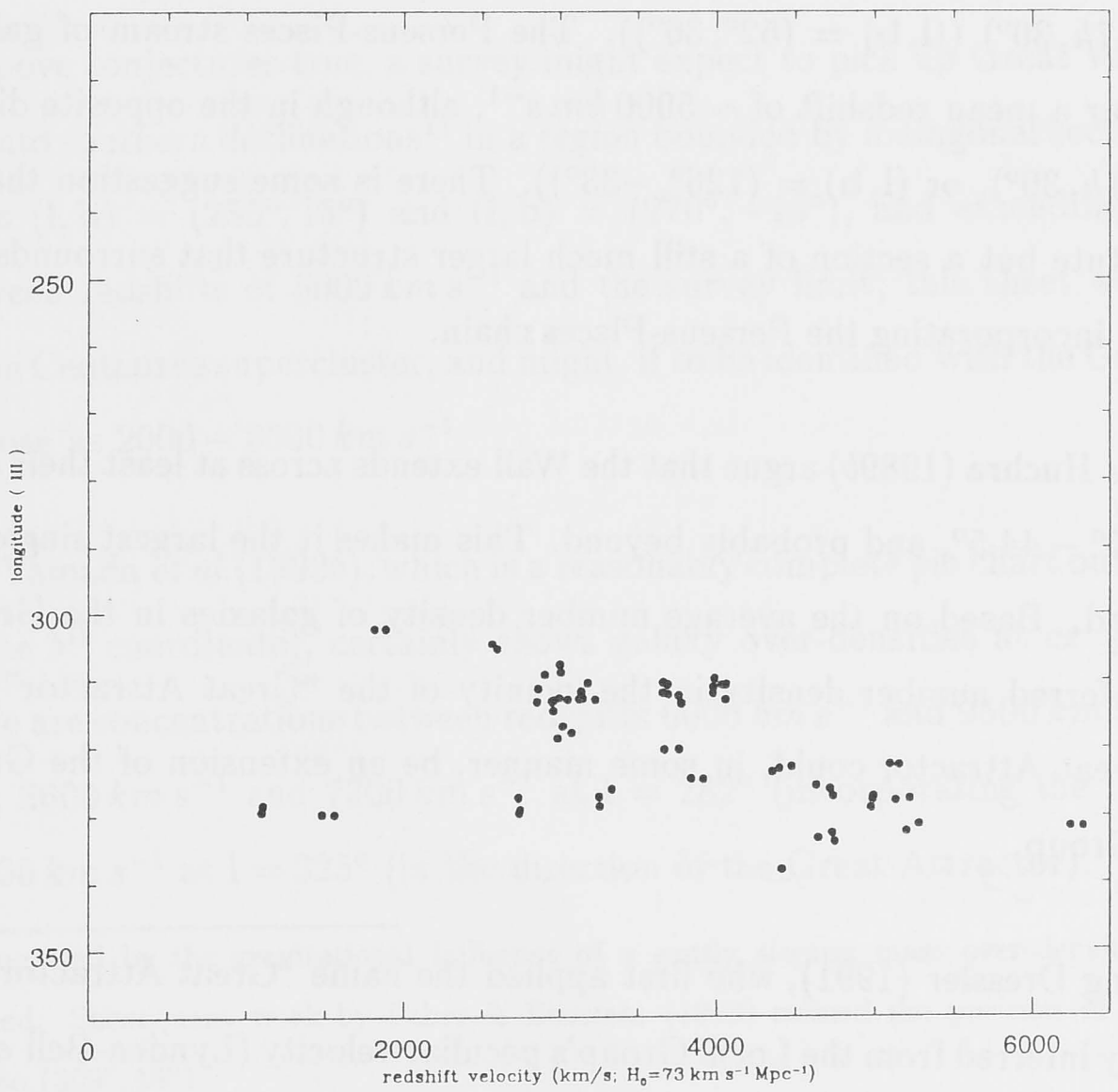

## 6.5 The "Great Wall" at Southern Latitudes?

Many galaxies lie in narrow sheet-like structures, and the largest such sheet detected so far is the "Great Wall". The minimum size of this structure is $60\,h^{-1}\,Mpc \times 170\,h^{-1}\,Mpc$ ($h = H_0$, in units of $100\,km\,s^{-1}\,Mpc^{-1}$) - i.e. for $H_0 = 73\,km\,s^{-1}\,Mpc^{-1}$, the extent of the Great Wall is $44\,Mpc \times 124\,Mpc$.

A good illustration of the Great Wall (in a right ascension versus redshift plot; declination suppressed) can be seen in Figure 5 of Geller & Huchra (1989*b*), which also plots the Perseus-Pisces chain of galaxies. The Great Wall of galaxies extends from an initial distance of $\sim 5000\,km\,s^{-1}$, near $(\alpha, \delta) = (9h, 30°)$ $((\mathbf{l}, \mathbf{b}) = (196°, 40°))$, to $\sim 12000\,km\,s^{-1}$ near $(\alpha, \delta) = (17h, 30°)$ $((\mathbf{l}, \mathbf{b}) = (52°, 36°))$. The Perseus-Pisces stream of galaxies is similarly situated near a mean redshift of $\sim 5000\,km\,s^{-1}$, although in the opposite direction in the sky ($(\alpha, \delta) = (1h, 30°)$, or $(\mathbf{l}, \mathbf{b}) = (126°, -33°)$). There is some suggestion that the Great Wall may constitute but a section of a still much larger structure that surrounds the Local Group like a shell, incorporating the Perseus-Pisces chain.

Geller & Huchra (1989*b*) argue that the Wall extends across at least their survey declination range of $8.5° - 44.5°$, and probably beyond. This makes it the largest single cosmic structure yet identified. Based on the average number density of galaxies in the Great Wall, and the similarly inferred number density in the vicinity of the "Great Attractor", it is conceivable that the Great Attractor could, in some manner, be an extension of the Great Wall towards the Local Group.

Following Dressler (1991), who first applied the name "Great Attractor" to the supposed over-density inferred from the Local Group's peculiar velocity (Lynden-Bell *et al.*, (1989)[9]), the

[9]Peculiar velocities are obtained by subtraction of the general cosmological expansion from galaxy velocities. Peculiar velocities may also decompose into more than one vector (see Visvanathan, 1990). The distances and velocities of 400 elliptical galaxies, out to $\sim 6000\,km\,s^{-1}$, are found to be skewed in such a way that the equivalent of an attracting mass of $5.4 \times 10^{16}\,M_\odot$ seems to be present, centred approximately on the coordinates $(307°, 9°)$, at $R_{\rm m} = 4350 \pm 350\,km/s$. Lynden-Bell *et al.* (1989) reported this result in terms of the detection of significant quadrupole terms in the flow of the large-scale streaming motion towards Virgo, suggesting that

Great Attractor describes the entire steradian on the sky centred around $(\mathbf{l}, \mathbf{b}) = (310°, 20°)$, at a depth of $2000 - 6000\, km\, s^{-1}$. It includes the Centaurus concentration, the Centaurus clusters and the Pavo-Indus-Telescopium clusters. The "Great Attractor" is also sometimes visualized as a thickening of the Supergalactic plane in this direction[10].

Strong number density enhancements are seen in this general direction in both the CfA optical and *IRAS* infra-red surveys, even without the possible contribution of new groups and clusters behind the Milky Way. The centre of the Centaurus concentration lies at $\sim 4300\, km\, s^{-1}$. If the GA is situated as a "dent" in the Great Wall, it may be that it is contributing to an infall of Great Wall galaxies into the Centaurus region. This notion is investigated in Dressler & Faber (1990), but is far from conclusive.

Were the above conjectures true, a survey might expect to pick up Great Wall galaxies as they intruded into southern declinations[11] in a region bounded by a diagonal section connecting the coordinates $(\mathbf{l}, \mathbf{b}) = (255°, 15°)$ and $(\mathbf{l}, \mathbf{b}) = (270°, -15°)$, and extending eastwards to $\mathbf{l} = 360°$, between redshifts of $5000\, km\, s^{-1}$ and the survey limit; this sheet would approach from beyond the Centaurus supercluster, and might, if to be identified with the Great Attractor, extend to as close as $2000 - 3000\, km\, s^{-1}$.

Figure 9 of Yamada *et al.*(1993*b*), which is a reasonably complete pie chart out to $10000\, km\, s^{-1}$ (suppressing the $b^{\mathrm{II}}$ coordinate), certainly shows galaxy over-densities at $cz \geq 5000\, km\, s^{-1}$. Most noticeable are concentrations between redshifts $6000\, km\, s^{-1}$ and $9500\, km\, s^{-1}$ at $\mathbf{l} = 245°$ (near Puppis), $3600\, km\, s^{-1}$ and $7300\, km\, s^{-1}$ at $\mathbf{l} = 282°$ (incorporating the Hydra cluster), and $2400 - 5300\, km\, s^{-1}$ at $\mathbf{l} = 325°$ (in the direction of the Great Attractor).

---

this flow was generated by the gravitational influence of a gently sloping mass over-density centred at the position mentioned. Subsequent work by Faber & Burstein (1988) refined the position of the centre of the Great Attractor to $(309°, 18°)$.

[10] However, Rowan-Robinson *et al.* (1990) argue that the galaxy concentrations already identified in Hydra, Centaurus and Pavo are adequate to account for the peculiar motion of the Local Group, as inferred from the microwave background dipole, and argue from this that the hypothetical hidden mass of galaxies near Centaurus may not need to exist.

[11] In the all-sky $1.2\, Jy$ survey of Fisher *et al.*, (1995), the Great Wall is identified as the over-density which extends out from $0 - 6000\, km\, s^{-1}$ in the direction of the SGP.

Because of the redshifts at which these over-densities occur, it is tempting to suggest that these are indeed sections of the Great Wall, as it stretches across into southern declinations. Near the Great Attractor region, this sheet would already have reached as far as 65° southern declination, in which case it would have extended itself over 110° in a north-south direction, or across 60% of the sky, between right ascensions of $\sim 6h$ and $\sim 19h$. However, Yamada's plot is of *IRAS* galaxies, while that of Geller & Huchra (1989*b*) is of optical CfA survey galaxies, and these comparisons might still be invalid at some level.

The results of galaxy surveys in the regions defined by $(\alpha, \delta) = (8.5h, 9°)$ and $(\alpha, \delta) = (10h, -5°)$, across to $(\alpha, \delta) = (14h, 9°)$ and $(\alpha, \delta) = (19h, -35°)$, will first need to be obtained and analyzed, before the question of the possible continuity of the Great Wall into southern declinations can be addressed with any further evidence.

While a more solid understanding may be required regarding the different selection effects pertaining to the CfA and *IRAS* samples, most investigators remark that *IRAS* samples, albeit tending to sample only the brighter spiral galaxies, seem to emulate the main features in optical surveys very well[12]. Babul & Postman (1990) find that *IRAS* galaxies are, on the average, clustered less strongly than optical galaxies. If clustering is therefore evident in an *IRAS* survey, it seems that much more likely to be real.

[12] *IRAS* galaxies also appear to trace mass in the universe quite well, especially because their surface-density distribution on the sky can be fitted by a dipole, the axis of which coincides with that of the cosmic microwave background.

# Chapter 7

# Conclusions

## 7.1 Summary of Results

The data in the CGMW brought to light two new concentrations of galaxies (Saito *et al.*, 1990, 1991) - namely the Monoceros supercluster near $(\mathbf{l}, \mathbf{b}) \approx (225°, 5°)$ at $120h^{-1}\,Mpc$ (Yamada & Saito, 1993) and the Puppis large groups centred around $(\mathbf{l}, \mathbf{b}) \approx (240°, 0°)$ at $20h^{-1}\,Mpc$ (Kraan-Korteweg & Huchtmeier, 1992; Yamada *et al.*, 1993*b*).

The current survey detects little, if anything, of the Monoceros supercluster, which begins at a redshift of $\sim 10000\,km\,s^{-1}$, but sample incompleteness beyond $\sim 7500\,km\,s^{-1}$ is most probably responsible for this. For the same reason, neither is anything of the Shapley Concentration detected in Centaurus. The Puppis large groups do, however, appear between $\sim 1000\,km\,s^{-1}$ and $\sim 3300\,km\,s^{-1}$, spread loosely between $\pm 10°$ of the Galactic equator around $\mathbf{l} \sim 240°$. Two new groups and two new clusters have been discovered in this area. Although, as pointed out in Chapter 1.2.1, it may be that one is attempting to draw conclusions on the basis of something like 55% of all *IRAS* galaxies, the general alignment with much more well-defined structures seen at higher latitudes in optical surveys lends weight to the results presented here.

An outline of the distribution of *IRAS* galaxies has now been determined down to $|\mathbf{b}| > 5°$. This study has also uncovered a number of new groups and clusters, all listed in Table 6.3; ten of these are located between $\mathbf{l} = 310°$ and $\mathbf{l} = 335°$, in the general direction of Centaurus and

the Great Attractor. NGC 5064, a known group near $(\mathbf{l}, \mathbf{b}) = (312°, 13°)$, has been shown to be part of a cluster at the same coordinates with a similar average redshift. All of the groups and clusters in this area are found in three bands delimited by $2740 - 3279\,km\,s^{-1}$, $3731 - 4014\,km\,s^{-1}$ and $4407 - 4983\,km\,s^{-1}$. The large groups in the direction of the constellation Puppis approach the scale of a cluster ($> 1500\,km\,s^{-1}$ in diameter). A number of small groups of galaxies are also found out to $70\,h^{-1}\,Mpc$ but the identifications of these are less reliable.

Although the *IRAS* galaxies seem, on the whole, to be uniformly distributed behind the Milky Way, and despite the fact that number densities approach the Rowan-Robinson all-sky average in the regions of lowest Galactic extinction, definite *over*-densities appear near $\mathrm{l} = 240°$, $\mathrm{l} = 280°$ & $\mathrm{l} = 330°$, where large-scale filamentary structures cross the galactic equator at various angles. These over-dense regions also seem to form boundaries to neighbouring regions which are *under*-dense (with respect to the average density), and therefore possible voids. If regions in which the *IRAS* galaxy density falls below 20% of the overall mean (taking account of variations in the extinction) are labelled as voids, then there appears to be a void centred near $(\mathbf{l}, \mathbf{b}) = (235°, 0°)$ (at $cz \sim 1000\,km\,s^{-1}$, crossing the Milky Way), another at $(\mathbf{l}, \mathbf{b}) = (250°, -7°)$ (at $cz \sim 1250\,km\,s^{-1}$, mainly at southern latitudes), one crossing the Milky Way at $\mathrm{l} \sim 290°$ at $750\,km\,s^{-1} \leq cz \leq 1000\,km\,s^{-1}$, possibly another at $\mathrm{l} \sim 315°$ near the galactic equator at a redshift of $\sim 750\,km\,s^{-1}$, and two more near $\mathrm{l} = 345°$ (out to $2250\,km\,s^{-1}$) and $\mathrm{l} = 355°$ (out to $3250\,km\,s^{-1}$).

In brief, grouping and clustering are clearly in evidence out to a radius of $50\,h_{73}^{-1}\,Mpc$, and within this distance several small voids are also detected. The groups and clusters which constitute the three large filaments crossing the Milky Way all fall within this limit. These structures appear to be continuations of structures seen in both optical and *IRAS* surveys at higher latitudes. Given that the regions of enhanced density in the large-scale distribution of *IRAS* galaxies are the same as those enhanced in optical galaxy distributions (Saunders *et al.*, 1991; Scharf *et al.*, 1992; Strauss *et al.*, 1992*a*), it seems exceedingly likely that the three filamentary structures in CfA survey (1989) are part of large-scale coherent structures which run right across the Milky Way.

The density enhancements of the population of bright $IRAS$ galaxies having $f_{60} > 1.936\,Jy$ occur in the same places as in the population of galaxies for which $f_{60} > 0.6\,Jy$. This suggests that the filamentary structures around the Milky Way region are located mainly within $cz \sim 6000\,km\,s^{-1}$, because clustering of the bright $IRAS$ galaxies is only seen at $cz \leq 6000\,km\,s^{-1}$ in the $f_{60} > 1.936\,Jy$ survey (Strauss *et al.*, 1992*a*). Both the Supergalactic-plane filament and the Hydra filament[1] are seen as a clustering of the bright $IRAS$ galaxies for $5° < |\mathbf{b}| < 15°$ (Strauss *et al.*, 1992*a*) in the velocity ranges $cz < 3000\,km\,s^{-1}$ and $3000 < cz < 6000\,km\,s^{-1}$ (see their Fig. 1). According to Dressler (1991), the number density of galaxies is high around $cz = 3000 - 5000\,km\,s^{-1}$ in the Supergalactic plane near the Milky Way. The Hydra cluster in the Hydra filament is at $cz \sim 3500\,km\,s^{-1}$ (Kraan-Korteweg, 1989). The bright $IRAS$ galaxies appear at $cz < 3000\,km\,s^{-1}$ only in the Puppis filament region (Strauss *et al.*, 1992*a*), and the Puppis cluster is at $cz \sim 2000\,km\,s^{-1}$ (Kraan-Korteweg & Huchtmeier, 1992). The Puppis filament is located nearer to our Galaxy than the Hydra filament.

From the combined CfA and Yamada data it is apparent that a narrow structure, whose average width is about three to four cluster widths, angles across the Milky Way near $\mathbf{l} = 320°$ in Centaurus. The approximate dimensions of this structure are $80\,h^{-1}\,Mpc \times 56\,h^{-1}\,Mpc$. The Vela filament is a much less densely populated sheet of galaxies with approximate dimensions of $45\,h^{-1}\,Mpc \times 40\,h^{-1}\,Mpc$, and is extended mainly to the north. The filament through the Puppis region is approximately $16\,h^{-1}\,Mpc \times 35\,h^{-1}\,Mpc$, and extends $\sim 9\,h^{-1}\,Mpc$ across its narrow dimension, but is much less flattened than the other two filaments.

The Supergalactic plane, which crosses the Milky Way in Centaurus, is like a wall of galaxies. Shaver (1990) estimated that its dimension may be as large as $\sim 100\,h^{-1}\,Mpc$. This survey confirms that it is probably larger than $\sim 80\,h^{-1}\,Mpc$ and so approaches about half the size of the Great Wall in the "CfA slice" (Geller & Huchra, 1989*b*); it looks like a filament to us because we lie in or near the plane of the galaxies. The Great Attractor region ($\mathbf{l} \sim 315°$, $\mathbf{b} \sim 15°$) may correspond to a large supercluster in the "Supergalactic-plane wall" - in the same way as the Coma concentration is a supercluster in the Great Wall. Just as some filamentary

[1]Referred to as the "Vela" filament in this study.

structures spread out from the Coma region delineating various sizes of void in the CfA slice, the Hydra filament and the Puppis filament seem to be filaments which spread out of the Supergalactic plane in the north, delineating voids of several tens of $h^{-1}\,Mpc$ in diameter.

Although the filament running across the Milky Way in Vela is more sparsely populated than that crossing in Centaurus, and contains far less overall mass, it nevertheless has dimensions which suggest that it too is a supercluster.

Such walls might be connected into structures at an even larger scale (Tully, 1987)[2]. Tully (1987) makes a case for the association of superclusters into vast "supercluster complexes" (SCCs) at scale-lengths of $\sim 300\,h_{75}^{-1}\,Mpc$, the individual superclusters being separated on average by something like $40\,h_{75}^{-1}\,Mpc$. He concludes that there are five such complexes out to $z < 0.1\,c$. One of these, which he refers to as the Pisces-Cetus supercluster complex[3], extends to nearly $300\,h_{75}^{-1}\,Mpc$ in the directions of the Supergalactic X and Y axes and $\sim 100\,h_{75}^{-1}\,Mpc$ along the SGZ axis. Within the $80\,h_{75}^{-1}\,Mpc$ of the present survey, it includes part of the southern extension of the Virgo-Hydra-Centaurus supercluster, about half of the Perseus-Pegasus chain and some intrusion of the Indus supercluster.

Tully (1987) believes that the Virgo-Hydra-Centaurus supercluster will eventually be found to be connected to the Pisces-Cetus complex, although this has not been proven as yet. He bases his conviction on the coincidence between the plane defined by the nearby (within $40\,h_{75}^{-1}\,Mpc$) Virgo-Hydra-Centaurus galaxies and the plane of flattening of the Pisces-Cetus SCC. The independent discoveries of the Centaurus Distant Cluster at $z \approx 0.05$ by Scaramella *et al.* (1989) in the direction of the suggested intrusion into southern latitudes of the Pisces-Cetus complex, tend to give credence to this possibility.

---

[2]For example, when Figures 5(a-c) of Rowan-Robinson *et al.* (1991) were set against Figures 2(a-c) of Faber & Burstein (1988) (the latter data derived from $D_{\rm n} - \sigma$ and Tully-Fisher galaxy studies) one could make out connective bridges between wall-like superclusters. What was originally the Centaurus supercluster has since been designated as the Virgo-Hydra-Centaurus supercluster.

[3]This is centred on the Pisces-Cetus supercluster at Supergalactic coordinates (100, -180, 0), located well beyond the present survey limit.

As early as 1990, Rowan-Robinson *et al.* described a 1 in 6 sparse-sampled redshift survey based on the QMW *IRAS* galaxy catalogue, using this survey to map the local gravitational field. They concluded at that time that the motion of the Local Group with respect to the microwave background must be generated by up to a dozen superclusters, all lying within $150\,h^{-1}\,Mpc$. The Puppis area in the zone of avoidance must also now be considered as possibly playing an important role in disturbing the expansion velocity of the Local Group (Kraan-Korteweg & Huchtmeier, 1992). It is the second most conspicuous feature in the density contour plots of Lahav *et al.* (1993) after the Great Attractor, and is even more pronounced than the Virgo cluster enhancement. It is centred at $(243°, -3°)$ in Puppis[4].

But it seems most likely of all that the motion of the Local Group is dictated by a tug-of-war between Centaurus/the Great Attractor and the Perseus-Pisces supercluster at opposite Galactic longitudes (cf. discussion in Kraan-Korteweg & Huchtmeier, 1992), although the net effect of the opposing influences may be to reduce the observed dipole[5] at our position in the Universe. Lynden-Bell *et al.* (1989) find that the Centaurus Concentration at $4300\,km\,s^{-1}$ must contribute to less than 25% of the streaming motion of the Local Group because of its distance relative to much nearer concentrations and that 80% of the amplitude of the final dipole arises from the influence of galaxies nearer than $4000\,km\,s^{-1}$. About half of the pull comes from galaxies closer than $2000\,km\,s^{-1}$ and about a third overall from the Hydra-Centaurus region between $2000 - 4300\,km\,s^{-1}$.

More observations need to be undertaken at latitudes $|\mathbf{b}| < 5°$, especially as a large proportion of the $> 2600$ *IRAS* sources might yet turn out to be galaxies. The simplest approach is just to systematically obtain redshifts for *all* of these *IRAS* sources, whether these are con-

---

[4]Interestingly, this is an *IRAS* over-density, and is not obvious in optical maps; it bears good testimony to the relative efficiency of an infra-red survey in an area of high optical opacity.

[5]Both the light flux and gravitational influence of a galaxy fall off as the inverse square of distance. Using an overall average mass-to-light ratio, the vector sum of all directed light fluxes from galaxies beyond the Local Group should be proportional to the gravity field acting on the Local Group. The surface brightness of the extra-galactic sky has been resolved into dipole, quadrupole and even higher components. The surface brightness dipole is effectively a gravitational dipole. Ideally this dipole should correspond directionally with the dipole implied by the skewing of the microwave background spectrum at our position in the universe.

strained by source confusion or not, as, apart from the possibility that many new galaxies will be found, this will at least give some indication of the percentage of the remaining $\sim$ 2600 sources that will turn out to be galaxies.

# Chapter 8

# References


- Allen, C. W., *Astrophysical Quantities* - 3rd ed., 1973, publ. University of London Press, 264.

- Babul, A. & Postman, M., 1990, *Astrophys. J.*, **359**, 280.

- Bloemen, J. B. G. M., 1983, in *Survey of Southern Galaxies*, in the *Astrophys. Space Sci. Library*, Vol. 105, eds Burton, W. B. & Israel, F. P., (Reidel, Dordrecht), 307.

- Burstein, D. & Heiles, C., 1982, *Astron. J.*, **8**, No. 8, 1165-1189.

- Burstein, D., Faber, S. M. & Dressler, A., 1990, *Astrophys. J.*, **354**, 18.

- Burton, W. B. & te Lintel Hekkert, P., 1986, *Astron. Astrophys. S. S.*, **65**, 427.

- de Lapparent, V., Geller, M. J. & Huchra, J. P., 1986, *Astrophys. J.*, **302**, L1.

- deVaucouleurs, G., deVaucouleurs, A. & Corwin, H., 1976, *Second Reference Catalogue of Bright Galaxies,* publ. by Univ. of Texas: Monographs in Astronomy, No.2 (RC2).

- deVaucouleurs, G., deVaucouleurs, A., Corwin, H., Buta, R., Paturel, G. & Forque, P., 1991, *Third Reference Catalogue of Bright Galaxies,* publ. by Springer, New York (RC3).

- Dressler, A., 1991, *Astrophys. J. S.*, **75**, 241.

- Dressler, A. & Faber, S. M., 1990*a*, *Astrophys. J.*, **354**, 13.

- ESO Catalogue: Lauberts, A., *The ESO/Uppsala Survey of the ESO-B Atlas* (European Southern Observatory, Garching, 1982).

- Faber, S. M. & Burstein, D., 1988, in *Large Scale Motions in the Universe: A Vatican Study Week*, eds V. C. Rubin & G. V. Coyne, (Princeton: Princeton Univ. Press), 116.

- Feitzinger, J. V. & Stuwe, J. A., 1984, *Astron. Astrophys. S. S.*, **58**, 365.

- Feitzinger, J. V. & Stuwe, J. A., 1986*a*, *Astron. Astrophys. S. S.*, **63**, 203.

- Feitzinger, J. V. & Stuwe, J. A., 1986*b*, *Astrophys. J.*, **305**, 534.

- Feitzinger, J. V. & Stuwe, J. A., 1986*c*, *Vistas in Astron.*, **29**, 291-293.

- Fisher, K. B., Strauss, M. A., Davis, M., Yahil, A., Huchra, J. P., 1992, *Astrophys. J.* **389**, 188.

- Fisher, K. B., Huchra, J. P., Strauss, M. A., Davis, M., Yahil, A. and Schlegel, D., 1995, *Astrophys. J. Supp.*, **100**, 69-103.

- Fouque, P., Gourgoulhon, E., Chamaraux, P. & Paturel, G., 1992, *Astron. & Astrophys. Supp. Ser.*, **93**, 211-233.

- Freedman, W. L., Madore, B. F., Mould, J. R., Hill, R., Ferrarese, L., Kennicutt Jr., R. C., Saha, A., Stetson, P. B., Graham, J. A., Ford, H., Hoessel, J. G., Huchra, J., Hughes, S. M. & Illingworth, G. D., Oct. 1994, *Nature*, **371**, 757-762.

- Geller, M. J., 1987, in *Large-Scale Structures in the Universe*, eds L. Martinet & M. Mayor (Sauverny: Geneva Observatory), 71.

- Geller, M. J. & Huchra, J. P., 1989*a*, in *Large Scale Motions in the Universe*, eds V. Rubin & G. V. Coyne (Princeston, New Jersey: Princeston University Press), 3.

- Geller, M. J. & Huchra, J. P., 1989*b*, *Science*, **246**, 897-903.

- Hartley, M. & Dawe, J. A., 1981, *Proc. astron. Soc. Australia*, **4**, 251.

- Huchra, J., 1988, in *Extragalactic Distance Scale* (eds van den Bergh, S. & Pritchet, C. J.),*Publ. astron. Soc. Pacif. Conf. Series*, **4**, 257-280.

- Huchra, J. P., 1993; private version of the redshift catalogue (zcat)

- Huchra, J. P., Geller, M. J. & Corwin Jr., H. G., 1995, *Astrophys. J. Supp.*, **99**, 391.

- *IRAS Explanatory Supplement* [ES], 1988, eds Beichman, C. A., Neugebauer, G., Habing, H. J., Clegg, P. E. & Chester, T. J., (Washington D.C.: U.S. Government Printing Office).

- *IRAS Point Source Catalog* [IPSC], *Version 2,* 1988, Joint *IRAS* Science Working Group, (Washington D.C.: U.S. Government Printing Office).

- Jacoby, G. H., Branch, D., Ciardullo, R., Davies, R. L., Harris, W. E., Pierce, M. J., Pritchet, C. J., Tonry, J. L. & Welch, D. L., 1992, *Publ. astron. Soc. Pacif.,* **104**, 599-662.

- Khavtassi, J. S., 1960, *Atlas of Galactic Dark Nebulae,* (Ambastumani Astrophysical Observatory).

- Kraan-Korteweg, R. C., 1989, in *Review in Modern Astronomy, Vol.2,* ed G. Klarc (Berlin Heidelberg: Springer-Verlag), 119.

- Kraan-Korteweg, R. C. & Huchtmeier, W. K., 1992, *Astron. & Astrophys.,* **266**, 150.

- Lahav, O., Yamada, T., Scharf, C. & Kraan-Korteweg, R.C., 1993, *Mon. Not. R. astr. Soc.,* **262** - Issue 3, 711-716.

- Lawrence, A., Rowan-Robinson, M., Leech, K., Jones, D. H. P. & Wall, J. V., 1989, *Mon. Not. R. astr. Soc.,* **240**, 329.

- Lonsdale, C. J., Helou, G., Good, J. C. & Rice, W., 1989, *Catalog of Galaxies and Quasars observed in the IRAS survey, Version 2* (Pasadena: Jet Propulsion Laboratory) [CGQ*IRAS*].

- Lu, N. Y., Dow, M. W., Houck, J. R., Salpeter, E. E. & Lewis, B. M., 1990, *Astrophys. J.,* **357**, 388.

- Lynden-Bell, D., Lahav, O. & Burstein, D., 1989, *Mon. Not. R. astr. Soc.,* **241**, 325.

- Lynds, B. T., 1962, *Astrophys. J. Supp. Ser.,* **7**, 1.
- May, J., Murphy, D. C. & Thaddeus, P., 1988, *Astron. Astrophys. S. S.,* **73**, 51.
- Meiksin, A. & Davis, M., 1986, *Astron. J.,* **91**, 191.
- Meurs, E. J. A. & Harmon, R. T., 1988, *Astron. & Astrophys.,* **206**, 53.
- Neckel, T. & Klare, G., 1980, *Astron. Astrophys. S. S.,* **42**, 251.
- Ostriker, J. P. & Cowie, L. L., 1981, Astrophys. J. (Letters), **243**, L127.
- Ramella, M., Geller, M. J. & Huchra, J. P., 1989, *Astrophys. J.,* **344**, 57 (CfA).
- Raychaudhury, S., 1989, *Nature,* **342**, no. 6247, 251-255.
- Rood, H. J. & Dickel, J. R., 1978, *Astrophys. J.,* **224**, 724.
- Rowan-Robinson, M., Lawrence, A., Saunders, W., Crawford, J., Ellis, R., Frenk, C. S., Parry, I., Xiaoyang, X., Allington-Smith, J., Efstathiou, G. & Kaiser, N., 1990, *Mon. Not. R. astr. Soc.,* **247**, 1.
- Rowan-Robinson, M., Saunders, W., Lawrence, A. & Leech, K., 1991, *Mon. Not. R. astr. Soc.,* **253**, 485.
- Saito, M., Ohtani, H., Asonuma, A., Kashikawa, N., Maki, T., Nishida, S. & Watanabe, T., 1990, *Publ. astr. Soc. Japan,* **42**, 603.
- Saito, M., Ohtani, H., Baba, A., Hotta, H., Kameno, S., Kurosu, S., Nakada, K. & Takata, T., 1991, *Publ. Astr. Soc. Japan,* **43**, 449.
- Saito, M., 1991, *Catalog of Galaxies behind the Milky Way, Vol. 1; Vol. 2* (Kyoto: Contributions from the Department of Astronomy, Kyoto University, No. 300) [CGMW].
- Sandage, A., Tammann, G. A. & Yahil, A., 1979, *Astrophys. J.,* **232**, 352.
- Sandage, A. R. & Tammann, G. A., 1993, *Astrophys. J.,* **415**, 1-9.
- Saunders, W., Rowan-Robinson, M., Lawrence, A., Efstathiou, G., Kaiser, N., Ellis, R. S. & Frenk, C. S., 1990, *Mon. Not. R. astr. Soc.,* **242**, 318-337.

- Saunders, W., Frenk, C., Rowan-Robinson, M., Efstathiou, G., Lawrence, A., Kaiser, N., Ellis, R., Crawford, J., Xaio-Yang, X. & Parry, I., 1991, *Nature,* **349**, 32.

- Scaramella, R., Baiesi-Pillastrini, G., Chincarini, G., Vettolani, G. & Zamorani, G., 1989, *Nature,* **338**, no. 6216, 562-564.

- Scharf, C., Hoffman, Y., Lahav, O. & Lynden-Bell, D., 1992, *Mon. Not. R. astr. Soc.,* **256**, 229.

- Shaver, P. A., 1990, *Proc. Astron. Soc. Australia,* **8**, 250.

- Strauss, M. A., Davis, M., Yahil, A. & Huchra, J. P., 1990, *Astrophys. J.,* **361**, 49.

- Strauss, M. A., Davis, M., Yahil, A. & Huchra, J. P., 1992*a*, *Astrophys. J.,* **385**, 421.

- Strauss, M. A., Huchra, J. P., Davis, M., Yahil, A., Fisher, K. B. & Tonry, J., 1992*b*, *Astrophys. J. Supp.,* **83**, 29.

- Takata, T., 1992, Thesis for Masters degree at Kyoto University (in Japanese).

- Takata, T., Yamada, T. & Saito, M., 1996, *Astrophys. J.,* **457**, 693-702.

- Tully, R. B., 1987, *Astrophys. J.,* **323**, 1-18.

- Tully, R. B. & Fisher, J. R., 1987, *Nearby Galaxies Atlas* (Cambridge University Press).

- Visvanathan, N., 1990, *Australian J. Phys.,* **43**, 189.

- Yamada, T., Takata, T., Djamaluddin, T., Tomita, A., Aoki, K., Takeda, A. & Saito, M., 1993*a*, *Mon. Not. R. astr. Soc.,* **262**, 79-84.

- Yamada, T. & Saito, M., 1993, *Publ. astr. Soc. Japan,* **45**, 25.

- Yamada, T., Takata, T., Djamaluddin, T., Tomita, A., Aoki, K., Takeda, A. & Saito, M., 1993*b*, *Astrophys. J. Supp.,* **89**, 57-84.

# Chapter 9

# Appendices

## 9.1 Previously Identified Groups and Clusters of Galaxies within $cz < 6500\,km\,s^{-1}$.

Table 9.1: Centaurus Clusters near the Milky Way, for $cz \leq 6500\,km/s$ - Table 1.
Key: Ray=Raychaudhury (1989); Sca=Scaramella *et al.* (1989).

| Centre of Grouping | | | Cluster | Author |
|---|---|---|---|---|
| l | b | $cz$ (km/s) | Name | |
| 302 | 22 | 3271 | Centaurus 3526 | Sca |
| 305 | 30 | 4945 | Centaurus 3537 | Sca |
| 314 | 28 | 3241 | Centaurus 3565 | Sca |
| 317 | 31 | 4183 | Centaurus 3574 | Sca |
| 275 | 15 | 2725 | Centaurus 27 | Ray |
| 273 | 19 | 2860 | Centaurus 29 | Ray |
| 270 | 27 | 3417 | Centaurus 34 | Ray |
| 277 | 62 | 5850 | Centaurus 59 | Ray |
| 298 | 23 | 3194 | Centaurus 32 | Ray |
| 302 | 22 | 3041 | Centaurus 30 | Ray |
| 305 | 30 | 5010 | Centaurus 50 | Ray |
| 310 | 29 | 4590 | Centaurus 46 | Ray |
| 313 | 29 | 3270 | Centaurus 33 | Ray |
| 314 | 28 | 3270 | Centaurus 33' | Ray |
| 317 | 31 | 4230 | Centaurus 42 | Ray |
| 320 | 27 | 4200 | Centaurus 42' | Ray |
| 323 | 33 | 6270 | Centaurus 63 | Ray |

Table 9.2: Previously Identified Groups and Clusters at $|\mathbf{b}| < 25°$ - Table 2.

Taken from Fouque *et al.* (1992), and supplemented from Kraan-Korteweg & Huchtmeier (1992) and Saunders (1991).

| Centre of Grouping | | | Catalogue | de Vaucouleurs | Tully |
|---|---|---|---|---|---|
| **l** | **b** | $cz$ (km/s) | Name | Name | Name |
| 223.1 | -21.4 | 2886 | IC 438 | | |
| 228.6 | -17.2 | 2559 | NGC 2207 | G36 | 34-8 |
| 234.8 | -18.3 | 1452 | NGC 2217 | | 34-1 |
| 236.9 | -13.1 | 1732 | NGC 2280 | | |
| 273.6 | -20.2 | 3002 | NGC 2417 | | |
| 281.0 | -21.7 | 1193 | NGC 2442 | | 53-17 |
| 263.0 | -12.7 | 823 | NGC 2427 | | |
| 246.1 | 5.3 | 1456 | NGC 2559 | | 31-21 |
| 244.7 | 13.2 | 1570 | ESO 563-16 | | |
| 255.9 | 5.8 | 1918 | NGC 2663 | | |
| 284.9 | -14.2 | 1357 | NGC 2836 | | 53-22 |
| 244.1 | 21.8 | 1794 | NGC 2781 | | 31-14 |
| 251.8 | 17.1 | 547 | NGC 2835 | | 54-3 |
| 252.5 | 18.3 | 2378 | NGC 2815 | | |
| 254.6 | 23.6 | 2027 | NGC 2986 | | |
| 262.5 | 16.8 | 851 | NGC 2997 | G 8 | 54-1 |
| 261.4 | 21.7 | 2282 | NGC 3054 | | |
| 266.1 | 17.2 | 2503 | NGC 3087 | | |
| 265.2 | 22.1 | 872 | NGC 3175 | | 54-2 |
| 265.5 | 24.4 | 2242 | NGC 3203 | | |
| 275.0 | 14.9 | 2570 | NGC 3250 | | |
| 277.5 | 11.6 | 2410 | NGC 3256 | | |
| 272.5 | 20.0 | 2849 | Antlia cr | | 31-2 |
| 278.4 | 11.2 | 2741 | NGC 3263 | | |
| 276.0 | 19.3 | 2805 | NGC 3347 | | |
| 281.5 | 21.2 | 2750 | NGC 3557 | | 31-10 |
| 298.1 | 23.3 | 2811 | IC 3370 | | |

Table 9.3: Previously Identified Groups and Clusters at $|\mathbf{b}| < 25^{\circ}$ - Table 3.

Taken from Fouque *et al.* (1992), and supplemented from Kraan-Korteweg & Huchtmeier (1992) and Saunders (1991).

| Centre of Grouping | | | Catalogue | de Vaucouleurs | Tully |
|---|---|---|---|---|---|
| l | b | $cz$ (km/s) | Name | Name | Name |
| 302.2 | 21.9 | 3225 | Centaurus cr | | 23-1 |
| 303.2 | 20.1 | 1837 | NGC 4751 | | |
| 305.7 | 13.2 | 1261 | NGC 4976 | | |
| 307.3 | 15.6 | 2809 | NGC 5064 | | |
| 308.2 | 19.1 | 3309 | NGC 5090 | | |
| 310.3 | 24.7 | 1328 | NGC 5121 | | 16-4 |
| 309.7 | 20.9 | 390 | NGC 5128 | G 4 | 14-15 |
| 312.3 | 13.4 | 2749 | NGC 5333 | | 23-3 |
| 315.3 | 17.3 | 2360 | NGC 5365 | | |
| 316.8 | 13.2 | 1330 | ESO 221-26 | | |
| 322.9 | -23.6 | 3519 | IC 4682 | | |
| 332.4 | -24.2 | 4575 | IC 4765 | | |
| 304 | 13 | 2764 | Centaurus s/cl | (Sa) | |
| 218 | -15 | 2525 | New s/cluster ? | (Sa) | |
| 210 | 13 | 2829 | New void | (Sa) | |
| 289 | 26 | 2429 | Vir-Hyd-Cent s/cl | (Sa) | |
| 281 | 0 | 6120 | New s/cluster ? | (Sa) | |
| 239 | 8 | 7064 | Tully void 3 | (Sa) | |
| 245.5 | 5.9 | 1450 | KKH1=NGC 2559? | | |
| 246.0 | 2.5 | 750 | KKH2 | | |
| 244.0 | -6.5 | 1800 | KKH3 | | |
| 242.0 | 5.0 | 2400 | KKH4 | | |
| 246.0 | 2.0 | 5000 | KKH5 | | |
| 310 | -22 | 4000 | Dressler void | | |
| 312 | 0 | 3000 | Centaurus cluster | | |
| 300 | 22 | 3200 | Centaurus cluster | | |
| 322 | 22 | 4000 | Centaurus cluster | | |
| 309 | 27 | 2000 | Centaurus cluster | | |

## 9.2 New Seyfert-like Galaxies in the Sample.

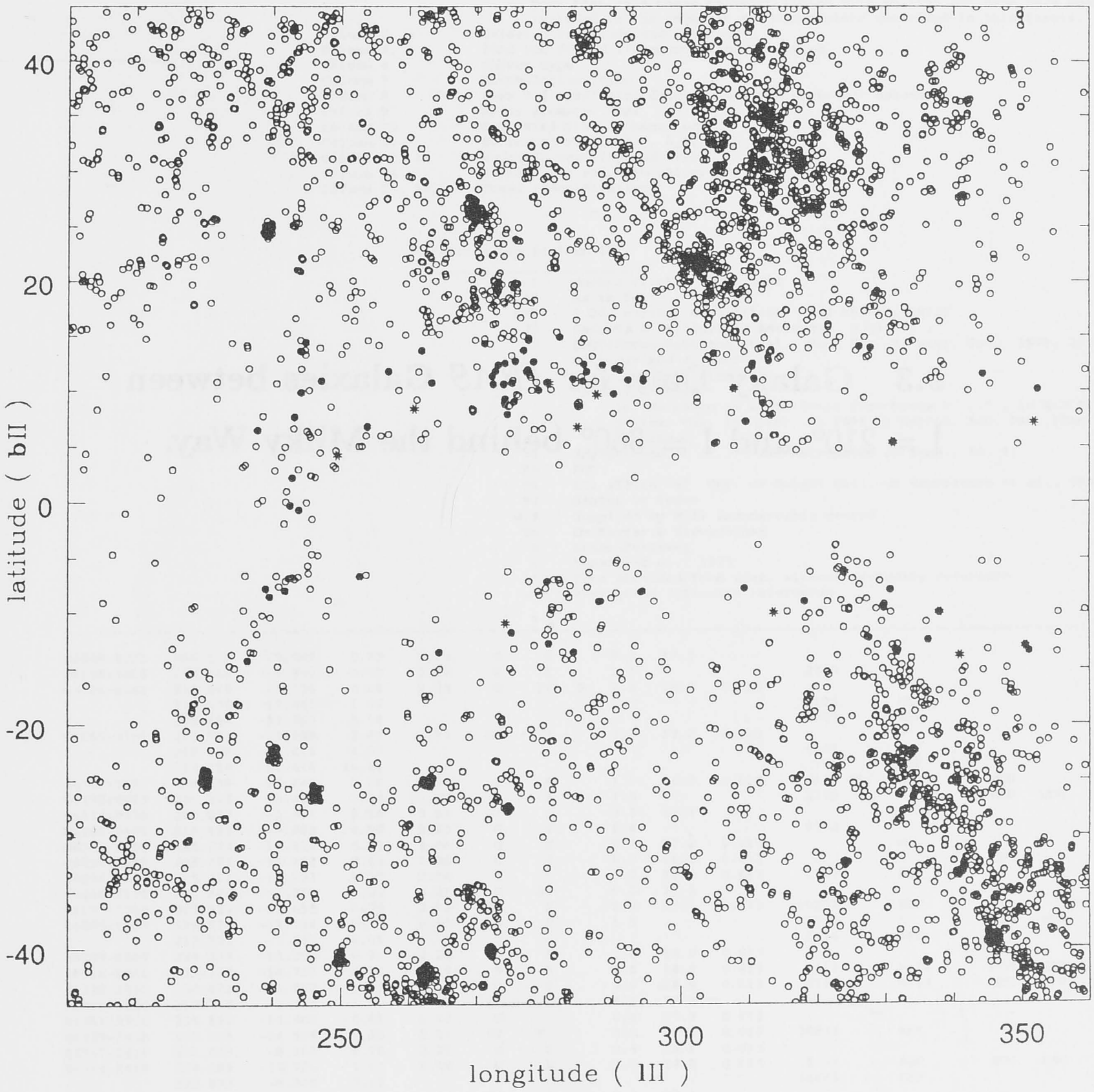


Figure 9.1: Locations of the Seyfert and "multiple"-source galaxies in the distribution of *IRAS* galaxies behind the Milky Way.

Key: open circles = normal galaxies, filled circles = "multiple"-source galaxies, stars = Seyfert or possible Seyfert galaxies.

## 9.3 Galaxy Data for *IRAS* Galaxies between l = 210° and l = 360° behind the Milky Way.

List of the Identified IRAS galaxies Behind the Milky Way

| | |
|---|---|
| Column 1 | IRAS PSC name<br>- Note that only those galaxies listed with an IRAS PSC name have been included in the redshift and other plots described in this thesis. |
| Column 2, 3 | Galactic longitude and latitude |
| Column 4, 5 | IRAS PSC 60 and 100 micron flux densities |
| Column 6 | Object type |
| Column 7 | Morphological type |
| Column 8 | Pair ? ("Pair" also denotes multiple or merger galaxies) |
| Column 9 | Major diameter (mm) |
| Column 10 | Estimated plate B magnitude |
| Column 11 | Estimated extinction, A_b, in B_band |
| Column 12, 13 | Redshift velocity and error |
| Column 14 | Sources for redshift velocities |
| Column 15, 16, 17 | Cross Identifications |

Reference key (column 14)

| | |
|---|---|
| -1 | Huchra et al., 1993, ZCAT |
| 0-49 | As in ZCAT |
| KBF | 1.2Jy survey, K. B. Fisher (PhD thesis, 1992) |
| -27 | DaCosta & Pelligrini, Astrophys. J.(1993, ) |
| 53 | QDOT(Rowan-Robinson et al., Mon. Not. R. astr. Soc., 1991, 253, 485) |
| 58 | Kirkahos and Steiner |
| 59 | Sekuguchi & Wolstencroft |
| 72 | Fairall & Jones, in "Workshop on Large-Scale Structures & ..." , in A.S.P. Conf. Series, Vol. 15, publ. in 1991 by Astron. Soc. Pac.,(San Francisco) |
| 76 | 2Jy(Strauss et al.,1992a, Astrophys. J. Supp., 83, 1) |
| 86 | PGC |
| 91 | RC3 (Third Ref. Cat. of Bright Gal., de Vaucoleurs et al., 1992.) |
| 93 | Elston or Vader |
| W,# | Supplied by Will Saunders/his source |
| DV | De Ruyter & Visvanathan |
| K | Kraan-Korteweg |
| Y | Yamada et al., 1993 |
| * | Data obtained from zcat, without secondary reference |
| av | Average of following references |

| | | | | | | | | | | | | | | |
|---|---|---|---|---|---|---|---|---|---|---|---|---|---|---|
| 06088+0221 | 206.232 | -7.809 | 0.93 | 2.60 | G | S | | 0.3 | 17.3 | | | | | |
| 06125+0012 | 208.585 | -7.997 | 0.69 | 2.07 | G | S | | 1.5 | | | 2340 | | * | |
| 06126-0244 | 211.248 | -9.336 | 0.66 | 1.73 | G | S? | P | 0.2 | 18.0 | 0.613 | | | | |
| | 213.279 | -13.907 | 1.39 | | | | | | | | 30104 | | KBF | |
| | 215.408 | -13.857 | 1.54 | | | | | | | | 10705 | | KBF | |
| 06165-0751 | 216.321 | -10.789 | 0.88 | 1.73 | G? | ? | | 0.1 | 19.2 | 0.613 | | | W | |
| | 218.030 | -13.076 | 1.30 | | | | | | | | 6647 | | KBF | |
| | 217.110 | -10.614 | 16.44 | | | | | | | | 755 | | KBF | |
| 06168-1655 | 224.739 | -14.646 | 0.68 | 1.95 | G | S | | 1.7 | 14.7 | 0.613 | 6148 | 35 | W,17 | MCG |
| 06192+0023 | 209.215 | -6.414 | 3.24 | 11.99 | G | ? | | 1.0 | | | 2728 | | * | MCG UCG |
| 06193+0130 | 208.237 | -5.871 | 0.96 | 2.54 | G? | S | | 0.3 | 17.3 | | | | | |
| 06206-0605 | 215.191 | -9.082 | 4.57 | 5.63 | G | S | | 0.4 | | | 6042 | | * | |
| 06233-1952 | 228.172 | -14.454 | 0.93 | 1.86 | G | S | | 0.4 | 17.2 | 0.613 | | | W | |
| 06234-1946 | 228.096 | -14.408 | 0.60 | 1.00 | G | S | | 0.7 | 16.2 | 0.613 | | | | ESO |
| 06234-1654 | 225.417 | -13.203 | 1.37 | 2.84 | G | ? | | 0.7 | 16.2 | 0.613 | 6187 | | KBF | |
| 06246+0130 | 208.846 | -4.712 | 1.20 | 3.01 | G | S? | | 0.3 | 17.3 | | | | | |
| 06293-1358 | 223.322 | -10.658 | 1.79 | 2.90 | G | S | | 0.3 | 17.3 | 0.613 | 10277 | | KBF | |
| 06295-1735 | 226.673 | -12.164 | 5.72 | 9.42 | G | S | | 1.0 | | | 6339 | | * | ESO ESO |
| | 218.753 | -7.845 | 4.11 | | | | | | | | 6974 | | KBF | |
| 06297-2007 | 229.053 | -13.204 | 0.79 | 2.28 | G | S | | 2.6 | 13.9 | 0.613 | | | | ESO |
| 06316-2456 | 233.772 | -14.769 | 0.86 | 2.10 | G | S | | 1.6 | 14.8 | 0.613 | 2665 | 35 | W,17 | MCG ESO |
| 06320-2538 | 234.472 | -14.959 | 1.22 | 3.18 | G | S | | 0.6 | 16.5 | 0.613 | 2488 | | W,53 | MCG ESO |
| 06330+0025 | 210.790 | -3.337 | 1.25 | 3.69 | G? | ? | | 0.1 | 19.2 | | | | | |
| 06351-2706 | 236.152 | -14.908 | 0.61 | 1.42 | G | | | 0.4 | 17.2 | 0.613 | | | | |
| 06357-2638 | 235.755 | -14.599 | 1.33 | 2.51 | G? | ? | | 0.2 | 18.4 | 0.613 | 20814 | | KBF | |
| 06357-1134 | 221.848 | -8.193 | 0.79 | 2.21 | G | S | | 0.6 | 16.1 | 0.613 | | | | |
| 06364-2448 | 234.088 | -13.726 | 1.67 | 5.30 | G | S | | 2.5 | 14.0 | 0.613 | 2708 | | KBF | MCG ESO |
| | 222.072 | -8.048 | 3.43 | | | | | | | | 14640 | | KBF | |
| 06375-0141 | 213.188 | -3.330 | 12.03 | 28.85 | G? | ? | | 0.3 | 17.3 | | | | | |
| 06378-1346 | 224.053 | -8.724 | 1.05 | 2.06 | G | S | P | 0.5 | 16.4 | 0.613 | 8964 | | W,53 | |
| 06381-2550 | 235.234 | -13.795 | 1.90 | 2.28 | G | ? | P | 1.3 | 15.1 | 0.613 | 7751 | | KBF | MCG ESO |
| 06383-2702 | 236.377 | -14.250 | 0.72 | 1.54 | G | S | P | 1.5 | 14.9 | 0.613 | 2132 | 35 | W,17 | MCG ESO |
| 06384-2709 | 236.494 | -14.272 | 0.67 | 1.23 | G | S | P | 0.7 | 16.2 | 0.613 | | | | MCG |
| 06391-0519 | 216.605 | -4.641 | 1.33 | 1.95 | G | S? | | | | | 6095 | | * | |
| 06411-2905 | 238.564 | -14.505 | 1.92 | 3.53 | G | ? | P | 0.3 | 17.7 | 0.613 | | | | |
| 06414-2316 | 233.150 | -12.038 | 3.34 | 4.70 | G | S | | | | | 6972 | | * | |
| 06416-2709 | 236.792 | -13.609 | 2.06 | 3.22 | G | S | | | | | 7053 | | * | MCG |
| 06421-2707 | 236.803 | -13.509 | 0.75 | 2.31 | G | S | | 1.5 | 14.9 | 0.613 | 1947 | 35 | W,17 | MCG ESO |
| 06421-2442 | 234.560 | -12.493 | 0.90 | 1.97 | G | S | | 0.3 | 17.7 | 0.613 | | | W | |
| 06422-1752 | 228.268 | -9.565 | 0.76 | 2.62 | G | S | | | | | 3395 | | * | MCG ESO |
| 06425-0901 | 220.303 | -5.560 | 0.69 | 2.30 | G | S | | 0.2 | 18.0 | 0.613 | | | | |
| 06425-0838 | 219.965 | -5.380 | 0.60 | 1.77 | G | S | | 0.2 | 18.0 | 0.613 | | | | |
| 06428-2735 | 237.305 | -13.553 | 4.73 | 17.15 | G | S | | | | | 1900 | | avKBF,W | MCG ESO |
| 06436-1809 | 228.667 | -9.386 | 4.84 | 16.27 | G | S | | | | | 850 | | * | MCG ESO |
| 06438-3110 | 240.789 | -14.788 | 3.14 | 4.57 | G | S | | 1.2 | 15.3 | 0.613 | 2731 | 76 | W,76 | MCG ESO |
| 06443-2602 | 236.009 | -12.607 | 1.19 | 2.62 | G | S | | | | | 2348 | | * | MCG ESO |
| 06452-2833 | 238.445 | -13.472 | 0.70 | 1.12 | G | ? | | 0.3 | 17.7 | 0.613 | | | W | |
| 06452-0601 | 217.932 | -3.601 | 6.79 | 18.48 | G? | S | | 0.2 | 18.0 | | | | | |
| 06462-2718 | 237.362 | -12.738 | 1.22 | 2.70 | G | S | | 0.2 | 18.4 | 0.613 | 12287 | | KBF | |
| | 242.704 | -14.897 | 1.24 | | | | | | | | 13820 | | KBF | |
| 06464-1650 | 227.768 | -8.217 | 9.53 | 38.41 | G? | ? | | 0.4 | 16.8 | 0.613 | | | | MCG |
| 06478-1111 | 222.835 | -5.381 | 6.28 | 10.63 | G | ? | | | | | 2709 | | * | |
| 06481-0517 | 217.603 | -2.620 | 20.06 | 32.05 | G? | S | | 0.4 | 16.8 | | | | | |
| 06483-1955 | 230.775 | -9.167 | 1.91 | 2.78 | G | S | | 0.7 | 16.2 | 0.613 | 7666 | | KBF | |
| | 234.215 | -8.935 | 1.60 | | | | | | | | 20088 | | KBF | |

| | | | | | | | | | | | | | | | |
|---|---|---|---|---|---|---|---|---|---|---|---|---|---|---|---|
| | 246.368 | -14.439 | 1.33 | | | | | | | | 34168 | | KBF | | |
| 06490-2055 | 231.754 | -9.453 | 1.50 | 2.78 | G? | ? | | 0.1 | 19.6 | 0.613 | | | | | |
| 06496-2010 | 231.139 | -8.997 | 1.12 | 2.53 | G | S | | 0.6 | 16.1 | 0.613 | 7645 | | W,53 | MCG | ESO |
| 06497-2839 | 238.947 | -12.606 | 0.63 | 1.51 | G | S | | 0.6 | 16.5 | 0.613 | 10972 | | W,53 | | |
| 06502-0040 | 213.733 | -0.042 | 2.09 | 7.79 | G? | S | | 0.2 | 18.0 | | | | | | |
| 06503-1202 | 223.865 | -5.220 | 0.84 | 2.41 | G | S | | 0.5 | 16.4 | 0.613 | | | | | |
| 06504-2717 | 237.751 | -11.898 | 0.74 | 1.38 | G | ? | | | | | 2489 | | * | | |
| 06514-2918 | 239.712 | -12.538 | 0.71 | 1.11 | G | S | | 0.7 | 16.2 | 0.613 | | | W | ESO | |
| 06520-0038 | 213.919 | 0.378 | 13.13 | 17.06 | G? | S | | 0.3 | 17.3 | | | | | | |
| 06522-3546 | 245.874 | -14.993 | 0.75 | 1.06 | G | S | | 0.3 | 17.7 | 0.613 | | | W | | |
| 06525-2021 | 231.609 | -8.455 | 0.83 | 2.40 | G | S | | 0.5 | 16.4 | 0.613 | | | | | |
| 06534-2632 | 237.348 | -10.967 | 0.84 | 2.70 | G | S | | | | | 2056 | | * | ESO | |
| 06535+0037 | 212.960 | 1.293 | 8.66 | 26.61 | G? | ? | P | 0.1 | 19.2 | | | | | | |
| 06540-2911 | 239.848 | -11.971 | 0.62 | 1.26 | G | E | | 0.2 | 18.4 | 0.613 | | | W | | |
| 06543-3443 | 245.066 | -14.185 | 0.61 | 1.61 | G | S | | 0.3 | 17.7 | 0.613 | | | W | | |
| 06547-2817 | 239.083 | -11.448 | 0.64 | 1.06 | G | ? | | 0.6 | 16.5 | 0.613 | 11983 | 73 | W,12 | ESO | |
| 06548-0505 | 218.190 | -1.036 | 1.92 | 2.85 | G | S | | 1.3 | 14.7 | | | | | | |
| 06553-2439 | 235.807 | -9.768 | 0.70 | 2.05 | G | S | | | | | 2581 | | * | ESO | |
| 06555-0516 | 218.441 | -0.970 | 2.25 | 5.13 | G | S | | | | | 2646 | | * | | |
| 06566-2830 | 239.466 | -11.159 | 0.64 | 1.59 | G | ? | P | 0.5 | 16.8 | 0.613 | | | W | | |
| 06573-0021 | 214.276 | 1.690 | 0.69 | 1.97 | G | S | | | | | 6964 | | * | | |
| 06574-1722 | 229.433 | -6.104 | 0.78 | 2.91 | G | S | | 0.9 | 15.4 | 0.613 | | | | | |
| 06584+0158 | 212.326 | 3.009 | 11.68 | 20.64 | G | S | | | | | 1774 | | * | MCG | UCG |
| 06586-2717 | 238.549 | -10.237 | 1.30 | 4.29 | G | S | | | | | 2652 | | avW,KBF | MCG | ESO |
| 06590-3740 | 248.237 | -14.508 | 2.68 | 6.02 | G | S | | | | | 8154 | | * | ESO | |
| | 248.199 | -13.004 | 1.60 | | | | | | | | 9654 | | KBF | | |
| 07001-2823 | 239.688 | -10.419 | 1.13 | 2.52 | G | ? | | 1.5 | 14.9 | 0.613 | 2188 | | W,53 | MCG | ESO |
| 07003+0144 | 212.755 | 3.313 | 1.81 | 2.37 | G | S? | | 0.2 | 18.0 | | | | | | |
| 07011-3743 | 248.448 | -14.148 | 0.66 | 1.27 | G | S | | | | | 7580 | | * | | |
| 07012-3605 | 246.930 | -13.463 | 0.73 | 1.67 | G | S | P | 0.8 | 16.0 | 0.613 | | | | | |
| 07023-3510 | 246.163 | -12.875 | 0.75 | 1.68 | G | S | | | | | 9303 | | * | | |
| 07026-0225 | 216.720 | 1.908 | 0.82 | 1.49 | G? | S | | 0.3 | 17.3 | | | | | | |
| 07035-1606 | 228.978 | -4.214 | 2.92 | 4.82 | G | S | P | 0.4 | 16.8 | 0.613 | | | | | |
| 07037-3102 | 242.459 | -10.865 | 0.88 | 1.51 | G | S | | 0.3 | 17.7 | 0.613 | | | W | | |
| 07038+0221 | 212.615 | 4.374 | 1.98 | 3.80 | G | ? | | | | | 5528 | | * | | |
| 07047-2738 | 239.460 | -9.173 | 1.03 | 2.42 | G | E | | 0.2 | 18.0 | 0.613 | 7296 | 13 | DV | | |
| 07047-2240 | 234.976 | -6.956 | 0.96 | 2.35 | G | S | | 0.5 | 16.4 | 0.613 | 12921 | | W,53 | | |
| 07062-2342 | 236.066 | -7.113 | 0.68 | 1.03 | G | S | | 0.3 | 17.3 | 0.613 | | | | ESO | |
| 07071-0520 | 219.831 | 1.538 | 0.77 | 3.31 | G | S? | | 2.2 | 13.8 | | | | | | |
| 07076-3100 | 242.818 | -10.088 | 1.98 | 2.73 | G | ? | | | | | 9562 | | * | | |
| 07077-2729 | 239.622 | -8.510 | 15.98 | 22.59 | G | S | P | | | | 2876 | | * | MCG | ESO |
| 07083-2327 | 236.045 | -6.584 | 0.74 | 2.26 | G | E? | | 0.4 | 16.8 | 0.613 | 3600 | | K,W,-27 | ESO | |
| 07086-3032 | 242.476 | -9.687 | 0.94 | 2.33 | G | S | | 0.3 | 17.3 | 0.613 | | | | | |
| 07089-3309 | 244.898 | -10.775 | 1.51 | 2.69 | G | S | P | | | | 7495 | | avW,KBF | | |
| 07091-2706 | 239.419 | -8.062 | 0.71 | 1.63 | G | E? | | 0.2 | 18.0 | 0.613 | | | | | |
| 07096-2637 | 239.028 | -7.750 | 7.81 | 14.91 | G | S | P | | | | 2611 | | * | ESO | |
| 07104-0913 | 223.641 | 0.460 | 0.77 | 2.97 | G | S | | 0.3 | 17.3 | | 2638 | 53 | DV | | |
| 07119-2834 | 241.031 | -8.174 | 1.29 | 3.02 | G | ? | | 0.3 | 17.3 | 0.613 | 9521 | | KBF | | |
| | 243.356 | -8.881 | 1.91 | | | | | | | | 10765 | | KBF | | |
| 07126-0645 | 221.727 | 2.099 | 0.68 | 2.01 | G? | S | | 0.2 | 18.0 | | | | | | |
| 07129-3524 | 247.330 | -11.029 | 0.71 | 2.07 | G | S | P | | | | 6670 | | * | | |
| 07133-2511 | 238.128 | -6.367 | 2.12 | 2.88 | G | ? | | 0.1 | 19.2 | 0.613 | | | | | |
| 07142-2815 | 240.967 | -7.574 | 1.10 | 2.12 | G | S | | | | | 5942 | | * | | |
| 07145-2914 | 241.877 | -7.965 | 4.40 | 6.05 | G | S | P | | | | 1642 | | avW,KBF | MCG | ESO |
| | 217.408 | 5.155 | 1.69 | | | | | | | | | | | | |
| 07153-1041 | 225.504 | 0.846 | 0.77 | 2.55 | G? | S | | 0.2 | 18.0 | | | | | | |
| 07155-2215 | 235.749 | -4.562 | 6.34 | 9.96 | G | S | | 0.5 | 16.4 | 1.499 | | | | | |
| 07155-3452 | 247.068 | -10.311 | 2.57 | 5.47 | G | S | | | | | 8731 | | * | ESO | |
| 07156-2758 | 240.854 | -7.169 | 1.89 | 4.52 | G | S | | | | | 7488 | | avW,KBF | ESO | |
| 07160-2938 | 242.399 | -7.850 | 1.01 | 1.91 | G | S | P | 0.3 | 17.3 | 0.613 | | | W | | |
| 07168-4245 | 254.459 | -13.501 | 1.62 | 2.40 | G | S | | 0.8 | 16.0 | 0.613 | 46407 | | KBF | ESO | |
| 07169-3504 | 247.388 | -10.135 | 1.76 | 3.71 | G | S | | | | | 8876 | | avW,KBF | | |
| 07170-0058 | 217.102 | 5.760 | 4.08 | 7.23 | G? | S | | | | | 9906 | | * | | |
| 07172-3451 | 247.228 | -9.992 | 1.21 | 2.36 | G | S | P | | | | 8935 | | avW,KBF | | |
| 07173-2729 | 240.593 | -6.620 | 0.72 | 2.86 | G | S | | 0.8 | 15.6 | 0.613 | 3400 | | K | ESO | |
| 07176-3533 | 247.896 | -10.236 | 3.55 | 6.97 | G | S | | | | | 2800 | | * | ESO | |
| | 241.958 | -7.061 | 1.56 | | | | | | | | 3119 | | KBF | | |
| 07178-0235 | 218.647 | 5.195 | 0.85 | 2.62 | G | S | | 0.2 | 18.0 | 0.613 | 15469 | | W,53 | | |
| 07181-0128 | 217.682 | 5.767 | 0.75 | 1.73 | G | S | P | 0.6 | 16.1 | 0.613 | | | W,zcat | CGCG | |
| 07183-2741 | 240.878 | -6.517 | 6.29 | 20.84 | G | ? | | 0.2 | 18.0 | 0.613 | | | | ESO | |
| 07193-3418 | 246.909 | -9.358 | 0.68 | 1.97 | G | S | | | | | 7706 | | * | ESO | |
| 07195-3444 | 247.333 | -9.512 | 0.77 | 1.98 | G | S | | | | | 12655 | | * | | |
| 07196-0549 | 221.721 | 4.072 | 1.50 | 1.97 | G | S | | | | | 1610 | | * | MCG | |
| 07200-2814 | 241.556 | -6.438 | 1.99 | 2.74 | G | ? | P | 0.1 | 19.2 | 0.613 | | | | | |
| 07202-2908 | 242.363 | -6.826 | 10.01 | 17.51 | G | S | | | | | 3068 | | * | MCG | ESO |
| | 242.568 | -6.839 | 1.69 | | | | | | | | 2877 | | KBF | | |
| 07206-3814 | 250.609 | -10.894 | 0.81 | 3.50 | G | S | | | | | 7127 | | * | ESO | |
| 07208-4539 | 257.466 | -14.069 | 1.00 | 1.91 | G? | ? | | 0.2 | 18.4 | 0.613 | | | | | |
| 07208+0242 | 214.258 | 8.323 | 2.06 | 4.50 | G | S | | | | | 1343 | | * | MCG | UCG CGCG |
| 07214-0322 | 219.758 | 5.608 | 0.89 | 2.03 | G | S | | 0.5 | 16.4 | 0.613 | | | | | |
| 07216-2957 | 243.238 | -6.921 | 5.70 | 14.82 | G | S | | | | | 2524 | | avW,KBF | ESO | |
| 07217-2933 | 242.887 | -6.726 | 2.85 | 9.41 | G | E | | | | | 1928 | | * | MCG | ESO |
| 07220-0437 | 220.936 | 5.158 | 0.60 | 1.24 | G | S | | 0.2 | 18.0 | 0.613 | | | | | |
| 07223+0004 | 216.791 | 7.422 | 1.02 | 1.54 | G | S | | 0.3 | 17.3 | 0.613 | | | | | |
| 07225-0933 | 225.352 | 2.939 | 8.93 | 17.94 | G | S | | | | | 2457 | | * | | |
| 07227-2904 | 242.572 | -6.297 | 0.79 | 1.48 | G | S | | | | | 9396 | | * | | |
| 07229-2725 | 241.130 | -5.493 | 1.47 | 2.51 | G | S? | | 0.3 | 17.3 | 0.613 | 7302 | | KBF | | |
| 07231-3223 | 245.570 | -7.779 | 1.64 | 4.85 | G | S | | | | | 1846 | | avW,KBF | ESO | |
| 07234-2858 | 242.551 | -6.113 | 1.51 | 2.42 | G | ? | | 0.2 | 18.0 | 0.613 | 8625 | | KBF | | |
| 07237-3018 | 243.761 | -6.694 | 2.73 | 6.80 | G | S | | | | | 2117 | | * | MCG | ESO |
| 07239-2631 | 240.437 | -4.866 | 0.85 | 3.68 | G | S? | | | | | 7347 | | * | | |
| 07242-4710 | 259.144 | -14.184 | 1.82 | 2.39 | G | S? | P | 0.3 | 17.7 | 1.499 | 21499 | | KBF | ESO | |
| 07245-3513 | 248.238 | -8.834 | 1.13 | 1.68 | G | S | | | | | 2843 | | * | ESO | |
| 07245-3548 | 248.762 | -9.083 | 1.54 | 3.03 | G | S | | | | | 8943 | | avW,KBF | | |
| 07246-0645 | 223.127 | 4.725 | 0.70 | 1.83 | G | S | | 0.5 | 16.4 | 0.613 | | | | | |
| 07247-2815 | 242.048 | -5.539 | 0.63 | 1.79 | G | ? | | 0.2 | 18.0 | 0.613 | | | | | |
| 07250-4910 | 261.072 | -14.916 | 0.70 | 1.71 | G? | ? | | 0.2 | 18.4 | 0.613 | | | | | |
| 07250-1226 | 228.177 | 2.093 | 0.74 | 2.77 | G? | S | | 0.1 | 19.2 | | | | | | |
| 07251-0248 | 219.688 | 6.691 | 6.66 | 6.63 | G? | ? | | 0.1 | 19.2 | 0.613 | | | | | |
| 07255-0502 | 221.717 | 5.726 | 1.86 | 2.08 | G? | ? | | 0.1 | 19.2 | 0.613 | | | | | |
| 07266-3538 | 248.813 | -8.637 | 1.95 | 3.20 | G | S | P | | | | 7243 | | * | | |
| 07274-2847 | 242.811 | -5.262 | 1.28 | 1.42 | G | S? | | 0.2 | 18.0 | 0.613 | 6672 | | KBF | | |
| | 253.058 | -10.580 | 3.25 | | | | | | | | 27919 | | KBF | | |
| 07283-3129 | 245.287 | -6.373 | 1.49 | 5.09 | G | S | | | | | 2012 | | avW,KBF | MCG | ESO |

| | | | | | | | | | | | | | | | |
|---|---|---|---|---|---|---|---|---|---|---|---|---|---|---|---|
| 07284-3554 | 249.216 | -8.438 | 1.04 | 1.80 | G? | S | P | 0.2 | 18.0 | 0.613 | | | | | |
| 07285-3437 | 248.079 | -7.822 | 0.75 | 2.49 | G | S | P | 0.3 | 17.3 | 0.613 | | | W | | |
| 07289-1218 | 228.518 | 2.988 | 0.63 | 1.65 | G | S | | 0.6 | 16.1 | | 10972 | | W,53 | | |
| 07300-1027 | 227.028 | 4.116 | 0.82 | 2.05 | G? | ? | | 0.1 | 19.2 | 0.613 | | | | | |
| 07303-1347 | 229.992 | 2.586 | 5.53 | 11.39 | G | S | | 1.0 | 15.2 | | | | | | |
| 07310-3104 | 245.196 | -5.676 | 2.01 | 1.79 | G | S | | | | | 1867 | | * | | |
| | 215.526 | 11.368 | 2.22 | | | | | | | | 5140 | | KBF | | |
| | 219.808 | 9.245 | 1.66 | | | | | | | | 8691 | | KBF | | |
| 07318-3520 | 249.046 | -7.553 | 1.00 | 2.05 | G | S? | | 0.1 | 19.2 | 0.613 | | | | | |
| 07332-2719 | 242.133 | -3.425 | 1.23 | 4.07 | G | S | | 0.5 | 16.4 | | | | | | |
| 07333-3558 | 249.759 | -7.604 | 0.72 | 2.76 | G | S | P | 0.3 | 17.3 | 0.613 | | | | | |
| 07333-2629 | 241.421 | -3.006 | 13.97 | 27.07 | G | S | | 0.6 | 16.1 | | | | | | |
| 07335-3527 | 249.310 | -7.316 | 0.63 | 2.55 | G | S | | 0.5 | 16.4 | 0.613 | | | | | |
| 07336-4648 | 259.531 | -12.590 | 2.04 | 5.18 | G | S | P | 3.1 | 13.6 | 0.613 | 2881 | 20 | Y | ESO | |
| 07339-4955 | 262.410 | -13.938 | 0.89 | 4.45 | G | S | | | | | 3003 | | * | ESO | |
| 07340-2742 | 242.550 | -3.467 | 0.97 | 2.16 | G | S | | | | | 7866 | | * | | |
| 07350-4731 | 260.291 | -12.696 | 3.22 | 13.15 | G | S | | | | | 973 | | avW,KBF | ESO | |
| 07357-1651 | 233.307 | 2.212 | 1.41 | 3.01 | G | S | | 0.6 | 16.1 | | | | | | |
| 07359-2832 | 243.481 | -3.513 | 1.03 | 2.87 | G | S | | 0.5 | 16.4 | | | | | | |
| 07362-4530 | 258.546 | -11.597 | 0.81 | 1.82 | G | S | P | 0.2 | 18.4 | 0.613 | | | | | |
| 07363-5210 | 264.670 | -14.583 | 1.02 | 3.19 | G | S | P | 2.0 | 14.4 | 0.613 | 12878 | | KBF | ESO | ESO |
| 07367-3104 | 245.789 | -4.608 | 0.78 | 1.96 | G? | ? | | | | | 2085 | | * | ESO | |
| 07368-2155 | 237.843 | -0.065 | 3.81 | 8.70 | G | S | | | | | 2182 | | * | ESO | |
| 07369-2848 | 243.831 | -3.455 | 0.67 | 2.54 | G | S | | 0.7 | 15.8 | | | | | | |
| 07378-3136 | 246.358 | -4.666 | 1.38 | 4.14 | G | S | | | | | 7731 | | * | | |
| 07383-3154 | 246.690 | -4.715 | 2.25 | 5.82 | G | S | | | | | 3986 | | * | ESO | |
| 07384-2611 | 241.721 | -1.862 | 1.06 | 2.90 | G | S | | | | | 2969 | | * | | |
| 07387-0344 | 222.143 | 9.247 | 2.98 | 6.06 | G | S | | | | | 16455 | | * | | |
| 07388-2248 | 238.833 | -0.104 | 1.30 | 3.61 | G | ? | | 0.2 | 18.0 | | | | | | |
| 07390-3157 | 246.798 | -4.609 | 0.85 | 3.19 | G | S | | 0.8 | 15.6 | 0.613 | | | | ESO | |
| 07393-0234 | 221.164 | 9.932 | 1.26 | 2.88 | G | S | | | | | 8180 | | avW,KBF | CGCG | |
| 07393-2911 | 244.417 | -3.188 | 0.88 | 2.49 | G | S | P | | | | 15130 | | * | | |
| 07395-2959 | 245.143 | -3.553 | 1.99 | 4.27 | G | S | | | | | 2093 | | * | | |
| 07395-2224 | 238.560 | 0.240 | 6.20 | 15.14 | G | S? | | | | | 3078 | | * | | |
| 07398-3021 | 245.489 | -3.668 | 0.79 | 2.61 | G | S | | | | | 7402 | | * | ESO | |
| 07403-2735 | 243.144 | -2.204 | 0.91 | 2.64 | G | ? | | 0.2 | 18.0 | | | | | | |
| 07405-2659 | 242.645 | -1.857 | 1.11 | 2.57 | G | ? | | 0.1 | 19.2 | | | | | | |
| 07413-3305 | 248.019 | -4.757 | 1.00 | 2.37 | G? | ? | | 0.1 | 19.2 | 3.273 | | | | | |
| 07416-2622 | 242.235 | -1.326 | 0.83 | 3.73 | G | S | | 0.2 | 18.0 | | | | | | |
| | 218.262 | 11.670 | 1.68 | | | | | | | | 14538 | | KBF | | |
| 07422-5133 | 264.523 | -13.503 | 1.74 | 5.06 | G | S | P | | | | 2593 | | avW,KBF | ESO | |
| 07422-0233 | 221.515 | 10.573 | 0.79 | 1.83 | G | S | P | | | | 8699 | | * | | |
| 07430-1712 | 234.469 | 3.549 | 2.71 | 5.05 | G | ? | | 0.3 | 17.3 | | 11182 | | W,53 | | |
| 07442-1825 | 235.663 | 3.181 | 1.73 | 5.47 | G | S | | | | | 3304 | | * | ESO | |
| 07443-4442 | 258.526 | -9.955 | 0.81 | 1.94 | G | S? | P | 0.3 | 17.7 | 0.613 | | | W | | |
| 07449-5446 | 267.661 | -14.612 | 3.42 | 3.17 | G | E | P | | | | 9332 | | * | | |
| 07451-3810 | 252.849 | -6.621 | 1.30 | 3.69 | G | S | P | 0.7 | 15.8 | 1.499 | 2817 | | KBF | ESO | |
| 07451-2130 | 238.443 | 1.806 | 2.10 | 3.20 | G? | S | P | 0.3 | 17.3 | | | | | | |
| 07456-1837 | 236.010 | 3.372 | 1.44 | 5.69 | G | S | | | | | 3242 | | * | MCG | ESO |
| 07460-2506 | 241.636 | 0.152 | 5.10 | 7.47 | G | | | 0.5 | 16.4 | | 7980 | 13 | W,72 | ESO | |
| 07464-3056 | 246.715 | -2.746 | 1.18 | 3.33 | G | ? | | 0.2 | 18.0 | | | | | | |
| 07464-2525 | 241.954 | 0.073 | 0.73 | 2.17 | G | S | | | | | 3975 | | * | | |
| 07465-2502 | 241.650 | 0.284 | 0.94 | 3.21 | G | S | P | 0.8 | 15.6 | | | | | | |
| 07466-2607 | 242.585 | -0.240 | 13.28 | 28.25 | G | S | P | | | | 2596 | | * | ESO | |
| 07474-3059 | 246.874 | -2.578 | 3.19 | 3.88 | G | ? | | 0.2 | 18.0 | | | | | | |
| 07475-1106 | 229.713 | 7.558 | 0.95 | 1.00 | G | S? | P | 0.1 | 19.2 | 0.613 | | | | | |
| | 221.123 | 11.938 | 1.32 | | | | | | | | 8745 | | KBF | | |
| | 253.023 | -6.081 | 1.61 | | | | | | | | 8833 | | KBF | | |
| 07479-3854 | 253.762 | -6.505 | 1.65 | 5.41 | G | S | | 0.5 | 16.4 | 0.613 | 6136 | | KBF | | |
| 07480-2724 | 243.848 | -0.637 | 2.71 | 6.31 | G | S | P | | | | 3166 | | * | | |
| 07484-3058 | 246.964 | -2.391 | 1.94 | 4.00 | G | S | | 0.5 | 16.4 | | | | | | |
| 07485-3742 | 252.785 | -5.793 | 0.73 | 3.25 | G | S | | 0.3 | 17.3 | 1.499 | | | | | |
| 07489-3336 | 249.276 | -3.651 | 4.79 | 8.35 | G? | | | 0.4 | 16.8 | | | | | | |
| 07494-2930 | 245.813 | -1.451 | 0.70 | 2.34 | G | S | | | | | 4754 | | * | ESO | |
| 07494-0307 | 222.899 | 11.884 | 0.67 | 1.04 | G | E | | 0.1 | 19.2 | 0.613 | | | W | | |
| 07500-1643 | 234.902 | 5.236 | 0.69 | 1.59 | G | S | P | 0.2 | 18.0 | 0.613 | | | | | |
| 07502-2500 | 242.054 | 1.023 | 0.63 | 2.33 | G | ? | | | | | 4842 | | * | ESO | |
| 07504-2537 | 242.606 | 0.743 | 2.94 | 5.04 | G | S? | | 0.2 | 18.0 | | | | | | |
| 07510-2209 | 239.700 | 2.647 | 8.36 | 12.64 | G | S | P | 0.3 | 17.3 | | | | | | |
| 07513-2121 | 239.059 | 3.128 | 0.66 | 1.53 | G | S | | 0.9 | 15.4 | | | | | ESO | |
| 07516-3148 | 248.028 | -2.237 | 1.07 | 4.74 | G | S? | | 0.2 | 18.0 | | | | | | |
| 07519-3404 | 250.005 | -3.345 | 14.41 | 18.46 | G | S | | 0.2 | 18.0 | | | | | | |
| 07520-3622 | 251.990 | -4.522 | 1.96 | 7.36 | G | S | | 0.2 | 18.0 | 3.273 | | | | | |
| 07526-2041 | 238.625 | 3.730 | 0.88 | 1.94 | G | ? | | 0.5 | 16.4 | | | | | | |
| 07526-3810 | 253.607 | -5.339 | 2.71 | 5.24 | G | S | | | | | 15395 | | * | | |
| 07529-3310 | 249.341 | -2.700 | 0.81 | 3.00 | G | S | | 0.5 | 16.4 | | | | | | |
| 07530-3441 | 250.645 | -3.482 | 85.24 | 145.60 | G | S | | 0.2 | 18.0 | | | | | | |
| 07531-2802 | 244.981 | 0.014 | 1.59 | 7.77 | G | S | | | | | 1692 | | * | ESO | |
| 07533-2235 | 240.352 | 2.883 | 0.62 | 2.10 | G | S | | | | | 3933 | | * | ESO | |
| | 268.409 | -13.698 | 1.60 | | | | | | | | 9922 | | KBF | | |
| 07551-1906 | 237.586 | 5.065 | 1.74 | 4.05 | G | S | | | | | 3487 | | avW,KBF | ESO | |
| 07555-2425 | 242.166 | 2.351 | 0.66 | 2.27 | G | S | | 0.3 | 17.3 | | | | | | |
| 07561-1413 | 233.501 | 7.796 | 0.74 | 2.21 | G? | ? | | 0.8 | 15.6 | 0.613 | | | | MCG | |
| 07565-4656 | 261.557 | -9.209 | 0.76 | 2.08 | G | S | | 0.3 | 17.7 | 0.613 | | | | | |
| 07566-2504 | 242.868 | 2.230 | 0.70 | 1.58 | G | S | P | | | | 6402 | | * | | |
| | 221.410 | 14.709 | 2.70 | | | | | | | | 3562 | | KBF | | |
| | 267.062 | -12.338 | 1.53 | | | | | | | | 13091 | | KBF | | |
| 07568-4942 | 264.013 | -10.579 | 8.06 | 27.00 | G | S | | | | | 1112 | | avW,KBF | ESO | |
| | 233.279 | 8.486 | 2.50 | | | | | | | | 17794 | | KBF | | |
| | 267.362 | -12.229 | 2.76 | | | | | | | | 12890 | | KBF | | |
| | 258.912 | -7.046 | 1.53 | | | | | | | | 38828 | | KBF | | |
| | 264.249 | -10.027 | 1.60 | | | | | | | | 11744 | | KBF | | |
| 07574-2355 | 241.989 | 2.993 | 1.17 | 2.65 | G | ? | | 0.3 | 17.3 | | | | | | |
| 07580-1202 | 231.848 | 9.306 | 0.61 | 1.67 | G | ? | | | | | 2741 | | * | | |
| 07581-2439 | 242.697 | 2.745 | 0.61 | 1.67 | G | S | | 0.5 | 16.4 | | | | W,-27 | | |
| 07583-5533 | 269.307 | -13.291 | 0.70 | 2.36 | G | S | P | 0.5 | 16.8 | 0.613 | | | W | | |
| 07583-2334 | 241.787 | 3.361 | 0.91 | 4.49 | G | S? | | 0.2 | 18.0 | | | | | | |
| 07588-3147 | 248.819 | -0.911 | 2.47 | 3.98 | G | S | | 0.4 | 16.8 | | | | | | |
| 07590-1814 | 237.316 | 6.288 | 0.71 | 1.93 | G | ? | | 0.4 | 16.8 | 0.613 | 14930 | | W,53 | | |
| 07591-4659 | 261.835 | -8.869 | 0.66 | 1.91 | G | S | P | 0.2 | 18.4 | 0.613 | | | W | | |
| 07593-2808 | 245.786 | 1.124 | 1.79 | 3.11 | G | S? | | 0.2 | 18.0 | | | | W | | |
| 08000-2248 | 241.342 | 4.089 | 1.32 | 3.00 | G | S? | | | | | 5796 | | * | ESO | |
| 08006-1730 | 236.899 | 7.014 | 1.17 | 2.62 | G | E? | | 0.2 | 18.0 | 0.613 | | | W | | |
| 08007-2817 | 246.071 | 1.291 | 36.09 | 141.70 | G? | ? | | 0.1 | 19.2 | | | | | | |

| | | | | | | | | | | | | | | |
|---|---|---|---|---|---|---|---|---|---|---|---|---|---|---|
| 08008-1833 | 237.827 | 6.495 | 0.82 | 1.58 | G | S | P | 1.3 | 14.7 | 0.613 | 3350 | K | MCG | ESO |
| 08013-4707 | 262.149 | -8.606 | 0.76 | 2.42 | G? | S? | | 0.2 | 18.4 | 0.613 | | W | | |
| 08016-2528 | 243.805 | 2.981 | 7.36 | 10.67 | G | S | | | | | 6133 | * | ESO | |
| 08021-5913 | 272.855 | -14.652 | 0.94 | 2.17 | G | S | | 0.6 | 16.5 | 0.613 | 9787 20 | DV | | |
| 08023-5918 | 272.953 | -14.669 | 0.89 | 1.88 | G | S | | 0.4 | 17.2 | 0.613 | 9887 42 | DV,W | | |
| 08028-5330 | 267.824 | -11.701 | 3.81 | 4.33 | G | S? | P | | | | 18111 | * | | |
| 08028-5544 | 269.798 | -12.828 | 0.70 | 1.99 | G | S | P | 0.4 | 17.2 | 0.613 | 14540 | W,53 | ESO | |
| 08037-2550 | 244.360 | 3.181 | 0.60 | 2.06 | G | S | | | | | 7657 | * | ESO | |
| 08039-2715 | 245.574 | 2.443 | 0.97 | 2.57 | G | S | | | | | 1021 | * | ESO | |
| 08041-2723 | 245.709 | 2.414 | 5.04 | 18.39 | G | S | | | | | 966 | * | ESO | |
| 08045-2245 | 241.864 | 4.992 | 1.20 | 3.43 | G | S | | | | | 4547 | * | ESO | |
| 08050-2754 | 246.255 | 2.299 | 2.01 | 5.03 | G | S | | | | | 1023 | * | ESO | |
| 08059-4512 | 260.933 | -6.921 | 0.89 | 3.25 | G | S? | | 0.2 | 18.4 | 0.613 | | | | |
| 08063-1305 | 233.822 | 10.488 | 0.74 | 0.87 | G | S | P | 0.3 | 17.3 | 0.613 | | W | | |
| 08064-1257 | 233.708 | 10.575 | 0.65 | 1.81 | G | ? | | 0.2 | 18.0 | 0.613 | 16343 | DV | | |
| 08065-2056 | 240.567 | 6.357 | 2.50 | 2.57 | G | ? | P | 0.2 | 18.0 | 0.613 | | | | |
| | 231.856 | 10.791 | 6.08 | | | | | | | | 1586 | KBF | | |
| 08069-1832 | 238.590 | 7.732 | 1.68 | 3.32 | G | S | | 0.7 | 15.8 | 0.613 | 6014 | KBF | MCG | ESO |
| 08077-2349 | 243.154 | 5.026 | 1.44 | 2.98 | G | S | | | | | 6960 | avW,KBF | | |
| 08080-6109 | 274.972 | -14.973 | 1.68 | 2.65 | G | | | 1.8 | 14.6 | 0.613 | 3086 12 | DV | | |
| 08109-2843 | 247.667 | 2.941 | 2.14 | 4.48 | G | S | | 0.2 | 18.0 | | | W | | |
| 08114-2306 | 243.020 | 6.130 | 0.64 | 1.76 | G | S | | | | | 6865 | * | | |
| 08126-4402 | 260.602 | -5.283 | 0.99 | 3.80 | G | S | P | 0.4 | 16.8 | 1.499 | | | | |
| 08128-2920 | 248.400 | 2.938 | 0.71 | 2.12 | G | S | | 0.2 | 18.0 | | | W | | |
| 08129-3417 | 252.525 | 0.199 | 1.17 | 2.40 | G | S | P | 0.3 | 17.3 | | | | | |
| 08132-5309 | 268.355 | -10.198 | 0.87 | 3.36 | G | E? | P | 0.3 | 17.7 | 0.613 | 11887 30 | DV,W | | |
| 08135-2254 | 243.122 | 6.642 | 1.22 | 1.69 | G | S | | | | | 4258 | avW,KBF | | |
| 08143-3942 | 257.169 | -2.605 | 2.76 | 13.11 | G | S? | | 0.2 | 18.0 | | | | | |
| 08146-6030 | 274.822 | -13.951 | 1.59 | 2.50 | G? | S | | 0.2 | 18.4 | 0.613 | | W | | |
| 08150-2718 | 246.979 | 4.482 | 25.99 | 65.63 | G | S | | | | | 1571 | * | MCG | ESO |
| 08152-5912 | 273.721 | -13.190 | 0.75 | 1.47 | G | S | P | 0.3 | 17.7 | 0.613 | 11337 21 | DV,W | | |
| 08153-2750 | 247.461 | 4.245 | 9.03 | 10.53 | G? | ? | P | 0.1 | 19.2 | 0.613 | | | | |
| 08155-2934 | 248.930 | 3.307 | 1.30 | 4.09 | G | S | | | | | 1659 | * | ESO | |
| 08156-2958 | 249.273 | 3.100 | 5.02 | 9.60 | G | S | | | | | 1651 | * | ESO | |
| 08166-2520 | 245.549 | 5.878 | 22.45 | 39.43 | G | S | | | | | 1649 | * | MCG | ESO |
| | 233.800 | 13.574 | 1.81 | | | | | | | | 15889 | KBF | | |
| 08171-2501 | 245.351 | 6.143 | 3.26 | 2.99 | G | S | | | | | 1628 | * | MCG | ESO |
| 08172-2437 | 245.033 | 6.394 | 1.31 | 2.41 | G | S | | | | | 1717 | avW,KBF | MCG | ESO |
| 08174-5100 | 266.884 | -8.480 | 0.86 | 3.57 | G | ? | P | 0.3 | 17.3 | 3.273 | 9621 14 | DV | | |
| 08174-2224 | 243.213 | 7.678 | 0.65 | 1.73 | G | S | P | | | | 5835 | * | MCG | ESO |
| 08177-3535 | 254.155 | 0.280 | 2.37 | 7.47 | G? | ? | | 0.1 | 19.2 | | | | | |
| | 236.557 | 12.005 | 4.89 | | | | | | | | 5732 | KBF | | |
| 08182-1823 | 239.933 | 10.051 | 1.28 | 2.47 | G | S | | 0.6 | 16.5 | 0.613 | 15004 | KBF | | |
| | 234.048 | 14.314 | 1.79 | | | | | | | | 4590 | KBF | | |
| 08193-2913 | 249.094 | 4.177 | 0.89 | 1.79 | G | ? | P | 0.5 | 16.4 | 0.613 | | | | |
| 08194-4925 | 265.740 | -7.320 | 29.75 | 74.63 | G? | S | | 0.6 | 16.1 | 3.273 | | | | |
| 08196-4931 | 265.838 | -7.357 | 53.30 | 74.63 | G? | ? | | 0.6 | 16.1 | 3.273 | | | | |
| 08207-2931 | 249.532 | 4.258 | 1.13 | 2.40 | G | S | P | 0.3 | 17.3 | 0.613 | 12788 45 | DV | | |
| 08211-2602 | 246.706 | 6.332 | 2.07 | 5.77 | G | S | | | | | 1705 | * | MCG | ESO |
| | 236.333 | 13.886 | 1.33 | | | | | | | | 6066 | KBF | | |
| | 236.219 | 14.108 | 2.14 | | | | | | | | 6044 | KBF | | |
| | 273.316 | -11.527 | 2.06 | | | | | | | | 16215 | KBF | | |
| | 238.494 | 12.825 | 3.41 | | | | | | | | 8984 | KBF | | |
| 08216-2906 | 249.298 | 4.656 | 0.88 | 1.78 | G | S | | | | | 2565 | * | | |
| 08219-1836 | 240.604 | 10.655 | 1.05 | 4.64 | G | S | | | | | 2569 | * | MCG | ESO |
| 08227-6042 | 275.547 | -13.217 | 0.68 | 1.98 | G | S | | 1.8 | 14.6 | 0.613 | 2589 12 | DV,W,38 | ESO | |
| 08230-1804 | 240.293 | 11.175 | 0.79 | 1.46 | G | S | | 0.4 | 17.2 | 0.613 | | W | | |
| 08240-3629 | 255.622 | 0.800 | 1.20 | 2.87 | G | S | | 0.6 | 16.1 | | | | | |
| 08247-1952 | 242.042 | 10.505 | 1.61 | 2.52 | G | S | P | 0.3 | 17.7 | 0.613 | 14061 | KBF | | |
| 08252-6421 | 278.858 | -14.972 | 0.72 | 1.57 | G | | | 0.2 | 18.4 | 0.613 | | | | |
| 08252-3619 | 255.628 | 1.089 | 2.47 | 3.96 | G | S | P | 0.2 | 18.0 | | | | | |
| 08267-3703 | 256.387 | 0.902 | 2.13 | 5.82 | G | S | | 0.7 | 15.8 | | | | ESO | |
| 08275-2418 | 246.123 | 8.501 | 0.82 | 1.21 | G | ? | | 0.2 | 18.0 | 0.613 | | | | |
| 08276-2158 | 244.184 | 9.864 | 0.74 | 1.49 | G | S | P | | | | 6350 | * | | |
| 08277-3336 | 253.732 | 3.102 | 0.62 | 1.86 | G | S | | 0.4 | 16.8 | | | W | | |
| 08279-1901 | 241.774 | 11.611 | 0.66 | 1.46 | G | S | P | 0.2 | 18.4 | 0.613 | 14990 | W,53 | | |
| 08282-1909 | 241.918 | 11.585 | 0.65 | 1.07 | G | ? | | 0.1 | 19.6 | 0.613 | | W | | |
| 08291-2019 | 243.019 | 11.097 | 0.71 | 1.31 | G | S | | 0.3 | 17.7 | 0.613 | | W | | |
| 08294-6449 | 279.517 | -14.848 | 0.85 | 2.74 | G | S | | 1.1 | 15.4 | 0.613 | 5342 10 | DV,W,53 | ESO | |
| 08298-2054 | 243.607 | 10.907 | 0.95 | 1.59 | G | S | | 0.6 | 16.5 | 0.613 | | | | |
| | 270.224 | -9.356 | 1.72 | | | | | | | | 12442 | KBF | | |
| 08305-2352 | 246.148 | 9.305 | 1.46 | 3.33 | G | S | P | | | | 7885 | avW,KBF | MCG | ESO |
| 08306-5936 | 275.175 | -11.785 | 1.79 | 8.29 | G | S | P | | | | 6415 | avW,KBF | ESO | |
| | 275.185 | -11.768 | 3.61 | | | | | | | | 6411 | KBF | | |
| 08310-1747 | 241.151 | 12.906 | 1.45 | 4.65 | G | S | | | | | 4600 | * | MCG | ESO |
| 08311-2459 | 247.159 | 8.779 | 4.96 | 5.80 | G? | S | | | | | 29988 | * | | |
| 08311-2248 | 245.360 | 10.055 | 6.77 | 20.39 | G | S | | | | | 1678 | * | MCG | ESO |
| 08322-5826 | 274.320 | -10.943 | 0.72 | 1.05 | G | S | P | 0.3 | 17.7 | 0.613 | 15910 98 | DV,W,53 | | |
| 08323-3138 | 252.721 | 5.044 | 2.58 | 4.25 | G | S | | | | | 1948 | | ESO | |
| | 244.091 | 11.377 | 1.49 | | | | | | | | 25504 | KBF | | |
| | 266.948 | -5.369 | 1.38 | | | | | | | | 7731 | KBF | | |
| 08332-2537 | 247.967 | 8.785 | 0.69 | 1.90 | G | S | | | | | 8138 | * | | |
| 08335-3158 | 253.133 | 5.056 | 1.19 | 3.49 | G | S | | | | | 1552 | * | ESO | |
| 08336-5553 | 272.329 | -9.297 | 1.39 | 1.97 | G | S | | 0.3 | 17.3 | 0.613 | 9176 16 | DV | | |
| 08340-2006 | 243.525 | 12.164 | 0.92 | 1.84 | G | S | | 0.9 | 15.8 | 0.613 | | W | MCG | ESO |
| 08340-2656 | 249.140 | 8.154 | 0.69 | 1.55 | G | S | | 0.3 | 17.3 | 0.613 | | W | | |
| 08341-2614 | 248.573 | 8.577 | 24.08 | 26.40 | G? | E | | | | | 864 | avW,KBF | MCG | ESO |
| 08350-2045 | 244.208 | 11.974 | 1.73 | 3.27 | G | S | | 1.6 | 14.8 | 0.613 | 2462 | KBF | MCG | ESO |
| | 267.523 | -5.393 | 9.68 | | | | | | | | 7780 | KBF | | |
| 08350-3419 | 255.206 | 3.898 | 1.00 | 3.11 | G | S | | 0.3 | 17.3 | | | | | |
| 08360-5456 | 271.775 | -8.457 | 4.37 | 10.59 | G | E | | | | | 1051 | * | ESO | |
| 08365-3549 | 256.588 | 3.231 | 1.09 | 1.55 | G | S | P | | | | 9467 | * | | |
| 08371-3528 | 256.388 | 3.521 | 0.79 | 2.01 | G | ? | P | 0.2 | 18.0 | | | W | | |
| 08373-2701 | 249.647 | 8.693 | 1.04 | 0.85 | G | S | P | 0.3 | 17.7 | 0.613 | | W | | |
| 08374-2033 | 244.366 | 12.550 | 0.69 | 1.36 | G | S? | P | 0.4 | 17.2 | 0.613 | | W,-27 | | |
| 08376-2315 | 246.629 | 10.991 | 0.75 | 0.90 | G | E | | 0.8 | 16.0 | 0.613 | | | MCG | |
| 08378-2553 | 248.799 | 9.460 | 0.76 | 1.42 | G | S? | P | 0.2 | 18.4 | 0.613 | | | | |
| 08381-1928 | 243.569 | 13.320 | 0.62 | 1.28 | G | S | | 0.3 | 17.7 | 0.613 | | W | | |
| 08386-6257 | 278.533 | -12.940 | 3.36 | 7.32 | G | S | | | | | 5024 | * | ESO | |
| 08387-2344 | 247.167 | 10.909 | 1.78 | 4.45 | G | ? | P | | | | 3830 | avW,KBF | MCG | ESO |
| 08387-3151 | 253.724 | 6.003 | 0.84 | 2.10 | G | S | | 2.0 | 14.0 | 0.613 | 900 | K | ESO | |
| 08397-5430 | 271.734 | -7.769 | 0.60 | 2.47 | G | S | | 0.2 | 18.0 | 3.273 | | | | |
| 08398-2520 | 248.624 | 10.145 | 0.70 | 1.69 | G | S | P | 0.7 | 16.2 | 0.613 | 9057 | W,59 | | |
| 08402-1941 | 244.053 | 13.594 | 0.74 | 1.04 | G | S | | | | | 1623 | * | MCG | ESO |

| | | | | | | | | | | | | | | | |
|---|---|---|---|---|---|---|---|---|---|---|---|---|---|---|---|
| 08407-1952 | 244.264 | 13.566 | 2.16 | 8.42 | G | S | P | | | | 1754 | | * | MCG | ESO |
| 08410-2028 | 244.814 | 13.266 | 0.82 | 1.59 | G | S | | | | | 1732 | | * | MCG | ESO |
| 08422-2010 | 244.729 | 13.686 | 1.02 | 3.71 | G | S | | | | | 3430 | | * | MCG | ESO |
| 08423-3430 | 256.284 | 4.965 | 1.37 | 2.98 | G | S | | 0.7 | 15.8 | 0.613 | | | W | ESO | |
| 08424-3130 | 253.921 | 6.830 | 6.27 | 9.77 | G | S | P | | | | 4846 | | * | ESO | |
| 08432-2847 | 251.865 | 8.651 | 0.85 | 1.37 | G | S? | P | 0.1 | 19.2 | 0.613 | | | W | | |
| 08436-2812 | 251.468 | 9.078 | 2.31 | 3.92 | G | S? | P | | | | 14708 | | * | | |
| 08437-1907 | 244.077 | 14.591 | 6.28 | 9.76 | G | S | | | | | 1706 | | * | MCG | ESO |
| 08450-1951 | 244.866 | 14.396 | 1.02 | 4.88 | G | S | P | | | | -410 | | * | MCG | ESO |
| 08457-2256 | 247.508 | 12.675 | 0.62 | 1.63 | G | S | P | 0.2 | 18.4 | 0.613 | | | W | | |
| 08462-2149 | 246.658 | 13.433 | 0.63 | 1.18 | G | S | | | | | 17642 | | * | | |
| 08482-6306 | 279.327 | -12.167 | 1.18 | 1.82 | G | S | | 0.3 | 17.7 | 0.613 | 10041 | 21 | DV | | |
| 08482-3229 | 255.469 | 7.191 | 0.64 | 1.33 | G | S | | | | | 14660 | | * | ESO | |
| 08485-4414 | 264.598 | -0.246 | 20.03 | 34.73 | G? | ? | | 0.5 | 16.4 | | | | | | |
| | 255.901 | 5.984 | 2.34 | | | | | | | | 2569 | | KBF | | |
| 08485-2146 | 246.958 | 13.886 | 8.22 | 16.57 | G | S | | | | | 2611 | | * | MCG | ESO |
| 08486-3731 | 259.438 | 4.063 | 0.95 | 2.61 | G | S? | | 0.2 | 18.0 | 0.613 | | | W | | |
| 08489-3420 | 257.009 | 6.122 | 1.17 | 5.09 | G | S | | | | | 2366 | | * | ESO | |
| 08492-2146 | 247.060 | 14.010 | 0.73 | 1.16 | G | E? | | 0.3 | 17.7 | 0.613 | 9953 | | W,53 | | |
| 08493-2721 | 251.574 | 10.601 | 0.81 | 1.12 | G | S | P | | | | 12205 | | * | | |
| 08494-3711 | 259.279 | 4.405 | 0.69 | 2.24 | G | S | | 0.4 | 16.8 | 0.613 | | | W | | |
| 08500-2722 | 251.687 | 10.693 | 0.79 | 1.35 | G | S | P | 0.3 | 17.7 | 0.613 | | | W | | |
| 08500-2440 | 249.537 | 12.382 | 0.68 | 1.57 | G | S | P | | | | 9164 | | * | | |
| 08511-6429 | 280.647 | -12.773 | 1.60 | 2.66 | G | S | P | 0.4 | 17.2 | 0.613 | 5688 | 7 | DV | | |
| 08511-3521 | 258.085 | 5.833 | 0.97 | 2.27 | G | S | | 0.3 | 17.3 | 0.613 | | | W | | |
| 08526-3012 | 254.284 | 9.368 | 0.99 | 1.24 | G | S? | | 0.1 | 19.2 | 0.613 | | | W | | |
| 08540-6337 | 280.157 | -11.990 | 1.14 | 3.02 | G | S | | 0.8 | 16.0 | 0.613 | 6425 | 15 | DV | | |
| 08542-2500 | 250.404 | 12.917 | 0.66 | 1.75 | G | ? | | | | | 7517 | | * | | |
| 08549-2433 | 250.139 | 13.319 | 1.01 | 2.41 | G | S? | | | | | 2377 | | * | MCG | ESO |
| 08549-6715 | 283.123 | -14.191 | 0.85 | 3.17 | G | S | | 2.0 | 14.4 | 0.613 | 3260 | 35 | W,17 | ESO | |
| 08549-2602 | 251.333 | 12.399 | 2.21 | 4.04 | G | S | P | 0.4 | 17.2 | 0.613 | 12446 | 39 | W,43 | | |
| 08553-3518 | 258.607 | 6.516 | 1.04 | 1.82 | G | ? | | 0.1 | 19.2 | 0.613 | | | W | | |
| 08574-2510 | 250.997 | 13.376 | 0.85 | 1.63 | G | E | | 0.5 | 16.8 | 0.613 | | | W | | |
| 08574-4006 | 262.524 | 3.691 | 4.88 | 10.28 | G | S | P | 0.5 | 16.4 | | | | | | |
| 08575-5512 | 273.916 | -6.229 | 2.03 | 2.24 | G | S | P | | | | 25150 | | * | | |
| 08576-6631 | 282.714 | -13.528 | 2.20 | 4.02 | G | S | | | | | 3283 | | * | ESO | |
| 08580-3020 | 255.151 | 10.164 | 3.73 | 6.85 | G | S | P | | | | 8752 | | * | | |
| 08581-6050 | 278.291 | -9.837 | 1.29 | 2.29 | G | S? | | 0.2 | 18.0 | 0.613 | 8684 | | KBF | | |
| 08586-3914 | 262.020 | 4.437 | 2.26 | 6.40 | G | S | | 0.7 | 15.8 | 0.613 | | | | ESO | |
| 08594-2435 | 250.837 | 14.091 | 1.09 | 2.76 | G | S | | | | | 422 | | * | ESO | |
| 08597-6336 | 280.559 | -11.484 | 1.76 | 5.33 | G | S | | 1.0 | 15.6 | 0.613 | 6368 | 21 | DV | ESO | |
| 09006-6404 | 280.990 | -11.710 | 4.10 | 5.80 | G | S | P | | | | 6621 | | avW,KBF | ESO | |
| 09009-5544 | 274.644 | -6.222 | 0.74 | 2.03 | G | S | | 0.2 | 18.0 | 0.613 | 1669 | | KBF | | |
| 09011-6442 | 281.515 | -12.077 | 2.07 | 5.21 | G | S | | | | | 1639 | | * | ESO | |
| 09018-3214 | 257.150 | 9.540 | 1.18 | 1.39 | G | S | | 0.5 | 16.8 | 0.613 | | | W | | |
| 09020-6801 | 284.175 | -14.158 | 0.75 | 1.80 | G | S | | | | | 4094 | | * | ESO | |
| | 260.236 | 6.951 | 11.48 | | | | | | | | 17880 | | KBF | | |
| 09026-3817 | 261.818 | 5.648 | 1.29 | 3.56 | G | S | | 0.5 | 16.4 | 0.613 | 4805 | | KBF | | |
| 09027-5757 | 276.483 | -7.500 | 2.90 | 6.04 | G | S | | | | | 16439 | | * | | |
| 09037-5414 | 273.780 | -4.914 | 0.82 | 2.40 | G | S | | 0.6 | 16.1 | 0.613 | | | W | | |
| 09052-2749 | 254.239 | 13.004 | 2.12 | 4.07 | G | S | P | | | | 10733 | | * | | |
| 09055-3349 | 258.866 | 9.062 | 0.72 | 1.81 | G | S | P | 0.2 | 18.0 | 0.613 | | | | | |
| 09060-3348 | 258.936 | 9.164 | 1.06 | 3.18 | G | S | | 0.3 | 17.3 | 0.613 | 9685 | | KBF | ESO | |
| 09067-3824 | 262.457 | 6.180 | 2.00 | 6.16 | G | S | | | | | 4942 | | * | ESO | |
| 09079-2620 | 253.495 | 14.431 | 0.78 | 1.67 | G | S | P | 0.3 | 17.7 | 0.613 | | | W | | |
| 09079-3256 | 258.548 | 10.039 | 0.75 | 2.11 | G | ? | | | | | 1541 | | * | MCG | ESO |
| 09083-6743 | 284.341 | -13.514 | 2.82 | 6.96 | G | S | P | | | | 1557 | | avW,KBF | ESO | |
| 09092-3039 | 257.005 | 11.763 | 0.66 | 1.32 | G | ? | P | | | | 2151 | | * | MCG | ESO |
| 09095-3544 | 260.863 | 8.384 | 1.05 | 2.91 | G | S | | 0.3 | 17.3 | 0.613 | 11361 | 48 | DV | | |
| 09097-2637 | 253.993 | 14.554 | 1.91 | 4.10 | G | S | | 0.8 | 16.0 | 0.613 | 2381 | | KBF | ESO | |
| 09105-4213 | 265.752 | 4.102 | 10.25 | 8.50 | G? | E | | 0.3 | 17.3 | 0.613 | | | | ESO | |
| 09106-6258 | 280.898 | -10.148 | 1.61 | 1.82 | G | E? | | 0.2 | 18.0 | 0.613 | 3087 | 9 | DV | | |
| 09112-5838 | 277.743 | -7.131 | 2.80 | 4.68 | G | S? | | | | | 2859 | | avW,KBF | ESO | |
| 09122-6034 | 279.259 | -8.378 | 12.12 | 15.65 | G | S | | | | | 2940 | | * | ESO | |
| 09129-2803 | 255.576 | 14.110 | 0.75 | 2.18 | G | S | | | | | 2181 | | * | MCG | ESO |
| 09133-6013 | 279.095 | -8.032 | 4.39 | 10.54 | G | S | | | | | 2857 | | * | ESO | |
| 09135-3526 | 261.197 | 9.189 | 4.84 | 7.90 | G | S | | | | | 2192 | | * | ESO | |
| 09136-6415 | 282.092 | -10.777 | 2.63 | 4.12 | G? | S? | | | | | 17546 | | * | | |
| 09137-3158 | 258.672 | 11.593 | 0.96 | 2.68 | G | S | | 0.8 | 16.0 | 0.613 | | | W | MCG | |
| 09144-6251 | 281.119 | -9.751 | 3.33 | 7.94 | G | S | | | | | 2868 | | avW,KBF | ESO | |
| 09148-3211 | 258.982 | 11.609 | 1.23 | 1.89 | G | S | | 0.3 | 17.7 | 0.613 | 8707 | | KBF | | |
| 09161-3216 | 259.233 | 11.755 | 0.85 | 2.06 | G | S | | 2.2 | 14.2 | 0.613 | | | W | ESO | |
| 09162-5932 | 278.849 | -7.307 | 0.72 | 2.19 | G | ? | | 0.2 | 18.0 | 0.613 | | | W | | |
| 09162-5516 | 275.775 | -4.311 | 1.60 | 3.72 | G | S | | 0.3 | 17.3 | 0.613 | | | | | |
| 09163-6240 | 281.131 | -9.464 | 0.79 | 1.77 | G | S | | 1.5 | 14.5 | 0.613 | 2266 | | avK,W,38 | ESO | |
| | 280.612 | -9.195 | 2.37 | | | | | | | | 17178 | | KBF | | |
| 09164-3904 | 264.254 | 7.090 | 1.70 | 4.50 | G | S | | 0.7 | 15.8 | 0.613 | 4720 | | * | ESO | |
| 09167-6037 | 279.670 | -8.006 | 1.72 | 3.26 | G? | | P | 0.1 | 19.2 | 0.613 | 27864 | | KBF | | |
| 09168-6141 | 280.458 | -8.741 | 0.63 | 1.66 | G | S | | 0.3 | 17.3 | 0.613 | | | W | | |
| 09182-3835 | 264.142 | 7.676 | 1.04 | 2.64 | G | E? | P | 0.2 | 18.0 | 0.613 | | | W | | |
| 09185-6456 | 282.960 | -10.871 | 0.85 | 2.75 | G | E | | 0.4 | 16.8 | 0.613 | 6387 | 24 | DV,W,53 | | |
| 09187-3008 | 258.035 | 13.629 | 1.20 | 2.26 | G | S? | P | | | | 18330 | | * | | |
| 09189-3258 | 260.168 | 11.691 | 1.11 | 3.75 | G | S | | 2.0 | 14.0 | 0.613 | | | | ESO | |
| 09190-2942 | 257.756 | 13.975 | 1.05 | 2.10 | G | S | | 0.5 | 16.8 | 0.613 | | | W | | |
| 09197-3306 | 260.391 | 11.727 | 0.88 | 3.58 | G | S | P | 0.6 | 16.1 | 0.613 | | | | ESO | |
| 09200-3308 | 260.458 | 11.760 | 2.37 | 3.58 | G | ? | P | | | | 16558 | | * | | |
| 09211-6050 | 280.205 | -7.776 | 1.97 | 7.47 | G | S | | | | | 2107 | | * | ESO | |
| 09214-5655 | 277.473 | -4.969 | 1.75 | 5.79 | G | S | | 0.3 | 17.3 | 1.499 | 6724 | | K | | |
| 09217-5648 | 277.411 | -4.857 | 1.41 | 4.60 | G | S? | P | 0.2 | 18.0 | 1.499 | | | | | |
| 09222-6327 | 282.181 | -9.542 | 0.78 | 1.97 | G | S | | 0.6 | 16.1 | 0.613 | 3185 | | avK,W,58 | ESO | |
| 09232-3353 | 261.471 | 11.697 | 1.41 | 2.76 | G | ? | | | | | 1153 | | * | ESO | |
| 09237-6700 | 284.846 | -11.948 | 1.97 | 3.25 | G? | ? | | | | | 3185 | | * | | |
| 09258-6505 | 283.619 | -10.426 | 0.71 | 1.21 | G? | ? | | 0.2 | 18.0 | 0.613 | 6187 | 14 | DV,W,53 | | |
| 09262-6033 | 280.454 | -7.139 | 1.64 | 4.14 | G | S | P | | | | 2211 | | * | ESO | |
| 09263-3554 | 263.388 | 10.712 | 1.44 | 2.69 | G | S | P | 0.5 | 16.8 | 0.613 | 4827 | | W,58 | ESO | |
| 09264-5853 | 279.318 | -5.920 | 1.09 | 2.25 | G | ? | | 0.2 | 18.0 | 0.613 | | | | | |
| 09281-4158 | 267.894 | 6.582 | 0.69 | 2.53 | G | S | | 0.6 | 16.1 | 0.613 | | | | | |
| 09291-4200 | 268.053 | 6.672 | 1.94 | 2.69 | G | ? | | | | | 6624 | | * | | |
| 09307-6528 | 284.267 | -10.350 | 1.23 | 3.39 | G | S | | 0.7 | 15.8 | 0.613 | 4530 | 14 | DV | | |
| 09312-3248 | 261.918 | 13.635 | 3.32 | 8.44 | G | S | P | | | | 929 | | * | MCG | ESO |
| 09316-6000 | 280.580 | -6.286 | 0.89 | 3.38 | G | | | 0.1 | 19.2 | 0.613 | | | W | | |
| 09328-6103 | 281.402 | -6.954 | 1.13 | 3.41 | G | S | | 0.6 | 16.1 | 0.613 | 2569 | 16 | DV | ESO | |
| 09335-4336 | 269.749 | 6.059 | 0.69 | 3.15 | G | S? | | 0.3 | 17.3 | 0.613 | | | | | |
| 09365-6155 | 282.311 | -7.301 | 2.06 | 6.50 | G | S | | | | | 2759 | | * | ESO | |

| | | | | | | | | | | | | | | |
|---|---|---|---|---|---|---|---|---|---|---|---|---|---|---|
| 09369-6315 | 283.248 | -8.265 | 6.63 | 11.20 | G | S | | | | | 2069 | | * | ESO |
| 09371-6136 | 282.151 | -7.014 | 1.66 | 6.23 | G | S | | | | | 2916 | | * | ESO |
| 09371-6130 | 282.095 | -6.943 | 0.73 | 3.47 | G | ? | | 0.6 | 16.1 | 0.613 | 2792 | | K | ESO |
| 09373-6344 | 283.606 | -8.600 | 2.60 | 3.22 | G | S | | | | | 4523 | | * | |
| 09375-6951 | 287.804 | -13.124 | 4.81 | 10.08 | G | S | | | | | 6066 | | * | ESO |
| 09375-4318 | 270.092 | 6.766 | 0.76 | 2.57 | G | ? | | 0.1 | 19.2 | 0.613 | | | W | |
| 09399-4152 | 269.456 | 8.132 | 1.33 | 2.12 | G | S? | | 0.5 | 16.4 | 0.613 | 6298 | | KBF | |
| 09403-4135 | 269.333 | 8.399 | 1.65 | 4.79 | G | S | | 1.4 | 14.6 | 0.613 | 4843 | | KBF | ESO |
| 09404-4142 | 269.431 | 8.317 | 1.32 | 4.77 | G | S? | | 0.5 | 16.4 | 0.613 | 4887 | | KBF | |
| 09405-3808 | 267.052 | 11.020 | 0.63 | 1.74 | G | ? | | 0.1 | 19.2 | 0.613 | | | | |
| 09407-4149 | 269.550 | 8.271 | 2.56 | 5.27 | G | S | | | | | 5527 | | * | ESO |
| 09424-5339 | 277.477 | -0.543 | 25.32 | 27.19 | G | S? | | 0.1 | 19.2 | | | | | |
| 09433-4445 | 271.837 | 6.344 | 1.30 | 2.31 | G | S | P | 0.3 | 17.3 | 0.613 | 18013 | | KBF | |
| 09444-4115 | 269.702 | 9.144 | 1.01 | 2.28 | G | S? | P | 0.3 | 17.3 | 0.613 | | | | ESO |
| 09447-6302 | 283.776 | -7.519 | 0.76 | 1.36 | G | S | | 1.0 | 15.2 | 0.613 | 3049 | | avK,W,38 | ESO |
| 09453-6840 | 287.528 | -11.782 | 0.71 | 2.46 | G | S | | 1.4 | 15.0 | 0.613 | | | W | ESO |
| 09465-3539 | 266.309 | 13.675 | 0.64 | 1.04 | G | S | P | 0.1 | 19.6 | 0.613 | | | W | |
| 09471-4223 | 270.824 | 8.603 | 2.15 | 3.14 | G | S | P | | | | 11363 | | * | ESO |
| 09473-4741 | 274.254 | 4.549 | 1.28 | 3.11 | G | E | | 0.9 | 15.4 | 0.613 | 1761 | 63 | avDV,K | ESO |
| 09477-4529 | 272.900 | 6.286 | 1.38 | 2.76 | G | S | P | 0.2 | 18.0 | 0.613 | 16196 | | KBF | |
| 09487-4928 | 275.560 | 3.300 | 0.63 | 2.76 | G | S | | 0.7 | 15.8 | | 12391 | | K,W | ESO |
| 09516-7304 | 290.849 | -14.794 | 1.32 | 1.68 | G | ? | P | 0.2 | 18.4 | 0.613 | 20596 | | W,53 | |
| 09532-4911 | 275.970 | 3.980 | 2.59 | 4.01 | G | S | | 0.3 | 17.3 | | 7745 | | K | |
| | 288.651 | -12.133 | 1.80 | | | | | | | | 39422 | | KBF | |
| 09538-6851 | 288.255 | -11.424 | 1.85 | 4.06 | G | S | | 0.8 | 16.0 | 0.613 | 6043 | | KBF | |
| 09543-4509 | 273.609 | 7.270 | 1.28 | 1.68 | G | S | | 0.4 | 16.8 | 0.613 | 6980 | | KBF | |
| 09547-3919 | 269.982 | 11.889 | 0.87 | 1.71 | G | ? | | 0.2 | 18.4 | 0.613 | | | W | |
| 09548-6751 | 287.685 | -10.579 | 0.69 | 1.29 | G | S | P | 0.3 | 17.3 | 0.613 | | | W | |
| 09555-3717 | 268.812 | 13.581 | 0.60 | 1.12 | G | S | P | 0.4 | 17.2 | 0.613 | | | W | |
| 09557-3907 | 270.014 | 12.165 | 1.89 | 3.91 | G | ? | | 0.5 | 16.8 | 0.613 | 4558 | 3 | KBF | ESO |
| 09558-3708 | 268.762 | 13.722 | 0.64 | 2.93 | G | S | | 0.2 | 18.4 | 0.613 | | | | |
| 09566-4650 | 274.962 | 6.188 | 1.31 | 2.47 | G | S | | 0.4 | 16.8 | 2.386 | 3572 | | KBF | |
| 09574-6846 | 288.450 | -11.152 | 0.61 | 1.41 | G | S | | 1.1 | 15.4 | 0.613 | 6266 | | W,53 | ESO |
| 09577-3950 | 270.773 | 11.847 | 0.92 | 2.57 | G | S | P | 0.6 | 16.5 | 0.613 | | | | ESO |
| 09590-3803 | 269.856 | 13.406 | 1.23 | 2.18 | G | S | P | 0.5 | 16.8 | 0.613 | 6913 | | avW,KBF | |
| 09594-4916 | 276.827 | 4.533 | 0.77 | 1.88 | G | S | | 0.5 | 16.4 | 0.613 | | | | |
| 10006-4515 | 274.550 | 7.868 | 1.93 | 3.55 | G | S | P | 0.7 | 15.8 | 0.613 | 3434 | | KBF | ESO |
| 10006-4150 | 272.470 | 10.589 | 1.40 | 3.27 | G | S | P | 2.4 | 14.1 | 0.613 | 2968 | | KBF | ESO |
| 10011-3835 | 270.530 | 13.232 | 0.65 | 1.80 | G | S | | | | | 12597 | | * | ESO |
| 10018-4417 | 274.145 | 8.768 | 1.68 | 3.99 | G | S | | 0.5 | 16.4 | 0.613 | 3523 | 19 | W,12 | ESO |
| 10019-6443 | 286.321 | -7.669 | 1.24 | 4.68 | G | S | | 1.2 | 14.9 | 0.613 | 2295 | | avK,W,38 | ESO |
| 10023-4411 | 274.143 | 8.905 | 0.91 | 1.51 | G | S? | P | 0.2 | 18.0 | 0.613 | 3734 | 14 | DV | |
| 10023-4110 | 272.313 | 11.320 | 1.77 | 5.38 | G | S | P | 2.5 | 14.0 | 0.613 | 5889 | | KBF | ESO |
| 10024-3705 | 269.788 | 14.573 | 1.29 | 2.90 | G | S | | | | | 4894 | | avW,KBF | ESO |
| 10034-4158 | 272.979 | 10.801 | 0.96 | 1.85 | G | S? | P | 0.1 | 19.6 | 0.613 | | | W | |
| 10037-4358 | 274.235 | 9.229 | 1.39 | 2.13 | G | S | P | | | | 3350 | | * | ESO |
| 10038-4446 | 274.729 | 8.598 | 1.34 | 4.21 | G | S | | 0.5 | 16.4 | 0.613 | 3874 | | KBF | |
| 10039-6730 | 288.165 | -9.778 | 1.07 | 1.91 | G? | ? | P | 0.3 | 17.3 | 0.613 | | | W | ESO |
| 10047-4123 | 272.815 | 11.408 | 0.96 | 2.25 | G | S | P | 0.7 | 16.2 | 0.613 | | | W | |
| 10048-3921 | 271.591 | 13.059 | 0.83 | 1.13 | G | S | P | 0.5 | 16.8 | 0.613 | | | W | |
| 10049-4448 | 274.891 | 8.683 | 1.74 | 4.80 | G | S | | | | | 3968 | | avW,KBF | ESO |
| 10049-4249 | 273.711 | 10.278 | 1.28 | 3.56 | G | S | P | 1.2 | 15.3 | 0.613 | 7700 | | W,72 | ESO |
| 10056-4105 | 272.773 | 11.760 | 2.40 | 5.47 | G | S | P | | | | 5668 | | * | ESO |
| 10069-3809 | 271.195 | 14.258 | 1.06 | 3.65 | G | S | P | | | | 4845 | | * | ESO |
| 10071-4245 | 274.007 | 10.575 | 1.60 | 2.62 | G | S | P | 0.9 | 15.4 | 0.613 | 4495 | | KBF | ESO |
| 10075-6647 | 288.018 | -8.994 | 16.05 | 31.31 | G | S? | P | | | | 1284 | | avW,KBF | ESO |
| 10082-3747 | 271.169 | 14.712 | 0.95 | 2.02 | G | S | | | | | 4137 | | * | ESO |
| 10089-4454 | 275.539 | 9.018 | 5.09 | 10.06 | G | S | P | | | | 5200 | | * | ESO |
| 10092-4053 | 273.214 | 12.317 | 0.70 | 2.39 | G | S | P | 0.8 | 16.0 | 0.613 | 4700 | 53 | W,12 | ESO |
| 10095-5843 | 283.546 | -2.266 | 181.40 | 313.90 | G | S? | P | 0.2 | 18.0 | | | | | ESO |
| 10096-6653 | 288.258 | -8.963 | 0.89 | 1.92 | G | S | | 0.5 | 16.4 | 0.613 | 5169 | 29 | DV | ESO |
| 10099-3838 | 271.979 | 14.226 | 0.79 | 2.38 | G | S | | | | | 5295 | | * | ESO |
| 10103-4703 | 276.987 | 7.400 | 1.84 | 5.86 | G | S | | | | | 2525 | | * | ESO |
| 10106-6217 | 285.684 | -5.121 | 27.77 | 30.48 | G | S | | | | | 3370 | | * | ESO |
| 10109-4525 | 276.146 | 8.793 | 0.94 | 1.78 | G | S | P | 0.1 | 19.2 | 0.613 | | | W | |
| 10111-6346 | 286.589 | -6.319 | 1.75 | 2.63 | G | S | | 0.5 | 16.4 | 0.613 | 3236 | | avK,KBF | |
| 10113-4327 | 275.060 | 10.447 | 1.03 | 3.13 | G | S | P | 2.3 | 13.8 | 0.613 | | | | ESO |
| 10126-4436 | 275.909 | 9.638 | 1.39 | 3.55 | G | S | | 0.9 | 15.4 | 0.613 | 969 | | KBF | ESO |
| 10128-4322 | 275.230 | 10.677 | 4.12 | 8.98 | G | S | P | | | | 3046 | | avW,KBF | ESO |
| 10134-4453 | 276.198 | 9.494 | 1.73 | 2.20 | G | S | | | | | 1050 | | * | ESO |
| 10138-4118 | 274.189 | 12.481 | 3.80 | 7.37 | G | S? | P | | | | 5974 | | * | ESO |
| 10142-4315 | 275.377 | 10.912 | 0.89 | 1.38 | G | S | | 0.5 | 16.4 | 0.613 | 5696 | | W,53 | |
| 10149-4837 | 278.522 | 6.529 | 2.85 | 12.15 | G | S | | | | | 2742 | | * | ESO |
| 10152-5136 | 280.218 | 4.084 | 1.58 | 6.44 | G | S | | 0.3 | 17.3 | 0.613 | | | | |
| 10166-6700 | 288.896 | -8.674 | 0.82 | 1.22 | G | S? | | 0.2 | 18.0 | 0.613 | | | | |
| 10173-4931 | 279.357 | 6.002 | 1.07 | 1.71 | G | S | P | 0.3 | 17.3 | 0.613 | | | W | |
| 10178-4732 | 278.329 | 7.708 | 0.75 | 1.87 | G? | ? | | 0.1 | 19.2 | 0.613 | | | W | |
| 10183-3906 | 273.625 | 14.779 | 1.97 | 5.07 | G | S | | | | | 2777 | | * | ESO |
| 10187-5810 | 284.242 | -1.132 | 144.10 | 296.20 | G | ? | | 0.1 | 19.2 | | | | | |
| 10196-4921 | 279.585 | 6.344 | 0.80 | 2.39 | G? | S | | 0.2 | 18.0 | 0.613 | | | W | |
| 10200-4116 | 275.157 | 13.158 | 2.49 | 2.69 | G? | S? | | 0.2 | 18.4 | 0.613 | | | | |
| 10209-4159 | 275.704 | 12.660 | 1.36 | 3.81 | G | S | P | | | | 2549 | | avW,KBF | ESO |
| 10211-4913 | 279.710 | 6.598 | 1.66 | 4.61 | G | S | | 1.0 | 15.2 | 0.613 | 5536 | 21 | DV | ESO |
| 10232-5315 | 282.152 | 3.346 | 1.67 | 2.66 | G | S | | 0.4 | 16.8 | | 6428 | 13 | DV | |
| 10232-3934 | 274.725 | 14.919 | 1.67 | 6.04 | G | S | | 2.0 | 14.4 | 0.613 | 2640 | | W,29 | ESO |
| 10234-4957 | 280.421 | 6.167 | 1.37 | 2.03 | G | S | P | 0.4 | 16.8 | 0.613 | 12717 | 20 | DV | ESO |
| 10240-6729 | 289.767 | -8.684 | 1.02 | 2.91 | G | S | | 0.9 | 15.8 | 0.613 | 5928 | 22 | DV,K,W | ESO |
| 10241-4528 | 278.119 | 10.024 | 1.83 | 5.23 | G | S | | | | | 4600 | | * | ESO |
| 10245-4811 | 279.639 | 7.773 | 1.59 | 2.55 | G | S | | 0.2 | 18.0 | 2.386 | 21307 | | KBF | |
| 10252-4252 | 276.875 | 12.332 | 0.98 | 3.03 | G | S | | 0.9 | 15.8 | 0.613 | | | W | ESO |
| 10255-4010 | 275.443 | 14.645 | 1.70 | 4.75 | G | S | | | | | 2565 | | avW,KBF | ESO |
| 10257-4338 | 277.371 | 11.726 | 94.63 | 121.80 | G | S | P | | | | 2739 | | avW,KBF | ESO |
| 10257-3949 | 275.273 | 14.956 | 0.97 | 2.98 | G | S | P | 1.2 | 15.3 | 0.613 | | | W | ESO |
| 10263-5026 | 281.079 | 6.011 | 0.89 | 2.75 | G | S | P | 0.6 | 16.1 | 0.613 | | | W,NED | ESO |
| 10264-6413 | 288.244 | -5.783 | 1.02 | 4.32 | G | S | P | 0.5 | 16.4 | 1.499 | | | | |
| 10267-5042 | 281.268 | 5.799 | 0.73 | 2.92 | G | S | | 1.0 | 15.2 | 0.613 | 6362 | | K,W | ESO |
| 10268-4423 | 277.954 | 11.198 | 2.36 | 10.38 | G | S | | | | | 2562 | | avW,KBF | ESO |
| 10268-4408 | 277.822 | 11.413 | 3.46 | 9.84 | G | S | | | | | 2693 | | avW,KBF | ESO |
| 10269-4335 | 277.534 | 11.892 | 2.17 | 6.66 | G | S | | | | | 2550 | | * | ESO |
| 10270-4351 | 277.702 | 11.672 | 7.50 | 19.21 | G | S | P | | | | 2929 | | avW,KBF | ESO |
| 10282-6554 | 289.293 | -7.121 | 0.75 | 1.46 | G | S | P | 0.1 | 19.2 | 0.613 | | | | |
| 10289-4847 | 280.582 | 7.632 | 1.85 | 4.17 | G | S | | 1.0 | 15.2 | 0.613 | 4780 | | KBF | ESO |
| 10290-4559 | 279.136 | 10.040 | 1.06 | 4.92 | G | ? | P | 1.6 | 14.4 | 0.613 | 2889 | 32 | W,17 | ESO |
| 10292-4148 | 276.934 | 13.632 | 3.50 | 7.83 | G | S | P | | | | 5870 | | * | ESO |

| | | | | | | | | | | | | | | |
|---|---|---|---|---|---|---|---|---|---|---|---|---|---|---|
| 10295-4513 | 278.806 | 10.741 | 1.36 | 3.66 | G | S | | 1.0 | 15.2 | 0.613 | 2664 | 16 | W,25 | ESO |
| 10299-7428 | 293.937 | -14.375 | 1.01 | 2.20 | G | S | | | | | 3700 | | * | ESO |
| 10321-6948 | 291.623 | -10.280 | 0.78 | 1.48 | G? | S? | | 0.2 | 18.4 | 0.613 | | | | |
| 10327-4039 | 276.905 | 14.964 | 1.41 | 2.14 | G | ? | | 0.4 | 17.2 | 0.613 | 4684 | | KBF | |
| 10329-4325 | 278.406 | 12.595 | 3.03 | 10.81 | G | S | P | | | | 2942 | | avW,KBF | ESO |
| 10329-7258 | 293.329 | -12.981 | 3.27 | 5.72 | G | S | | | | | 3390 | | * | ESO |
| 10333-6727 | 290.525 | -8.202 | 1.24 | 2.31 | G | S | | 0.6 | 16.5 | 0.613 | 5943 | | avK,KBF | |
| 10334-4056 | 277.172 | 14.786 | 1.42 | 3.07 | G | S | | 1.0 | 15.6 | 0.613 | 7053 | | KBF | ESO |
| 10338-5350 | 283.806 | 3.655 | 2.89 | 4.62 | G | S | | 0.7 | 15.8 | | | | | |
| 10344-6957 | 291.872 | -10.305 | 0.71 | 2.38 | G | E | | 0.2 | 18.4 | 0.613 | | | W | |
| 10350-4122 | 277.670 | 14.568 | 4.97 | 12.65 | G | S | P | | | | 2768 | | * | ESO |
| 10350-4251 | 278.450 | 13.286 | 0.79 | 2.26 | G | S | | 0.7 | 16.2 | 0.613 | | | W | |
| 10353-4112 | 277.635 | 14.738 | 0.63 | 1.74 | G | S | | 1.3 | 15.1 | 0.613 | 2757 | 16 | W,25 | ESO |
| 10355-4426 | 279.336 | 11.954 | 0.84 | 1.36 | G | S | P | 1.0 | 15.6 | 0.613 | | | W | ESO |
| 10355-5218 | 283.270 | 5.118 | 2.15 | 3.60 | G | S | | | | | 6320 | | * | |
| 10359-4411 | 279.275 | 12.208 | 0.63 | 1.93 | G | S | | | | | 7250 | | * | ESO |
| 10361-4426 | 279.428 | 12.001 | 0.91 | 1.66 | G | S | P | 0.5 | 16.8 | 0.613 | | | W | |
| 10369-5009 | 282.403 | 7.095 | 1.31 | 3.36 | G | S | | 0.4 | 16.8 | 0.613 | 7181 | | KBF | |
| 10369-4601 | 280.348 | 10.708 | 2.45 | 6.03 | G | S | P | | | | 5330 | | * | ESO |
| 10376-4451 | 279.880 | 11.781 | 0.98 | 2.91 | G | S | P | 1.2 | 15.3 | 0.613 | | | W | ESO |
| 10380-4650 | 280.929 | 10.085 | 3.01 | 6.70 | G | S | | | | | 3310 | | * | ESO |
| 10382-4609 | 280.617 | 10.692 | 0.87 | 1.90 | G | ? | | 0.5 | 16.8 | 0.613 | 7132 | 39 | DV | |
| 10388-4606 | 280.695 | 10.798 | 0.84 | 2.72 | G | S | | 0.7 | 16.2 | 0.613 | 6509 | 11 | DV,W,53 | |
| 10409-4557 | 280.945 | 11.106 | 5.74 | 13.45 | G | S | P | | | | 7000 | | * | ESO |
| 10413-4705 | 281.547 | 10.140 | 0.73 | 1.89 | G | S? | | 0.5 | 16.8 | 0.613 | 8902 | | W | |
| 10421-7520 | 295.093 | -14.712 | 0.81 | 1.08 | G | S | P | 0.5 | 16.8 | | | | W | |
| 10433-4414 | 280.480 | 12.816 | 0.65 | 1.68 | G | S | P | 0.3 | 17.7 | 0.613 | | | W | |
| 10462-7209 | 293.806 | -11.783 | 0.64 | 1.54 | G | S | | 0.7 | 16.2 | 0.613 | 7474 | 22 | DV,W,37 | |
| 10463-6503 | 290.524 | -5.467 | 2.44 | 3.82 | G | S | | | | | 3360 | | * | |
| 10465-4509 | 281.433 | 12.268 | 1.18 | 4.53 | G | S | | 1.6 | 14.8 | 0.613 | 5623 | 38 | W,43 | ESO |
| 10487-4345 | 281.140 | 13.686 | 0.87 | 2.38 | G? | ? | P | 0.1 | 19.6 | 0.613 | | | W | |
| 10488-6454 | 290.694 | -5.215 | 2.43 | 4.46 | G | S | | | | | 5935 | | * | |
| 10493-5138 | 284.842 | 6.706 | 1.01 | 3.44 | G | S? | | 0.2 | 18.0 | 0.613 | 14109 | 28 | DV,W | |
| 10495-6707 | 291.755 | -7.165 | 1.05 | 1.79 | G? | E? | | 0.3 | 17.3 | 0.613 | 21932 | | KBF | |
| 10500-7135 | 293.811 | -11.145 | 0.87 | 1.82 | G | ? | | 0.4 | 17.2 | 0.613 | | | | |
| 10501-4606 | 282.458 | 11.717 | 3.31 | 5.15 | G | S | | | | | 5889 | | avW,KBF | ESO |
| 10524-4831 | 283.902 | 9.726 | 1.38 | 6.00 | G | S | | 0.5 | 16.4 | 0.613 | | | | ESO |
| 10541-5017 | 284.932 | 8.247 | 0.98 | 3.10 | G | S | | 1.3 | 14.7 | 0.613 | | | | ESO |
| 10547-4943 | 284.774 | 8.793 | 0.90 | 3.50 | G | S | | 0.4 | 16.8 | 0.613 | 2795 | 19 | DV | |
| 10550-4959 | 284.938 | 8.583 | 1.60 | 5.11 | G | S | P | | | | 5559 | | * | |
| 10564-6923 | 293.320 | -8.923 | 1.54 | 2.19 | G | S | P | 0.5 | 16.4 | 0.613 | 8948 | | KBF | ESO |
| 10564-5003 | 285.172 | 8.620 | 2.11 | 4.77 | G | S | | | | | 2859 | | * | ESO |
| 10566-4942 | 285.049 | 8.950 | 1.25 | 2.69 | G | S | | | | | 2741 | | avW,KBF | ESO |
| 10567-4310 | 282.206 | 14.861 | 5.74 | 11.48 | G | S | P | | | | 5156 | | * | ESO |
| 10572-4725 | 284.160 | 11.052 | 1.85 | 3.48 | G | S | P | 0.4 | 16.8 | 0.613 | 6128 | 14 | DV | |
| 10574-6603 | 292.001 | -5.859 | 10.32 | 19.13 | G | S | | | | | 1470 | | * | ESO |
| 10581-4755 | 284.508 | 10.670 | 1.38 | 2.06 | G | S | | 0.4 | 16.8 | 0.613 | 5626 | | KBF | |
| 10589-4346 | 282.839 | 14.486 | 0.68 | 1.88 | G | S | | | | | 11240 | | * | ESO |
| 10590-4859 | 285.104 | 9.765 | 2.08 | 5.37 | G | S | P | | | | 14627 | | * | |
| 10593-6723 | 292.725 | -6.997 | 0.98 | 3.15 | G | S | | 0.2 | 18.0 | 0.613 | | | W | |
| 11003-4321 | 282.914 | 14.968 | 0.86 | 1.61 | G | S | P | 0.2 | 18.4 | 0.613 | 13170 | 24 | DV | |
| 11019-4811 | 285.216 | 10.694 | 2.01 | 3.73 | G | S | P | | | | 13812 | | * | |
| 11025-7212 | 294.980 | -11.287 | 0.66 | 2.19 | G | S? | | 0.2 | 18.4 | 0.613 | | | | |
| 11033-4407 | 283.734 | 14.503 | 0.74 | 1.28 | G | S? | P | 0.3 | 17.7 | 0.613 | | | W | |
| 11042-4746 | 285.398 | 11.228 | 2.56 | 4.45 | G | S | | | | | 5586 | | * | ESO |
| 11044-4812 | 285.609 | 10.837 | 1.65 | 2.69 | G | S | P | 0.5 | 16.4 | 0.613 | 2747 | 10 | DV,W,53 | ESO |
| 11055-4615 | 284.981 | 12.702 | 6.05 | 17.74 | G | S | | | | | 1319 | | avW,KBF | ESO |
| 11068-4746 | 285.813 | 11.394 | 0.68 | 1.48 | G | S | P | 0.4 | 16.8 | 0.613 | 13017 | 34 | DV | |
| 11073-6958 | 294.444 | -9.083 | 0.65 | 1.53 | G | S | | 0.4 | 16.8 | 0.613 | 9178 | 21 | DV | |
| 11083-4849 | 286.453 | 10.515 | 5.46 | 9.56 | G | S | | | | | 2755 | | avW,KBF | ESO |
| 11083-6858 | 294.135 | -8.115 | 0.68 | 1.96 | G | S | | 0.6 | 16.1 | 0.613 | 3238 | 95 | DV | ESO |
| 11085-4646 | 285.680 | 12.424 | 1.15 | 3.25 | G | S | P | 0.9 | 15.8 | 0.613 | | | W | ESO |
| 11089-4650 | 285.775 | 12.396 | 0.67 | 1.68 | G | S | P | 0.6 | 16.5 | 0.613 | 5399 | 13 | DV,W,43 | ESO |
| 11096-4738 | 286.193 | 11.696 | 0.66 | 1.80 | G | ? | P | | | | 4312 | | * | ESO |
| 11111-4711 | 286.261 | 12.218 | 0.89 | 1.62 | G | ? | | 0.1 | 19.6 | 0.613 | | | W | |
| 11111-6859 | 294.381 | -8.047 | 1.33 | 3.45 | G | S | P | | | | 1383 | | * | ESO |
| 11111-6715 | 293.736 | -6.434 | 2.67 | 3.77 | G | S? | | | | | 5762 | | * | |
| 11113-4453 | 285.407 | 14.351 | 1.02 | 2.40 | G | S | | 0.3 | 17.7 | 0.613 | 5250 | 13 | DV | |
| 11116-4642 | 286.165 | 12.686 | 1.43 | 3.59 | G | E? | P | 0.2 | 18.4 | 0.613 | 12939 | 21 | DV | |
| 11125-4556 | 286.005 | 13.464 | 0.63 | 1.38 | G | ? | | 0.2 | 18.4 | 0.613 | | | W | |
| | 288.078 | 8.088 | 2.23 | | | | | | | | 14498 | | KBF | |
| 11129-5006 | 287.641 | 9.616 | 1.28 | 2.68 | G | S | | 0.4 | 16.8 | 0.613 | 16237 | 20 | DV | |
| 11138-4442 | 285.764 | 14.701 | 1.44 | 2.72 | G | S | | 0.6 | 16.5 | 0.613 | 5910 | 15 | DV | |
| 11143-7556 | 297.225 | -14.412 | 47.65 | 70.38 | G | S | | | | | 1825 | | avW,KBF | ESO |
| 11147-4855 | 287.491 | 10.821 | 0.81 | 2.19 | G | S | | 1.0 | 15.2 | 0.613 | 4229 | 13 | DV,W,91 | ESO |
| 11168-4637 | 286.982 | 13.105 | 1.03 | 1.79 | G | ? | | 0.2 | 18.4 | 0.613 | 5846 | 67 | DV | |
| 11172-4654 | 287.143 | 12.861 | 0.68 | 1.85 | G | ? | | 0.3 | 17.7 | 0.613 | | | W | |
| 11182-4523 | 286.762 | 14.336 | 0.72 | 1.00 | G? | ? | | 0.1 | 19.6 | 0.613 | | | W | |
| 11183-4547 | 286.927 | 13.962 | 1.15 | 1.39 | G | S | | 0.2 | 18.4 | 0.613 | 14648 | 25 | DV,W,53 | |
| 11205-6909 | 295.227 | -7.908 | 1.75 | 4.70 | G | S | P | | | | 12510 | | * | |
| 11209-5002 | 288.841 | 10.135 | 0.97 | 3.40 | G | S | P | 0.3 | 17.7 | 0.613 | | | W | |
| 11218-4634 | 287.797 | 13.445 | 0.80 | 2.13 | G | S | P | 0.4 | 17.2 | 0.613 | | | W | |
| 11233-4752 | 288.488 | 12.310 | 1.03 | 3.33 | G | S | P | 2.0 | 14.4 | 0.613 | 5578 | 35 | W,17 | ESO |
| 11237-5230 | 290.089 | 7.945 | 0.70 | 2.83 | G | S | | | | | 4941 | | * | ESO |
| 11251-4918 | 289.255 | 11.053 | 0.72 | 1.61 | G | S | P | 0.2 | 18.4 | 0.613 | 16159 | | W,53 | |
| 11256-7026 | 296.081 | -8.974 | 1.02 | 2.28 | G | S | | 0.5 | 16.4 | 0.613 | 5115 | 17 | DV | |
| 11262-4828 | 289.151 | 11.888 | 0.76 | 1.54 | G | S | | 0.5 | 16.8 | 0.613 | | | | |
| 11274-5548 | 291.659 | 4.993 | 0.75 | 3.11 | G | ? | | 0.1 | 19.2 | 0.613 | | | | |
| 11276-5051 | 290.132 | 9.702 | 0.92 | 1.16 | G | S | P | 0.5 | 16.8 | 0.613 | 6299 | 11 | DV,W,86 | ESO |
| 11307-5516 | 291.944 | 5.638 | 2.03 | 7.93 | G | S | | 0.5 | 16.4 | 0.613 | 5472 | 16 | DV | |
| 11307-5228 | 291.108 | 8.321 | 0.70 | 2.34 | G | S | P | 0.4 | 17.2 | 0.613 | 15682 | 46 | DV | |
| 11308-4643 | 289.339 | 13.791 | 0.61 | 1.54 | G | ? | | 0.4 | 17.2 | 0.613 | | | W | |
| 11316-5035 | 290.673 | 10.147 | 0.62 | 1.52 | G | E? | | 0.2 | 18.4 | 0.613 | | | W | |
| 11323-5856 | 293.249 | 2.198 | 2.18 | 4.79 | G | E? | | 0.3 | 17.3 | | 1502 | 23 | DV | ESO |
| 11328-4844 | 290.292 | 11.982 | 4.09 | 8.47 | G | S | P | | | | 5624 | | * | ESO |
| 11329-4601 | 289.485 | 14.581 | 0.84 | 1.99 | G | S | | 0.8 | 16.0 | 0.613 | | | W | |
| 11340-7031 | 296.778 | -8.840 | 0.83 | 1.27 | G | S? | | 0.2 | 18.0 | 0.613 | 7665 | 24 | DV | ESO |
| | 292.360 | 5.889 | 1.61 | | | | | | | | 15097 | | KBF | |
| 11340-5114 | 291.233 | 9.642 | 0.82 | 3.01 | G | S | P | 0.3 | 17.7 | 0.613 | 14934 | | KBF | |
| 11353-4854 | 290.739 | 11.940 | 1.48 | 4.19 | G | S | P | | | | 5070 | | * | ESO |
| 11353-4650 | 290.130 | 13.916 | 1.18 | 2.51 | G | ? | | 0.3 | 17.7 | 0.613 | | | W | |
| 11354-4858 | 290.787 | 11.878 | 0.95 | 4.19 | G | S | P | | | | 5113 | | * | ESO |
| 11367-4908 | 291.038 | 11.782 | 0.79 | 1.88 | G | S | | | | | 5565 | | * | ESO |
| 11368-5316 | 292.226 | 7.812 | 1.00 | 2.75 | G | S | | 0.8 | 15.6 | 0.613 | | | | ESO |

| | | | | | | | | | | | | | |
|---|---|---|---|---|---|---|---|---|---|---|---|---|---|
| 11375-4841 | 291.046 | 12.253 | 1.42 | 4.66 | G | S | | | | | 5442 | avW,KBF | ESO |
| 11376-5406 | 292.571 | 7.041 | 0.62 | 2.34 | G | S | | | | | 4676 | * | ESO |
| 11381-4612 | 290.423 | 14.653 | 0.71 | 1.07 | G? | S? | | 0.3 | 17.7 | 0.613 | | W | |
| 11407-5303 | 292.729 | 8.183 | 0.67 | 2.07 | G | S | | 0.2 | 18.0 | 0.613 | | | |
| 11413-7212 | 297.816 | -10.290 | 1.29 | 2.02 | G | ? | | 0.2 | 18.0 | 0.613 | 3845 12 | DV | |
| 11423-5015 | 292.245 | 10.947 | 0.67 | 1.52 | G | S | P | | | | 4997 | * | ESO |
| 11435-5026 | 292.482 | 10.814 | 0.71 | 1.40 | G | S | P | 0.5 | 16.8 | 0.613 | | W | |
| 11436-5606 | 293.929 | 5.338 | 17.45 | 34.41 | G | S | | | | | 1859 | avW,KBF | ESO |
| 11442-7214 | 298.042 | -10.268 | 0.79 | 1.62 | G | S | | 0.5 | 16.8 | 0.613 | | | |
| 11443-5040 | 292.664 | 10.625 | 1.38 | 2.81 | G | ? | P | 0.2 | 18.4 | 0.613 | 14976 | KBF | |
| 11470-6824 | 297.325 | -6.500 | 2.56 | 4.75 | G | S | | | | | 7476 | * | |
| 11471-5235 | 293.557 | 8.877 | 1.43 | 2.88 | G | S | | 0.6 | 16.5 | 0.613 | 4476 | avK,KBF | |
| 11493-5145 | 293.698 | 9.767 | 1.04 | 1.81 | G | S | | 0.6 | 16.5 | 0.613 | | W | |
| 11508-5320 | 294.296 | 8.279 | 1.97 | 4.53 | G | S? | | 0.5 | 16.4 | 0.613 | 6718 36 | W,43 | |
| 11512-7335 | 298.877 | -11.454 | 1.10 | 1.80 | G | S | | 0.8 | 16.0 | 0.613 | | W | ESO |
| 11513-7209 | 298.561 | -10.056 | 1.52 | 1.82 | G | S | P | 0.3 | 17.7 | 0.613 | 12296 | KBF | |
| 11517-5117 | 293.957 | 10.303 | 0.62 | 1.41 | G | S | P | 0.9 | 15.8 | 0.613 | | W | ESO |
| 11557-5051 | 294.489 | 10.863 | 0.76 | 2.22 | G | S | P | | | | 5082 | * | ESO |
| 11557-5041 | 294.457 | 11.022 | 0.61 | 1.98 | G | S | | | | | 4210 | * | ESO |
| 11566-5307 | 295.093 | 8.667 | 1.05 | 3.08 | G | ? | | | | 0.613 | 4228 | * | ESO |
| 11568-4652 | 293.829 | 14.790 | 0.94 | 1.69 | G | S | P | 0.8 | 16.0 | 0.613 | | W | ESO |
| 11579-5346 | 295.419 | 8.081 | 0.89 | 2.77 | G | S? | | 0.7 | 15.8 | 0.613 | | W | |
| 11592-5018 | 294.921 | 11.517 | 0.61 | 1.85 | G | S | | | | | 4051 | * | ESO |
| 12002-5333 | 295.713 | 8.354 | 1.92 | 2.09 | G | S | | 0.3 | 17.3 | 0.613 | 8384 | KBF | |
| 12021-5211 | 295.742 | 9.741 | 1.27 | 3.69 | G | S | P | 0.9 | 15.8 | 0.613 | 8074 | KBF | ESO |
| 12033-4821 | 295.220 | 13.560 | 0.83 | 1.75 | G | S | P | 0.4 | 17.2 | 0.613 | | W | |
| 12040-4704 | 295.110 | 14.843 | 0.64 | 2.02 | G | S | P | | | | 9571 | * | ESO |
| 12097-5210 | 296.907 | 9.953 | 1.04 | 2.93 | G | S? | | | | | 4650 | * | ESO |
| 12110-5602 | 297.679 | 6.168 | 1.22 | 5.50 | G | S? | | | | | 8256 | * | |
| 12116-5615 | 297.807 | 5.960 | 9.68 | 12.34 | G | ? | | | | | 8141 | * | |
| 12137-5139 | 297.445 | 10.558 | 0.65 | 1.57 | G | S | | 0.2 | 18.4 | 0.613 | | W | |
| 12142-4841 | 297.109 | 13.507 | 3.24 | 8.79 | G | E | | | | | 5385 | * | |
| 12154-5627 | 298.356 | 5.834 | 1.05 | 3.81 | G | S? | | 0.6 | 16.1 | 0.613 | | | |
| 12168-6827 | 300.042 | -6.049 | 0.62 | 3.09 | G? | ? | | 0.2 | 18.0 | 0.613 | | | |
| 12181-7108 | 300.487 | -8.698 | 0.74 | 2.11 | G | S | | 0.3 | 17.7 | 4.160 | | W | |
| 12199-5820 | 299.184 | 4.044 | 2.37 | 5.63 | G | S | | | | | 1497 | * | ESO |
| 12269-5404 | 299.739 | 8.380 | 0.99 | 2.12 | G | S | | 1.0 | 15.2 | 0.613 | | | ESO |
| 12279-5116 | 299.639 | 11.190 | 0.60 | 1.19 | G | S? | | 0.4 | 17.2 | 0.613 | | W | |
| 12288-4741 | 299.501 | 14.773 | 1.26 | 2.02 | G | S | P | 0.6 | 16.5 | 0.613 | 8290 | KBF | |
| 12291-5127 | 299.845 | 11.014 | 0.69 | 1.01 | G | S | | 2.5 | 14.0 | 0.613 | 2632 20 | W,38 | ESO |
| 12295-6803 | 301.172 | -5.530 | 0.89 | 3.81 | G | S | | 0.5 | 16.4 | 0.613 | | | ESO |
| 12304-5150 | 300.092 | 10.546 | 0.77 | 2.19 | G | S | | 0.4 | 17.2 | 0.613 | | | |
| 12308-5446 | 300.363 | 7.735 | 0.89 | 2.22 | G | ? | | 0.2 | 18.0 | 0.613 | | | |
| 12320-5232 | 300.377 | 9.971 | 1.46 | 4.76 | G | S? | | 0.2 | 18.0 | 0.613 | 12224 | KBF | |
| 12355-5223 | 300.921 | 10.163 | 0.62 | 1.46 | G | ? | | 0.2 | 18.0 | 0.613 | | | |
| 12400-5843 | 301.838 | 3.849 | 2.06 | 6.10 | G | S | | 0.7 | 15.8 | | | | |
| 12446-5340 | 302.350 | 8.924 | 0.78 | 2.04 | G | ? | | | | | 1887 | * | ESO |
| 12447-5316 | 302.359 | 9.315 | 2.38 | 3.99 | G | S? | | | | | 1817 | * | ESO |
| | 302.675 | -5.781 | 1.57 | | | | | | | | 23136 | KBF | |
| 12483-5316 | 302.901 | 9.319 | 1.33 | 1.75 | G | S | P | 0.2 | 18.0 | 0.613 | 17233 | | |
| 12506-4828 | 303.273 | 14.120 | 3.66 | 11.18 | G | S | | | | | 3735 | * | ESO |
| 12526-4948 | 303.607 | 12.790 | 0.95 | 3.50 | G | S | | | | | 2294 | avW,KBF | ESO |
| 12547-4928 | 303.953 | 13.109 | 0.92 | 3.78 | G | S | | | | | 4476 | * | ESO |
| 12547-5307 | 303.875 | 9.467 | 1.10 | 2.76 | G | S | | | | | 6829 | * | ESO |
| 12548-5036 | 303.943 | 11.979 | 0.62 | 1.53 | G | S | | 0.2 | 18.4 | 0.613 | | W | |
| 12550-4801 | 304.051 | 14.560 | 0.94 | 2.71 | G | S | | 0.3 | 17.7 | 0.613 | | | |
| 12585-5300 | 304.462 | 9.571 | 0.86 | 1.87 | G? | S? | | 0.4 | 17.2 | 0.613 | | W | |
| 12588-5349 | 304.468 | 8.747 | 2.36 | 2.70 | G | ? | | | | | 7905 | * | |
| 12594-5004 | 304.712 | 12.497 | 1.24 | 4.75 | G | S | | | | | 1483 | avW,KBF | ESO |
| 12594-4912 | 304.757 | 13.359 | 1.15 | 2.66 | G | S | P | | | | 1093 | * | ESO |
| 12595-5403 | 304.557 | 8.506 | 1.65 | 2.78 | G | S | | 0.3 | 17.3 | 0.613 | 8019 | KBF | |
| 12596-5212 | 304.661 | 10.354 | 0.84 | 3.21 | G | S | P | 0.3 | 17.7 | 0.613 | | W | |
| 13003-7151 | 303.896 | -9.274 | 0.63 | 1.62 | G | S | | 0.5 | 16.4 | 0.613 | | W | |
| 13025-5049 | 305.177 | 11.725 | 0.84 | 3.21 | G | S | | 0.3 | 17.7 | 0.613 | 22200 | KBF | |
| 13025-4911 | 305.268 | 13.341 | 388.10 | 685.60 | G | S | | | | | 560 | * | ESO |
| 13028-5010 | 305.264 | 12.370 | 1.01 | 1.73 | G | ? | | 0.2 | 18.4 | 0.613 | | | |
| 13031-5717 | 304.919 | 5.256 | 2.93 | 5.16 | G | S | P | | | | 5880 | * | ESO |
| 13042-5351 | 305.278 | 8.671 | 0.68 | 3.17 | G | S | | 0.8 | 15.6 | 0.613 | | | ESO |
| 13052-5711 | 305.207 | 5.339 | 7.82 | 11.73 | G | S | | | | | 6390 | * | |
| 13064-5712 | 305.365 | 5.316 | 0.68 | 3.34 | G | S | | 0.5 | 16.4 | 0.613 | | | |
| 13065-4742 | 306.044 | 14.794 | 0.65 | 2.62 | G | ? | | 1.2 | 15.3 | 0.613 | | W | ESO |
| 13069-4740 | 306.123 | 14.810 | 0.63 | 1.02 | G | S | | 1.0 | 15.6 | 0.613 | | W | ESO |
| 13109-4912 | 306.685 | 13.229 | 2.42 | 7.76 | G | S | | | | | 3476 | avW,KBF | ESO |
| 13120-5453 | 306.337 | 7.559 | 41.49 | 46.74 | G | S | | | | | 9222 | * | |
| 13160-4738 | 307.699 | 14.708 | 3.14 | 10.15 | G | S | | | | | 3002 | * | ESO |
| 13173-7716 | 304.613 | -14.757 | 0.81 | 2.48 | G | S | | | | | 2566 | * | ESO |
| 13185-4734 | 308.148 | 14.724 | 0.68 | 1.52 | G? | E | | 0.2 | 18.4 | 0.613 | 3262 8 | DV | ESO |
| 13188-5420 | 307.389 | 7.996 | 1.23 | 3.86 | G | S | | 1.3 | 14.7 | 0.613 | 3982 77 | DV | ESO |
| 13192-5208 | 307.716 | 10.188 | 4.63 | 7.17 | G | S | | 0.9 | 15.4 | 0.613 | 5006 26 | DV,W,43 | ESO |
| 13195-4927 | 308.075 | 12.843 | 0.66 | 1.62 | G | S | P | 0.3 | 17.7 | 0.613 | | W | |
| 13215-5311 | 307.919 | 9.093 | 0.88 | 1.92 | G | S | | 0.3 | 17.3 | 0.613 | | W | |
| 13230-4758 | 308.868 | 14.237 | 0.74 | 2.70 | G | S | | | | | 3008 | | ESO |
| 13239-4903 | 308.863 | 13.137 | 0.84 | 1.62 | G | S | P | 0.5 | 16.8 | 0.613 | | W | ESO |
| 13242-5713 | 307.768 | 5.044 | 76.32 | 89.86 | G | S | | | | | 3006 | * | ESO |
| 13256-4839 | 309.216 | 13.499 | 4.14 | 11.63 | G | S | | | | | 2906 | avW,KBF | ESO |
| 13280-5100 | 309.237 | 11.119 | 0.66 | 1.88 | G? | E | | 0.1 | 19.6 | 0.613 | | W | |
| 13307-7723 | 305.345 | -14.977 | 1.67 | 6.01 | G | S | | 2.4 | 14.1 | 0.613 | 2598 | W,36 | ESO |
| 13308-5014 | 309.817 | 11.809 | 1.19 | 2.37 | G | ? | | | | | 3985 | * | ESO |
| 13320-5311 | 309.508 | 8.872 | 2.25 | 3.59 | G | S | | | | | 14425 | * | |
| | 309.402 | 7.226 | 1.55 | | | | | | | | 4290 | KBF | |
| 13339-4944 | 310.406 | 12.212 | 1.83 | 3.98 | G | S | P | 0.8 | 16.0 | 0.613 | 3661 | KBF | ESO |
| 13340-5449 | 309.514 | 7.204 | 0.94 | 3.95 | G | S | P | 0.6 | 16.1 | 0.613 | 3976 | KBF | |
| 13342-5838 | 308.864 | 3.437 | 15.52 | 14.64 | G | ? | P | 0.5 | 16.4 | | | | |
| 13342-4929 | 310.491 | 12.447 | 3.56 | 7.36 | G | S | P | | | | 3178 | avW,KBF | ESO |
| 13349-5613 | 309.389 | 5.805 | 1.08 | 3.65 | G | S | | 0.5 | 16.4 | 2.386 | | | |
| | 309.890 | 8.341 | 1.64 | | | | | | | | 21496 | KBF | |
| 13364-7052 | 306.906 | -8.636 | 1.27 | 3.45 | G | S | | 1.1 | 15.0 | 0.613 | 5283 28 | DV | ESO |
| 13370-5047 | 310.698 | 11.098 | 1.94 | 4.09 | G | S | P | | | | 4060 | avW,KBF | ESO |
| 13370-4706 | 311.411 | 14.700 | 0.96 | 1.44 | G | E? | | 0.2 | 18.4 | 0.613 | | | |
| 13370-5053 | 310.691 | 10.991 | 2.55 | 6.01 | G | S | | | | | 3689 | avW,KBF | ESO |
| 13373-5049 | 310.752 | 11.052 | 1.90 | 8.28 | G | S | | | | | 4031 | KBF | ESO |
| 13375-4805 | 311.305 | 13.730 | 1.80 | 5.72 | G | S | | | | | 2864 | avW,KBF | ESO |
| 13399-4755 | 311.750 | 13.818 | 1.22 | 4.37 | G | E | | | | | 3137 | avW,KBF | ESO |
| 13401-7101 | 307.181 | -8.833 | 1.62 | 3.08 | G | S | | 0.5 | 16.4 | 0.613 | 7234 14 | DV | |

| | | | | | | | | | | | | | |
|---|---|---|---|---|---|---|---|---|---|---|---|---|---|
| 13412-5206 | 311.086 | 9.665 | 1.69 | 4.49 | G | S | | | | | 3977 | * | ESO |
| 13413-6525 | 308.407 | -3.380 | 7.81 | 13.47 | G? | S | | 0.5 | 16.4 | | | | |
| 13415-4655 | 312.229 | 14.742 | 0.89 | 1.56 | G | /I | | 1.2 | 15.3 | 0.613 | 3410 19 | DV,W | ESO |
| 13451-5043 | 311.993 | 10.892 | 4.37 | 6.36 | G | ? | | | | | 1447 | * | |
| 13451-5010 | 312.118 | 11.428 | 1.61 | 3.24 | G | S? | | 0.8 | 16.0 | 0.613 | 8195 | avW,KBF | ESO |
| 13452-4943 | 312.237 | 11.858 | 1.38 | 2.12 | G | S | P | 0.6 | 16.5 | 0.613 | 15939 | KBF | |
| 13454-4718 | 312.819 | 14.213 | 0.74 | 2.12 | G | ? | P | 0.5 | 16.8 | 0.613 | 9863 | W,53 | |
| 13466-4830 | 312.736 | 13.007 | 1.01 | 3.09 | G | S | | 0.7 | 16.2 | 0.613 | 2996 11 | DV | ESO |
| 13471-4839 | 312.795 | 12.830 | 0.76 | 2.35 | G | S | | | | | 3147 | * | ESO |
| 13472-5241 | 311.867 | 8.900 | 0.71 | 2.88 | G | S | | 0.6 | 16.1 | 0.613 | | | |
| 13472-5224 | 311.937 | 9.173 | 2.32 | 7.97 | G | S | | | | | 3657 | avW,KBF | ESO |
| 13473-4801 | 312.967 | 13.442 | 5.64 | 6.37 | G | ? | | | | | 3225 | avW,KBF | ESO |
| 13475-4841 | 312.843 | 12.788 | 0.74 | 2.35 | G | S | | 0.6 | 16.5 | 0.613 | 3050 | W,65 | ESO |
| 13477-4848 | 312.860 | 12.666 | 13.09 | 23.05 | G | S | | | | | 3122 | avW,KBF | ESO |
| 13482-5240 | 312.024 | 8.887 | 2.20 | 5.02 | G | S | P | | | | 3976 | * | |
| | 313.191 | 13.591 | 1.85 | | | | | | | | 2950 | KBF | |
| | 313.207 | 13.648 | 1.52 | | | | | | | | 4300 | KBF | |
| | 311.418 | 5.907 | 2.46 | | | | | | | | 4070 | KBF | |
| 13489-4755 | 313.268 | 13.479 | 3.06 | 8.54 | G | S | | | | | 2856 | * | ESO |
| 13506-5339 | 312.146 | 7.848 | 0.72 | 3.23 | G | ? | | 0.2 | 18.0 | 0.613 | 3693 8 | DV | |
| | 312.380 | 8.401 | 1.78 | | | | | | | | 3758 | KBF | |
| 13543-5231 | 312.967 | 8.805 | 3.05 | 6.77 | G | S | | | | | 4056 | * | ESO |
| | 314.375 | 13.758 | 1.81 | | | | | | | | 8314 | KBF | |
| 13553-4816 | 314.243 | 12.868 | 1.57 | 5.31 | G | S | | 1.3 | 15.1 | 0.613 | 2655 14 | DV | ESO |
| 13570-4801 | 314.580 | 13.038 | 1.94 | 5.28 | G | S | | | | | 2960 | avW,KBF | ESO |
| 13571-5329 | 313.130 | 7.775 | 1.40 | 3.28 | G | S | P | 0.5 | 16.4 | 0.613 | 4810 44 | DV | |
| 13589-5318 | 313.440 | 7.879 | 5.26 | 6.58 | G | S | | | | | 3775 | * | ESO |
| 13589-6915 | 309.160 | -7.498 | 1.02 | 2.82 | G | S | | 0.2 | 18.0 | 0.613 | | W | |
| 13592-5252 | 313.612 | 8.283 | 0.98 | 4.36 | G | S | | 0.5 | 16.8 | 0.613 | | | |
| 14011-6929 | 309.286 | -7.778 | 0.98 | 3.80 | G | S | P | 0.3 | 17.3 | 1.499 | 600 89 | DV,W | |
| | 315.105 | 11.544 | 1.79 | | | | | | | | 18878 | KBF | |
| 14032-5507 | 313.549 | 5.956 | 1.53 | 4.93 | G | ? | | | | | 3775 | avW,KBF | ESO |
| 14051-4626 | 316.406 | 14.168 | 0.74 | 3.10 | G | S | | 0.2 | 18.4 | 0.613 | | | |
| | 313.863 | 5.988 | 1.58 | | | | | | | | 4313 | KBF | |
| 14060-4642 | 316.480 | 13.870 | 1.54 | 3.63 | G | S | | 0.5 | 16.8 | 0.613 | 1507 91 | DV | |
| 14072-5205 | 315.016 | 8.684 | 1.87 | 3.45 | G? | ? | | 0.4 | 17.2 | 0.613 | 3074 | KBF | |
| 14088-7045 | 309.543 | -9.186 | 0.83 | 2.58 | G | S | | 0.7 | 15.8 | 3.273 | | W | |
| 14088-4909 | 316.171 | 11.395 | 5.70 | 13.31 | G | S | | | | | 2900 | * | ESO |
| 14092-6506 | 311.323 | -3.806 | 248.70 | 315.90 | G | S | | | | | 438 | * | ESO |
| 14125-4724 | 317.328 | 12.855 | 0.60 | 2.29 | G | S | | | | | 6800 | * | ESO |
| | 315.895 | 8.722 | 10.38 | | | | | | | | 4458 | KBF | |
| 14137-5518 | 314.916 | 5.318 | 2.56 | 7.10 | G | S | | | | | 3954 | * | |
| 14167-7236 | 309.533 | -11.130 | 1.77 | 1.47 | G? | ? | | 0.4 | 17.2 | 0.613 | 7818 24 | DV,W,93 | |
| 14169-5450 | 315.505 | 5.618 | 1.50 | 5.54 | G | ? | | 0.4 | 16.8 | 0.613 | 2844 11 | DV | |
| 14179-4604 | 318.692 | 13.808 | 9.58 | 17.33 | G | S | | | | | 1847 | avW,KBF | ESO |
| 14241-5153 | 317.550 | 8.003 | 1.45 | 2.64 | G | S | | 0.6 | 16.1 | 0.613 | 17164 | KBF | |
| 14242-4707 | 319.336 | 12.441 | 0.70 | 1.35 | G | S | P | 0.5 | 16.8 | 0.613 | | W | ESO |
| 14245-4425 | 320.424 | 14.933 | 1.17 | 2.66 | G | S | | 0.6 | 16.5 | 0.613 | 8750 14 | DV,W,53 | |
| 14284-5514 | 316.909 | 4.652 | 6.06 | 13.23 | G | S | | | | | 3019 | * | ESO |
| 14285-4548 | 320.554 | 13.376 | 0.85 | 2.40 | G | S | | 1.2 | 15.3 | 0.613 | | W | ESO |
| 14325-5411 | 317.868 | 5.394 | 1.55 | 5.31 | G | S | | 0.6 | 16.1 | 0.613 | 3074 | avDV,KBF | |
| 14363-4448 | 322.255 | 13.754 | 0.73 | 3.19 | G | S | | | | | 2806 | * | ESO |
| | 319.191 | 7.207 | 1.32 | | | | | | | | 1471 | KBF | |
| 14368-5231 | 319.117 | 6.674 | 2.10 | 5.07 | G? | ? | | | | | 13273 | * | |
| 14369-4406 | 322.649 | 14.351 | 4.02 | 13.32 | G | S | | | | | 2945 | avW,KBF | ESO |
| | 318.658 | 5.589 | 1.54 | | | | | | | | 2987 | KBF | |
| 14386-4324 | 323.248 | 14.852 | 1.59 | 5.17 | G | S | | | | | 4858 | * | ESO |
| 14425-4523 | 323.017 | 12.756 | 0.64 | 1.56 | G | S | | 0.4 | 17.2 | 0.613 | | W | |
| 14454-4343 | 324.250 | 14.035 | 4.83 | 5.54 | G | S? | P | | | | 11530 | * | ESO |
| | 314.354 | -6.488 | 2.82 | | | | | | | | 15507 | KBF | |
| 14529-4331 | 325.590 | 13.591 | 1.89 | 3.17 | G | ? | | 0.7 | 16.2 | 0.613 | 4629 | KBF | ESO |
| 14535-5411 | 320.650 | 4.097 | 1.60 | 6.69 | G | S | | 1.0 | 15.2 | 0.613 | | | ESO |
| 14541-5145 | 321.859 | 6.208 | 1.26 | 6.16 | G? | S | | 1.0 | 15.2 | 2.386 | | | |
| 14544-4255 | 326.116 | 13.983 | 7.77 | 14.00 | G | S? | P | | | | 4715 | avW,KBF | ESO |
| | 324.001 | 9.909 | 4.48 | | | | | | | | 1052 | KBF | |
| 14556-4148 | 326.879 | 14.854 | 5.06 | 15.04 | G | S | | | | | 3054 | * | ESO |
| 14565-6955 | 313.608 | -9.991 | 0.64 | 1.25 | G | S | | 0.4 | 16.8 | 0.613 | 7922 43 | DV | |
| 14574-4207 | 327.020 | 14.417 | 0.76 | 1.45 | G | S | | 0.6 | 16.5 | 0.613 | | W | ESO |
| | 322.887 | 6.516 | 1.35 | | | | | | | | 10579 | KBF | |
| 15000-4247 | 327.120 | 13.612 | 1.32 | 2.88 | G | S | | 0.4 | 17.2 | 0.613 | 15944 55 | DV | |
| 15006-4119 | 327.972 | 14.818 | 0.78 | 1.31 | G | S | | 0.3 | 17.7 | 0.613 | | W | |
| 15013-4109 | 328.169 | 14.899 | 0.84 | 2.13 | G | S | | 0.5 | 16.8 | 0.613 | 11936 32 | DV,W | |
| | 323.384 | 6.982 | 1.23 | | | | | | | | 10421 | KBF | |
| 15018-4318 | 327.139 | 12.989 | 1.97 | 5.55 | G | S | | | | | 4735 | avW,KBF | ESO |
| 15023-4215 | 327.774 | 13.855 | 2.41 | 5.57 | G | S | P | | | | 5130 | avW,KBF | ESO |
| 15031-4302 | 327.486 | 13.111 | 1.39 | 2.61 | G | S | | 0.6 | 16.5 | 0.613 | 5219 17 | DV | ESO |
| 15058-5221 | 323.150 | 4.814 | 4.44 | 17.80 | G | S | | | | | 1282 | * | ESO |
| | 327.269 | 12.642 | 2.20 | | | | | | | | 28967 | KBF | |
| | 328.912 | 14.758 | 1.49 | | | | | | | | 14975 | KBF | |
| 15066-7240 | 312.942 | -12.777 | 7.19 | 20.79 | G | S | | | | | 3050 | avW,KBF | ESO |
| 15073-7235 | 313.028 | -12.727 | 1.36 | 2.52 | G | S | | 2.2 | 14.2 | 0.613 | 2963 | KBF | |
| 15093-6901 | 315.049 | -9.766 | 4.36 | 9.65 | G | E | | | | | 8227 | * | ESO |
| 15108-4637 | 326.812 | 9.335 | 1.39 | 2.75 | G | S | | | | | 522 | * | ESO |
| 15109-5248 | 323.593 | 4.044 | 18.23 | 60.02 | G | S | | 2.0 | 14.0 | 0.613 | | | |
| 15110-4349 | 328.343 | 11.696 | 1.16 | 2.92 | G | S | | 0.5 | 16.4 | 0.613 | | W | |
| 15123-4352 | 328.516 | 11.537 | 0.66 | 2.15 | G | S | | 0.9 | 15.4 | 0.613 | | W | ESO |
| 15126-6629 | 316.654 | -7.770 | 0.66 | 1.76 | G | S | | 0.2 | 18.0 | 0.613 | 14647 19 | DV,W | |
| 15127-4617 | 327.267 | 9.440 | 2.10 | 6.59 | G | S | | | | | 10058 | * | |
| 15154-6850 | 315.619 | -9.904 | 1.76 | 2.67 | G | S | | 1.0 | 15.6 | 0.613 | 4945 11 | DV | ESO |
| 15160-4102 | 330.655 | 13.548 | 1.46 | 4.11 | G | S | | | | | 1334 | * | ESO |
| 15175-3957 | 331.520 | 14.301 | 0.67 | 2.85 | G | S | | 0.7 | 16.2 | 0.613 | 7479 41 | DV | |
| 15198-3924 | 332.231 | 14.509 | 3.84 | 4.72 | G | ? | | | | | 7519 | * | |
| 15206-6256 | 319.301 | -5.240 | 10.89 | 13.84 | G | S | | | | | 8779 | * | ESO |
| 15207-3858 | 332.622 | 14.767 | 0.87 | 3.61 | G | S | | 0.6 | 16.5 | 0.613 | 7395 17 | DV | |
| 15210-3854 | 332.712 | 14.784 | 1.06 | 3.61 | G | S | | 0.8 | 16.0 | 0.613 | | | ESO |
| 15215-4838 | 327.258 | 6.662 | 0.94 | 4.00 | G | S | | 0.5 | 16.4 | 2.386 | 10525 23 | DV | |
| 15226-4149 | 331.266 | 12.207 | 4.58 | 7.18 | G | S | | | | | 4896 | * | |
| 15232-6400 | 318.959 | -6.279 | 1.12 | 4.47 | G | S | | | | | 3381 | avW,KBF | ESO |
| | 328.861 | 8.265 | 1.36 | | | | | | | | 17073 | KBF | |
| | 332.614 | 13.490 | 3.24 | | | | | | | | 4729 | KBF | |
| 15251-3854 | 333.376 | 14.335 | 3.04 | 10.58 | G | ? | | | | | 4642 | * | ESO |
| 15263-4213 | 331.610 | 11.488 | 1.89 | 2.84 | G | S? | | 0.4 | 16.8 | 0.613 | 11141 26 | DV | |
| 15268-3828 | 333.927 | 14.489 | 3.42 | 10.32 | G | S | | | | | 4746 | avW,KBF | ESO |
| 15272-4813 | 328.278 | 6.482 | 1.10 | 3.26 | G | ? | | 0.1 | 19.2 | 0.613 | | | |

| | | | | | | | | | | | | | | |
|---|---|---|---|---|---|---|---|---|---|---|---|---|---|---|
| 15280-4935 | 327.612 | 5.276 | 0.99 | 4.64 | G | S | P | 0.3 | 17.3 | 0.613 | | | | |
| | 328.697 | 7.123 | 3.40 | | | | | | | | 5568 | | KBF | |
| 15281-7242 | 314.294 | -13.686 | 1.29 | 2.43 | G | S | P | 0.5 | 16.8 | 0.613 | 20693 | | KBF | |
| 15295-4018 | 333.269 | 12.705 | 1.84 | 2.41 | G | ? | | 0.3 | 17.7 | 0.613 | 14708 | | DV | |
| 15304-7137 | 315.089 | -12.909 | 1.11 | 1.83 | G | E | | 0.6 | 16.5 | 0.613 | | | W | |
| 15312-3839 | 334.533 | 13.835 | 0.69 | 3.04 | G | ? | | 0.4 | 17.2 | 0.613 | | | | |
| 15316-4501 | 330.759 | 8.655 | 2.28 | 3.52 | G? | S | | | | | 11863 | | * | |
| 15317-6641 | 318.139 | -8.991 | 2.19 | 7.77 | G | S | P | | | | 3513 | | avW,KBF | ESO |
| 15362-3822 | 335.503 | 13.483 | 0.94 | 3.34 | G | S | | | | | 4316 | | * | ESO |
| 15366-5955 | 322.599 | -3.853 | 1.45 | 5.95 | G | S | | 0.6 | 16.1 | | 5151 | 25 | DV | |
| 15370-5949 | 322.708 | -3.798 | 1.61 | 5.53 | G | S | | 0.5 | 16.4 | | 5918 | 15 | DV | |
| 15389-6618 | 318.953 | -9.112 | 0.73 | 1.89 | G | S | | 0.3 | 17.3 | 0.613 | | | | |
| 15412-6050 | 322.507 | -4.917 | 3.27 | 8.31 | G | S | | 0.5 | 16.4 | 0.613 | 5093 | 21 | DV | |
| | 320.350 | -6.163 | 1.53 | | | | | | | | 12967 | | KBF | |
| 15421-6747 | 318.278 | -10.481 | 0.66 | 2.24 | G? | S | | 0.6 | 16.5 | 0.613 | 3412 | 16 | DV | |
| 15440-6710 | 318.821 | -10.102 | 1.07 | 3.31 | G | S | | | | | 4920 | | * | ESO |
| | 336.331 | 12.091 | 1.94 | | | | | | | | 14844 | | KBF | |
| 15445-4729 | 331.066 | 5.349 | 1.57 | 5.03 | G? | ? | | 0.2 | 18.0 | 1.499 | 6070 | 29 | DV | |
| 15452-4104 | 335.191 | 10.294 | 4.30 | 8.86 | G | S | | | | | 7303 | | * | ESO |
| 15462-4010 | 335.925 | 10.863 | 0.96 | 3.71 | G | S | | | | | 4445 | | * | ESO |
| | 322.979 | -5.201 | 1.41 | | | | | | | | 12916 | | KBF | |
| 15464-3935 | 336.326 | 11.300 | 1.60 | 4.86 | G | ? | | 0.5 | 16.8 | 2.386 | 7533 | 22 | DV | |
| 15484-5814 | 324.837 | -3.450 | 3.25 | 11.55 | G | ? | | 0.6 | 16.1 | | 12403 | 69 | DV | |
| | 336.548 | 11.083 | 1.75 | | | | | | | | 5706 | | KBF | |
| 15487-3729 | 338.052 | 12.614 | 3.75 | 7.16 | G? | S | | | | | 4414 | | * | ESO |
| | 322.836 | -6.068 | 1.62 | | | | | | | | 4473 | | KBF | |
| 15492-3842 | 337.339 | 11.629 | 3.38 | 8.26 | G | S | | | | | 4549 | | * | ESO |
| 15497-6834 | 318.342 | -11.524 | 1.42 | 3.72 | G | S | | 1.2 | 15.3 | 0.613 | 6217 | 15 | DV,W,91 | ESO |
| 15509-7211 | 316.009 | -14.343 | 0.60 | 1.98 | G | S | | 0.3 | 17.7 | 0.613 | 12480 | 30 | DV | |
| 15509-3953 | 336.809 | 10.507 | 3.39 | 7.34 | G | S | | 0.7 | 15.8 | 0.613 | 7355 | 29 | DV | |
| 15514-3729 | 338.474 | 12.277 | 0.89 | 3.03 | G | S | | | | | 5901 | | * | |
| | 323.131 | -5.869 | 1.54 | | | | | | | | 4397 | | KBF | |
| | 323.500 | -5.652 | 1.86 | | | | | | | | 10769 | | KBF | |
| | 322.528 | -7.101 | 1.84 | | | | | | | | 7837 | | KBF | |
| | 338.033 | 11.150 | 1.26 | | | | | | | | 4413 | | KBF | |
| 15540-6654 | 319.748 | -10.520 | 0.97 | 2.96 | G | S | P | 0.7 | 16.2 | 0.613 | 9550 | 28 | DV,W,53 | |
| 15551-5952 | 324.456 | -5.257 | 1.37 | 4.54 | G | S | | 0.4 | 16.8 | 0.613 | 3826 | 84 | DV | |
| 15554-6614 | 320.300 | -10.104 | 2.19 | 5.81 | G | S | | | | | 3760 | | avW,KBF | ESO |
| 15554-3645 | 339.581 | 12.317 | 1.11 | 2.58 | G | E | | 0.1 | 19.6 | 0.613 | | | | |
| 15555-6610 | 320.348 | -10.065 | 2.68 | 4.38 | G | S | | | | | 3668 | | avW,KBF | ESO |
| 15559-6058 | 323.812 | -6.152 | 2.11 | 9.28 | G | S | | | | | 6045 | | * | |
| 15567-6439 | 321.457 | -8.999 | 0.94 | 2.25 | G | S | | 0.4 | 17.2 | 0.613 | 4869 | 13 | DV,W,31 | ESO |
| 15571-4436 | 334.600 | 6.187 | 2.21 | 6.41 | G | S | | 0.2 | 18.0 | 2.386 | | | | |
| 15574-6100 | 323.937 | -6.299 | 1.82 | 6.16 | G | S | | 0.4 | 16.8 | 0.613 | 3511 | 31 | DV | |
| 15582-6138 | 323.587 | -6.835 | 1.57 | 4.32 | G? | S | | 0.6 | 16.1 | 0.613 | 4352 | 10 | DV,W,25 | ESO |
| 15586-6358 | 322.062 | -8.624 | 2.22 | 6.16 | G | S | P | | | | 7842 | | avW,KBF | ESO |
| | 337.915 | 9.202 | 1.59 | | | | | | | | 8123 | | KBF | |
| 16001-3339 | 342.441 | 13.967 | 1.98 | 4.99 | G | S | | | | | 7706 | | * | |
| 16037-5905 | 325.794 | -5.382 | 2.03 | 6.59 | G | S | | | | | 4514 | | * | |
| 16045-3950 | 338.836 | 8.823 | 1.43 | 4.64 | G | S | | | | | 8133 | | * | |
| 16073-6014 | 325.361 | -6.530 | 2.15 | 5.06 | G | S | | | | | 6683 | | * | |
| 16078-6038 | 325.125 | -6.879 | 0.71 | 3.48 | G | ? | | | | | 4510 | | * | ESO |
| 16079-3111 | 345.426 | 14.626 | 4.25 | 7.13 | G | E | | | | | 4451 | | * | |
| 16082-3229 | 344.535 | 13.656 | 0.96 | 2.09 | G | ? | | 0.2 | 18.4 | 0.613 | | | W | |
| 16084-3428 | 343.155 | 12.199 | 1.29 | 2.36 | G | S | P | 0.2 | 18.4 | 0.613 | 18316 | | KBF | |
| 16091-6316 | 323.417 | -8.898 | 0.99 | 2.90 | G | S | | 0.8 | 16.0 | 0.613 | 3278 | 15 | DV | ESO |
| 16115-3503 | 343.190 | 11.336 | 0.76 | 3.63 | G | S | | 0.2 | 18.4 | 0.613 | | | | |
| 16122-3647 | 342.076 | 10.004 | 1.92 | 4.11 | G | S | | 0.3 | 17.3 | 3.273 | 5126 | | W,53 | |
| 16129-5811 | 327.302 | -5.540 | 6.27 | 8.76 | G | S | | | | | 2734 | | avW,KBF | ESO |
| | 323.712 | -9.260 | 1.28 | | | | | | | | 13336 | | KBF | |
| 16144-3414 | 344.212 | 11.500 | 1.59 | 3.00 | G | E | P | | | | 4771 | | * | ESO |
| 16150-3119 | 346.438 | 13.461 | 0.92 | 3.48 | G | S | | | | | 3626 | | * | ESO |
| 16153-7001 | 319.026 | -14.128 | 6.65 | 19.76 | G | S | | | | | 3476 | | avW,KBF | ESO |
| | 338.739 | 5.373 | 3.42 | | | | | | | | 11148 | | KBF | |
| | 326.121 | -7.460 | 2.44 | | | | | | | | 642 | | KBF | |
| 16176-6325 | 323.993 | -9.671 | 3.86 | 5.22 | G | ? | | | | | 5160 | | * | ESO |
| 16211-3408 | 345.276 | 10.588 | 1.37 | 3.90 | G | S | | 0.3 | 17.3 | 0.613 | 5280 | | KBF | ESO |
| 16213-6256 | 324.649 | -9.620 | 0.73 | 3.11 | G | S | | 0.2 | 18.0 | 0.613 | 3913 | 13 | DV | |
| 16220-6304 | 324.598 | -9.782 | 2.51 | 8.09 | G | S | | | | | 3836 | | * | ESO |
| 16228-6518 | 323.025 | -11.374 | 1.59 | 5.84 | G | S | P | 1.3 | 15.1 | 0.613 | 7511 | 28 | DV | ESO |
| 16229-6640 | 322.009 | -12.320 | 4.73 | 9.53 | G | S | P | | | | 6535 | | * | ESO |
| 16232-4917 | 334.657 | -0.282 | 355.50 | 539.10 | G? | S | | 0.2 | 18.0 | | 7585 | | W,53 | |
| 16238-2947 | 348.915 | 13.153 | 0.88 | 3.31 | G | S | P | 0.2 | 18.4 | 0.613 | 22214 | | W,53 | |
| 16247-6234 | 325.187 | -9.656 | 1.72 | 2.51 | G | S | | 0.2 | 18.0 | 0.613 | 9753 | | KBF | |
| 16254-6735 | 321.483 | -13.125 | 0.89 | 1.29 | G | ? | | 0.5 | 16.8 | 0.613 | 12104 | 75 | DV,W | |
| 16259-6125 | 326.128 | -8.975 | 3.25 | 8.07 | G | S? | | | | | 3332 | | * | |
| 16264-5518 | 330.665 | -4.814 | 1.77 | 4.69 | G? | E? | | 0.3 | 17.3 | 0.613 | 4860 | 12 | DV | |
| 16265-3333 | 346.490 | 10.172 | 0.97 | 3.81 | G | ?/I | | 0.3 | 17.3 | 0.613 | | | | |
| 16269-5505 | 330.861 | -4.716 | 1.16 | 5.12 | G? | S | | 0.3 | 17.3 | 1.499 | | | | |
| 16276-6440 | 323.843 | -11.330 | 1.01 | 2.44 | G | S | | 1.0 | 15.6 | 0.613 | 4432 | 8 | DV | |
| 16285-2759 | 350.994 | 13.584 | 6.27 | 15.66 | G | S | | 1.0 | 15.6 | 0.613 | | | | MCG ESO |
| 16297-2739 | 351.443 | 13.606 | 2.47 | 7.65 | G | S | P | 0.4 | 17.2 | 0.613 | | | | |
| | 349.939 | 12.557 | 1.86 | | | | | | | | 5307 | | KBF | |
| | 349.723 | 12.197 | 1.47 | | | | | | | | 6546 | | KBF | |
| | 326.367 | -9.365 | 1.51 | | | | | | | | 9845 | | KBF | |
| | 328.255 | -7.788 | 3.18 | | | | | | | | 28741 | | KBF | |
| 16304-6030 | 327.189 | -8.758 | 16.52 | 32.35 | G | S | | | | | 3250 | | * | ESO |
| | 343.085 | 5.708 | 1.55 | | | | | | | | 6853 | | KBF | |
| 16330-6820 | 321.399 | -14.147 | 7.16 | 12.37 | G | S? | P | | | | 14053 | | avW,KBF | ESO |
| 16338-6224 | 326.027 | -10.326 | 3.65 | 4.69 | G? | ? | | | | | 16655 | | * | |
| 16354-6721 | 322.323 | -13.686 | 1.05 | 1.41 | G | S | | 1.0 | 15.6 | 0.613 | 6601 | 45 | DV,W,53 | ESO |
| 16383-6644 | 322.988 | -13.510 | 0.61 | 1.39 | G | ? | | 0.6 | 16.5 | 0.613 | | | W | |
| 16394-6359 | 325.228 | -11.831 | 1.96 | 2.89 | G | S? | | | | | 15214 | | * | |
| 16400-3050 | 350.479 | 9.841 | 0.90 | 4.19 | G | S | | 1.0 | 15.6 | 0.613 | 6781 | 42 | DV | ESO |
| 16403-6659 | 322.920 | -13.817 | 0.77 | 2.86 | G | S | | 1.3 | 15.1 | 0.613 | 4632 | 20 | DV,W | ESO |
| | 329.128 | -7.095 | 1.71 | | | | | | | | 2747 | | KBF | |
| 16421-6253 | 326.285 | -11.357 | 0.94 | 2.14 | G | S | | 0.5 | 16.8 | 0.613 | 17912 | | KBF | |
| 16430-5721 | 330.676 | -7.897 | 3.93 | 14.25 | G | ? | P | | | | 805 | | avW,KBF | ESO |
| 16432-6003 | 328.593 | -9.654 | 2.66 | 8.41 | G | S | | | | | 3255 | | * | ESO |
| 16434-3130 | 350.438 | 8.855 | 0.94 | 3.64 | G | | | 0.7 | 15.8 | 0.613 | 6546 | 14 | DV | ESO |
| 16434-2633 | 354.319 | 12.006 | 1.51 | 2.92 | G? | | | 0.1 | 19.6 | 0.613 | 20336 | | DV | |
| 16437-3611 | 346.875 | 5.772 | 2.90 | 11.21 | G? | | | 0.3 | 17.3 | 0.613 | 6528 | 51 | DV | |
| 16443-2916 | 352.317 | 10.119 | 9.32 | 13.21 | G | ? | P | | | | 6264 | | * | ESO |
| 16448-2456 | 355.807 | 12.767 | 1.62 | 3.12 | G | S | | 0.7 | 16.2 | 0.613 | | | | ESO |

| | | | | | | | | | | | | | | |
|---|---|---|---|---|---|---|---|---|---|---|---|---|---|---|
| 16454-6715 | 323.028 | -14.373 | 1.42 | 2.41 | G | S | P | 0.6 | 16.5 | 0.613 | 7761 | 20 | DV | |
| 16467-5854 | 329.781 | -9.266 | 26.13 | 48.77 | G | S | | | | | 1560 | | * | ESO |
| 16470-5909 | 329.609 | -9.440 | 2.65 | 2.40 | G | S | | | | | 2740 | | * | ESO |
| 16482-6221 | 327.165 | -11.569 | 2.10 | 3.03 | G | ? | | | | | 4989 | | * | |
| 16484-5908 | 329.738 | -9.571 | 36.32 | 84.50 | G | S | P | | | | 1482 | | * | ESO |
| 16493-6254 | 326.795 | -12.013 | 2.05 | 3.96 | G | S | | | | | 4168 | | * | |
| 16532-6238 | 327.294 | -12.204 | 1.46 | 3.89 | G | S | | | | | 4000 | | * | ESO |
| 16535-3132 | 351.777 | 7.159 | 1.86 | 5.62 | G | S | | 0.7 | 15.8 | 0.613 | 7156 | 54 | DV | ESO |
| 16543-5824 | 330.799 | -9.727 | 0.66 | 2.76 | G | ? | | 0.6 | 16.5 | 0.613 | | | | |
| | 349.362 | 5.197 | 3.62 | | | | | | | | 5895 | | KBF | |
| 16545-6008 | 329.426 | -10.804 | 1.88 | 9.37 | G | S | | | | | 1099 | | avW,KBF | ESO |
| 16550-6228 | 327.561 | -12.269 | 1.48 | 3.86 | G | S | P | 0.8 | 16.0 | 0.613 | 4986 | 11 | DV | ESO |
| 16555-5836 | 330.727 | -9.969 | 1.97 | 4.85 | G | S? | | | | | 4818 | | avW,KBF | ESO |
| | 359.382 | 11.838 | 1.81 | | | | | | | | 6028 | | KBF | |
| | 356.243 | 9.359 | 1.90 | | | | | | | | 8372 | | KBF | |
| 16580-2759 | 355.208 | 8.568 | 2.48 | 3.86 | G | S | | | | | 8048 | | * | |
| 16582-3159 | 352.052 | 6.090 | 2.15 | 4.82 | G? | ? | | | | | 8444 | | * | |
| 17030-4820 | 339.646 | -4.617 | 2.68 | 8.51 | G | S | | 0.8 | 15.6 | 0.613 | | | | |
| 17043-2534 | 358.034 | 8.888 | 1.03 | 3.69 | G | S | | 0.5 | 16.8 | 0.613 | | | | |
| 17051-2501 | 358.575 | 9.064 | 1.12 | 3.69 | G? | ? | | 0.1 | 19.6 | 2.386 | | | | |
| 17053-2538 | 358.102 | 8.658 | 1.09 | 3.85 | G | S | | 0.7 | 16.2 | 0.613 | 8824 | 50 | W,36,DV | ESO |
| 17056-6151 | 328.820 | -12.901 | 1.11 | 3.29 | G | S | | 1.1 | 15.4 | 0.613 | 4974 | 15 | DV,W,53 | ESO |
| | 334.223 | -8.569 | 1.98 | | | | | | | | 17983 | | KBF | |
| | 327.378 | -13.570 | 1.42 | | | | | | | | 5395 | | KBF | |
| 17086-2541 | 358.516 | 8.028 | 1.81 | 6.29 | G | S | | 1.0 | 15.6 | 1.499 | 6259 | 50 | W,36 | ESO |
| 17113-5150 | 337.599 | -7.772 | 0.79 | 3.41 | G | S | | 0.3 | 17.3 | 0.613 | 14397 | 23 | DV | |
| 17156-6006 | 331.001 | -12.921 | 0.75 | 2.18 | G | S | | | | | 4501 | | * | ESO |
| 17161-5748 | 333.003 | -11.706 | 0.64 | 1.70 | G | S? | | 0.5 | 16.8 | 0.613 | 14181 | 21 | DV,W,53 | |
| 17175-5757 | 332.988 | -11.949 | 0.73 | 2.24 | G? | E | | 0.3 | 17.7 | 0.613 | | | W | |
| 17181-5927 | 331.737 | -12.837 | 0.85 | 1.64 | G | S | | 1.2 | 15.3 | 0.613 | 2601 | 14 | DV | ESO |
| | 331.309 | -12.164 | 8.49 | | | | | | | | 30262 | | KBF | |
| | 328.491 | -14.052 | 16.98 | | | | | | | | 1107 | | KBF | |
| | 337.458 | -8.797 | 1.26 | | | | | | | | 21313 | | KBF | |
| 17185-5239 | 337.557 | -9.137 | 0.80 | 3.07 | G | S | | 0.6 | 16.1 | 0.613 | | | | |
| 17194-5957 | 331.397 | -13.240 | 1.53 | 6.75 | G | S | | | | | 3204 | | avW,KBF | ESO |
| | 344.169 | -5.348 | 1.87 | | | | | | | | 5614 | | KBF | |
| 17220-5941 | 331.809 | -13.370 | 1.30 | 3.23 | G | S | | 1.0 | 15.6 | 0.613 | 3889 | 18 | DV | ESO |
| 17221-5454 | 335.936 | -10.823 | 0.66 | 2.91 | G | S | | 0.6 | 16.5 | 0.613 | 4136 | 16 | DV | |
| 17222-5953 | 331.648 | -13.506 | 10.18 | 10.76 | G | S | P | | | | 6241 | | * | ESO |
| 17225-6050 | 330.840 | -14.036 | 1.83 | 3.39 | G | E? | | | | | 1905 | | avW,KBF | ESO |
| 17227-5954 | 331.667 | -13.568 | 1.70 | 3.35 | G | S | | 0.4 | 17.2 | 0.613 | 6324 | 21 | DV,W,53 | |
| | 346.446 | -5.375 | 6.85 | | | | | | | | 2548 | | KBF | |
| 17240-5252 | 337.833 | -9.957 | 1.03 | 1.94 | G? | ? | P | 0.3 | 17.3 | 0.613 | 329 | 64 | DV | |
| 17277-6041 | 331.300 | -14.506 | 0.99 | 1.88 | G | ? | | | | | 5278 | | * | ESO |
| 17282-5634 | 334.962 | -12.442 | 0.71 | 1.44 | G | S | P | 0.4 | 17.2 | 0.613 | | | | |
| 17294-5336 | 337.643 | -11.021 | 0.89 | 2.76 | G | S | | 0.7 | 16.2 | 0.613 | 7920 | 11 | DV | |
| 17329-5531 | 336.230 | -12.459 | 1.04 | 2.35 | G | S | P | 0.9 | 15.8 | 0.613 | 5049 | 35 | DV,W,43 | ESO |
| 17331-5954 | 332.352 | -14.691 | 0.61 | 1.85 | G | S | | | | | 5200 | | * | ESO |
| 17344-5823 | 333.788 | -14.075 | 2.12 | 3.23 | G | S | | | | | 3781 | | * | |
| 17348-4912 | 341.892 | -9.439 | 1.31 | 2.69 | G? | S | | 0.2 | 18.0 | 0.613 | 10205 | 24 | DV | |
| | 340.163 | -11.974 | 1.28 | | | | | | | | 52463 | | KBF | |
| 17382-5848 | 333.678 | -14.713 | 0.62 | 1.06 | G | S | | 0.8 | 16.0 | 0.613 | 2646 | 13 | DV,W,53 | |
| 17413-5807 | 334.495 | -14.733 | 0.86 | 1.39 | G? | ? | | 0.1 | 19.6 | 0.613 | | | W | |
| 17472-5510 | 337.570 | -14.060 | 0.83 | 1.74 | G | ? | | 0.5 | 16.8 | 0.613 | 6769 | 14 | avDV,KBF | ESO |
| 17477-4025 | 350.696 | -6.895 | 1.30 | 4.08 | G? | S | | 0.4 | 16.8 | 0.613 | 12808 | | KBF | |
| 17483-5324 | 339.253 | -13.366 | 1.39 | 1.54 | G? | S? | | 0.4 | 17.2 | 0.613 | 27043 | | KBF | |
| 17559-5214 | 340.858 | -13.832 | 1.47 | 3.62 | G | S? | P | 0.5 | 16.8 | 0.613 | 13810 | 24 | DV | |
| | 341.626 | -14.945 | 1.52 | | | | | | | | 5462 | | KBF | |
| | 345.003 | -13.269 | 1.89 | | | | | | | | 4587 | | KBF | |
| 18133-3748 | 355.418 | -9.987 | 0.81 | 2.13 | G | S | | 0.9 | 15.8 | 0.613 | 5872 | 10 | DV | ESO |
| 18134-3918 | 354.071 | -10.682 | 0.61 | 2.88 | G | S | P | 0.6 | 16.5 | 0.613 | | | | |
| 18139-3722 | 355.871 | -9.896 | 0.90 | 2.59 | G | S | | 0.6 | 16.5 | 0.613 | 7214 | 28 | DV | |
| 18162-4326 | 350.525 | -12.980 | 1.09 | 1.68 | G | S | | 0.3 | 17.7 | 0.613 | 3608 | 89 | DV | |
| 18172-4016 | 353.522 | -11.775 | 0.86 | 2.35 | G? | ? | | 0.1 | 19.6 | 0.613 | | | | |
| 18176-3915 | 354.482 | -11.392 | 1.52 | 4.03 | G | S | | 1.2 | 15.3 | 0.613 | 7038 | | avW,KBF | ESO |
| 18192-3952 | 354.065 | -11.942 | 1.61 | 3.95 | G | S | | 1.0 | 15.6 | 0.613 | 7056 | | avDV,KBF | ESO |
| 18197-4309 | 351.055 | -13.436 | 0.61 | 2.48 | G | S | P | 3.1 | 13.6 | 0.613 | 6021 | 35 | W,17 | ESO |
| 18199-4017 | 353.733 | -12.233 | 0.89 | 2.13 | G | S | | 0.5 | 16.8 | 0.613 | 6968 | | KBF | |
| | 347.795 | -14.957 | 1.85 | | | | | | | | 5788 | | KBF | |
| 18206-3921 | 354.657 | -11.947 | 1.89 | 2.26 | G | S | P | 0.4 | 17.2 | 0.613 | 9731 | | KBF | |
| 18210-3412 | 359.398 | -9.756 | 1.81 | 5.56 | G | S | | 0.9 | 15.8 | 0.613 | 4896 | | KBF | ESO |
| 18216-3528 | 358.309 | -10.427 | 0.74 | 2.29 | G | S | | 0.5 | 16.8 | 0.613 | | | | |
| 18217-4250 | 351.523 | -13.624 | 0.82 | 1.58 | G | ? | | 0.2 | 18.4 | 0.613 | | | | |
| | 354.564 | -12.172 | 2.39 | | | | | | | | 34005 | | KBF | |
| 18220-3839 | 355.416 | -11.901 | 0.96 | 1.72 | G | S | | 1.0 | 15.6 | 0.613 | 3676 | 12 | DV | ESO |
| 18266-3532 | 358.684 | -11.369 | 0.76 | 1.55 | G | S | | 1.1 | 15.4 | 0.613 | | | | ESO |
| 18281-4213 | 352.598 | -14.455 | 1.58 | 2.13 | G | S | | 0.3 | 17.7 | 0.613 | 14231 | | KBF | |
| | 355.247 | -13.502 | 1.50 | | | | | | | | | | KBF | |
| | 357.037 | -14.476 | 1.66 | | | | | | | | | | KBF | |